Stress response and inorganic poly-phosphate in the Bacillus group bacteria

Atkinson, Deborah

Award date:
2010

Awarding institution:
University of Bath

Stress response and inorganic poly-phosphate in the *Bacillus cereus* group bacteria

Deborah Jane Atkinson

A thesis submitted for the degree of Doctor of Philosophy

University of Bath

Department of Biology and Biochemistry

October 2010

Acknowledgements

I would like to thank Prof. Mike Brown, Dr. David Clarke, and Dr. Nick Waterfield who have been my supervisors over past few years at the University of Bath over the years and Dr. Sue Charlton and Mike Hudson who were my supervisors based at CEPR, HPA, Porton Down.

I would like to thank Dr. Anne Moir at the University of Sheffield and Dr. Patrick Trieu- Cuot, Institute Pasteur, Paris for providing some of the plasmids used in this work and thank you to Dr. Colin Berry for providing the *Bacillus thuringiensis* strains.

I would also like to thank Ursula Potter at the University of Bath for her help and support to produce the SEM and TEM micrographs.

I am also very grateful to the Anthrax Vaccines Group, Dr. Nigel Silman and a long list of colleagues at CEPR, HPA, Porton Down for all their help and support throughout my PhD.

A final thank you goes to my family and Barry for putting up with me through the hard times.

I especially want to dedicate my thesis to my Dad who I miss with all my heart and sadly didn't get to see me finish.

I acknowledge gratefully, receipt of financial support from the University of Bath and the Health Protection Agency.

Table of Contents

Table of Figures

Abbreviations

ACDP	Advisory Committee for Dangerous Pathogens
ATP	adenosine triphosphate
bp	base pairs
°C	degrees centigrade
CEPR	Centre for Emergency Preparedness and Response
CDM	chemically defined medium
cfu	colony forming units
CL2, CL3	Containment Level 2, Containment Level 3
CO_2	carbon dioxide
CT	crossing threshold
DNA	deoxyribonucleic acid
EDTA	ethylenediamine tetra-acetic acid
EF	oedema factor
ELISA	enzyme linked immunosorbent assay
ET	oedema toxin
GDP	guanosine diphosphate
GTP	guanosine triphosphate
HPA	Health Protection Agency
HRP	Horseradish peroxidase
Kb	kilo base
kDa	kilo Daltons
LB	Luria-Bertani medium
LF	lethal factor

LT	lethal toxin
Mg	Magnesium
µl, ml, l	microlitre, millilitre, litre
µM, mM, M	micromolar, millimolar, molar
mRNA	messenger RNA
NCBI	National Centre for Biotechnology Information
NCTC	National Collection of Type Cultures
Nhe	non-haemolytic enterotoxin
nm, µm, mm, cm, m	nanometre, micrometre, millimetre, centimetre, metre
OD	optical density
PA	protective antigen
PBS	phosphate buffered saline
PCR	polymerase chain reaction
pg / ng / µg / mg / g	picogram, nanogram, microgram, milligram, gram
poly P	Polyphosphate
ppm	parts per million
RNA	ribonucleic acid
rpm	revolutions per minute
RT	reverse transcriptase
RT-PCR	reverse transcription/transcriptase polymerase chain reaction
SD	standard deviation
sec, min, h, d	seconds, minutes, hours, days
SEM	Scanning Electron Microscope
TEM	Transmission Electron Microscope

UV	ultra violet
w/v	weight / volume

Abstract

This thesis concentrates on the *Bacillus cereus* group of organisms and interactions that they may encounter in their natural environment. Inorganic polyphosphate has been identified as an important factor of stress and survival in *B. cereus*. One of the aims of this project was to create knock out mutants of certain enzymes involved in polyphosphate metabolism in *B. anthracis*, the etiological agent of anthrax. Unfortunately, even though *B. anthracis* is very closely related to *B. cereus* and despite the application of published methods it was not possible to create these *B. anthracis* knockout mutants. In order to address the importance of inorganic polyphosphate in *B. anthracis,* a real time RT-PCR assay was developed to monitor the mRNA levels of these enzymes when the bacterium is faced with harsh nutrient environments Real time RT-PCR analysis showed that mRNA levels of the metabolizing enzymes were upregulated in low nutrient conditions but that the profiles of gene expression were varied when grown in a chemically defined media.

In addition to abiotic stresses such as low nutrients, *B. anthracis* is also likely to face biotic stress such as predation by amoeba in the soil. Investigations were performed into the outcome of the interaction of *B. cereus* group bacteria with a model amoeba, *Acanthamoeba polyphaga.* Amoebae are bacterial predators but can also be utilised as hosts by bacterial symbionts and pathogens, such as *Legionella pneumophila.* It was theorised that amoebae may provide a host environment similar to that of the professional macrophages, which *B. anthracis* encounters in mammalian infection. These investigations confirmed that the *B. cereus* group bacteria demonstrate a range of interactions with amoeba cells, from surface attachment through to intracellular persistence. These studies went on to show that *B. cereus*, *B. thuringiensis* and *B. anthracis* can all be engulfed by amoebae when challenged in their vegetative form and that spores were able to survive, and apparently germinate. Finally these studies have identified a new developmental stage of the *B. cereus* group bacteria. When grown in static conditions, especially in the presence of amoeba, the bacterial cells cease to septate and large (often motile) continuous hyphae like filaments form. These filaments can be seen to “weave” together to form large “rope” like macrofibre structures which can even become visible by eye. Previously this macrofibre growth has also been seen in *B. subtilis*, suggesting it may be common to the whole genus. In the light of these findings we speculate that this group of pathogens have evolved complex behaviours to interact with soil amoeba in order to facilitate survival in harsh environmental conditions.

1 Introduction

1.1 Inorganic Polyphosphate

1.1.1 Background

Inorganic polyphosphate (poly P) consists of chains of tens to hundreds of orthophosphate residues linked by high - energy phosphoanhydride bonds (figure 1), similar to ATP (Kornberg *et al.*, 1999). Due to lack of proven function it has been generally considered as a molecular fossil.

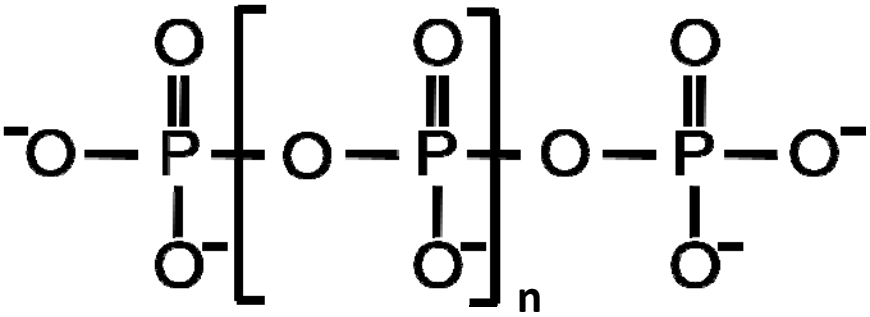

Figure 1.1 Structure of Inorganic Polyphosphate molecule

Inorganic poly P was first isolated in yeast but has now been found in every cell in nature. In eukaryotes, it is found in subcellular organelles and in yeast vacuoles at very high levels, sometimes as much as 20% of total dry weight (Brown & Kornberg, 2004). Its chemical functions as a biomolecule are becoming increasingly evident which reflect a massively influential role in nature. It can also be found at elevated temperatures in places like volcanic condensates and deep oceanic steam vents where it is formed by the dehydration of orthophosphate at the elevated temperatures (Kornberg, 1995, Kornberg et al., 1999).

It has been speculated that poly P has been present since prebiotic times and may have been an important factor in evolution. As a polyanion it possesses the ability to chelate a wide variety of cations specifically Mg^{2+}, Mn^{2+}, Ca^{2+}, Zn^{2+} and Fe^{3+}. When present in living cells, this characteristic has a major influence on biological roles. The ability of poly P to sequester toxic metals such as Cd^{2+} and Hg^{2+} can help facilitate their removal from the environment.

This chelating ability may provide a high energy scaffold of varying polymer lengths to orient or assemble some of the major polymers such as phospholipids, nucleic acids and proteins (Brown & Kornberg, 2004).

Poly P was once thought to be a significant diagnostic feature of medically important bacteria such as *Corynebacterium diphtheriae* (Kornberg *et al.*, 1999). Later, poly P was linked to the biochemical studies of oxidative phosphorylation, through which the first source of inorganic poly P was identified and curiosity the led to the investigation of how the phosphoanhydride - linked residues were assembled in poly P. This consequently led to the discovery of the associated enzymes and their functions with regards to the assembly and degradation of poly P.

Manipulating the expression of the poly P synthesising enzymes can provide a favourable route for the investigation of poly P in metabolic pathways. Several enzymes have been identified and purified for these studies.

1.1.2 The Inorganic Polyphosphate enzymes

1.1.2.1 Polyphosphate Kinase

Polyphosphate kinase (Ppk) has been identified in *E. coli* where it has been studied the most. It is a homotetramer of 80 kDa subunits bound to the inner cell membrane (Ahn & Kornberg, 1990).

Ppk catalyses the reversible synthesis of poly P using the terminal γ phosphate of ATP. Other activities include the conversion of ADP to ATP and the conversion of other nucleotides especially GDP to GTP (Brown & Kornberg, 2008). Depending on the conditions, the rates of GDP to GTP conversion are only 5% that of ADP to ATP; those of cytidine diphosphate and uridine diphosphate are even less.

Polyphosphate kinase has been identified in a variety of pathogenic bacteria such as *Salmonella typhimurium*, *Vibrio cholera* and *Mycobacterium tuberculosis* and the sequences identified demonstrate a high degree of conservation between them (Tzeng & Kornberg, 1998).

Poly P is found in large quantities within vacoules in yeast cells but there has been no Ppk activity identified. In higher eukaryotes high levels of inorganic poly P have also been identified but again, the presence of a Ppk-like enzyme has not been identified (Brown & Kornberg, 2008). Although *ppk* usually occurs as part as of an operon coupled with the *ppx* gene, other Ppk activity has been identified in species of bacteria not associated with the *ppx* gene. The gene designated *ppk2* has been found in numerous bacteria (Zhang *et al.*, 2002) and was initially found in a Ppk1 null mutant of *P. aeruginosa* (Ishige *et al.*, 2002). The Ppk1 null mutants of *P. aeruginosa* displayed no detectable level of Ppk1 but they still possessed up to 20% of the wild type poly P (Rashid *et al.*, 2000). These results suggested another source of Ppk type activity which was later confirmed to be Ppk2 (Zhang *et al.*, 2002).

Ppk2 is widely conserved, similar to the conservation of Ppk1, however the activity differs slightly. Ppk2 can be distinguished from Ppk1 as it can synthesis poly P from either GTP or ATP and has a preference for the presence of Mn^{2+} over Mg^{2+} during the enzyme reaction, whereas it is the opposite for Ppk1 (Zhang et al., 2002, Ishige et al., 2002).

1.1.2.2 Exopolyphosphatase

Exopolyphosphatase (Ppx) has also been identified and studied in *E. coli*. Its activity levels are similar to Ppk.

Ppx removes poly P by hydrolysis of the end chains of poly P producing single phosphate molecules (Pi) until only inorganic pyrophosphate is left.

The genes that code for Ppx and Ppk occur in the same operon; *ppx* occurs downstream of the *ppk* gene. However, in some species such as *H. pylori* and *P. aeruginosa*, the genes occur separately (Kornberg *et al.*, 1999).

Overexpression of *ppx* leads to depletion of cellular poly P, resulting in the same cellular effects that would result knocking out the *ppk* gene.

1.1.2.3 Phosphotransferases

Phosphotranferase works in conjunction with Ppk to convert AMP to ATP. Poly P AMP - phosphotransferase (Pap) has been purified from *E. coli*, *Acinetobacter* and *Myxococcus xanthus* (Shiba *et al.*, 2005, Zhang *et al.*, 2005b).

1.1.2.4 Endopolyphosphatases

Endopolyphosphatase acts on long chains of poly P, cleaving chains of poly P longer than 60 residues. If chains of 3 - 60 residues are used as a substrate, no hydrolytic products from cleavage are observed (Kornberg *et al.*, 1999). The best characterised examples have been purified from *Saccharomyces cerevisiae* and a similar enzyme from rat and bovine brain (Kumble & Kornberg, 1996).

1.1.3 Inorganic polyphosphate in all cells in nature

1.1.3.1 Poly P and bacteria

The influence of inorganic poly P has been studied on numerous pathogenic and non - pathogenic bacteria with extremely interesting results.

By creating knockout mutants of the specific genes *ppk*, *ppx* and *pap,* the activity and subsequent effects of the specific enzyme can be examined. Numerous groups have used this method of looking at the effect of the polyphosphate enzymes of a variety of human pathogenic bacteria.

Once the knockout mutants have been established, phenotypic experiments can be performed which can help clarify the role of inorganic poly P on bacterial virulence factors.

Motility is a key virulence factor in certain human pathogens as it aids dissemination of the pathogen through the body of the host and the pathogens entry into cells, promoting bacterial colonisation and establishing systemic infections (Josenhans & Suerbaum, 2002).

The ability to move using flagella is a key virulence factor for numerous human pathogenic bacteria including *Helicobacter pylori, Pseudomonas aeruginosa and Salmonella. ppk* knockout mutants of *Salmonella typhimurium, Vibrio cholerae, P. Aeruginosa* and *Helicobactor pylori* have all shown impaired motility (Rashid *et al.*, 2000). The results from Rashid *et al.* showed a reduced motility on swim plates when compared with the wild type. Further experiments in liquid culture proved there was no growth defect but the effect on motility was likely to be due to altered functioning of the flagella (Rashid et al., 2000, Rashid & Kornberg, 2000). *P. aeruginosa* is a very motile bacterial pathogen which can cause disease in insects, plants and animals. In humans it is an opportunistic pathogen infecting immunocompromised patients such as victims of cancer, burns and cystic fibrosis (Van Delden & Iglewski, 1998). *P. aeruginosa* relies on flagella for swimming and swarming motilities and type IV pili for twitching motilities both of which are deficient in *ppk* knockout mutants. The *ppk* mutants have apparently normal flagella which suggests that the defects are at the functional rather than structural levels (Rashid & Kornberg, 2000). The mutants were complemented with the *ppk* gene on an independent plasmid that restored motility therefore proving that the *ppk* gene was the causative factor. The actual mechanism of this defect remains obscure but does suggest fundamental roles for poly P in a range of bacterial systems.

Similar defects in motility have been shown to affect the colonisation characteristics of *H. pylori* (Ayraud *et al.*, 2005). *ppk* knockout mutants were compared with the wild type in motility studies, which were then expanded to *in vivo* studies with mice to examine the colonisation characteristics. Results showed that reduced motility corresponded with reduced colonisation of the gastric mucosa. A loss of poly P granules in cells was also consistent in the *ppk* knockout mutant. These granules of poly P have been suggested to be an alternative energy reservoir when ATP is no longer available (Ayraud *et al.*, 2005).

Salmonella and *Shigella ppk* mutants have been shown to have defects in growth rates, lowered response to stress and starvation and defects in surface attachment, all indicative of a lowered virulence (Kim *et al.*, 2002).

Poly P has been linked to the adaptation of bacteria to certain stresses and extreme environments. In order to survive, bacteria have to monitor and adapt to their environment relying on sensory systems to regulate their physiological growth characteristics. The stringent response is a method that bacteria use in order to reduce levels of rRNA synthesis and prepare and adapt for nutrient limitation. During the stringent response the bacteria produces guanosine 5' – diphosphate – 3' (ppGpp) and guanosine 5' – triphosphate 3' (pppGpp; collectively referred to as (p)ppGpp). These alarmones function to promote bacterial adaptation when faced with unfavourable conditions (Dalebroux *et al.*, 2010).

These alarmones are synthesised by the enzymic phosphorylation of GDP and GTP to ppGpp and pppGpp respectively, using ATP as a phosphate donor. In *E. coli* the proteins RelA and SpoT catalyse this reaction. During growth of *E. coli*, poly P has been found to be present at low concentrations during exponential phase but will accumulate up to 1000 – fold in concentration in response to amino acid starvation (Kuroda *et al.*, 1997). The production of (p)ppGpp during the stringent response inhibits the action of the Ppx enzyme which results in the accumulation of long chain inorganic poly P. The (p)ppGpp seems to have no effect on Ppk so long chain poly P is continually synthesised and not degraded by the inhibited Ppx. This long chain poly P then forms a complex with the ATP – dependant Lon protease which degrades free ribosomal proteins which releases amino acids for the bacteria to use in its adaptation to the low nutrient environment (Kuroda, 2006).

The stringent response can be utilised by a number of pathogenic bacteria in order to initiate their virulence programs (Dalebroux *et al.*, 2010). *Francisella tularensis* infects its host and is phagocytosed by macrophages. Whilst in the phagosome it uses (p)ppGpp to initiate and control the activation of the *Francisella* pathogenicity island which then contributes to phagosomal escape and the intracellular survival of the bacterium (Charity *et al.*, 2009, Dalebroux et al., 2010).

In Gram positive bacteria the protein RelA combines the functions of the *E. coli* RelA and SpoT. Non-spore forming bacteria such as *Mycobacterium tuberculosis* and *Listeria monocytogenes* have shown that the deletion of the *RelA* gene effects virulence properties (Dahl *et al.*, 2003, Taylor *et al.*, 2002).

Conversely, in *B. anthracis* the role of the stringent response has been shown to contribute to sporulation but not to virulence (van Schaik *et al.*, 2007). Studies using *B. anthracis RelA* mutants showed that expression of the virulence gene *pagA* and virulence in mouse models were not affected. When studying sporulation efficiency levels in *RelA* mutants, results showed that spore counts and sporulation efficiency was 1000-fold lower in the mutant when compared to the parent strain (van Schaik *et al.*, 2007). Considering the close relationship between inorganic poly P and the stringent response it could be suggested that inorganic poly P may have a major role in the process of sporulation. Even if the stringent response does not contribute to virulence, inorganic poly P may still play a part in the production of toxins. Poly P accumulates as part of the stringent response during stationary phase and this is when the toxins are produced.

1.1.3.2 Poly P in other cells in nature

Poly P has also been found in the social slime mould *Dictyostelium discoideum*. A homologue of *ppk* in *Dictyostelium sp*. has been knocked out to study the effects of poly P and Ppk on growth characteristics.

The *D. discoideum ppk* mutants were shown to be deficient in development of fruiting bodies. Fruiting bodies were significantly smaller and fewer spores were produced. Predation of bacteria by *D. discoideum* also seemed to be affected and it was suggested that poly P has a role in phagocytosis (Zhang *et al.*, 2005a).

The importance of poly P in virus replication has also recently been reported. Using an *E. coli ppk* mutant deficient for *ppk*1 it was shown that poly P was essential for the lytic growth of bacteriophages P1 and fd (Li *et al.*, 2007).

Inorganic poly P has been isolated from rodent brain, heart, liver, kidneys and lungs. Results have suggested that the synthesis of poly P from Pi bypasses the intracellular Pi and ATP pool which indicates the direct involvement of the membrane components (Kumble & Kornberg, 1995).

A role for poly P in modulation of blood coagulation has also been suggested by studies which showed that without poly P clot formation was impaired (Smith *et al.*, 2006). Studies have also shown the importance of poly P in developmental roles in young rat brain cells and programmed cell death in human cells (Lorenz *et al.*, 1997, Hernandez-Ruiz *et al.*, 2006).

Inorganic poly P has been shown to affect cancerous tumour and mammary cancer cells by stimulating mTOR (mammalian target of rapamycin) (Wang *et al.*, 2003). The exopolyphosphate gene, *ppx*1 from yeast was inserted into the chromosome of the mammary cancer cells. Ppx reduced the levels of poly P by hydrolysis of the end chains of inorganic poly P reducing the length of the molecule to its key components of pyrophosphate. Results showed that cells were deficient in their response to mitogens such as insulin and amino acids and had extremely reduced growth in serum - free medium. These results suggest that poly P (and / or Ppx1) has a regulatory effect on the proliferation of cancer cells (Wang *et al.*, 2003).

1.2 *Bacillus cereus* group

1.2.1 Background

The *Bacillus cereus* group is a group of six gram positive, spore forming, soil dwelling organisms sharing very similar growth characteristics. Members of the group share similarities in their genetic material such as the plasmids that encode their virulence factors and toxins. This similarity enables them to be able to naturally share and exchange genetic material (Koehler, 2009). Members of the *Bacillus cereus* group include *B. anthracis*, *B. cereus* and *B. thuringiensis, B. weihenstephanensis, B. mycoides and B. psuedomycoides* (Kolsto *et al.*, 2009).

This study concentrates on the three species of this genus, *B. anthracis*, *B. cereus* and *B. thuringiensis.*

1.2.2 Bacillus anthracis

1.2.2.1 Background

Bacillus anthracis is the etiological agent of anthrax. Natural outbreaks of the disease through history prompted the initial research and interest in the bacterium. The ability of *B. anthracis* spores to be dispersed as an aerosol lead to the research and development of a bio - warfare program during World War II in which an effective biological weapon was developed, but not deployed. This development of *B. anthracis* as a bio - weapon was also highlighted in 1979 when the Soviet military research facility (Sverdlovsk) had an accidental release of spores into the environment causing the death of numerous civilians (Meselson *et al.*, 1994). In 2001, *B. anthracis* was used as a bio – terror agent for the first time in history. Mail laced with *B. anthracis* spores was sent through the post addressed to important members of the media world and two US senators. This attack resulted in 22 cases 11 of which were confirmed cases of inhalational anthrax of whom five died (Spencer, 2003). These events have resulted in a renewed interest in research surrounding the disease; methods of treatment and vaccine prophylaxis are being reassessed and diagnostic assays are continuously updated.

B. anthracis is a gram positive, non - motile, spore forming, rod shaped bacterium. The dormant spore can survive in soil under adverse environmental conditions for long periods of time. Its life cycle is dependent on being ingested or inhaled by a mammalian host where it can perform its full cycle from germination, via multiplication to sporulation (Figure 1.2). During this cycle the capsule and toxins are produced which attack the host immune defences often resulting in fatal consequences.

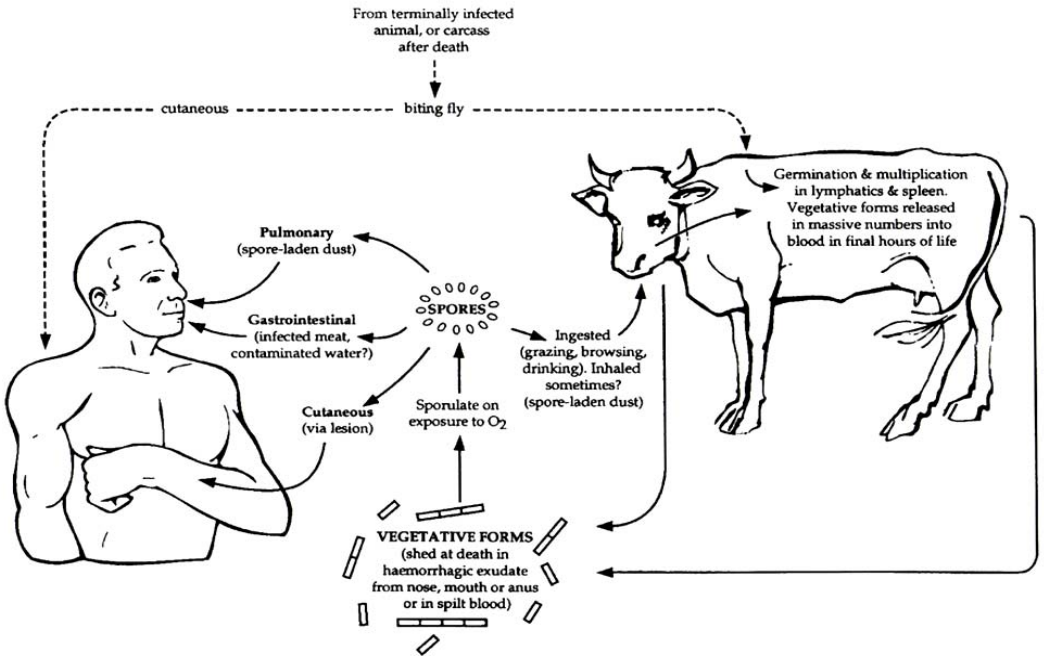

Figure 1.2. The anthrax cycle of infection (taken from Turnbull, 2002a). The spore is central to the cycle as the disease is usually contracted through uptake of the spore by the host, however, infection can also be acquired through uptake of the vegetative forms. For example, when humans and animals eat meat from an animal which died of anthrax, or when biting flies transmit the disease. .

B. anthracis is naturally prevalent in the environment and there are many natural outbreaks of anthrax around the world every year. In the UK, places such as tanneries and slaughter houses are at a higher risk of being contaminated and the surrounding soils have to be tested before any disruptive building work can commence. Anthrax spores can sometimes be found in horse hair plaster in houses built before 1895, at which time rules were introduced requiring decontamination of potentially contaminated hair.

In the environment *B. anthracis* is commonly found in its spore form which is produced when faced with a nutrient deprivation and exposure to oxygen. It has been debated heavily as to whether anthrax spores would germinate naturally in the soil if the right conditions were presented, however, the only documented case of germination outside a host occurred in a root nodule (Saile & Koehler, 2006). In this instance the root nodule was sterilised and therefore not truly indicative of the natural environment.

1.2.2.2 Disease and Infection

Anthrax is primarily a disease of herbivores, however all mammals including humans are susceptible to varying degrees.

The disease presents itself in three distinct forms; cutaneous anthrax, gastrointestinal anthrax and inhalational anthrax depending on the route of infection.

Cutaneous anthrax is the most common and the least fatal form of the disease. The bacteria usually enter through a cut or lesion on the skin and multiply locally causing a small pimple that develops into a painless black scab or eschar. This can be easily diagnosed and treated with a number of common antibiotics. The most common incidences of cutaneous anthrax are usually from contact with infected animals or untreated animal hides and skins. The term "wool sorters disease" is used to describe cutaneous anthrax. The disease has also been nicknamed "mail sorters disease" after the bio - terrorist attacks where post workers were victims of inhalational and cutaneous anthrax.

Gastrointestinal and inhalational anthrax are the most severe forms of the disease. They present after the ingestion or inhalation of anthrax spores into the mammalian host. Herbivores contract this form of the disease by grazing on contaminated soil. If diagnosed and treated at the early stages of infection the prognosis is good, however if untreated the disease can progress rapidly often ending in septicaemia or meningitis followed by death.

Cases of Anthrax in the UK are usually rare, however in the past few years there have been 2 cases of anthrax resulting from the use of imported, contaminated animal hides used in the production of drums. A drum maker in Scotland died in July 2006 when he contracted *Bacillus anthracis* spores from using the hides to make drums and artefacts. Viable spores were found in his workshop and in places where the drums had been played. No other people contracted anthrax and it was found that underlying health conditions may have complicated the disease and made him more susceptible (ProMed, 2006). A similar case occurred in November 2008 when a man died in London after contracting anthrax from contaminated animal hides used in drum making (ProMed, 2008).

Since December 2009 there has been a localised outbreak of multiple anthrax cases in heroin users in Scotland, with related cases in England and Germany. There are several theories surrounding the introduction anthrax spores into the supply of heroin. One theory is that a cutting agent, such as bone meal, contaminated with *Bacillus anthracis* spores may have been responsible. This theory has recently been dropped in favour of the idea that animal hides used to transport or contain the heroin may in fact be responsible. In these cases, anthrax presented in the cutaneous form from the scratch of the needle when injecting. However, the presentation was not typical of cutaneous anthrax and it has recently been defined as a new form; 'injectional anthrax' (Ramsay *et al.*, 2010). Cutaneous anthrax is only 0-10% fatal and is treatable with antibiotics when diagnosed. Investigations into this outbreak are still ongoing with forty five people confirmed positive of which thirteen have died (ProMed, 2010). This situation is unique as the patients were already immunocompromised from drug use, therefore, more susceptible to the disease and more likely to develop complications from cutaneous anthrax which is the mildest form of the disease.

1.2.2.3 The Toxins

The two main virulence factors of *B. anthracis* can be found on its two plasmids pX01 and pX02 which code for the toxins and the poly - D - glutamic acid capsule respectively. The fully virulent Vollum and Ames strains of *B. anthracis* have both plasmids present but the avirulent Sterne strain just possesses pX01 and is not infectious to humans. Loss of both of these plasmids results in an avirulent form which can be confused with *Bacillus cereus.*

The toxins play a key role in the pathogenesis of anthrax. The toxins are composed of three main proteins: protective antigen (PA), lethal factor (LF) and edema factor (EF).

Protective antigen is named after its ability to produce a protective immune response against (Mock & Fouet, 2001).

Although separately these proteins are not toxic, when combined they can generate fatal effects. PA and LF combine to produce lethal toxin (LT) which, when injected, can provoke death of an animal. PA and EF combine to produce edema toxin (ET) which produces edema in the skin (Mock & Fouet, 2001).

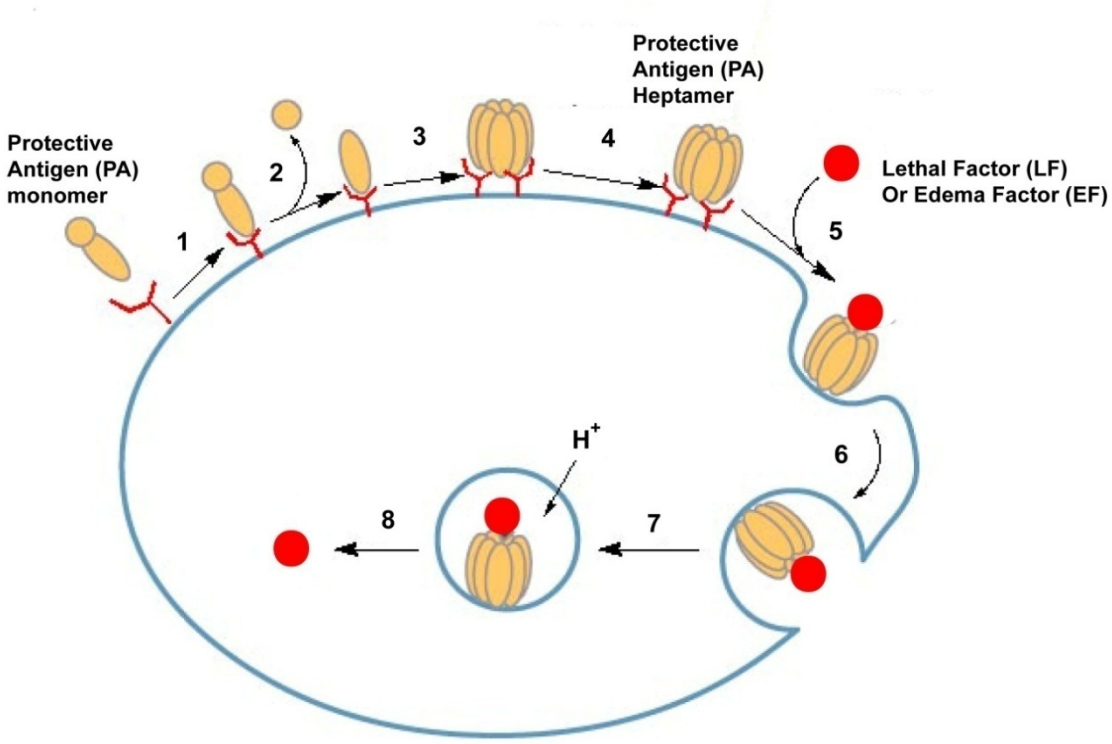

Figure 1.3 Mode of action of the anthrax toxins. 1. PA binds to the cell receptor. 2. Proteolytic cleavage of PA by furin which exposes the LF and EF binding site. 3. Assembly of PA monomers to form the heptamer. 4. The heptamer acts as a pre-pore which allows toxins to enter the cell. 5. LF or EF bind to the PA heptamer. 6. The whole toxin complex is internalised into the cell. 7. The acidic endosome causes the PA to create a pore in the bi - lipid membrane. 8. The EF and LF are released into the cell cytosome (Adapted from Mourez *et al.*, 2002).

The targets for LF and EF are located in the cytoplasm. PA acts as an escort to target the toxin to the host cell and then facilitate the translocation of the protein across the bi - lipid membrane. PA binds to two known specific cell receptors; ANTXR1 (tumor endothelial marker - 8) and ANTXR2 (capillary morphagenesis protein 2) (Young & Collier, 2007). A 20kDa peptide is then removed from the N terminus of PA through proteolytic cleavage by a furin protease in order for PA to heptamerise and form a pore in the bi - lipid membrane. It has also recently been discovered that not only does PA form a heptamer but also an octomer to aid in the translocation of EF and LF. Both forms of PA share translocation rates and efficiencies (Kintzer *et al.*, 2009). This cleavage also exposes the LF and EF binding site on PA. This is a critical step in intoxication and deletion mutants of PA without this cleavage site have shown to be completely non - toxic to macrophages when combined with LF (Mock & Fouet, 2001). Once the 14 stranded transmembrane porin β - barrel is assembled and the EF and LF binding sites

have been exposed, LF and EF bind to the heptamer. This triggers receptor mediated endocytosis and the PA, LF and EF are internalised into an acidified endosome. The acidic environment causes a conformational change on the PA heptamer which produces a pore for the translocation of EF and LF into the cell cytoplasm (Mourez *et al.*, 2002).

The 14 stranded transmembrane porin - like ß - barrel formed by PA may well be similar to that of the translocation of bacterial proteins that use the type V secretion system (Abrami *et al.*, 2005).

EF is an adenylate cyclase that converts intracellular ATP to cyclic AMP (cAMP) in a process that is dependant on the eukaryotic protein calmodulin (Leppla, 1982). This process occurs in the target cell which results in a substantial increase in intracellular cAMP levels leading to an imbalance of water homeostasis (Abrami *et al.*, 2005). After entry into the cytosol, EF stays associated with the membrane unlike LF which dissociates. This association to the membrane and adenylate cyclase activity of EF has been suggested to resemble the membrane - associated eukaryotic adenylate cyclase (Mock & Fouet, 2001).

LF is a zinc - metalloprotease similar to *Clostridium botulinum* and tetanus toxins. LF has been shown to cleave the amino terminus of mitogen - activated protein kinase kinases (MAPKKs). MAPKKs lie in the middle of three-component phosphorylation cascades activated by a wide variety of cellular stimuli, including growth factors, cytokines and stress (Chopra *et al.*, 2003, Widmann *et al.*, 1999).The MAPK pathway regulates gene expression by protein phosphorylation in response to environmental signals to transcriptional apparatus in the nuclease (Mock & Fouet, 2001).

Both EF and LF can target a range of cell types and are internalised with the subsequent increases in cAMP and cleaved MAPKKs. LF has shown to prompt apoptosis in endothelial cells (Kirby, 2004), however, the main target cells in anthrax pathogenesis seem to be those of the immune system, either professional phagocytes or antigen presenting cells (Fukao, 2004). Once LT has entered the macrophage cytosol it has been shown to inhibit the production of a multitude of immune responses such as the production of proinflammatory cytokines, the

lipopolysaccharide (LPS), interferon (IFN) γ - induced release of nitric oxide and tumour necrosis factor (Pellizzari *et al.*, 1999).

1.2.2.4 Capsule and S-layer

The ability to produce toxins is obviously a very important virulence factor for *B. anthracis* but this alone is not sufficient to inflict the fully virulent form of the disease. The capsule is the second important virulence factor that enables the bacteria to invade the host and hold off the attacks of the immune system. The poly - D - glutamic acid capsule is coded for on the virulence plasmid pX02. The coding region for the capsule is made up of three genes *capB*, *capC* and *capA*, arranged in this order (Makino *et al.*, 1989).

The capsule was first described in 1903 when McFadyean devised the staining method which uses polychrome methylene blue to visualise the capsule (M'Fadyean, 1903). This technique is still used today as a diagnostic tool.

The capsule enables the bacteria to evade the host's immune system by inhibiting phagocytosis and provoking septicaemia. Studies have shown that inhibition of phagocytosis is capsule - mediated in neutrophils and macrophages (Makino et al., 1989, Schneerson *et al.*, 2003).

The capsule synthesis is dependent on increased levels of bicarbonate and temperature; environmental conditions indicative of being inside the mammalian host. When a spore is in the presence of serum and elevated CO_2, capsule is excreted through openings on the spore surface in the form of blebs which may then combine before shedding of the exosporium and the spore outgrows into a vegetative cell (Ezzell & Welkos, 1999).

When the capsule is not present, the outer wall consists of the S - layer. The S -layer overlays the peptidoglycan and is made up from two proteins; namely Sap (surface array protein) and EA1 (extractable antigen 1) (Etienne-Toumelin *et al.*, 1995, Mesnage *et al.*, 1997). These two

proteins are immunogenic in animals but immunisation of the proteins on their own does not provide protection (Baillie *et al.*, 2003). The Sap and EA1 proteins are coded for by *sap* and *eag* respectively. The production and surface location of these two proteins are controlled at the transcriptional level and depend on the phase of growth. During exponential phase the predominant protein is the Sap layer which is replaced in the stationary phase with the EA1 layer (Mignot *et al.*, 2002).

The S - layer itself seems to have no influence on virulence; however, when present in conjunction with the capsule a cumulative effect can be observed which increases resistance to complement mediated pathways defences (Mock & Fouet, 2001).

1.2.2.5 Genetics

B. anthracis is a member of the "*Bacillus cereus* group" which also includes *B. cereus* and *B. thuringiensis*. This group of bacteria are so closely genetically related that it has been questioned that they may be the same species but carrying different plasmids (Rasko *et al.*, 2005). The suggestion has been raised that the group should be reclassified as a single species (*Bacillus cereus)* and that the specialized groups should be designated as subspecies (Helgason *et al.*, 2000). The practical taxonomic separation within the group has historically been determined with the capsule staining method (M'Fadyean, 1903) and γ - phage sensitivity (Brown & Cherry, 1955) along with characteristics such as motility and haemolysis when grown on blood agar.

Distinguishing between the members of the group has progressed to the analysis and comparison of horizontally transferred plasmids but even these can complicate the results as *B. anthracis* plasmids have been found in *B. cereus* strains (Hoffmaster *et al.*, 2006, Okinaka *et al.*, 2006).

There are many complications within the classification of *Bacillus* species but with the improved molecular identification techniques such as Variable Number of Tandem Repeats (VNTR), Multiple Locus VNTR analysis (MLVA), and Multiple Locus Sequence Typing (MLST) analysis *Bacillus* genetics are becoming clearer. These molecular typing methods can be used to map evolutionary pathways and decipher the intricate relationships between strains within

the *Bacillus* genus using the chromosomal sequences which give a more accurate portrayal of the evolutionary tree (Priest *et al.*, 2004, Helgason et al., 2000).

The *B. anthracis* species is divided into three major lineages (A, B, and C) with the A clade being the most important and globally dispersed cause of anthrax (Van Ert *et al.*, 2007, Keim *et al.*, 2009). The B clade has two lineages. The B1 clade has been found in South Africa and the B2 clade has been found more widely in southern and eastern Europe (Keim *et al.*, 2000) and a single case in California in the USA (Van Ert *et al.*, 2007). The C clade is considered an enigma due to its rarity and source (Keim *et al.*, 2009). However, as with all analysis of bacterial isolates there is sometimes the risk of bias due to the inability to sample a fair and equal distribution of strains from everywhere in the world.

The *B. anthracis* plasmids pX01 and pX02 code for its two virulence factors; the toxins and the poly - D glutamic acid capsule respectively. A *B. anthracis* strain containing both of these plasmids results in a fully virulent form of *B. anthracis* however these transmissible plasmids can sometimes be lost resulting in an avirulent strain such as the Sterne strain ($pX01^+$ and $pX02^-$). The *B. anthracis* plasmids are also transmissible into other *Bacillus* strains. *B. cereus* has been reported to naturally acquire the toxin genes and consequently caused a pneumonic disease in Texas, USA (Hoffmaster *et al.*, 2004). Further analysis of the clinical isolates revealed that the *B. cereus* strain contained almost all of the pXO1 toxin virulence plasmid which was most likely acquired from horizontal transfer in the environment (Hoffmaster *et al.*, 2006). A *B. cereus* strain that contains plasmids with high identity to both pX01 and pX02 has also been isolated from great apes in the Ivory Coast and Cameroon which had died from an anthrax like illness (Klee *et al.*, 2006).

1.2.2.6 Antibiotic Treatment

The treatment for anthrax has historically been penicillin as only very rarely has naturally occurring penicillin resistant strains been identified (Spencer, 2003).

In vitro, *B. anthracis* is susceptible to penicillins, fluoroquinolones, tetracycline, chloramphenicol, aminoglycisides, macrolides, imipenem, rifampicin and vancomycin (Spencer, 2003, Turnbull *et al.*, 2004). For treatment of mild cutaneous anthrax the recommended

dosage is ciprofloxacillin (500 mg twice daily), doxycyline (100 mg twice daily) or amoxicillin (500 mg three times daily) (Inglesby *et al.*, 1999). In case of a bioterrorist attack it is recommended that treatment should be continued for 60 days instead of the usual 7 – 10 days for the naturally acquired infection. This is due to an unknown prolonged latency period as there is no guarantee of the germination time of the inhaled spore (Friedlander *et al.*, 1993).

1.2.2.7 Anthrax Vaccines

In the late 1800's early research on *B. anthracis* produced the first successful use of a whole cell anthrax vaccine by Jean - Joseph Henri Toussaint, William Smith Greenfield, and Louis Pasteur (Scorpio *et al.*, 2006). A vaccine for *B. anthracis* was originally developed to reduce the incidence of disease in livestock and their workers; however, the present focus is the defence against bio - terrorism and biological warfare. Pasteur developed the first animal *B. anthracis* vaccine in 1881. The Pasteur vaccine was a live attenuated strain lacking the toxin plasmid ($pX01^-$ and $pX02^+$). This was followed in 1939 by the Sterne vaccine strain, which lacked the capsule plasmid ($pX01^+$ and $pX02^-$). The Sterne vaccine was an attenuated spore vaccine of the avirulent non-capsulated 34_{F2} strain produced from a subculture of a case of bovine anthrax. The Sterne vaccine has shown much greater protection indicating that the presence of pX01, therefore the expression of the toxins, holds a great importance for protection (Turnbull, 2000, Turnbull, 1991). In 1940 the Soviet Union introduced a Sterne - like vaccine (ST1), a live spore vaccine, which has been used in millions of people (Scorpio *et al.*, 2006).

The current UK anthrax vaccine, an acellular vaccine manufactured from alum precipitated culture supernatants of *B. anthracis* $34F_2$ Sterne strain, was introduced in 1965 for workers in high risk occupations (animal workers and handlers of animal hides) (Spencer, 2003). It was later officially licensed for human use in 1979 after the addition of biological agents to the European directive. The UK anthrax vaccine is manufactured using a simple method which has not significantly changed since the vaccine was first licensed. Manufacture of anthrax vaccine precipitate (AVP) involves growth of the non - capsulated *B. anthracis* $34F_2$ Sterne strain (Sterne, 1939) in a chemically defined medium supplemented with casamino acids and activated charcoal (Charlton *et al.*, 2007). The cultures are grown statically in Thompson bottles at 37°C until the pH falls below pH 7.6. At the end of this growth period the cultures are harvested and the pooled supernatants are filter sterilised. Alum solution is added and the

pH is adjusted to 5.8 - 6.2. The precipitate is allowed to settle under gravity at 5°C. Supernatants are aspirated to effect a 15 fold concentration, producing Bulk Vaccine Concentrate. This is then diluted 1 : 3 with saline to produce AVP (Charlton *et al.*, 2007). The immunisation schedule for the UK anthrax vaccine consists of four initial doses at zero, three, six and 32 weeks followed by an annual booster. The immunisations may result in a painful vaccination site and may sometimes cause flu - like symptoms, however, these side effects often differ from batch to batch.

The US anthrax vaccine (anthrax vaccine adsorbed - AVA) is similar to the UK AVP. It consists of culture supernatant from *B. anthracis* V770 - NP1 - R, which is $pX01^+$ and $pX02^-$. This Sterne based strain is grown in a protein - free defined medium, filtered then adsorbed to aluminium hydroxide (Alhydrogel) (Scorpio *et al.*, 2006). The vaccination schedule is a little more intense than the UK version consisting of six injections over 18 months and yearly boosters from then onwards (Scorpio *et al.*, 2006).

There are many disadvantages to these types of vaccines and the production methods are in desperate need of redeveloping. The manufacturing processes are extremely labour intensive as they are performed at CL3 and they are hard to scale up to produce the amounts needed during vaccine production. There are a number of new types of anthrax vaccine in the research stages including subunit vaccines and DNA vaccines (Ferrari *et al.*, 2004, Galloway & Baillie, 2004, Chawla *et al.*, 2009). Protective antigen (PA) is a major immunogenic protein and has shown to be one of the main components in the AVP and AVA vaccines, therefore, research groups are focusing on possibilities of using a recombinant PA protein in the development of a subunit vaccine (Williamson *et al.*, 2005, Chawla et al., 2009).

1.2.3 Bacillus cereus

Bacillus cereus is an ACDP hazard group 2 organism. The bacteria is a soil dwelling microbe as are most bacilli and it is very common in the environment.

1.2.3.1 Disease and Infection

B. cereus is commonly recognised as a cause of food poisoning. *B. cereus* may be present in certain foodstuffs where it will multiply when incubated at ambient temperatures. During this time, it produces its toxins which can lead to severe food poisoning if ingested. Two distinct forms of food poisoning can be caused by this *Bacillus* depending on the type of toxin that is ingested.

The "short incubation" or emetic form results in the onset of nausea and vomiting as quickly as 1 - 5 hours after consumption and is caused by the pre - formed heat stable emetic toxin ETE. The diarrheal form is caused by the heat susceptible enterotoxin Nhe or / and the haemolytic enterotoxin HBL. This form has a longer incubation time of 8 – 16 hours after consumption of the contaminated food. The diarrhoea is coupled with abdominal pain. Both forms of the disease are self-limiting and usually last less than 24 hours after the onset.

Food poisoning from *B. cereus* is commonly caused by the re - heating of cooked rice especially in restaurants where boiled rice is held at an ambient temperature for long periods of time and then refried quickly as part of a dish. Spores that were not effectively killed during the initial cooking step germinate if inadequately refrigerated or kept at an ambient temperature for a long time. During the multiplication stages, the toxins are produced (Granum, 1994, Kotiranta *et al.*, 2000).

Non - gastrointestinal infections from *B. cereus* have also been reported. These occur more commonly in immunocompromised patients such as drug addicts or patients with surgical wounds, traumatic wounds or catheters. Production of the enterotoxins and emetic toxin is likely to be an important step in the development of the infection (Turnbull *et al.*, 1979, Drobniewski, 1993). Although the majority of *B. cereus* localised infections are mild, they can sometimes develop in deep tissue resulting in more severe manifestations such as gangrene and necrotising fasciitis (Fitzpatrick *et al.*, 1979, Drobniewski, 1993).

1.2.3.2 Virulence Factors

1.2.3.2.1 Toxins

B. cereus produces a number of toxins; the emetic toxin, cereulide, and at least five different enterotoxins including Non - heamalytic enterotoxin (Nhe) and Haemolysin BL (HBL). Cereulide is highly resistant to heat and proteolytic cleavage and is stable between pH 2 – 11. . It is this heat resistance that causes the problems with regards to food poisoning (Granum & Lund, 1997).

Only two of the enterotoxins, Nhe and HBL, are involved in diarrheal food poisoning (Lund & Granum, 1997). They both consist of three different protein subunits that act together. There are a number of other enterotoxins also produced by *B. cereus* that contribute to its virulence. The cytotoxin, CytK, was isolated from a *B. cereus* strain that caused an outbreak of food poisoning. The protein is highly cytotoxic, necrotic and haemolytic (Lund *et al.*, 2000). The enterotoxin entFM and *B. cereus* enterotoxin T (bceT) have also been found to contribute to the virulence of *B. cereus* but may not play a major role in food poisoning (Choma & Granum, 2002, Luxananil *et al.*, 2003).

1.2.3.2.2 Exotoxins

B. cereus also produces other virulence factors in the form of exotoxins and membrane degrading enzymes. There are three haemolysins; cereolysin and haemolysin II and III. These have a wide range of effects on tissues and often initiate cell lysis possibly by binding to the cell receptor allowing pore formation and subsequently cell leakage leading to lysis (Drobniewski, 1993). Phospholipase C (PLC) is a metalloenzyme which has been shown to interfere with a number of cell signalling pathways indicating that PLC may be involved in mediating tissue damage during infection (Firth *et al.*, 1997). Sphingomyelinase (SMase) has shown to be able to induce apoptosis in several mammalian cell types (Flores *et al.*, 1998).

1.2.3.2.3 Proteases

Extracellular metalloproteases have been detected from a number of strains of *B. cereus.* One of these proteases has been sequenced and has homology to a metalloprotease from *B. thuringiensis*. This thermolysin-like protease has shown to be highly conserved in the evolution of the *B. cereus* group (Donovan *et al.*, 1997, Bach *et al.*, 1999). Another neutral protease has shown to have a destructive effect on albumin and haemoglobin which suggests that the *B. cereus* proteases are virulence factors in non-gastrointestinal diseases (Sierecka, 1998).

1.2.4 Bacillus thuringiensis

B. thuringiensis is an insect pathogen, commonly isolated from the guts of moths and caterpillars. During sporulation the bacterium produces proteinaceous crystalline inclusions that have insecticidal activity. This property has been exploited commercially in biological insecticides. Strains have been isolated from a variety of different environments ranging from soil, insects, and various leaves (Roh *et al.*, 2007).

B. thuringiensis is very closely related to *B. cereus.* Recent studies have shown that *B. cereus* and *B. thuringiensis* could be considered as one strain (Carlson *et al.*, 1994) as previously proposed for *B. cereus* and *B. anthracis* (Helgason et al., 2000, Keim et al., 2009) further demonstrating the intricate relationship within this group. Indeed, if many strains of *B. thuringiensis* are plasmid cured they result in a strain that is phenotypically indistinguishable to that of *B. cereus* (Roh *et al.*, 2007) using most common techniques.

1.1.1.1

1.2.4.1 Crystal Proteins

The crystal (Cry) proteins, or δ-endotoxins, are encoded on a transmissible plasmids similar to that of the virulence factors of *B. cereus* and *B. anthracis* (Gonzalez & Carlton, 1980). Individual Cry proteins are specifically toxic to a small range of insect species and expression of particular toxins defines the activity spectrums of that particular strain. The *cry* genes code for toxins which range in size from 50 to 140kDa (Roh *et al.*, 2007). They are classified on the basis of amino acid sequence homology and are numbered depending on its position in a phylogentic tree (Roh *et al.*, 2007).

As well as the Cry toxins, *B. thuringiensis* also produces the Cryt toxins which occur as a different group. The Cryt toxins are slightly smaller ranging from 20 – 28 kDa and have cytolytic activity.

Whether naturally occurring or when used as a pesticide, crystal proteins act after ingestion by the susceptible insect. The protoxin is solubilised and proteolytically digested in the insect gut, which releases the active toxic fragments (Hofte & Whiteley, 1989, de Maagd *et al.*, 2003). The Cry toxin acts via a multi stage process. After the proteolytic cleavage to activate the protoxin into its active fragments they bind to the cell receptors located on the microlvillus membrane of the epithelial midgut cells. After the toxin has bound to the receptor the toxin structure is thought to change allow the toxin to insert into the membrane. This is followed by oligomerization of the toxin which forms a pore that leads to osmotic cell lysis (Lorence *et al.*, 1995). Nevertheless, the precise mode of action of the Cry toxins and their ecological relevance remain controversial.

1.3 *Bacillus cereus* and inorganic polyphosphate

In *B. cereus* the three enzymes Ppk, Ppx and Pap have been identified and their genetic loci determined. *ppk* and *ppx* occur in an operon similar to that of *E. coli* and the amino acid code shares the same high level of identity to other bacteria (Shi *et al.*, 2004). Furthermore, inorganic polyphosphate (poly P) has been discovered to be very important in growth and sporulation in *B. cereus.* The deletion of the key enzymes involved in the metabolism of inorganic poly P in *B. cereus* resulted in a decrease in sporulation efficiency (Shi *et al.*, 2004). *ppx* mutants displayed the highest decrease in sporulation, whereas the *ppk* and *pap* mutants displayed similar levels to the wild type. The fact that poly P has such a noticeable effect on the level of sporulation suggests that poly P is essential as part of the stress response and subsequently prolonged survival in the environment.

Shi *et al.* have also shown that each of the *B. cereus* mutants showed impairment in both types of motility; swimming and swarming. A surface attachment assay showed that attachment and biofilm formation was greatly reduced in the *ppk* and *ppx* mutants and moderately reduced in the *pap* mutants. Such defects in motility and biofilm formation are typically indicative of

reduced virulence. It is interesting to speculate that inorganic polyphosphate may have similar importance in the growth, development and virulence of *B. anthracis*.

1.4 Protozoa and bacterial interactions

1.4.1 Background

Protozoa are ubiquitous and have been isolated from numerous natural environments; soil, freshwater, salt water, dust and air. Interestingly they have also been found in man-made environments such as piped water systems, air conditioning units and cooling towers. There are many different species including the Flagellates, Amoeboids, Sporozoans, and Ciliates. Protozoa are predators of environmental bacteria occurring in their natural environment and it is not surprising that some of these bacteria have evolved ways to evade predation and even exploit the intracellular niche to their advantage (Molmeret *et al.*, 2005). Indeed it is likely that many virulence factors seen in mammalian pathogens were first evolved as a means of combating predation by amoeba.

1.4.2 Protozoa as environmental hosts

Free - living protozoa have been identified in conjunction with bacterial symbionts from the groups *Alphaproteobacteria*, *Betaproteobacteria*, *Gamaproteobacteria*, *Bacteriodetes*, and *Chlamydiales* for many years (Molmeret et al., 2005, Horn & Wagner, 2004). These symbionts were identified using specific PCR amplification of bacterial rRNA genes and fluorescence in situ hybridisation. Other bacteria have also been isolated from protozoa such as *Mycobacterium avium,* which was isolated from *Acanthamoeba castellanii*, a water born amoeba (Cirillo *et al.*, 1997). The existence of two phylogentically different endosymbionts in a single protozoan isolate had not been seen (Horn *et al.*, 2001) until recently when two distinct groups were identified in *Acanthamoeba sp*. Using 16srRNA a *Betaproteobacteria* and *Chlamydiae* were identified to be present within the amoeba separated in membrane bound intracellular compartments (Heinz *et al.*, 2007). In many cases we can only speculate as to the nature of such associations and as to which partner gains an advantage. Are these symbiotic or parasitic associations?

One of the best studied intracellular associated bacteria is *Legionella pneumophila*. *L. pneumophila* is the causative agent of Legionnaires Disease which is often the consequence of contaminated water in environments such as cooling towers for air conditioning, shower heads, whirlpool spas and decorative water fountains. The aerosolised water droplets are inhaled into the lungs, thought to be the primary site of infection, where the bacteria is ingested by alveolar macrophages (Horwitz & Silverstein, 1980). *L. pneumophila* has been shown to multiply and kill both human macrophages and free-living amoebae (Rowbotham, 1980, Horwitz & Silverstein, 1980). Further studies have shown that *L. pneumophila* uses the same genes to multiply within *Acanthamoeba* and macrophages (Segal & Shuman, 1999). These observations have led to suggestions that bacteria evolved to become intracellular pathogens after surviving phagocytosis and adapting to the intracellular environment of the protozoa (Molmeret *et al.*, 2005). *L. pneumophila* has also been shown to survive in *Acanthamoeba* cysts after decontaminating with chlorine (Kilvington & Price, 1990) which raises concerns with regards to eradication.

Numerous other pathogenic bacteria also show similarities between growth in a protozoan host and their intracellular growth in human macrophages. *Francisella tularensis* is the causative agent of tularaemia (Oyston, 2008). *F. tularensis* is an intracellular pathogen and can utilise a number of different cells, however, *in vivo* the primary target appears to be the macrophage (Fortier *et al.*, 1994). It can also replicate in protozoa (Abd *et al.*, 2003) which may act as a reservoir in aquatic environments. Growth in protozoa shares the same intracellular characteristics when compared to growth in macrophages (Titball *et al.*, 2003). These studies showed that *F. tularensis* was present in amoebae cysts, suggesting that utilising this environmental niche could hinder detection and disinfection in the natural environment.

The ability of *Burkholderia sps*. to reside within protozoa has resulted in difficulties disinfecting drinking water in Australia (Howard & Inglis, 2005). The minimum disinfection and contact time of 1mg/L chlorine for 30 minutes was only found to reduce a *B. pseudomallei* population by 2 $\log_{10}$ (Howard & Inglis, 2003) and further studies show that the level of monochloramine needs to be 100 times more concentrated when protozoa are present (Howard & Inglis, 2005).

Other species that have been shown to be able to persist in protozoa are largely human pathogens, for example *Yersinia pestis* (Sinclair *et al.*, 2008), *Salmonella typhimurium* (Gaze *et*

al., 2003), *Vibrio cholera* (Abd *et al.*, 2007) and *Helicobacter pylori* (Winiecka-Krusnell *et al.*, 2002).

As well as acting as a training ground for these pathogenic intracellular bacteria, the protozoan host can aid bacterial survival in the environment and help in dispersal, complicating the spread of disease from the human health perspective (Huws *et al.*, 2006, Fenner *et al.*, 2006). In particular, the ability of *E. coli* 0157 and MRSA to persist and grow in the common soil protozoa *A. polyphaga* highlights a substantial risk to infection control in hospitals and other healthcare establishments (Huws et al., 2006, Barker *et al.*, 1999). *Acanthamoebae* form cysts when faced with a nutrient deprived environment. These cysts are notoriously resistant to chlorine which can cause numerous difficulties when attempting to eradicate protozoa from water supplies (Khan, 2006). If this situation was to occur in a health care environment where chlorine was being used as a disinfectant, a variety of pathogenic bacteria would have an extra layer of protection provided from the protozoan host. Fresh flowers taken into hospitals may be seen as a nice gesture but the consequences of introducing a pathogenic bacterium within protozoa is reminiscent of the "Trojan Horse" (Barker & Brown, 1994).

1.4.3 *Bacillus* interactions

Bacteria which have been identified in association with protozoa are those which occur naturally in the environment. *Bacillus sp*. are prevalent in the environment and due to their ability to sporulate can survive for many years in adverse conditions (Turnbull, 2002a). *B. anthracis* has been studied in detail and yet a non-mammalian host has never been identified. Its seasonal cycle of outbreaks is thought to relate to the prevalence of rain and these specific environmental conditions influence the way in which the host comes into contact with the spores. It is thought that spontaneous multiplication in the environment would require very specific conditions and the event would be extremely rare (Turnbull, 2002a). Multiplication and persistence has only been observed once outside of a host, which was performed in laboratory conditions in sterilised soil. The results from this showed that *B. anthracis* could indeed grow in and around the rhizosphere of grass plants and had genetic exchange between bacteria (Saile & Koehler, 2006). However, in my opinion, these results do not represent the natural environment as there would be an abundant amoebae population in the soil as well as

numerous other environmental bacteria which would surely contribute to the growth characteristics of *B. anthracis*.

Many of the identified protozoan associated bacteria are, like *B. anthracis,* capable of growth in macrophages as well as their environmental host. Although there are no references to *B. anthracis* and protozoan relationships, relationships between protozoa and other *Bacillus* species have been observed and studied.

B. subtilis has shown that during predation by the protozoan *Tetrahymena thermophila* the wild-type dormant spores were neither killed nor digested. The spore was found to be resistant to the phagosomal enzymes which suggest a defence mechanism against predation (Klobutcher *et al.*, 2006). Bacteria within the *Bacillus* genus are very similar and this suggests that other *Bacillus* spores may also be resistant which would surely help to contribute to their environmental survival.

B. thuringiensis subsp. *israelensis*, is used worldwide as a biological control to lower numbers of black-flies and mosquitoes which act as vectors for a wide variety of human diseases. During the evaluation of environmental survival of these bacteria it has been discovered that they can survive in the excreted food vacuoles of the protozoa *Tetrahymena pyriformis* (Manasherob *et al.*, 1998). The spores were able to germinate in the excreted food vacuoles and interestingly germinated faster when grown in *Tetrahymena* lysate, probably due to the availability of free nutrients (Manasherob *et al.*, 1998). It would be surprising if this was the only species of *Bacillus* that could germinate in conjunction with a protozoan.

As mentioned previously, the many intracellular bacterial associates identified within protozoa are also equipped to grow in the mammalian macrophage for example, *L. pneumophila* and *F. tularensis*. *L. pneumophila* expresses the same genes to multiply within *A. castellanii* and human macrophages (Segal & Shuman, 1999). *B. anthracis* also utilises the mammalian macrophage as an important part of its infectious cycle and therefore we speculate that it may use a similar genes and strategies to survive encounters with protozoan.

Macrophages play an important role in the pathogenesis of *B. anthracis* contributing to the progression of the disease. The uptake of the spore by a professional phagocyte can provide a form of transport around the body to specific lymph tissue and also provides a favourable niche for germination and expression of toxins (Guidi-Rontani *et al.*, 1999). The production of lethal toxin and edema toxin result in lysis of the macrophage, releasing the germinated bacilli throughout the host (Guidi-Rontani, 2002). It has been shown that after inhalation of *B. anthracis* spores most are phagocytosed by alveolar macrophages. It has been suggested that this step is mediated by the interactions between the BclA protein expressed on the spore surface and the Mac - 1 protein expressed by professional phagocytes, such as alveolar macrophages (Oliva *et al.*, 2008).

L. pneumophila uses different strategies to invade amoeba and mammalian cells but then proceed to cause a very similar infection ending in the destruction of the host cell (Gao *et al.*, 1997, Solomon *et al.*, 2000). When *L. pnemophila* invades the protozoan host *Hartmanella vermiformis,* entry is mediated by a 170kDa Gal or GalN AC lectin receptor present on the surface of the protozoa (Harb *et al.*, 1998) whereas attachment in mammalian cells has shown to be mediated by complement and non – complement receptors (Rodgers & Gibson, 1993). However, mutants that were defective in the invasion of mammalian cells were also defective with regards to invasion of the protozoa (Gao *et al.*, 1997). In the same study, a different group of *L. pneumophila* mutants showed defects in attachment to macrophages but not to *A. polyphaga* which suggests that although some mechanisms are similar others are unique to certain protozoa. *L. pneumophila* has been shown to invade at least 13 different strains of amoeba and ciliated protozoa (Fields, 1996) and the mechanisms may vary between strains *(Gao et al., 1997).*

A single study examining the interaction between *B. cereus* vegetative cells and *A. polyphaga* has previously been published (Huws *et al.*, 2008). This study concluded that *A. polyphaga* predated on *B. cereus* cells and there was no evidence to suggest replication or survival within the amoeba. In contrast to this we have shown that all the members of the *B. cereus* group bacteria are in fact capable of a range of different behaviours against *A. polyphaga,* including intracellular persistence. In addition, no previous studies on the interactions of protozoa and *B. anthracis* have been published. We argue that this is in fact highly relevant given the known intracellular interactions with macrophages.

2 Materials and Methods

All work with *B. anthracis* was carried out in containment level 3. Work with *Bacillus* hazard group 2 organisms were carried out at containment level 2.

2.1 Bacterial strains and media

2.1.1 *Bacillus* strains used in these studies

Bacillus strains used in these studies (seeTable 2.1):

Strain	NCTC/ASC number or reference	Virulence	ACDP hazard group categorisation
Bacillus cereus	NCTC 14579 (Ivanova *et al.*, 2003)	Causes food poisoning in humans	2
Bacillus anthracis Sterne	ASC 1	Causes disease in immunocompromised humans	3
Bacillus anthracis Ames	ASC 68	Causes severe disease in humans	3
Bacillus thuringiensis Q5	(Berry *et al.*, 2002)	Insect pathogen	2
Bacillus thuringiensis Q7	(Berry et al., 2002)	Insect pathogen	2
Bacillus thuringiensis Q7 gfp	(Berry et al., 2002)	Insect pathogen	2

Table 2.1 *Bacillus* strains used in these studies

2.1.2 Culture of *Bacillus* strains

B. anthracis was cultured on horse blood agar (bioMerieux) or Tryptone Soya Agar (TSA) (bioMerieux) at 37˚C overnight. *B. anthracis* was also cultured in brain heart infusion (BHI) broth (CEPR, Porton Down Media department) at 37˚C overnight, shaking at 220rpm.

B. cereus was cultured on horse blood agar, L - Agar (bioMerieux), and L - Agar 10µg/ml Tetracycline at 37°C. *B. cereus* was also cultured in brain heart infusion (BHI) broth (CEPR, Porton Down Media department) at 37˚C overnight, shaking at 220rpm.

B. thuringiensis was cultured in LB broth, BHI broth (CEPR, Porton Down Media department) and on LB agar (bioMerieux).

15% glycerol bacterial stocks were prepared by adding 700µl of the culture to 300µl of 50% glycerol (Sigma). These were then stored at -80°C.

2.1.3 Spore Preparation

Cultures were grown in CCY media (Stewart *et al.*, 1981) for the production of spore stocks.

CCY salts are added from a 100x stock solution to the CCY broth prior to inoculation with an overnight culture of *Bacillus spp.*. 2-3ml of culture is added per 100ml of broth. The culture is incubated at 37°C (220rpm) for 2 - 5 days.

After 2 - 5 days the spores are harvested by centrifugation at 3000rpm for 15 minutes. These are then washed in sterile ice-cold water three times before re-suspending in sterile water. Sporulation efficiency is determined by performing a viable cell count and following a heat shock step a spore cell count. The heat shock step consists of incubating the spore culture for 30 minutes at 65-70°C. The neat spore stock is stored at 4°C.

2.1.4 Sterility testing of products for further processing

All samples from Containment Level 3 laboratory had to be sterility tested before the sample could be transferred to a Containment Level 2 laboratory for further analysis.

A 10 µl loop of sample (DNA, RNA or culture supernatant) was spread on a blood agar plate and placed into BHI broth. This was then incubated for 7 days at 37°C. After the 7 day incubation the plates and broth were checked for any signs of growth. If no growth was present the sample was deemed sterile and could be further processed at CL2.

2.1.5 Media

2.1.5.1 Complex Media

Brain Heart infusion broth

Brain heart infusion (BHI) broth was used for culturing *Bacillus* sp. and as the high nutrient broth in the growth curve analysis.

Miller's LB broth

Miller's LB broth (sigma) was prepared according to the manufacturer's instructions. Media were solidified with 1.2 % agar (Oxoid, UK) where necessary. The medium was sterilised by autoclaving at 121°C for 30 min.

Peptone Yeast Glucose medium (Amoeba medium)

PYG medium was made according to the following recipe:

Proteose peptone (Oxoid L85) – 15g

D-glucose – 18g

Yeast extract – 2.5g

Page's Amoeba Saline (PAS) solution (Page, 1988)

Stocks per 500ml of water

PAS 1: NaCl – 12.0g

MgSO4.7H2O – 0.40g

CaCl2.6H2O – 0.60g

PAS 2: Na2HPO4 – 14.20g

KH2PO4 - 13.60g

5ml of stock PAS 1 and 2 are added to the PYG ingredients then made up to 1 litre with water and autoclaved at 110ºC.

Basal Medium – without charcoal

Basal medium was prepared by HPA Media Supplies, Porton Down. Recipe as follows:

5.956 g l^{-1} casamino acids

0.518 g l^{-1} KOH

52 mg l^{-1} DL-serine

25 mg l^{-1} $MgSO_4.7H_2O$

24.5 mg l^{-1} $CaCl_2.6H_2O$

20 mg l^{-1} L-cystine

0.167 mg l^{-1} thiamine hydrochloride

This was sterilised by autoclaving at 121˚C for 15 minutes.

2.1.5.2 Chemically defined media

Three chemically defined media types were also used in the growth curve analysis. The media varied the defined phosphate levels previously optimised from research performed by Zoe Betteridge (PhD Thesis).

Table 2.2 Recipe for CDM20 (Potassium phosphate concentrations of 3.2, 0.4 and 0 mM phosphate)

Component	Concentration
3-[N-Morpholino]-2-hydroxy-propanesulfonic acid (MOPSO) (pH 6.9 with 5 M NaOH)	50 mM
Magnesium sulphate	101 mM
Calcium chloride 6-hydrate (BDH, UK)	114 μM
Potassium phosphate	3.2 or 0.4 or 0 mM
Ammonium sulphate	40 mM
Manganese (II) sulphate 4-hydrate (BDH, UK)	4.48 μM
Thiamine	2.96 μM
D+ Glucose	41.7 mM
L-alanine	1 mM
L-arginine (hydrochloride)	1 mM
L-aspartic acid	1 mM
L-asparagine (anhydrous)	1 mM
L-cysteine (free base)	1 mM
L-glutamic acid	1 mM
L-glutamine	1 mM
L-glycine (amino-acetic acid)	1 mM
L-histidine (hydrochloride, monohydrate, L-α-amino-β-[4-imidazolyl] propionic acid,)	1 mM
L-isoleucine	1 mM
L-leucine (L-2-amino-4-methylpentanoic acid)	1 mM
L-lysine (L-2,6, diaminohexanoic acid, monohydrochloride)	1 mM
L-methionine	1 mM
L-phenylalanine (L-2-amino-3-phenylpropanoic acid)	1 mM
L-proline	1 mM
L-serine	1 mM
L-threonine (L-α-amino- β-hydroxybutyric acid)	1 mM

L-tryptophan	1 mM
L-tyrosine	1 mM
L-valine (L-2-amino-3-methylbutanoic acid)	1 mM

2.1.6 Antibiotics

All antibiotics were ordered from Sigma and were used at the following concentrations: Kanamycin, 50μg/ml; Ampicillin, 100μg/ml; Tetracycline, 10μg/ml; Spectinomycin, 100μg/ml.

2.2 Molecular methods

2.2.1 *Bacillus anthracis* DNA boilates

50μl of BHI broth was added to 2 PCR tubes (0.2ml) for each strain of *B. anthracis.*

A colony pick was taken and emulsified in the relevant PCR tubes. These were then heat shocked for 1min at 37°C (to germinate any existing spores) and 95°C for 10mins (to inactivate the bacteria). A sterility test was then performed in order to use them outside of containment level 3 (CL3)

2.2.2 Phenol / chloroform DNA extraction

Crude DNA boilates were cleaned up by adding 200μl of PCR grade water to 7μl of the crude boilate. 200μl of phenol was then added and the tube was vortexed for 1 min.

This was then centrifuged for 5 minutes at 13,000rpm (18,000 x *g*) at room temperature.

The top layer was removed and put into another tube. 200μl of phenol:chloro:isoamyl alcohol (ratio of 25:24:1) was added to the new tube and vortexed for 1 min. This was then centrifuged as before and the upper layer transferred to a new tube. 900μl of 100% Ethanol and 10μl of 3M NaOH was added to precipitate the DNA. This was vortexed briefly and

centrifuged for 30mins at 13,000g at 4˚C. The liquid was carefully removed, leaving precipitated DNA in the tube. 200µl of 70% ethanol was added to the tube. After centrifugation for 15min (13,000 x *g*, 4˚C) the sample was dried in the speed VAC for 10 minutes.

The DNA was re-suspended in 5µl of PCR grade water which was then further diluted for use in PCR.

2.2.3 Bacterial DNA extraction

DNA extraction from bacterial cultures was performed using the QIAgen DNeasy Blood and Tissue kit. The manufacturer's instructions were followed. DNA was eluted in PCR grade water.

2.2.4 DNA / RNA quantification

DNA and RNA were quantified using a Nanodrop NB - 1000 spectrophotometer (Thermo Scientific). 1µl of sample is used to determine the DNA or RNA concentration as well as 260 nm and 280 nm absorbance readings.

2.2.5 RNA extraction using Trizol

Guanidinium thiocynate (GTC) 5M lysis solution was prepared in an empty 1 litre PCR water bottle to ensure the solution is RNase free. 591g Guanidinium thiocynate GTC (5M), 5g N lauryl sarcosine (0.5%), 7.3g trisodium citrate (25mM), 5ml tween 80 (0.5%) are added and made up to 1 litre with RNase free water. The mixture is incubated at 37°C to dissolve the components and stored in the dark at room temperature. 2-mercaptoethanol is added to the GTC solution immediately prior to use (560µl for every 80ml). All components used to prepare the GTC solution were acquired from Sigma.

GTC solution was used with bacterial cells at a 4:1 ratio.

The appropriate amount of *Bacillus* was extracted and added directly to the required amount of GTC lysis solution. This was then incubated at room temperature for 1 hour before RNA

extraction. Bacterial cells were then pelleted and re-suspended in Trizol (Invitrogen). Samples were either stored at -20°C as the RNA remains stable in the Trizol solution for up to 7 days or processed directly.

Samples were then placed into lysing matrix B (Q-Biogene, UK) ribolyser tubes and ribolysed for 45 seconds at speed 6.5^{-1} using a Hybrid Ribolyser (Hybrid, UK). The pink supernatant was aspirated off and added to a tube of 240µl chloroform. This was then shaken vigorously for 20 seconds and centrifuged in a microfuge at 13,000 rpm for 10 minutes. The aqueous phase was then removed and placed in 600µl of chloroform and the spin was repeated. This wash step was repeated 3 times and each time the aqueous phase removed. After the last wash the aqueous phase was added to isopropanol, sterility tested and frozen at -20°C.

2.2.6 Analysis of sequence data and designing of the oligonucleotide primers

Sequence data was obtained from the NCBI online database.

B. anthracis Sterne AE017225 and *B. anthracis* Ames NC003997 were used in the sequence analysis.

The three genes polphosphate kinase (*ppk*), exopolyphosphatase (*ppx*) and poly-AMP-phosphotranferase (*pap*), were identified in *B. anthracis* by using the BLAST (blastn) search database (Altschul, Madden et al. 1997).

Endogenous control primer and probes were identified from a previous gene expression study on *B. anthracis* (Drysdale et al., 2004).

Sequence analysis was performed using DNA star – Lasergene V6 software. Alignments of the three target genes (*ppk, ppx* and *pap*) were done using MegALine. Analysis of restriction sites were done using SeqBuilder and sequencing results were constructed using SeqMan.

Oligonucleotide primers were designed manually and checked for primer dimers, GC content and TM using Primer Express software and Sigma Genosys online ordering website.

Oligonucleotide primers and fluorescently labelled probes were purchased from Sigma Genosys and MWG and supplied in a lyophilised form which was then re-hydrated in sterile DNA/RNA free water (Sigma) and stored at 100mM at -20ºC.

Primers used in the final cloning experiments can be seen in Table 2.3.

Primer	Sequence 5' to 3'	Modification
*ppk*1	cgatggatccgaatccgtctactgg	*Bam*H1
*ppk*2	atcggtcgactgatagtcaagtgaag	*Sal* 1
*ppk*3	atcggtcgacgtaataagctgtatc	*Sal* 1
*ppk*4	atcgagatctattgtcgttcatag	*Bgl* II
*ppx*1	cgatggatccgatactttatatcctg	*Bam*H1
*ppx*2	cgatgtcgacgacaaagatcgcttg	*Sal*1
*ppx*3	cgatgtcgaccgcattgtattagatcc	*Sal*1
*ppx*4	cgatagatcttgtatgacagctataat	*Bgl* II
*pap*1	cgatggatccgcaatgatctgggcagcag	*Bam*H1
*pap*2	cgatgtcgactactttagcaagaactcc	*Sal*1
*pap*3	cgatgtcgaccataatatagaattaccttcg	*Sal*1
*pap*4	cgatagatctctggacgaagcataac	*Bgl* II

Table 2.3 Primers used in the final cloning method. Red text denotes the restriction enzyme modification site.

Real Time Primers and probe sequences can be seen in Table 2.4.

Real time Primers and Probes	Sequence (5' – 3')	Fluorescence label
gyrB fwd	ACTTGAAGGACTAGAAGCAG	
gyrB Rvs	TCCTTTTCCACTTGTAGATC	
gyrB Probe	CGAAAACGCCCTGGTATGTATA	5' FAM BHQ1
16s rRNA fwd	TTCGGGAGCAGAGTG	
16s rRNA rvs	AACATCTCACGACACGAG	
16s rRNA Probe	CAGGTGGTGCATGGTTGTC	5' FAM BHQ1
ppk fwd	CCCAACAACACTAACTACCCGAAT	
ppk Rvs	AACTCATCGTTCGAGGAACATGT	
ppk Probe	TTTTCACTTACATTTGGAATACCAGGTCGTAGGC	5' FAM BHQ1
ppx Fwd	ACAAATGCTGGCGCCTCTA	
ppx Rvs	GGCAAAAGATCGAGCAGATACA	
ppx Probe	AAGCGTATGAAATACTTCGACTGCTGGAACAA	5' FAM BHQ1
pap Fwd	GAAGCTACCTCAGTATGGGCAAA	
pap Rvs	CCTTCAACACGCTCCACTAACA	
pap Probe	TACTATTTTTGATCGCTCATGGTACGGCCG	5' FAM BHQ1

Table 2.4 Real Time PCR primers and probes used in this study. All probes were labelled with a FAM fluorescent dye and Black Hole Quencher 1 (BHQ1).

2.2.7 Polymerase chain reaction (PCR)

All PCR's were performed in either 50µl or 25µl reactions.

Each reaction contained a forward and reverse oligonucleotide primer, $MgCl_2$, dNTP's, manufacturer specific PCR buffer and DNA template (≤ 1µg per reaction).

Throughout the study, different polymerase kits were used to optimise the PCR reaction. Four main kits were used in the process; QIAgen Core Kit (QIAgen), Pfu polymerase (NEB), HiFi KOD Polymerase (Novagen) and GoTaq Flexi (Promega).

Thermocycling conditions were based around the following standard cycle of a denaturing step at 95°C for 5minutes followed by 25-30 cycles of a denature at 95°C for 30 seconds, an annealing step at 55°C for 30 seconds and an extension step at 72°C for 30 seconds, with a final extension step at 72°C for 10 minutes. For the Taq Polymerase, 1 minute per Kb of

amplicon product was allowed for the cycled extension step. For Pfu Polymerase, 2 minutes per Kb of amplicon product was allowed for the cycled extension step due to its proof reading capabilities. Each PCR cycle was optimised according to specific requirements. For example, the annealing step temperatures were varied using a gradient thermocyler allowing for simultaneous testing of a range of temperatures.

PCR results were analysed by using 9µl of each PCR product mixed with 2µl of running buffer (sigma) and depending on the expected size of the amplicon, run on a 1% or 2% agarose gel containing 0.5µg/ml ethidium bromide (Sigma). The gels were then run at 110 Volts for 40 min using TBE in the gel tank as a running buffer. Gels were then viewed and photographed on a Gene Genius (Syngene, UK).

2.2.8 Overlapping PCR

Initial PCR conditions were kept the same but used a proofreading enzyme instead of Taq polymerase. Taq polymerase adds an A tail onto the end of the PCR product which would interfere with the second round PCR as the end would not be homologous.

A cooling step prior to the second PCR was added to try and anneal the fragments. The mix consisted of 4-7µl of each fragment, 10µl 10x buffer, 2 µl dNTPs, 1µl Taq, and PCR grade water to make the reaction up to 50µl.

A cooling cycle was used which started at 99.9°C for 10 minutes and then cooled at 0.1°C per second until 20°C was reached. There was then an extension step at 72°C for 10 minutes. Reaction mixtures were then run on a 1% agarose gel and extracted at around 2.1kb or PCR purified and used in a second round of PCR.

2.2.9 PCR purification

PCR purification was performed using the QIAgen PCR Purification kit according to the manufacturer's instructions. DNA was eluted in PCR grade water.

2.2.10 Gel extraction

Extraction of DNA from agarose gels was performed using the QIAgen Gel extraction kit according to the manufacturer's instructions. DNA was eluted in PCR grade water.

2.2.11 TA Topo Cloning

TA Topo cloning kits were purchased from Invitrogen and used according to the manufacturer's instructions.

2.2.12 Plasmids

pMAD (Arnaud *et al.*, 2004) and pIC156 (Spc*R* cassette) (Steinmetz & Richter, 1994) were supplied by Anne Moir, University of Sheffield. Both plasmids were lyophilised and were re - constituted in 10µl of PCR grade water.

pAT113 (Trieu-Cuot *et al.*, 1991) was supplied by Patrick Trieu- Cuot, Institute Pasteur, Paris.

pKD4 : Donor for Kanamycin cassette (Datsenko & Wanner, 2000) was supplied by David Clarke, University of Bath.

pAEX - 4 was used as a positive control plasmid thoughout the electroporation experiment (CEPR, Health Protection Agency, Vaccine Research Group).

2.2.13 Plasmid DNA purification

Plasmid DNA purification was performed using the QIAgen Miniprep Spin Kit according to the manufacturer's instructions. DNA was eluted in PCR grade water.

2.2.14 Restriction Digest

Varied amounts of DNA were digested in either 50µl or 20µl reactions.

Each reaction contained the restriction enzymes from Promega and the matching buffer provided. BSA at a final concentration of 0.1µg/µl was added to each reaction and PCR grade water was added to make up the reaction to the required volume.

Each reaction was incubated at the specified temperature for the recommended time. The digests were then either run on an agarose gel to visualise the results or directly cleaned using a QIAgen PCR purification kit (according to the manufacturer's instructions).

2.2.15 Sequencing

20µl sequencing reactions consisted of 8µl BigDye v3.1 (ABI), 3.2µl Forward/ Reverse Primer (1/3 dilution of the working stock), 3.8µl PCR grade water and 5µl DNA sample. The thermocycler program consisted of a 25 round cycle of a 96°C step for 10 seconds, 50°C for 5 seconds then a 60°C step for 4 minutes. Dye terminator removal was achieved using the QIAgen DyeEx 2.0 spin kit according to the manufacturer's instructions. The dried sample was re-suspended in 12µl of HiDi Formamide (Applied Biosystems) This was then denatured at 80°C for 3 minutes and transferred immediately to ice. 12µl of each sample was loaded into a 96 well plate, centrifuged and placed in the ABI 3100 sequencer. Sequencing results were aligned and analysed using Lasergene v7 SeqMan software.

2.2.16 Optimisation of Real Time PCR Primers and Probes

Forward and reverse Taqman primers were prepared at 1 µM, 6 µM and 18 µM concentrations in sterile water. DNA control extracted from overnight *B. anthracis* cultures grown in BHI was diluted in sterile water as a template for the PCR reaction.

Reactions were prepared in triplicate. Each reaction contained 0.25 µl of 25 µM probe; 1.25 µl of forward primer (at concentrations of 1 µM, 6 µM or 18 µM); 1.25 µl reverse primer (at concentrations of 1 µM, 6 µM or 18 µM); 2.5 µl of 10^{-3} diluted DNA template (or 2.5 µl PCR grade water for negative controls); 12.5 µl of 2x Universal Mastermix (Applied Biosystems) and 7.25 µl PCR grade water. The total reaction volume (25µl) was added to a 96 well optical plate (Applied Biosystems). The plate was then sealed with an optical adhesive cover (Applied Biosystems) and briefly centrifuged at 500g for 30 seconds to ensure all liquid was at the bottom of the wells. The plate was then placed in a 7900HT real time PCR system (Applied Biosystems) and an absolute quantitation assay was completed with the following conditions; 48°C for 30 min then 95°C for 10 min, followed by 45 cycles of 95°C for 15 sec and 60°C for 1 min.

Average CT values were then plotted for each combination of forward and reverse primer concentration. The primer combination with the lowest average CT value and error (18µM forward primer and 18µM reverse primer) was then selected for use in further assays.

2.2.17 Real Time RT PCR gene expression assay

Real Time RT PCR was performed on the TaqMan 7900HT using the optimised primer concentrations.

The optimisation of the Real Time Gene expression assay used a number of different reagents (manufacturer's instructions were followed):

Reverse Transcriptase kits:

Quantitect RT - PCR Kit (Qiagen)

High capacity cDNA Reverse Transcriptase Kit (Applied Biosystems)

One Step RT – PCR Master Mix (Applied Biosystems)

Real Time PCR Mastermix:

Universal Mastermix 2x (Applied Biosystems)

Gene Expression Mastermix (Applied Biosystems)

After concluding the primer efficiencies of the target gene and endogenous controls were not efficient when compared to each other it was decided to run the gene expression assay as the standard curve method instead of the Delta Ct comparison method (See page 92). The standard curve of DNA consisted of 100ng, 10ng, 1ng, 0.1ng and 0.01ng. After RNA extraction from each time point sample was performed, the total RNA was established using the nanodrop. RNA was added to each reaction for total of 5ng RNA per well.

The RT reactions were set up using the Quantitect RT – PCR Kit using the genomic wipeout step to begin with. The genomic wipeout step was set up with 2µl Genomic wipeout buffer, 100 ng RNA (variable amount), PCR grade water (variable) and made up to a total of 14µl with PCR grade water. This was incubated at 42°C for 2 minutes then put straight onto ice.

The RT step was set up with 1µl Quantitect Reverse Transcriptase, 4µl RT buffer, 1µl RT Primer mix and the all of the 14µl from the previous genomic wipeout step. An RT negative control for each sample was also run. In this reaction the Quantitect RT enzyme was replaced with PCR grade water. The total 20µl reaction was incubated at 42°C for 15 minutes then incubated at 95°C for 3 minutes. The resulting cDNA was either stored at -20°C or used directly in the Real Time PCR reaction.

The Real Time PCR assay was set up on 384 well optical PCR plates (Applied Biosystems). All samples and standard curve samples were run in triplicate. 1µl from the RT reaction was used as this contained 5 ng of cDNA.

Each Real Time PCR reaction contained 5µl Universal Mastermix (Applied Biosystems), 1µl of forward and reverse primer, 0.1µl of Probe and 2.9µl PCR grade water. After these reagents were added in each of the wells the 1µl cDNA template was added. The plate was then manually sealed with an optical adhesive cover (Applied Biosystems) and briefly centrifuged at 500g for 30 seconds to ensure all liquid was at the bottom of the wells. The plate was then placed in a 7900HT Real Time PCR system (Applied Biosystems) and a Taqman assay was

completed with the following conditions; 48°C for 30 min then 95°C for 10 min, followed by 45 cycles of 95°C for 15 sec and 60°C for 1 min.

2.3 Growth curve study methods

2.3.1 Growth Curves

Medium was pre-warmed to 37°C before inoculating with 0.1% of glycerol stock of *Bacillus* culture at 2 x 10^6 cfu per ml. Culture was incubated at 37°C at 220rpm. Optical density (OD) measurements were taken with a spectrophotometer at 600nm throughout the growth curve to establish the optimal sampling times. Samples were taken as the culture OD started to increase in order to acquire samples from all stages of the growth curve. Samples were then processed with the RNA extraction method. The time point samples were also subjected to cell counts to establish cell numbers when compared to the OD reading.

B. anthracis growth curves were performed in a flexible film isolator containing an incubator to enable a quick and more accurate sampling of the culture whilst maintaining containment.

In some cases growth curves had to be assembled from two experiments due to time limitations caused by a slower growth rate.

2.3.2 Protein Gels

Protein gels were performed using NuPage SDS gels (Invitrogen) according to the manufacturer's instructions.

Samples are diluted 1 in 4 with the sample running buffer (Invitrogen) and heated at 70°C for 10mins.

5µl of Mark12 markers (Invitrogen) were used for protein gels and 3µl of SeeBlue (Invitrogen) was used when a gel would be Western blotted.

Protein gels were stained using Simply Blue Safe Stain (Invitrogen). The gel was washed three times for 5 minutes in demineralised water. Simply Blue Safe Stain was then added over the top of the gel and stained for 1 hour with continuous swirling. After 1 hour the gel was washed with numerous changes of demineralised water to produce a clear gel image.

Images were visualised and recorded on an Imagemaster VDS – CL scanner (GE Healthcare).

2.3.3 Western Blots

Protein gels were performed as in step 2.3.2 and transferred to nitrocellulose membranes using the Xcell blot module according to the manufacturer's instructions (Invitrogen).

10 x Stock Transfer Buffer:

144.01g Tris (Sigma)

29.96g Glycine (Sigma)

Made up to 2litre with distilled water

1x Transfer Buffer:

200ml 10x Stock Transfer Buffer

1800ml distilled water

After running the blot the membranes were blocked in a solution of PBST (phosphate buffered saline (PBS) 0.1% (v / v) Tween 20) with 2% (w / v) bovine serum albumin (BSA) (sigma) for 1 hour or overnight at 4ºC.

The blot was then incubated with PBST and 2% BSA with the appropriate antibody for 1 hour at room temperature with gentle agitation. Rabbit polyclonal hyperimmune antisera (αPA Rab 446B at 1/4000 or αLF Rab 727B at 1/4000) were used in these experiments. These were produced at CEPR, HPA, Porton Down (Charlton *et al.*, 2007). Blots were then washed 3 times for 5 minutes each in PBST.

Secondary antibody enzyme conjugate (anti - rabbit horse radish peroxidise conjugate (Sigma) was then added to the blot, diluted 1/4000 in PBST and 2% BSA;. This was left for 1 hour.

Blots were then washed 3 times (5 minutes each) in PBST.

An Enhanced ChemiLuminescent substrate system was used to visualise the blots (GE Healthcare details) according to the manufacturer's instructions. Blots were developed and scanned using the Imagemaster VDS – CL scanner (details as above).

2.4 Amoeba interaction study methods

2.4.1 Amoeba and their growth conditions

Acanthamoeba polyphaga was obtained from Dr. T. J. Rowbotham (Public health Laboratories, Leeds, UK) and grown in proteose peptone –yeast-glucose (PYG) medium as monolayers in 76cm^2 tissue culture flasks at 23°C. Amoebae were sub-cultured weekly by gently tapping the flasks and washing the monolayer to detach cells before diluting 1:10 in fresh medium. Stationary phase (3-5 days) cultures were used throughout this study. Amoebae were harvested by replacing the excess medium with fresh media and gently washing the monolayer to detach the cells.

2.5 Co-culture assays

Co-culture assays were performed in a 25 well culture plate (Nunc) or in single 25ml cell culture flasks (Corning) for *Bacillus anthracis* in containment level 3. Co-culture assays were performed with specified ratios of amoeba to spore or amoeba to vegetative cell. Ratios were 100:1, 10:1, 1:1, 1:10, and 1:100. Each assay was performed in 100% PBS, 100% PYG or 10% PYG to study the effect of nutrient availability on the interactions. Number of amoeba per well was adjusted to approximately 2 x 10^5 cells/ml using a haemocytometer. The amoebae were allowed to settle for 10 minutes prior to the addition of the bacteria. Results were analysed using a Nikon TES2000 inverted microscope at a magnification of x20 and x40. Images, videos and time lapse data were taken using a Nikon camera and NIS-Elements software.

2.6 Gentamycin assay

The gentamycin assay was used to obtain numbers of viable bacterial cells inside the amoeba. The gentamycin wash was used to kill the external bacteria leaving the internal bacteria protected inside the amoeba.

The co-culture assay was set up as required. At the required time point gentamycin sulphate was added to the well at a final concentration of 100μg/ml or 200μg/ml. After a 2 hour incubation at room temperature the amoeba were gently dislodged from the surface of the well and placed into microtubes where they were subjected to 3 washes in PBS in a microfuge at 5000rpm. Sterile cold water was added after the final wash and vigorous pipetting ensured the lysing of the amoeba. This lysed solution was serial diluted and plated out on LB agar to establish the bacterial count of internal bacteria. A sample without the gentamycin wash was used to compare the accuracy of the assay by obtaining numbers of both external and internal bacteria.

2.7 Scanning Electron Microscopy

The co-culture assay was set up as previously described but with a Thermanox coverslip (Nunc) on the base of the well. This acted as a surface for the amoeba to adhere to and allowed for more efficient processing of the sample. At the required point the media was aspirated and replaced with the fixative solution of 2.5% glutaraldehyde and 1% Potassium Ferrocyanide, post-fixed in aqueous 1% Osmium Tetroxide and stained in 2% aqueous Uranyl Acetate in the dark. The sample was then dehydrated through an acetone series and dried. Samples were then coated with gold and analysed under a JEOL JSM6480LV Scanning Electron Microscope (JEOL Tokyo, Japan).

2.8 Transmission Electron Microscopy

The co-culture assay was set up as previously described. At the critical time point the media was aspirated and replaced with 2.5% glutaraldehyde and PBS fixative solution and post fixed

in aqueous 1% osmium tetroxide + 1% potassium ferrocyanide. Samples were then encapsulated in 3% agarose and stained with 2% aqueous Uranyl Acetate in the dark. The sample was then dehydrated through an acetone series and infiltrated and embedded in Spurrs epoxy resisn (TAAB, premix). Ultra thin sections were cut using an ultra-microtome (Leica, Reichert Ultracut E). Sections were then analysed under a JEOL JEM1200 Transmission Electron Microscope (JEOL Tokyo, Japan).

3 Sequence Analysis and Knockout Mutants

Studies on *B. cereus* have shown the importance of inorganic polyphosphate on motility and sporulation efficiencies among other characteristics previously mentioned. The *B. cereus* polyphosphate kinase (Ppk), exopolyphosphatase (Ppx) and poly-AMP phosphotransferase (Pap) mutants were constructed by Kornberg's group at Stanford University, California (Shi *et al.*, 2004). The *B. cereus* mutants were created using a simple procedure which incorporated the generation of the 5' and 3' flanking regions of the target gene by PCR. The tetracycline resistance gene was also amplified by PCR with 5' and 3' tails consisting of sections complimentary to the flanking regions of the target gene. These products were mixed as a template for a second round of PCR which used primers designed to amplify the whole product. See Figure 3.1 for a simple visual representation.

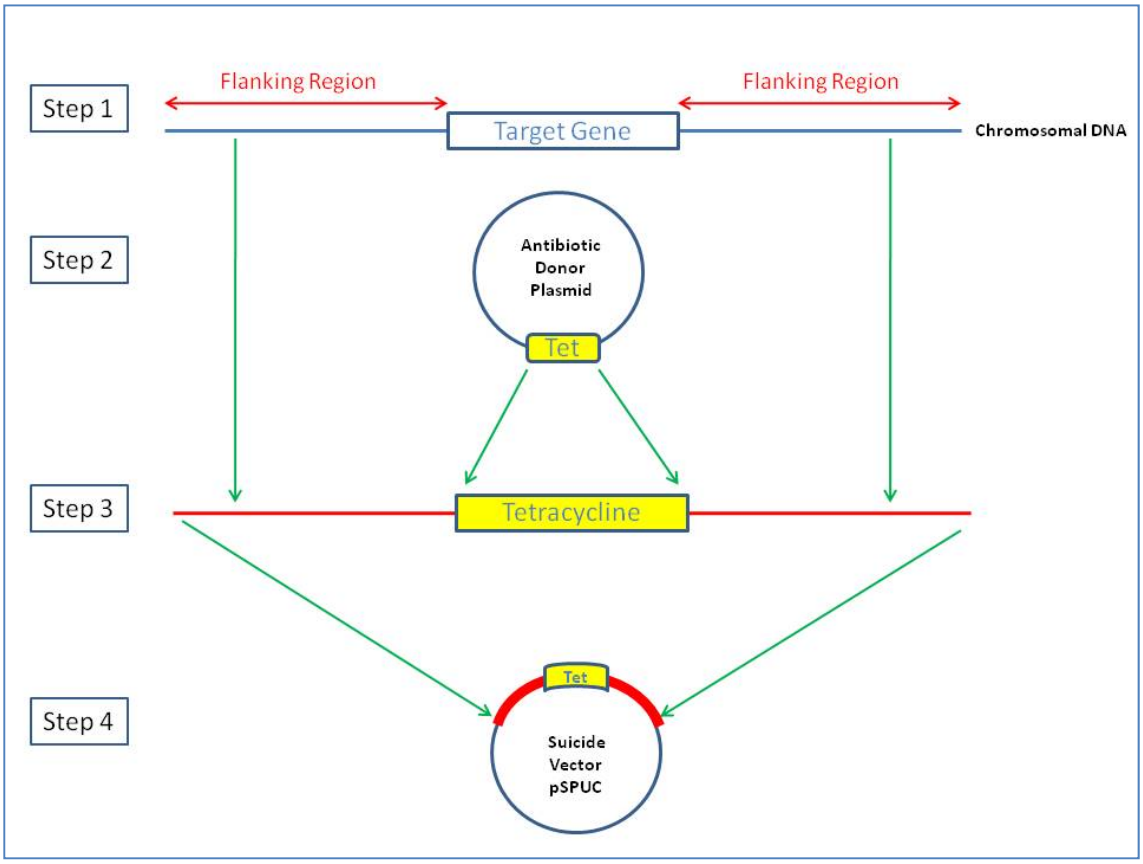

Figure 3.1 Construction of the *B. cereus* knockout plasmids. Step 1: Amplification of the flanking regions of the target gene (*ppk*, *ppx* or *pap*). Step 2: Amplification of the antibiotic resistance gene from a donor plasmid. Step 3: Combining all three products using PCR by mixing them together as the DNA template. Step 4: Digestion of the whole product and ligation into the *B. cereus* suicide vector.

After producing the whole product, it was digested with *Bam*HI and *Hind*III and ligated into pSPUC a *B. cereus* suicide vector precut with the same restriction enzymes. The pSPUC vector also carried a spectinomycin resistance gene allowing for selection of double cross-over mutants.

The final plasmids were transformed into *B. cereus* by electroporation and single cross- over mutants (containing the whole plasmid) were selected on tetracycline/ spectinomycin agar. These transformants were grown on tetracycline LB agar for 4-6 days with regular sub-culturing to encourage excision and loss of the plasmid. Double cross-over mutants (containing just the flanking regions with the tetracycline gene in between) were selected as tetracycline resistant and spectinomycin sensitive. PCR and DNA analysis was used to verify the correct insertion of the mutations.

B. anthracis and *B. cereus* share a very high homology in their chromosomal DNA and by creating similar knockout mutants in *B. anthracis* the significance of inorganic poly P can be studied with regards to this important human and animal pathogen.

We investigated various methods for creating the knockout mutants as well as trying to resuscitate the *B. cereus* mutants created by Kornberg *et al.* By resuscitating the *B. cereus* null mutants we could have continued studies with them and used them as a comparison for the *B. anthracis* null mutants.

The specific aims of the experiments represented in this chapter were:

1. Resuscitation of the *B. cereus* mutants
2. Sequences analysis of *ppk, ppx* and *pap* in *B. cereus* and *B. anthracis*
3. Construction of a knockout cassette for *B. anthracis*
4. Analysis of the knockout cassette
5. Electroporation of the knockout cassette into e-competent *B. anthracis*
6. Analysis of the *ppx* mutation in the Kruger B isolates from the Kruger National Park

3.1 *Bacillus cereus* mutants

3.1.1 Culturing of the *B. cereus* mutants

The *B. cereus* mutants were attained from Stanford (Shi, et al. 2004). The strains were difficult to culture. Numerous culturing techniques were tried such as using high nutrient agar, horse blood agar, and high nutrient broth; brain heart infusion broth but failed to grow the mutants. Limited nutrient agar and broth was also tried but without success. After many attempts at culturing, only the *ppk* mutant and the WT *B. cereus* strains grew. Glycerol stocks were made and stored at -80°C. The *ppk* mutant however could not be subsequently sub-cultured from either stored plates or from the glycerol stocks. The reason for this is unclear but is likely to indicate the importance of these genes in stress survival.

3.2 Sequence Analysis

Gene sequence data of polyphosphate kinase (*ppk*), exopolyphosphatase (*ppx*), and poly - AMP - phosphotransferase (*pap*) were highly analogous when comparing *Bacillus cereus* and the two *Bacillus anthracis* strains Sterne and Ames. Alignments were constructed from the genes with a 1kb flanking region both upstream and downstream of the gene (data not shown).

B. anthracis Sterne and Ames had 100% homology when comparing the *ppk*, *ppx* and *pap* regions; this was not unexpected as there are minimal differences between the chromosomal sequence of these strains .

B. anthracis Sterne and Ames have 90.1% identity to *B. cereus* in the *ppk* region.

B. anthracis Sterne and Ames have 91.3% identity to *B. cereus* in the *ppx* region.

The *pap* region shows the most variation although *B. anthracis* Sterne and Ames still have 58.6% identity to *B. cereus*.

One of the most notable points from the analysis is the *B. cereus pap* gene is larger than its *anthracis* relative; the *B. cereus pap* gene is 804bp and the *B. anthracis pap* gene is 765bp.

3.3 Construction of the knockout cassette

3.3.1 Method 1

Primers were designed to span the flanking regions of each of the three target genes. The primer positions can be seen in Figure 3.2.

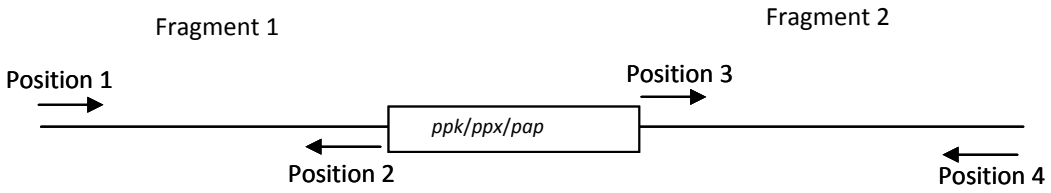

Figure 3.2 Location of the primer sets for method 1. Primers 1 and 2 were used to amplify fragment 1 and primers 3 and 4 were used to amplify fragment 2.

These regions were amplified using PCR and cloned in the Topo 2.1 cloning vector. Due to the restriction sites added into the primers these fragments could be cut out and used for further cloning.

To confirm the insertion and orientation of the fragment, the cloning region of the Topo 2.1 plasmid was sequenced. All flanking regions from all three of the genes were cloned successfully.

The Topo plasmid was then cut using *Sal* 1 and *Eco*RV in preparation to clone fragment 2 into Topo next to fragment 1. Fragment 2 was cut with the corresponding restriction sites and cloned into the plasmid.

The tetracycline gene from plasmid pBR322 was also amplified using primers Tet 1 and Tet 2. Both primers had *Sal* 1 sites integrated in order for them to fit between the two flanking regions when cloned together.

After cutting the Topo plasmid with *Sal* 1 the Tet resistance gene was ligated in, transformed into *E. coli* and plated out on L agar with 10μg/ml Tetracycline. However no *E. coli* clones were recovered. It is possible that this strategy failed due to plasmid re-circularization preventing insertion of the tetracycline gene. The method was repeated with a dephosphorylation step before the ligation of the Tet fragment into the plasmid. Different ratios of plasmid and fragment DNA were also used in the reaction in case the concentrations were effecting the reaction. There were still no colonies after the transformation stage. The same strategy was attempted using Nova blue cells instead of Top 10 cells, however the cloning was still unsuccessful. A spectinomycin resistance gene was amplified from pIC56 with the addition of *Sal* 1 sites on either end. The same methods were used in the cloning steps and transformations were plated on L - agar with 100μg/ml spectinomycin but each condition used again gave no clones.

As an alternative to the Topo-based suicide vector dependant recombination approach we decided to try and use a temperature sensitive plasmid approach for homologous recombination into the chromosome. The pMAD plasmid (a pE194::pBR322 derivative) was chosen to use as the vector instead of Topo as it has previously been shown to work well with *B. cereus* (Arnaud et al., 2004). Also, being a temperature sensitive plasmid the final electroporation into *B. anthracis* would require only a single transformant to proceed.

A more detailed analysis of the primer locations for the tetracycline gene indicated that it had been amplified from pBR322 without its native promotor. Therefore when cloned between the two flanking fragments in pMAD, it would not have been expressed and therefore the *E. coli* containing the plasmid would not have grown on the tetracycline medium.

3.3.2 Method 2 – overlapping PCR construction approach

Primers were designed around the same sequence positions as in method 1. It was decided to concentrate on the *ppk* gene. Primers in positions 2 and 3 contained an approximate 16bp overlap homologous to the Tet primers. When used in a second round of PCR the homologous

regions should bind and the whole 2.1kb construct should be amplified as one fragment. See Figure 3.3.

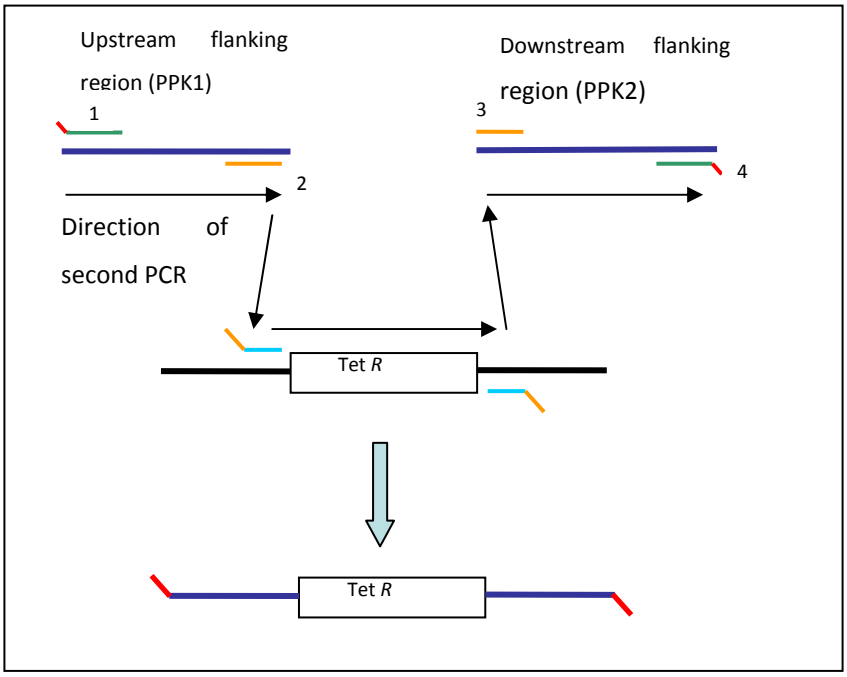

Figure 3.3 Demonstration of overlapping PCR.

After optimisation of the primer concentration and Mg^{2+}, the first round PCR produced all the separate fragments of the expected sizes.

However, when using these in the second round of PCR the complete fragment was not obtained. The fragments were both gel extracted and PCR purified in case there was any difference between the two purifying procedures. Attempts were made using different amounts of separate fragments and varying of the cycles with different annealing temperatures. Surprisingly the gel extracted and PCR purified products produced different banding patterns in the second round of PCR. See Figure 3.4.

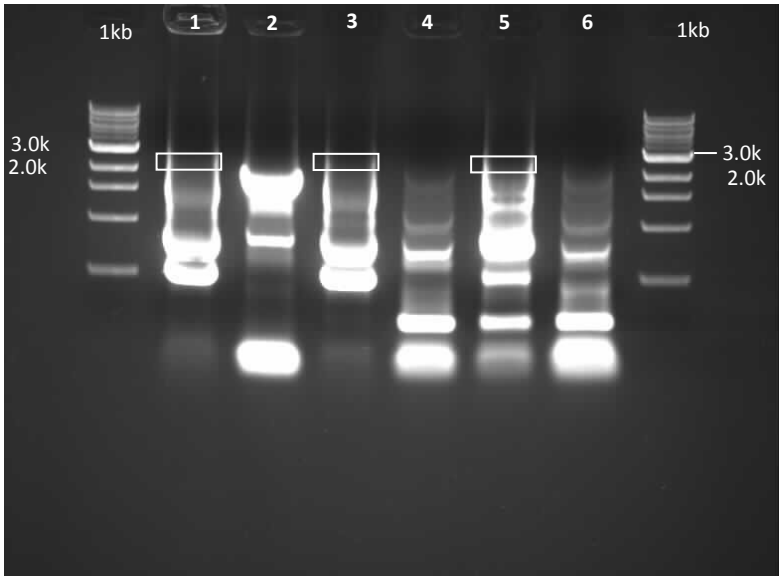

Figure 3.4 A 2% agarose gel showing the second round of PCR with the different annealing temperatures. Lane 1, PCR purified DNA ,49.3°C. Lane 2, Gel purified DNA, 49.3°C. Lane 3, PCR purified DNA, 55.8 °C. Lane 4, Gel purified DNA, 55.8 °C. Lane 5, PCR purified DNA, 62.6°C. Lane 6, Gel purified DNA, 62.6°C. Boxed regions represent the 2.1kb region which was gel extracted.

The area around 2.1kb (see Figure 3.4) was gel extracted and used again in the second PCR. Clearly defined products could not be obtained and the result was always a smear of DNA.

Addition of a slow cooling cycle before the second round of PCR was thought to encourage the initial annealing of the fragments by cooling the mixture at a slow rate. However, these results often produced a smear on a gel. The area around 2.1kb was gel extracted and used in the second PCR. A clean band could not be obtained and the result was always a smear.

It was decided to increase the length of the overlapping regions on the PCR primers and so tetracycline primers were designed that contained an overlap of approximately 30bp.

After optimisation, the PCR produced products; however, the *ppk*2 fragment always produced a weak band suggesting these primers were not ideal.

The products were nevertheless gel extracted and used in the second round of PCR as before. When repeating the same methods used previously yet again the second round of PCR always produced a smear and a clear band could not be obtained.

It is remains unclear as to why the overlapping PCR construction method did not work. This method was based around the *B. cereus* knockout method but the flanking regions were smaller.

3.3.3 Method 3

A kanamycin cassette from the pKD4 plasmid was selected to use for the antibiotic resistance gene. This cassette has a promoter which would drive expression independently to the target gene (Datsenko and Wanner 2000).

Primers were designed to incorporate the start and stop codons of the *ppk* gene. A different set of primers were also designed to span the cloning region in pMAD for quick analysis to see if the fragments had inserted. These primers can also be used for sequencing purposes in order to check insertion and orientation of the fragments. The forward and reverse primers had the sequences gaaggccatccagcctcg and ggatccgaccttaattatattatag respectively.

PCR was performed using KOD (HiFi) polymerase in 50µl reactions. The initial PCRs showed that the *ppk*2 fragment and the kanamycin fragment amplified successfully but the *ppk*1 fragment failed to amplify, see Figure 3.5.

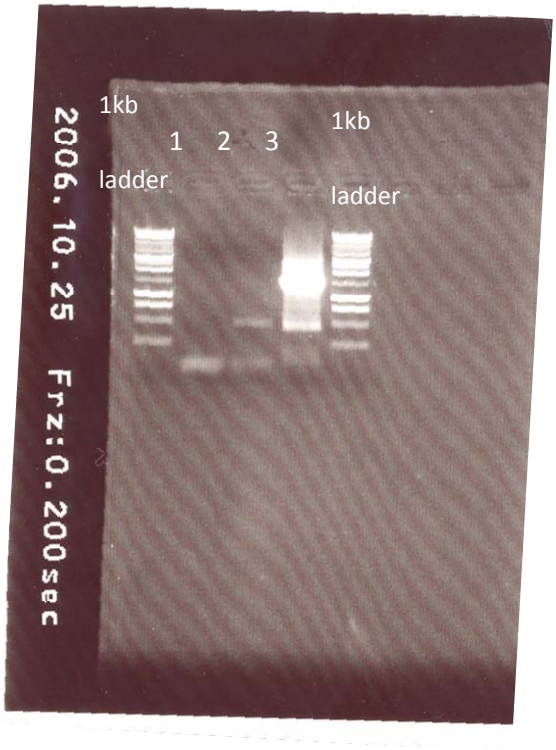

Figure 3.5 1% Agarose gel. Lane 1, *ppk*1 fragment. Lane 2, *ppk*2 fragment Lane 3 kanamycin cassette.

The *ppk*2 fragment was then successfully cloned into pMAD and stored to later add fragment 1. The insertion of the *ppk*2 fragment into pMAD was confirmed by restriction digest.

The *ppk*1 PCR reaction was run on the gradient cycler and with varied $MgCl_2$ concentrations in the range 1.5mM – 4.0mM, but no clean band was obtained. The PCR often showed a smear, which could be due to DNA concentration or too much $MgCl_2$. A serial dilution of the DNA was performed and used in a repeat of the PCR conditions used previously. No band was obtained. The location of the reverse primer could not be changed due to the incorporation of the *ppk* stop codon. So it was decided to re - design primer 1. Both primers had a high AT content due to the nature of the region of DNA being amplified. All PCR conditions, including a range of primer concentrations, were repeated with the new *ppk*1 forward primer, but were still not successful after many attempts. The new *ppk*1 forward primer was run with the *ppk*2 reverse primer as it had been shown to work previously. This would indicate if there was a problem with the primer 1 specifically. This PCR also did not work.

Further analysis of the sequence in the *ppk*1 fragment region showed a very AT rich region. This often hinders PCR as the primer may not anneal well to the low melting temperature DNA. Even after re - designing the new *ppk*1 primer the PCR failed to work. This was a problem that had limited solutions as the location of the primer needed to include the *ppk* stop codon. A different method needed to be used which would incorporate a different region of the DNA.

3.3.4 Method 4 – Amplification of the whole gene with the flanking regions and internal digestion with unique restriction sites

Primers were designed to span the whole *ppk* gene with the flanking regions. Restriction sites were integrated into the primers to enable cloning in the pMAD vector. The *ppk* Forward primer had an integrated BamH I restriction site and the reverse primer had a Bgl II restriction site. The forward and reverse primers had the sequences 5' atcggatccgctctatgtcaatcgaggtctcg 3' and 5' cgatagatctgcataaagagcgagttagattagc 3'respectively. Unique sites within the *ppk* gene were located. After cross referencing for the absence of their restriction sites in the kanamycin cassette and the pMAD vector, the restriction enzymes *Spe* 1 and *Mlu* 1 were chosen because

of their absence from the sequence analysis. Primers were then also designed for the kanamycin cassette to include these restriction sites. The KD4 forward and reverse primers had the sequences 5'atcgacgcgttaatgtgtaggctggagctgcttcg 3', and 5' atcgactagtcatatgaatatcctccttag 3' respectively.

This PCR was run with KOD polymerase and due to the expected size of the product, 3.1kb, the extension time was adjusted accordingly. A PCR product could not be obtained. Reagents were replaced and DNA was cleaned up using phenol / chloroform DNA extraction. PCR was repeated using the serial dilution of clean DNA, different $MgCl_2$ concentrations and run on a gradient cycler to broaden the range of annealing temperatures. Each separate reaction gave a smear, including the negative control. After changing the PCR water and making up new primers there was still no success with the repeated PCRs.

New primers were designed again with larger flanking regions. The GC content was increased and the region of DNA was less AT rich. Pure phenol / chloroform extracted DNA was used which would eliminate any impurities from the previous stock of DNA boilates. The PCR was run with the new primers. The gradient cycler was used for a broad range of temperatures from 50˚C to 65˚C. Different $MgCl_2$ concentrations and a serial dilution of the DNA was also used in order to cover a variety of conditions. None of these conditions produced a PCR product at the expected size.

The region of DNA around *ppk* is very AT rich and difficult to amplify. By increasing the flanking regions to nearly 1kb, the AT rich area which has been causing major problems could be avoided. This method of increasing the flanking regions was employed in method 5.

3.3.5 Method 5

Primers were re-designed based heavily on the *B. cereus* knockout method. Restriction sites were added on the ends of each primer in order to clone into the pMAD vector. There are 4 primers for each gene knockout. See Table 3.1.

Primer	Sequence	Restriction Site
K1	cgatggatccgaatccgtctactgg	BamH1
K2	atcggtcgactgatagtcaagtgaag	Sal 1
K3	atcggtcgacgtaataagctgtatc	Sal 1
K4	atcgagatctattgtcgttcatag	Bgl II
X1	cgatggatccgatactttatatcctg	BamH1
X2	cgatgtcgacgacaaagatcgcttg	Sal 1
X3	cgatgtcgaccgcattgtattagatcc	Sal 1
X4	cgatagatcttgtatgacagctataat	Bgl II
A1	cgatggatccgcaatgatctgggcagcag	BamH1
A2	cgatgtcgactactttagcaagaactcc	Sal 1
A3	cgatgtcgaccataatatagaattaccttcg	Sal 1
A4	cgatagatctctggacgaagcataac	Bgl II

Table 3.1 Table showing the primer sequences and modifications used in method 5.

Flanking regions were increased to ~900bp.

PCR product sizes are as follows:

ppk fragment 1 = 963bp

ppk fragment 2 = 965

ppx fragment 1 = 1kb

ppx fragment 2 = 979bp

pap fragment 1 = 754bp

pap fragment 2 = 959bp

The first sets of PCRs were run using KOD polymerase. See Figure 3.6.

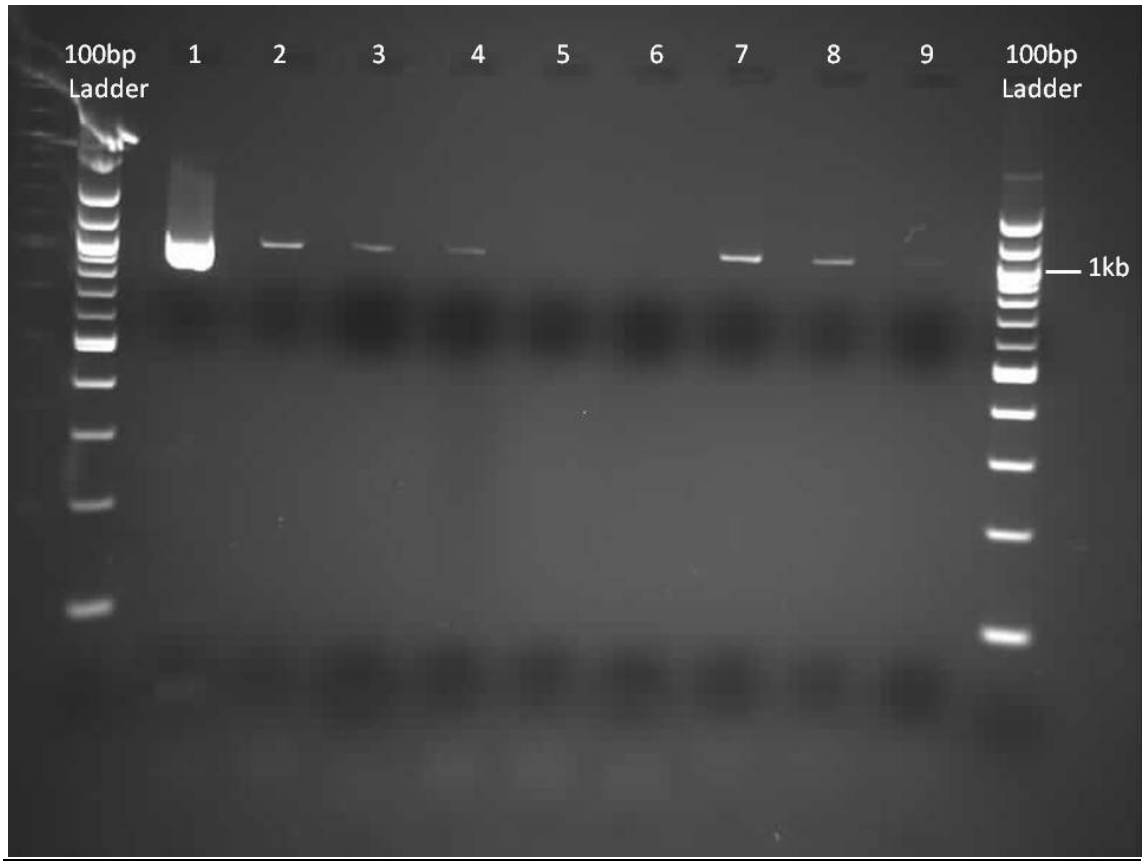

Figure 3.6 2% Agarose gel. Lanes 1, 2, Sterne *ppk*1 Lanes 3, 4, Sterne *ppk*2. Lane 5 Neg control (No template DNA) Lanes 6, 7 Ames *ppk*1. Lanes 8, 9, Ames *ppk*2.

ppk fragments were amplified from *B. anthacis* Sterne and Ames either in repeats or just once from the reaction. See Figure 3.7

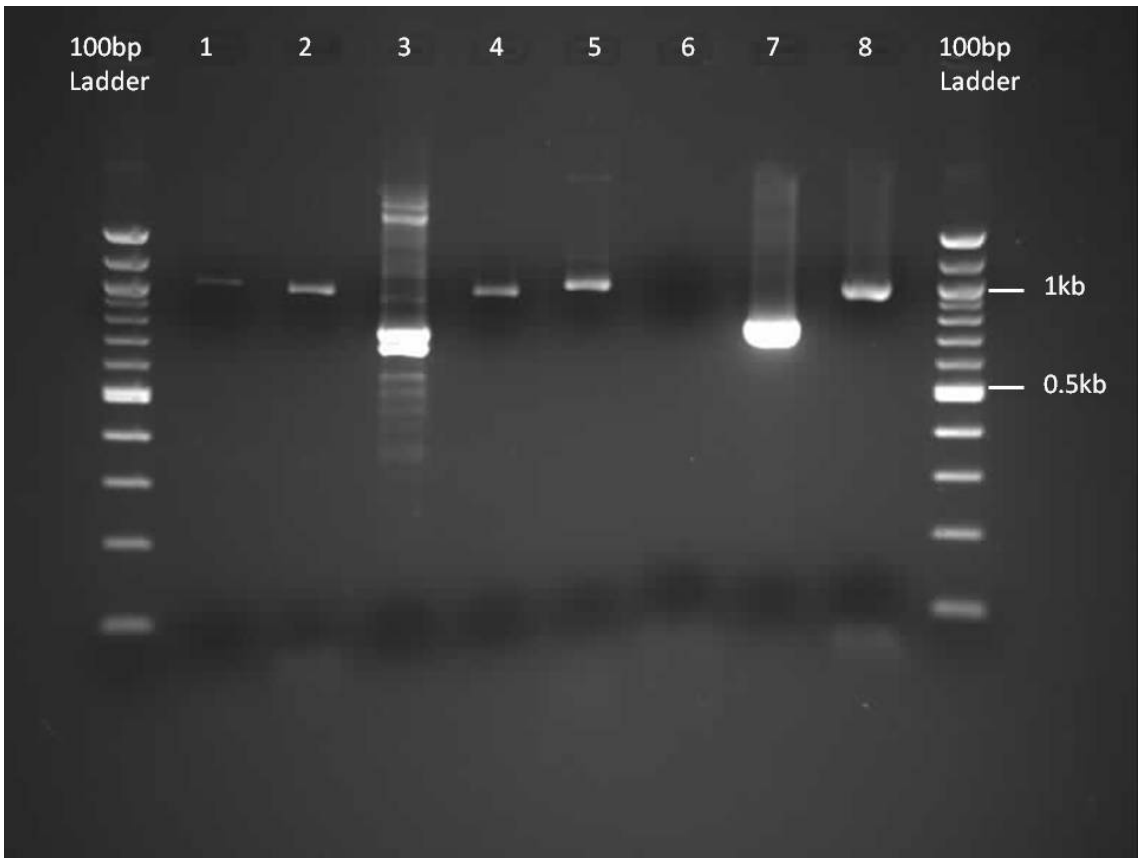

Figure 3.7. 2 % agarose gel. Lane 1, Ames *ppx*1. Lane 2, Ames *ppx*2. Lane 3, Ames *pap*1. Lane 4, Ames *pap2*. Lane 5, Sterne *ppx*1. Lane 6, Sterne *ppx*2. Lane 7, Sterne *pap*1. Lane 8, Sterne *pap*2.

All the PCRs produced fragments at the expected sizes apart from Sterne *ppx*2 fragment which produced no product. The Ames *pap*1 fragment seemed to produce a double band of approximately the correct size (750bp) so the product was gel extracted prior to use in cloning.

Both Sterne and Ames *ppk* 1 and 2 fragments were gel extracted and cut with *Sal* 1. These were then ligated together and run on a gel for confirmation. See Figure 3.8.

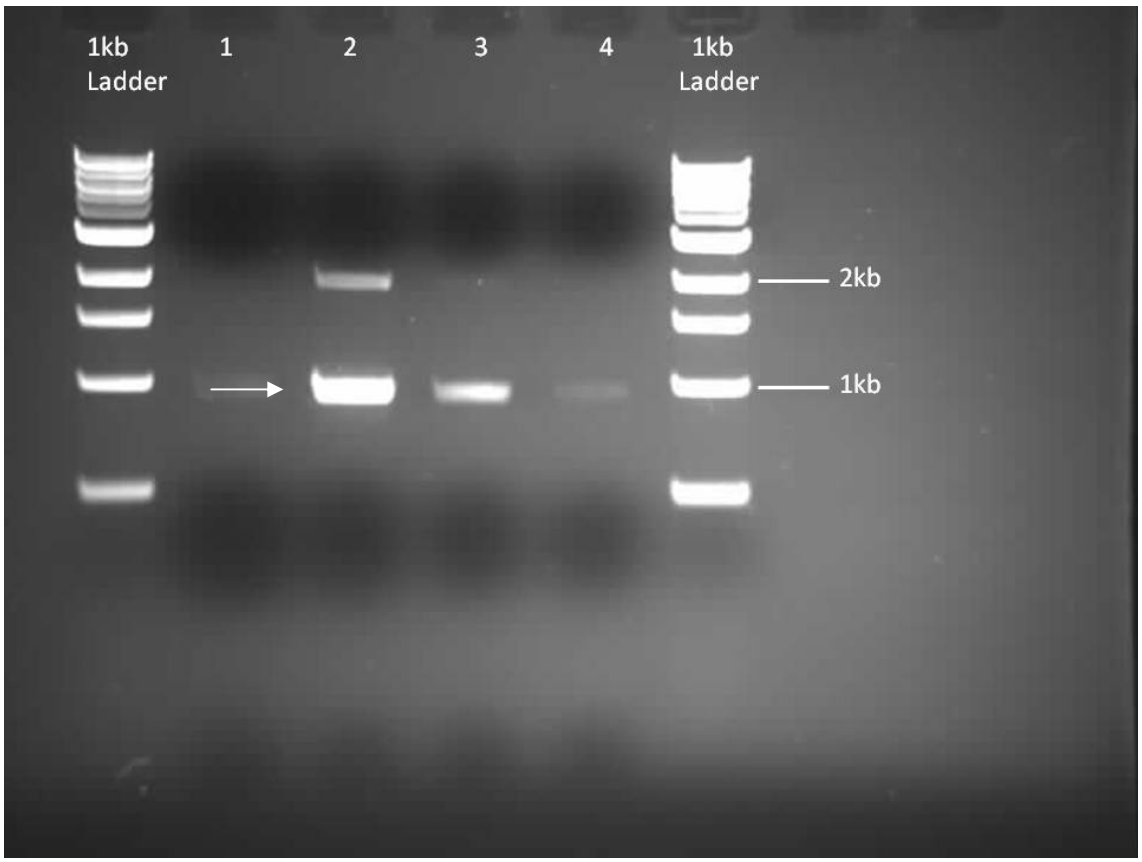

Figure 3.8. 1% Agarose gel. Lane 1 and 2 replicate Ames *ppk* ligation. Lanes 3 and 4 replicate Sterne *ppk* ligation.

In lane 2 the Ames *ppk* ligation can clearly be seen to have worked and in lane 3 there is a very faint band, again of the correct size.

Both of these products were gel extracted and cloned into the pMAD vector degested with the corresponding *Bam*H 1 and *Sal* 1 enzymes.

After the transformation numerous *E. coli* clones were obtained. 27 of the *E.coli* colonies were subjected to colony PCR with the pMAD primers that span the cloning region resulting in a product of 2.0kb. A selection of *E. coli* clones produced from the Ames and Sterne *ppk* fragments were chosen and grown up for analysis. Unfortunately a restriction digest of the plasmid DNA did not work well and only produced faint bands that could not be clearly distinguished.

After further optimisation of the *ppx* PCR, fragments were gel extracted, *Sal* 1 digested and used in a ligation. Both Ames and Sterne fragments were used. Products were run on a gel for extraction. See Figure 3.9.

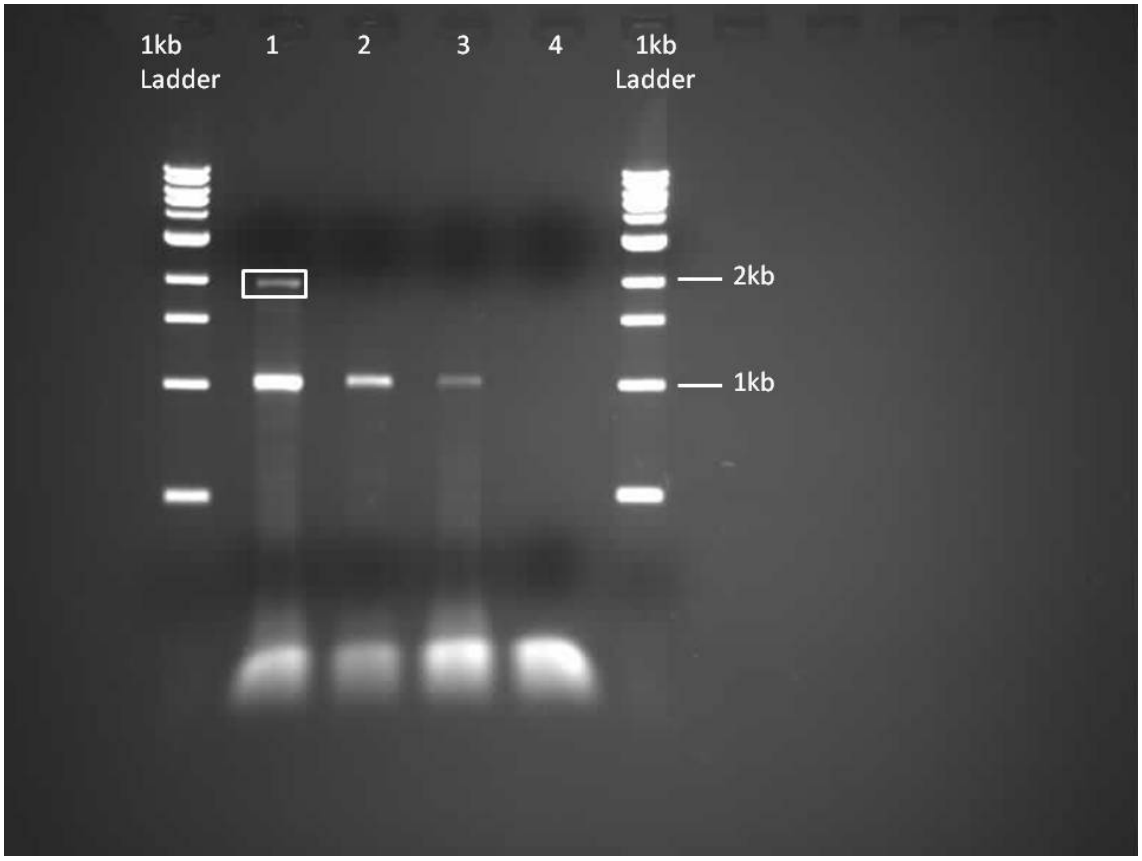

Figure 3.9. 1% Agarose Gel. Lane 1 and 2, Ames *ppx* ligation. Lane 3 and 4, Sterne *ppx* ligation

Results from the ligation (see Figure 3.9) (highlighted band) show that only the Ames *ppx* fragments ligated together. This product was extracted and stored at -20°C for future cloning.

The *ppk* and *ppx* ligated fragments of the flanking regions were digested with *Bam*H I and *Bgl* II ready to clone into the pMAD plasmid. The pMAD plasmid was also cut with the corresponding sites and dephosphorylated for the ligation. The cloning of these fragments did not work after many repeats using different conditions. As each fragment amplified well with the new PCR primer set, the separate cloning of each individual fragment was performed. Although this was laborious, each step could be carefully controlled and optimised in order to maximise chances of success.

3.3.6 Method 6 – Cloning the individual fragments separately

Using the primers designed on the *B. cereus* primers the flanking regions of *ppk*, *ppx* and *pap* were cloned into the pMAD vector.

The PCR using these primers produced products of the correct size in the first PCR reactions as shown previously. The products were gel extracted and cleaned up to be cloned into the pMAD plasmid. After cutting the Flanking region 1 amplicons and pMAD with the corresponding restriction sites, *Bam*H1 and *Sal* 1, the amplicons were ligated into the pMAD vector and transformed into Top 10 *E. coli.* The *E.coli* clones were cultured and stored at -80°C in 15% glycerol.

A plasmid extraction was performed on the clones in order to analyse the pMAD plasmid. A restriction digest using *Bam*H1 and *Sal*1 confirmed the insertion of the flanking region 1 amplicons from *ppk*, *ppx* and *pap*. The fragment sizes produced from the digest correlated to the expected sizes of the newly cloned amplicons; *ppk* flanking region 1 was 0.951kb, *pap* flanking region 1 was 0.740kb and *ppx* flanking region 1 was 0.988kb. See Figure 3.10, 3.11, 3.12 and 3.13.

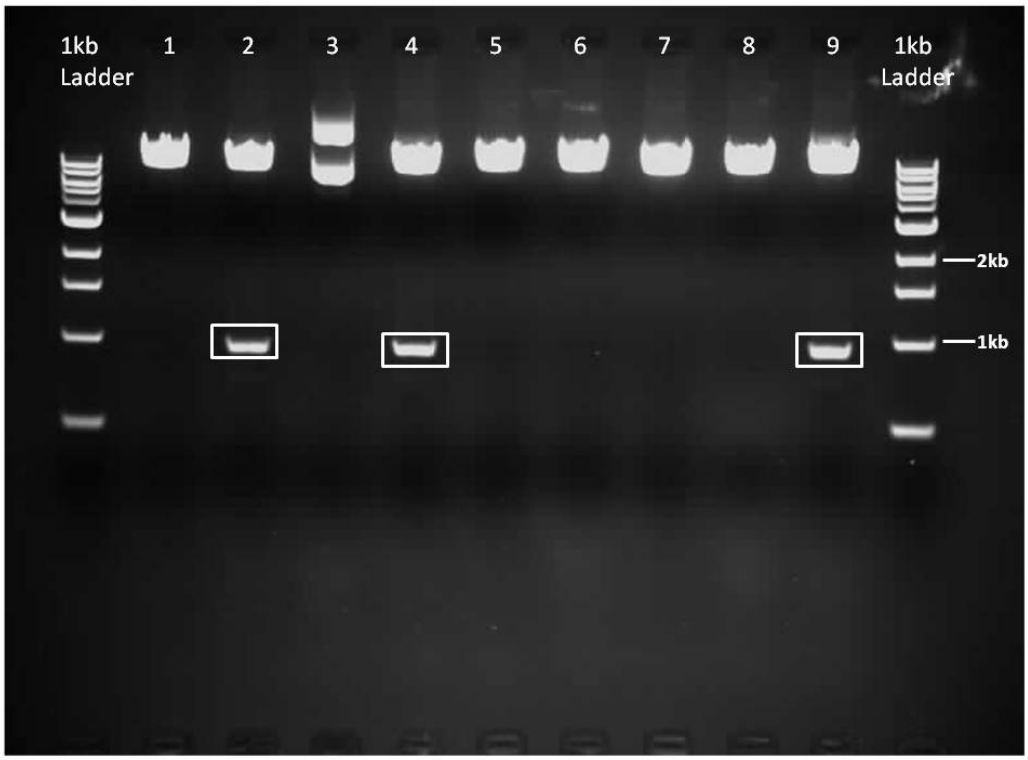

Figure 3.10. Lanes 1-9, Clones of *ppk* Flanking region 1 in pMAD. Highlighted bands show the expected insert.

Figure 3.11. Lane 10 and 11, Clones of *ppk* Flanking region 1 in pMAD. Highlighted bands show the expected insert.

Figure 3.12. Lanes 1-7, Clones *pap* Flanking region 1 in pMAD. Lanes 8-9, Clones *ppx* Flanking region 1 in pMAD. Highlighted bands show the expected insert.

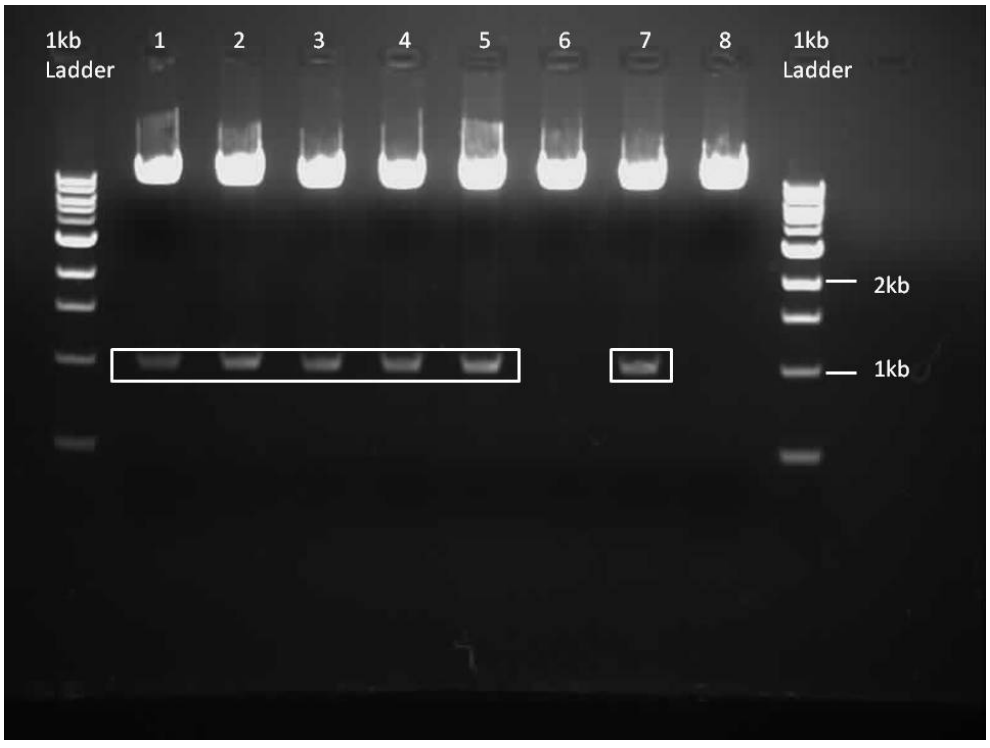

Figure 3.13. Lanes 1-8, Clones *ppx* Flanking region 1 in pMAD. Lanes 8, Negative control. Highlighted bands show the expected insert.

The *ppk*, *ppx* and *pap* flanking region 2 were then amplified and cloned into the pMAD plasmid using the corresponding *Sal* 1 and *Bgl* II restriction sites. After transformation into Top 10 *E.coli*

the clones were stored and plasmids extracted for analysis. A restriction digest using *Sal* 1 and *Bgl* II confirmed the insertion of the flanking region 2 amplicons from *ppk*, *ppx* and *pap*. The fragment sizes produced from the digest correlated to the expected sizes of the newly cloned amplicons which had inserted next to flanking region 1. The *ppk* flanking region 1 and 2 was 1.906kb, the *ppx* flanking region 1 and 2 was 1.953kb and the *pap* flanking region 1 and 2 was 1.685kb. See Figure 3.14, 3.15 and 3.16.

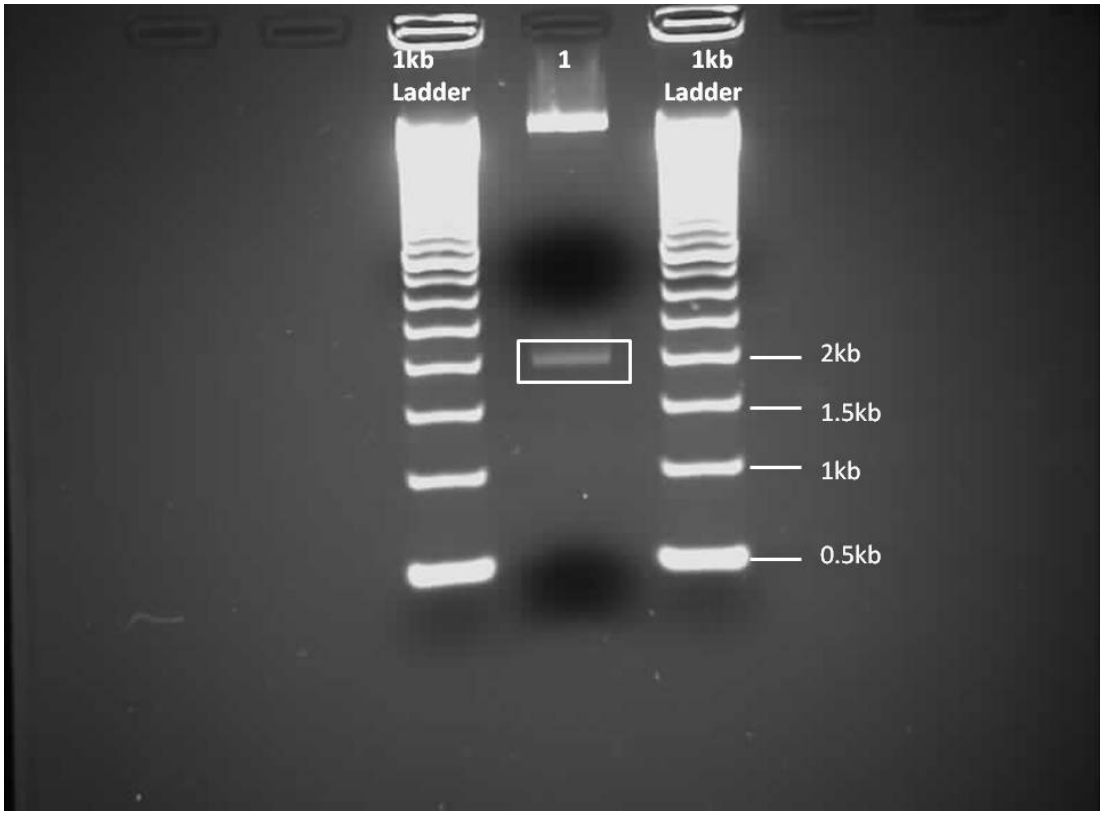

Figure 3.14. Lane 1 Clone *ppk* Flanking region 1 and 2 in pMAD. Highlighted band shows the expected insert.

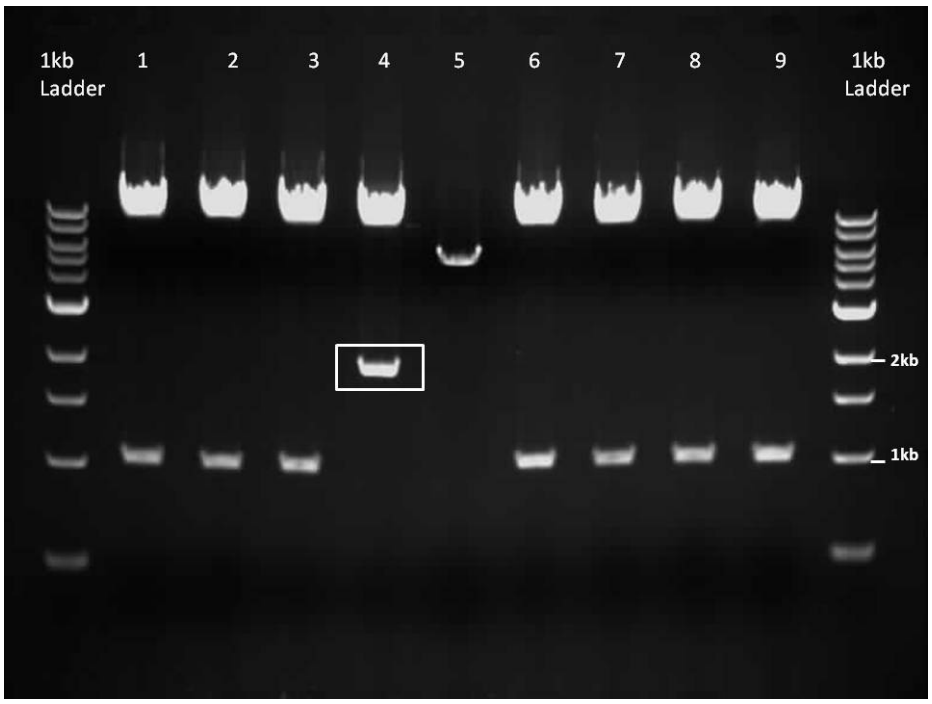

Figure 3.15. Lanes 1-9, Clones *ppx* Flanking region 1 and 2 in pMAD. Highlighted bands show the expected insert.

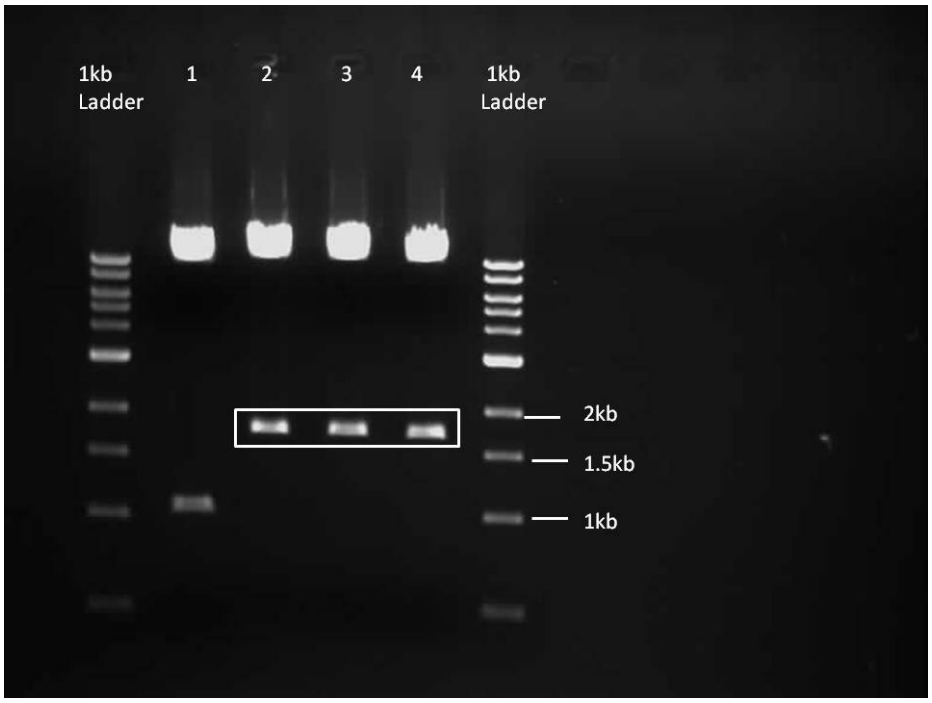

Figure 3.16. Lane 1, Clone *ppx* Flanking region 1 and 2 in pMAD. Lanes 2-4, Clones *pap* Flanking region 1 and 2 in pMAD. Highlighted bands show the expected insert.

3.3.7 Cloning of the kanamycin cassette

The kanamycin cassette was amplified from the Tn30 transposon with additional *Sal* 1 sites incorporated into the primers. Primer sequences for the forward and reverse primers were 5' atcgtcgacgaattgtgtctcaaaatct 3' and 5' caggtcgactctagaggatccccgcca 3' respectively.

After a successful amplification, the product was gel purified and cleaned up ready to clone into the *Sal* 1 site in each of the pMAD constructs. See Figure 3.17.

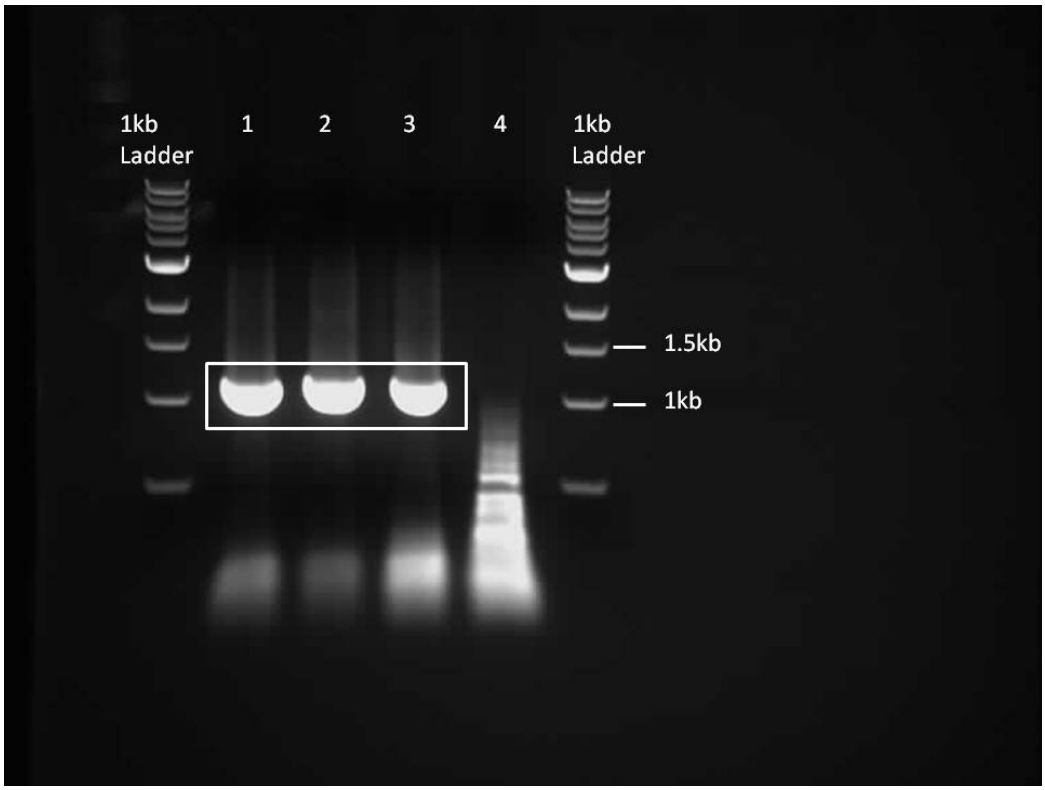

Figure 3.17. Lane 1-3, Kanamycin cassette product. Lane 4, Negative control. Highlighted bands show the expected size product, 1.2kb.

Both plasmid (pMAD with flanking regions 1 and 2) and insert (kanamycin cassette) were cut with *Sal* 1 and ligated together. After transformation into Top 10 *E. coli*, clones were selected and analysed for the correct orientation and insertion of the Kanamycin cassette.

3.3.8 Analysis of the final constructs

A *Sal* I digest was performed on all clones; *ppk*:Kan, *ppx*:Kan and *pap*:Kan. The results showed a 1.143kb band which represents the kanamycin cassette and the larger 11 - 12kb band which represents the remaining plasmid. All of the clones produced the desired band that confirmed insertion of the kanamycin cassette.

The orientation of the kanamycin cassette was determined as ideally it needed to be inserted in the same direction of the designated gene (*ppk*, *ppx* or *pap*). Although the kanamycin cassette has its own promoter and stop codon, when faced in the same orientation of the wild type operon it may work more efficiently

Primers were designed to incorporate the kanamycin gene and part of the flanking region of the three genes. See Figure 3.18.

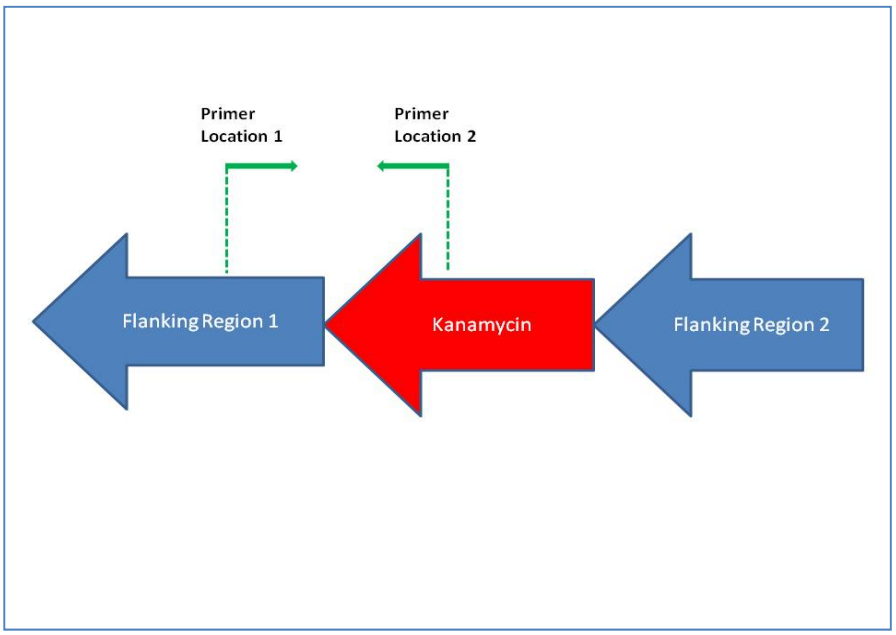

Figure 3.18. Representation of the knockout cassette and location of the primers to check kanamycin orientation.

All *ppx* and *pap* clones produced PCR products but the PCR needed to be optimised due to some smearing and non - specific bands. The *ppk* PCR did not work. After optimisation of

annealing temperature and $MgCl_2$ concentrations, a clean band was only acquired from the *ppx* and *pap* clones. All products produced from this PCR were gel extracted, cleaned up and sequenced. The correct sequence and therefore orientation were obtained from the sequencing results. These results proved that the *ppx* and *pap* constructs were now ready to be electroporated into *B. anthracis.*

A restriction enzyme screen using Seqbuilder Lasergene 7 was performed to check for 2 enzymes that cut the final constructs up to 3 times so the final plasmids could be mapped. As the PCR method of confirmation had not worked on the *ppk*:Kan clones, this method would have to be relied on.

Age 1 and *Eco*R V were used as enzymes to digest the plasmids. See Figures 3.19, 3.20 and 3.21. Expected band sizes were as follows:

ppk= (3 bands) 1.552kb, 4.750kb, 6.339kb

ppx = (3 bands) 1.552kb, 4.797kb, 6.339kb

pap= (3bands) 1.552kb, 4.529kb, 6.339kb

pMAD = (3bands) 1.552kb, 1.775kb, 6.339kb

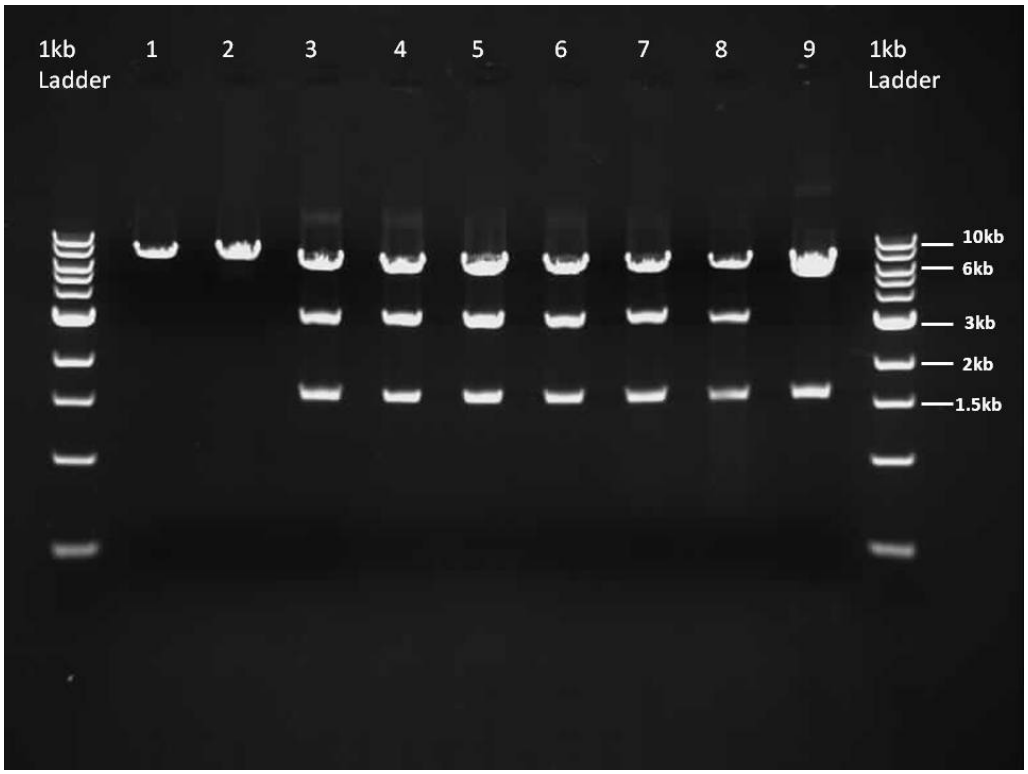

Figure 3.19. Lane 1-9 *ppk*:Kan final cassettes

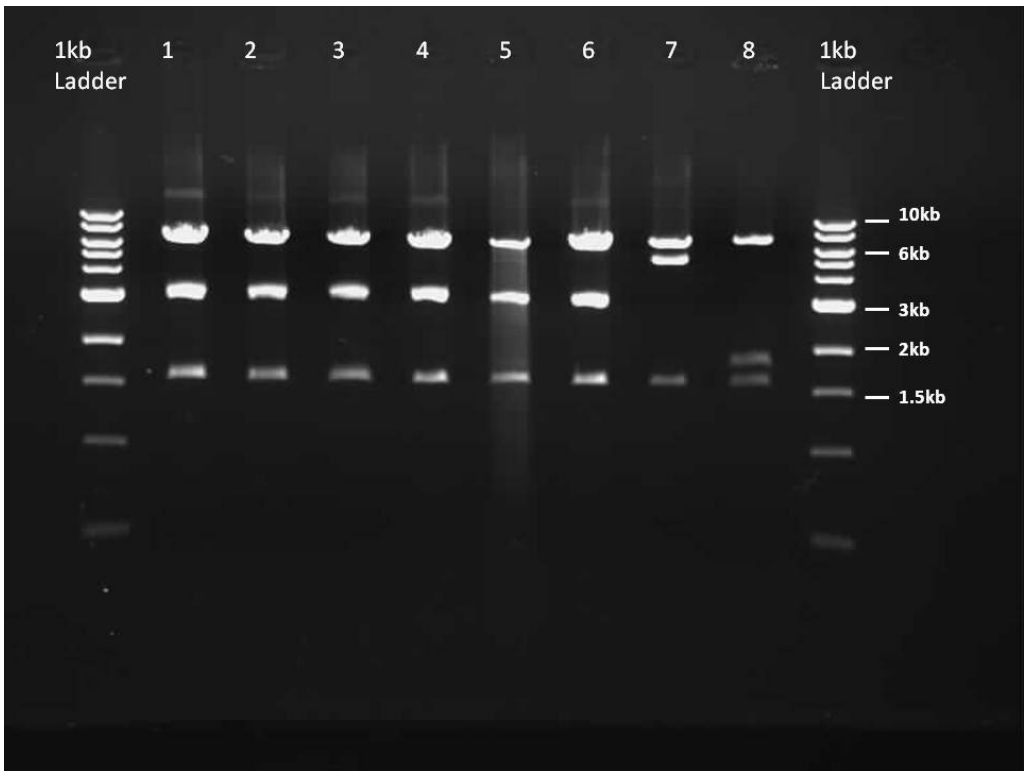

Figure 3.20. Lane 1 - 6 *ppk*:Kan final cassettes, Lane 7 PPX:Kan final cassette, Lane 8 pMAD.

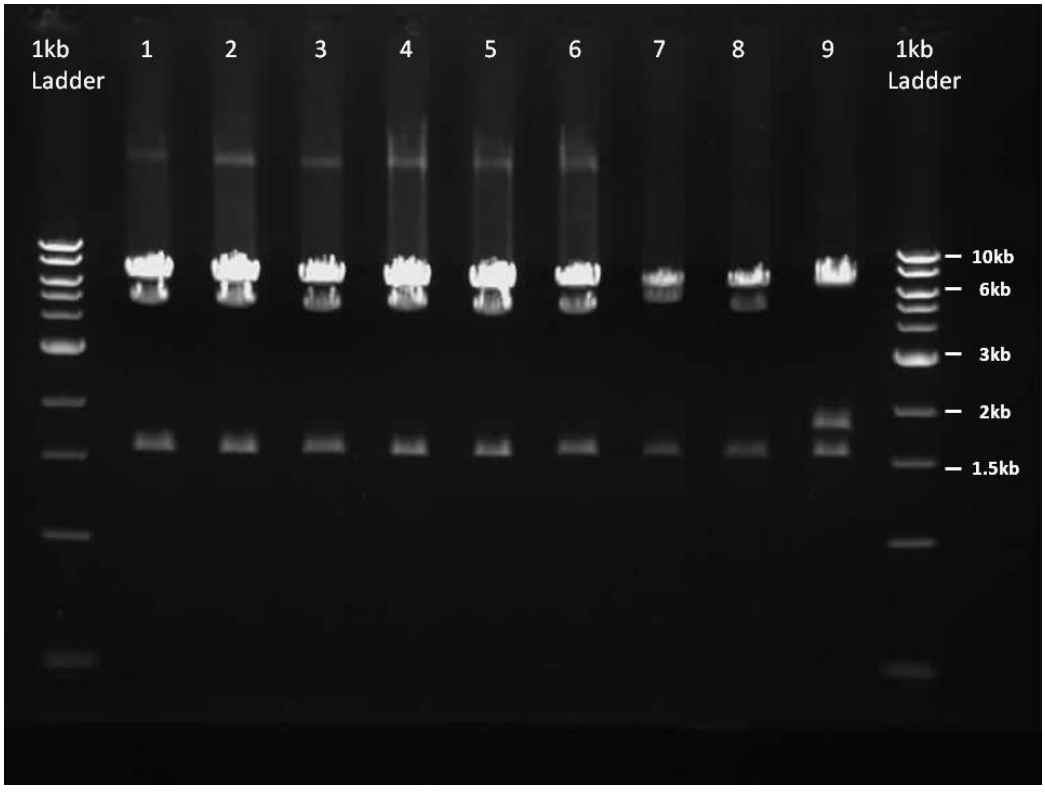

Figure 3.21. Lanes 1-6 *pap*:Kan final cassettes, Lane 7, *ppx*:Kan final cassettes. Lane 8 ppk:Kan final cassettes, Lane 9 pMAD.

Using *Age* I and *Eco*R V, 3 bands are produced from each of the cassette digests. The pMAD control shows the expected sizes and the *pap* and *ppx* final cassettes have also digested in the expected places. The *ppk* final cassettes however, seems to show the largest and smallest bands at the correct sizes but instead of the 4.750kb there is a band of ~3.1kb. This band fragment contains the cloning region of the pMAD vector which indicates that the final cassette may have not assembled correctly. This would also support the results from the confirmation PCR which did not work.

It is quite difficult to accurately see the sizes of the bands in this digest. Although it gives a representation of the band sizes, another digest which produces smaller fragments could be used to map the plasmid allowing easier analysis of the cassettes.

After further analysis of the construct sequences, enzymes were chosen that cut 5 - 6 times and that produced manageable size fragments so that these could be used to map the plasmids and further confirm the correct orientation and insertion of the flanking regions and kanamycin cassette.

The best three enzymes for mapping the plasmid were found to be *Cla* I, *Bsp*HI, and *Sml* I. Using these three enzymes as single digests rather than a multiple digest would limit the variables in the experiment leading to a more accurate set of results. See Figure 3.22, 3.23 and 3.24.

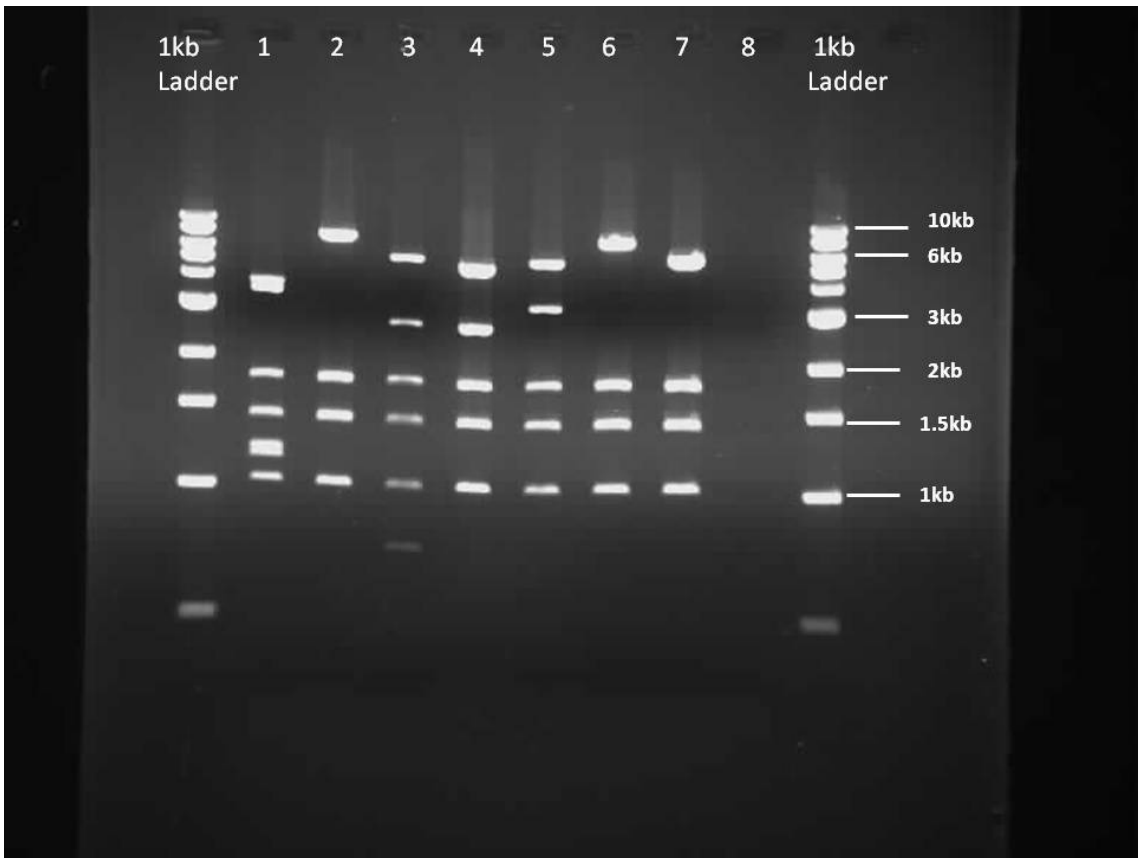

Figure 3.22. Restriction Digest with BspH I. Lane 1, *ppk*:Kan Clone. Lane 2, *ppk* Flanking. Lane 3, *ppx*:Kan Clone. Lane 4, *ppx* Flanking. Lane 5, *pap*:Kan Clone. Lane 6, *pap* Flanking. Lane 7, pMAD. Lane 8, Negative control.

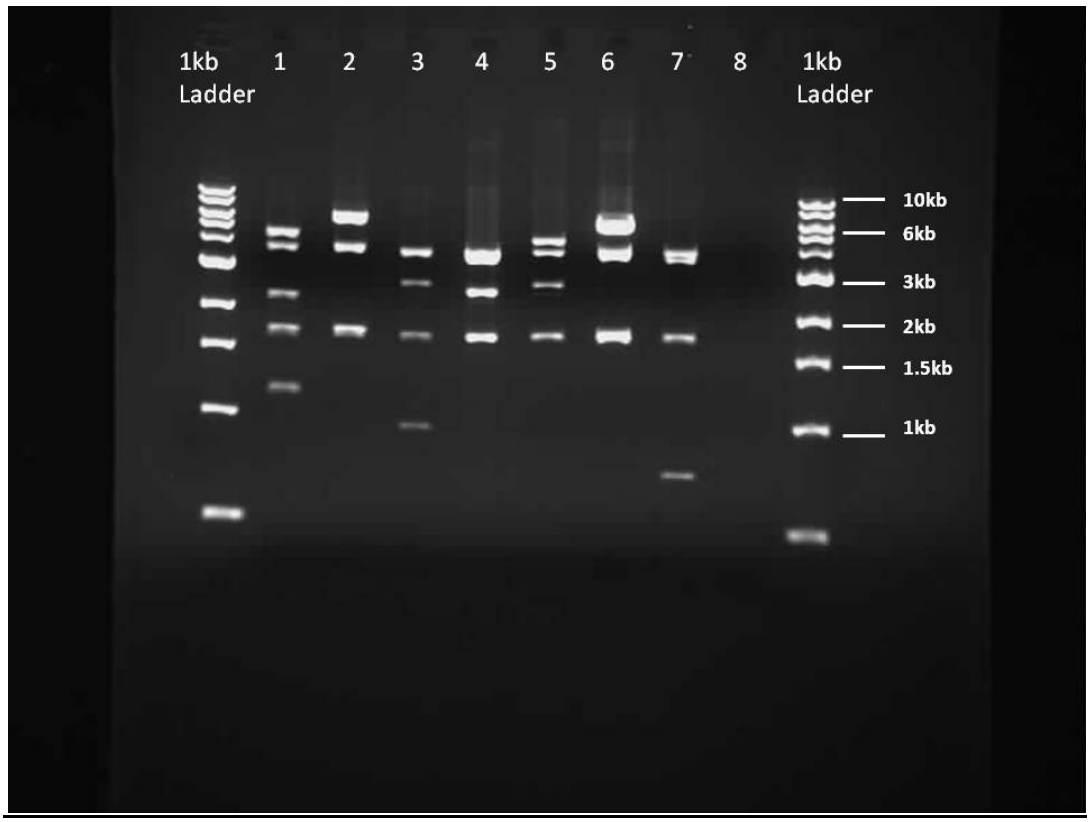

Figure 3.23. Restriction Digest with Cla I. Lane 1, *ppk*:Kan Clone. Lane 2, *ppk* Flanking. Lane 3, *ppx*:Kan Clone.4, *ppx* Flanking. Lane 5, *pap*:Kan Clone. Lane 6, *pap* Flanking. Lane 7 pMAD. Lane 8, Negative control.

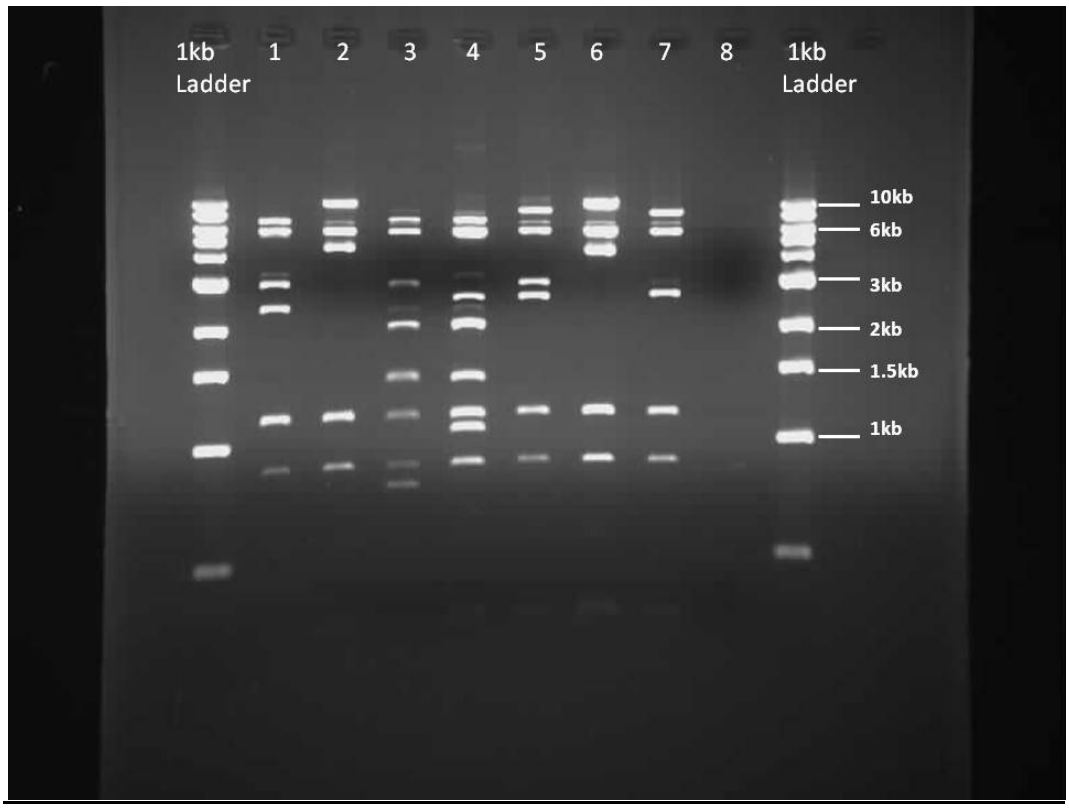

Figure 3.24. Restriction Digest with Sml I. Lane 1, *ppk*:Kan Clone. Lane 2, *ppk* Flanking. Lane 3, *ppx*:Kan Clone. Lane 4, *ppx* Flanking. Lane 5, *pap*:Kan Clone. Lane 6, *pap* Flanking. Lane 7 pMAD. 8, Negative control.

The pMAD plasmid was used as a control as the exact sequence is known. When analysing the digest results, the *Cla* I and *BSp*H I digests show the expected size bands. The smaller bands, less than 0.5kb, cannot be seen on the gel but due to their size this is not unexpected. The larger bands are the ones of interest. The *Sml* I digest does not show all the expected sizes. The pMAD plasmid is 9.666kb and the *Sml* I digest shows bands of approximately 6.0kb and 8.0kb which is not correct. This may suggest a partial digestion of the plasmid or that some of the restriction sites have been lost or mutated, which is unlikely but possible. The *Cla* I and *BSp*H I results have worked well so these were used to map the plasmid.

3.3.8.1 Digest Results

The expected digest results (sizes of bands) can be seen in Table 3.2 . The actual digest results (sizes of bands) can be seen in Table 3.3.

Expected sizes	**Restriction endonuclease**		
Plasmid construct	***Cla* I**	***Bsp*H I**	***Sml* I**
ppk:Kan:pMAD Lane 1	0.237, 0.360, 1.323,1.7, 3.728, 5.293	0.105, 1.008, 1.403, 1.725, 4.130, 4.270	0.262, 0.277, 0.868, 1.975, 3.576, 5.683
ppk:pMAD Lane 2	0.237, 0.360, 1.7, 3.728, 5.473	0.105, 1.008, 1.725, 7.257, 1.403,	0.262, 0.277, 0.868, 4.408, 5.683
ppx:Kan:pMAD Lane 3	0.237, 0.360, 1.333, 1.661, 1.7, 3.669, 3.728	0.105, 1.008, 1.403, 1.725, 1.751, 2.556, 4.140	0.262, 0.277, 0.569, 0.868, 1.416, 1.639, 1.974, 5.683
ppx:pMAD Lane 4	0.237, 0.360, 1.333, 1.661, 1.7, 3.669, 3.728	0.105, 1.008, 1.403, 1.725, 1.751, 2.556, 4.140	0.262, 0.277, 0.569, 0.868, 1.416, 1.639, 1.974, 5.683
pap:Kan:pMAD Lane 5	0.237, 0.360, 1.7, 1.994, 3.728, 4.401	0.105, 1.008, 1.403, 1.725, 3.034, 5.145	0.262, 0.277, 0.868, 2.5, 2.830, 5.683
pap:pMAD Lane 6	0.237, 0.360, 1.7, 3.728, 5.252	0.105, 1.008, 1.403, 1.725, 7.036	0.262, 0.277, 0.868,4.187, 5.683
pMAD Lane 7	0.143, 0.237, 0.360, 1.7, 3.728, 3.498	0.105, 1.008, 1.725, 5.425, 1.403	0.262, 0.277, 0.868, 2.576, 5.683

Table 3.2. A table representing the expected band sizes from the restriction digests if the correct insertions had been achieved.

Digest Results	**Restriction endonuclease**		
Plasmid construct	***Cla* I**	***Bsp*H I**	***Sml* I**
ppk:Kan:pMAD Lane 1	1.3, 1.7, 2.2, 3.7, 4.5	1.0, 1.2, 1.25, 1.4, 1.7, 3.5, 4.0	0.9, 1.2, 2.5, 3.0, 6.0, 7.0
ppk:pMAD Lane 2	1.7, 3.7, 6.0	1.0, 1.4, 1.7, 8.0	0.9, 1.2, 4.5, 6.5, 10
ppx:Kan:pMAD Lane 3	0.9, 1.7, 2.8, 3.7	0.7, 1.0, 1.4, 1.7, 2.5, 5.0	0.8, 0.9, 1.2, 1.5, 2.0, 3.0, 6.0, 7.0
ppx:pMAD Lane 4	1.7, 2.5, 3.5	1.0, 1.4, 1.7, 2.5, 4.0	0.9, 1.1, 1.2, 1.5, 2.0, 2.5, 6.0, 7.0
pap:Kan:pMAD Lane 5	1.7, 2.8, 3.9, 4.5	1.0, 1.4, 1.7, 3.0, 5.0	0.9, 1.2, 2.5, 3.0, 6.0, 8.0,
pap:pMAD Lane 6	1.7, 3.5, 6.0	1.1, 1.4, 1.7, 8.0	0.9, 1.2, 4.5, 5.0, 10
pMAD Lane 7	0.7, 1.7, 3.5	1.0, 1.4, 1.7, 6.0	0.9, 1.2, 2.5, 6.0, 8.0

Table 3.3 Restriction digest results in numeric form from gel pictures in Figures 3.22, 3.23 and 3.24. Plasmids were cut with *Cla*I, *Bsp*H I and *Sml* I. Numbers are expressed in Kb.

(The results from the digest do not include bands below 0.5kb as they would have run off the gel.)

When looking at the *Bsp*H I results the *pap*:Kan:pMAD construct has the expected size bands from the assembled sequence which means that it has assembled correctly with only one insertion of the kanamycin cassette. With the correct orientation proven with previous sequencing results this construct is complete.

The *ppk*:Kan:pMAD and *ppx*:Kan:pMAD constructs do not have the correct band sizes for the final cassettes. The *ppk*:pMAD cassette without the kanamycin insert does show around the correct size bands when cut with *Cla* 1 which suggests that the flanking regions have inserted correctly and that the kanamycin gene insert was not as expected. However the same construct, *ppk*:pMAD when cut with *Bsp*H1 only produces two of the correct band sizes.

ppx:pMAD produces the correct bands when cut with *Bsp*H1 but not when cut with *Cla* 1.

Electroporation of the pMAD vector and the positive control pAEX – 4 was performed into freshly prepared electrocompetent *B. anthracis* Sterne cells. The *pap*:Kan:pMAD construct was also used in the electroporation in order to produce the first knockout mutants.

The positive control plasmid transformation, pAEX - 4, worked well and colonies were isolated on kanamycin 50µg / ml L-agar plates. Kanamycin resistance is only expressed when the plasmid has been incorporated into the *B. anthracis* cells. However, colonies were not isolated from the ampicillin or ampicillin and kanamycin plates when electroporating either the pMAD vector on its own or with the *pap* assembled cassette in the vector. Numerous attempts were made with adjustments to the incubation temperature and varied ratios of cells to DNA concentration, each failing to produce the desired clones. It is not clear why the pMAD derived plasmids would not transform into *B. anthracis.* pMAD has not been used in *B. anthracis* before but has been successfully used to construct mutants in *B. cereus* and *B. thuringiensis.* pMAD is a plasmid derived from pBR322 and pE194. This enables intermediate growth in *E. coli* using the pBR322 replicon for replication and for cloning in *Bacillus* the pE194 replicon is used. pE194 is a plasmid derived from *Staphlococcus aureus* (Dempsey & Dubnau, 1989) and is used frequently for mutagenesis in *B. subtilis*. pE194 has also been used for genetic mutagenesis studies in *B. anthracis* (Koehler, T. 2002). It would be surprising if plasmid incompatibility is indeed the problem in this particular case but it should be taken into consideration.

3.4 Discussion

Throughout this study, six different methods were attempted to try and initially construct the cassettes for electroporating into *B. anthracis* Sterne to create the same gene knockouts as constructed in *B. cereus*. All six methods used techniques shown to work on previous studies within the lab and are published methods (Shi et al., 2004, Trieu-Cuot *et al.*, 1991, Sambrook J. *et al.*, 1989, Arnaud et al., 2004, Steinmetz & Richter, 1994).

Method 6, which was heavily based on the methods used to create the *B. cereus* clones (Shi et al., 2004), gave the best results with the correct assembly of a plasmid containing the *pap* knockout cassette. Conversely, the *ppk* and *ppx* constructs were not correctly assembled even though the same method was used for all three constructs. The method differed slightly from the one used for the *B. cereus* constructs because in the original method they were able to make the construct by amplifying the flanking regions and the antibiotic cassette and adding all the products together in one PCR to use as a template. This method did not work in this study although tried numerous times with negative results. The method that worked involved the addition of each individual part of the cassette separately which was laborious and time consuming.

The failure to recover the final *B. anthracis* transformants was very disappointing, especially as the pAEX-4 positive controls always worked. It is not clear whether the presence of the *pap* construct caused a problem, but the failure to recover pMAD transformants suggests a problem with this replicon in *B. anthracis* that does not occur in *B. cereus*. The origin of replication in pX01 does not show any homology to any of the *rep* genes that have been previously associated to the replicon in large plasmids of other Gram positive bacteria (Okinaka et al., 1999). In order to test this possible incompatibility of pMAD and pX01 plasmids, the final constructs could be electroporated into the *B. anthracis* UM23C strain which is cured of both pX01 and pX02. If this experiment was successful then plasmid incompatibility would be the logical explanation. Unfortunately there was not enough time to continue to pursue these experiments.

It is also not clear why the previously constructed *B. cereus* mutants failed to recover from frozen store. It seems likely that the mutations cause a very severe debilitating phenotype preventing freeze thaw stability or longer term survival in culture. The *ppx* knockout mutants have shown to have highly reduced sporulation efficiencies which may lead to a reduced survival rate if stored for a long time either at 4°C or in glycerol at -80°C.

3.5 Analysis of *B. anthracis* strains from the Kruger National Park

The two distinct groups of *B. anthracis* A and B are both prevalent in the Kruger National Park (KNP), South Africa. This occurrence provides a unique opportunity to analyse and compare these strains and their exact location from which they were isolated. Both groups A and B have been isolated from contrasting soil from within the KNP. Group B was isolated from a significantly higher calcium and pH soil than group A. (Smith, K.L. 2000). This is an interesting finding as the geographical distributions of the two groups are also significantly distinct.

3.5.1 Analysis of Kruger isolates from the Anthrax Strain Collection

Dr. M. Mock's group at the Institute Pasteur discovered a deletion in the *ppx* gene of one of their *B. anthracis* group B strains from the KNP (personal communication). When comparing the *ppx* gene from *B. anthracis* Kruger B AAEQ00000000 and *B. anthracis* Ames NC003997 an in frame three base pair deletion was apparent. The GAA codes for glutamic acid which can be seen more clearly when analysing the *B. anthracis* Kruger B and *B. anthracis* Ames protein sequences.

After examining the *Bacillus* strains available in the Anthrax Strain Collection (ASC) at the HPA, Porton Down, it was discovered that 19 of the available strains were isolated from the KNP.

The majority of the ASC have not been molecularly typed and designated groups for the 19 strains were not known.

Primers were designed to incorporate the *ppx* gene in a PCR to then use for sequencing to compare the *ppx* region of these strains.

The PCR was optimised and performed on all available strains from the KNP. All strains except one produced a band at 525bp. ASC 207 did not produce a band from the PCR. The PCR product was cleaned up and used directly for sequencing. See Figure 3.25 for the alignment results produced from the sequenced strains.

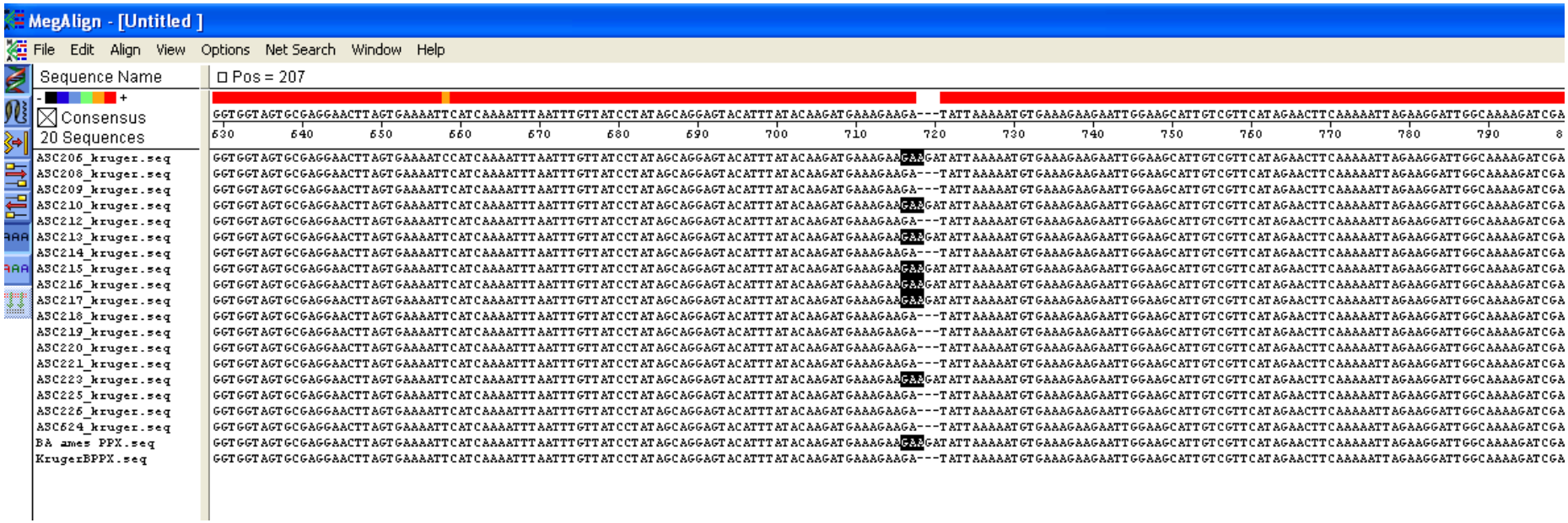

Figure 3.25 Alignment results from Megaline Lasergene v7 by the Clustal W method.

Comparing all 18 *B. anthracis* Kruger isolates from the ASC with *B. anthracis* Ames and the sequenced *B. anthracis* Kruger B strain. The highlighted region shows the glutamic acid which has been lost in 11 of the strains.

3.5.2 Discussion

The *ppx* gene encodes for the enzyme exopolyphosphatase which converts long chain polyphosphates into single phosphate molecules which may then be used for ATP production. Knockout mutants of *ppx* have shown serious side effects such as the *B. cereus* mutants. *ppx* null mutants were found to have a three hours delay in sprorulation and sporulation efficiencies only reached 60% when compared to the wild type (Shi *et al.*, 2004). With the notable deletion of a glutamic acid in the *ppx* sequence in the *B. anthracis* group B strains it may suggest that the exopolyphosphatase structure is altered slightly leading to an alteration of the activity of the enzyme.

Results from the sequencing reaction showed that 11 strains from the KNP isolates had the same 3 base pair deletion when comparing to the *B. anthracis* Ames NC003997 sequence. This would suggest that these strains belong to *B. anthracis* group B. Further VNTR analysis would have to be performed in order to confirm the molecular typing of these strains.

The crystal structure and active sites of the *E. coli* 0157:H7 *ppx* gene has been completed by Rangarajan et al in 2006. Using the *E.coli* 0157:H7 sequence, alignments were constructed with other well characterised *ppx* protein sequences. The conserved regions were identified and a putative poly p binding site was established. Using these alignments the region around the glutamic acid deletion was analysed. The glutamic acid deletion occurs within the α9 chain of the structure and does not form part of the active site or the metal binding site for $MgCl_2$ needed for activity. Unless the crystal structure of the *B. anthracis* Kruger B *ppx* gene was completed it is difficult to say as to whether the structure of the α9 chain would affect the optimal activity of the overall enzyme.

4 Growth Curve Analysis of *Bacillus anthracis* and *Bacillus cereus*

The normal expression levels of the three enzymes; polyphosphate kinase (Ppk), exopolyphosphatase (Ppx) and poly – AMP phosphotransferase (Pap) have not previously been studied in detail in *Bacillus* species. Knockout mutants of *B. cereus* have shown the importance of these enzymes with regards to motility and sporulation. It would be informative to understand when these enzymes are expressed when faced with certain growth environments and in different stages of growth. Inorganic polyphosphate has been associated with the stress response in bacteria so it would be expected that the levels of *ppk* mRNA might increase when entering the stationary phase of growth. At this point the bacteria would sense depleting levels of nutrients (amino acids) and typically switch on genes related to long term survival, triggering what is termed the stringent response. During the stringent response in bacteria, ppGpp is produced which inhibits *ppx* but not *ppk* which leads to the accumulation of long chain poly P. The mRNA levels in this situation should reflect this and therefore show that *ppk* expression continues but *ppx* expression is inhibited during the stationary phase of growth (Kuroda, 2006).

Advances in real time PCR have dramatically changed the field of measuring gene expression. Real time PCR is a technique for collecting data throughout the PCR process as it occurs thus combining the amplification and detection into a single step. Detection is achieved by using fluorescent chemistries that correlate to a specific PCR product. The intensity of the fluorescence during a reaction directly indicates the quantity/concentration of the target PCR product (Higuchi *et al.*, 1993). Consequently, the greater the quantity of target DNA present in the starting material the faster the increase in fluorescent signal yielding a lower crossing threshold (Ct) (Heid *et al.*, 1996).

There are numerous advantages of using real time PCR over traditional PCR with agarose gel based analysis. It can produce quantitative data with an increased dynamic range and does not require a post-amplification processing step as results are collected during the exponential phase not as part of an end point PCR (Wong & Medrano, 2005). Sensitivity of real time PCR is increased substantially. Traditional end point PCR can measure yields of a ten-fold change but real time PCR can detect as little as a two-fold change.

In this particular study the development of a real time RT-PCR assay will indirectly reflect levels of gene expression by measuring the levels of mRNA produced by the target genes.

We investigated the effect of various nutrient defined media on the growth rates of *B. anthracis* and *B. cereus* and compared levels of mRNA expression of the target genes *ppk, ppx* and *pap* against the endogenous 16sRNA internal control gene. The media are a range of specific nutrient content that covers the spectrum between high nutrient availability to very low defined levels of phosphate using the chemically defined medium (CDM) 20 developed specifically for *B. cereus* (Zoe Betteridge, PhD Thesis). The medium includes brain heart infusion broth (BHI) which makes a high nutrient medium. BHI broth was used as a regulator for comparison when analysing gene expression levels because it produces optimal growth conditions with no nutrient limitation until stationary phase is reached. The three defined levels of CDM 20 media are 3.2mM, 0.04mM and 0mM Potassium Phosphate. These media were used as a model to represent a phosphate limited environment to investigate how the poly P genes of interest will be expressed when faced with this nutrient limitation. Basal medium is the medium currently used in the production of the anthrax vaccine. This was also included in this study to look at the levels of gene expression during vaccine production when compared to growth in a high nutrient media. Studies using basal medium were performed with *B. cereus* as a model for *B. anthracis* due to CL3 limitations.

The specific aims of the experiments represented in this chapter were:

1. Test the growth rate of *B. anthracis* in nutrient rich media
2. Test the expression levels of toxins from *B. anthracis* when grown in nutrient rich media
3. Develop and optimise a real time RT-PCR assay to test the mRNA expression levels of the target genes *ppk*, *ppx* and *pap* in relation to an endogenous control
4. Compare growth and mRNA expression levels of *B. cereus* in a variety of media using the optimized real time RT-PCR assay

B. anthracis Sterne ASC1 ($pX01^+$ and $pX02^-$) and *B. cereus* ATCC 14579 were used in these experiments. Each step of the experiment had to be optimized including the amount of culture inoculum used and an accurate measurement of the timing of the different growth phases. Growth in the limited nutrient media meant that a sampling across a growth curve had to be

split over either two or three cultures, each with staggered inoculation times, as the full growth curve from a single culture could not be followed during the core work hours after which the lone working policy is enforced.

During the growth optimisation steps it was found that *B. anthracis* did not grow confluently in the CDM 20 medium. The growth instead formed a clumpy and thick texture which disrupted the optimal density readings and resulted in misleading bacterial counts. Therefore the study concentrated on the mRNA expression levels in *B. cereus*. It turned out to be quite difficult to acquire the results from the *B. anthracis* growth curves due to the length of time needed to perform the experiments and the limitations with regard to the usage of the flexible film isolator. However, results that were produced were useful as a comparison when grown in BHI broth.

4.1 *B. anthracis* growth curve and toxin production in high nutrient broth

B. anthracis was inoculated into pre-warmed high nutrient BHI broth and Optical Density$_{600nm}$ readings were taken every hour to establish when growth started to reach a level which could be sampled for further analysis. The OD_{600nm} was plotted against the time after inoculation in order to work out the generation time of the bacteria.

The generation time was calculated to be 42 minutes for the OD_{600nm} reading to double from 2 to 4 (mid exponential). The *B. anthracis* growth curve can be seen in Figure 4.1.

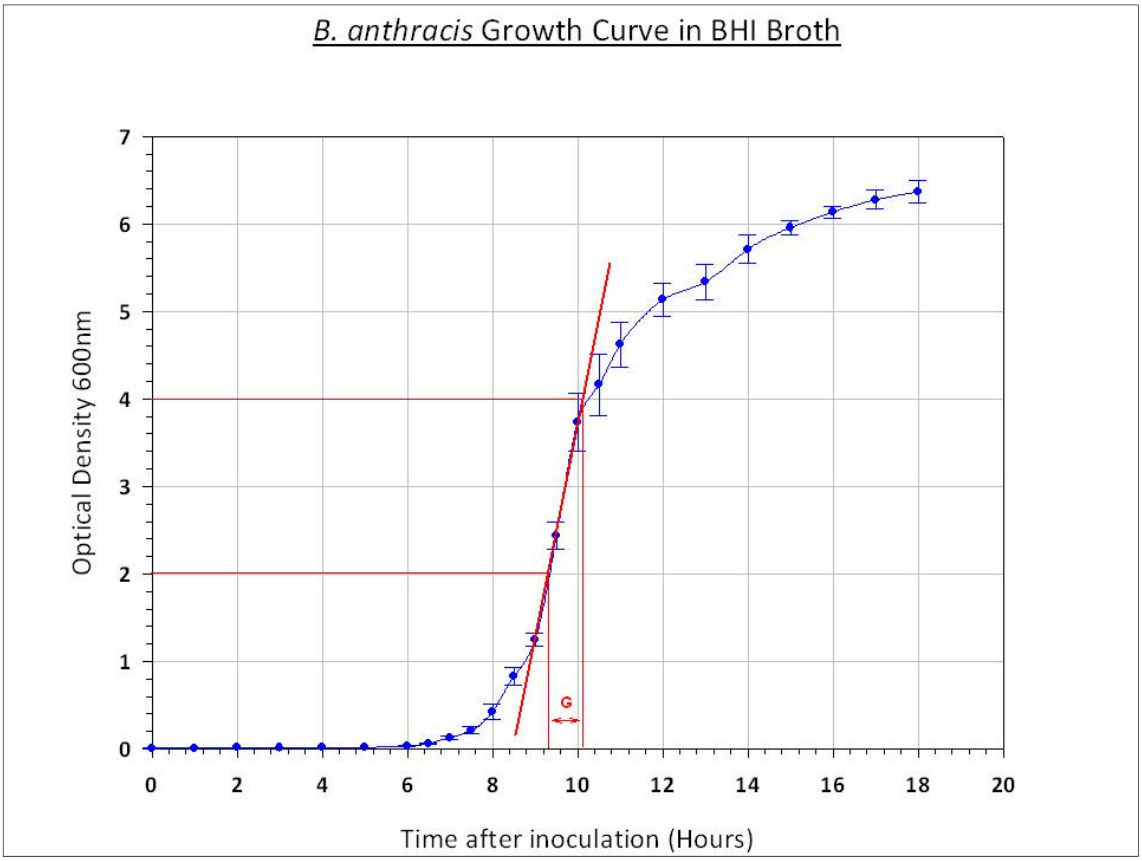

Figure 4.1 *B. anthracis* growth in BHI broth. G = Generation Time.

Samples were taken from time points 5 ½ hours to 10 hours and filtered to assay at containment level 2 after a sterility test was performed. The samples were run on a protein gel to establish the expression levels of toxin proteins PA and LF in comparison with the stage of bacterial growth. Samples taken from 5 ½ hours to 10 hours represent the exponential phase of growth. The 10 hour sample represents the beginning of the stationary phase where growth has started to slow. PA has a mass of 83 kDa and LF had a mass of 90 kDa. The positive controls are marked by an arrow on the gels. These results can be seen in Figure 4.2 and 4.3.

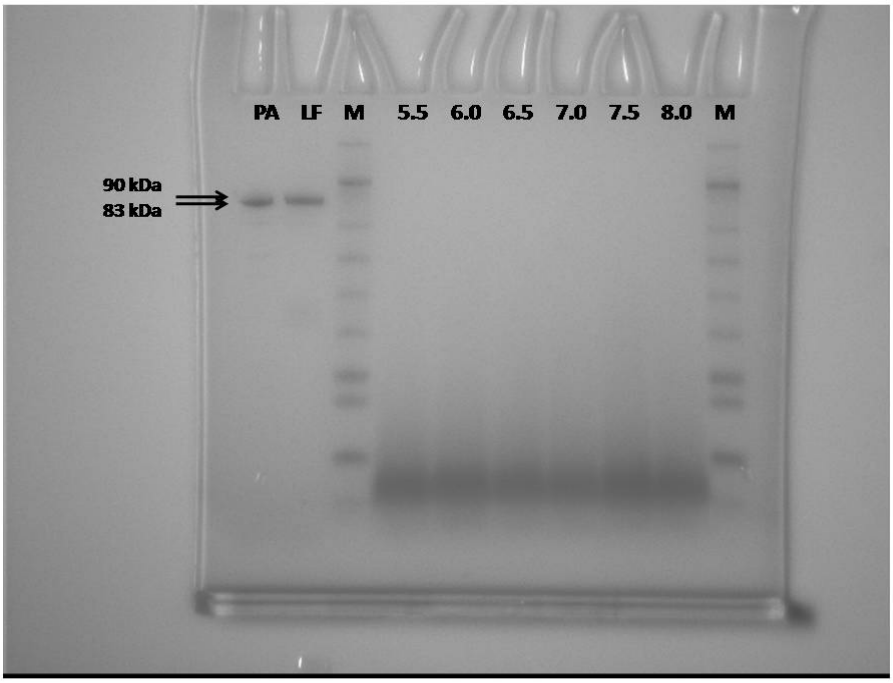

Figure 4.2 *B. anthracis* filtered supernatant from growth curve timepoints. Timepoints 5 ½ hours to 8 hours. Lanes 1 and 2 contain positive control Protective Antigen (PA) and Lethal Factor (LF), Lanes 3 and 10 (labelled M) contain the simply blue protein marker.

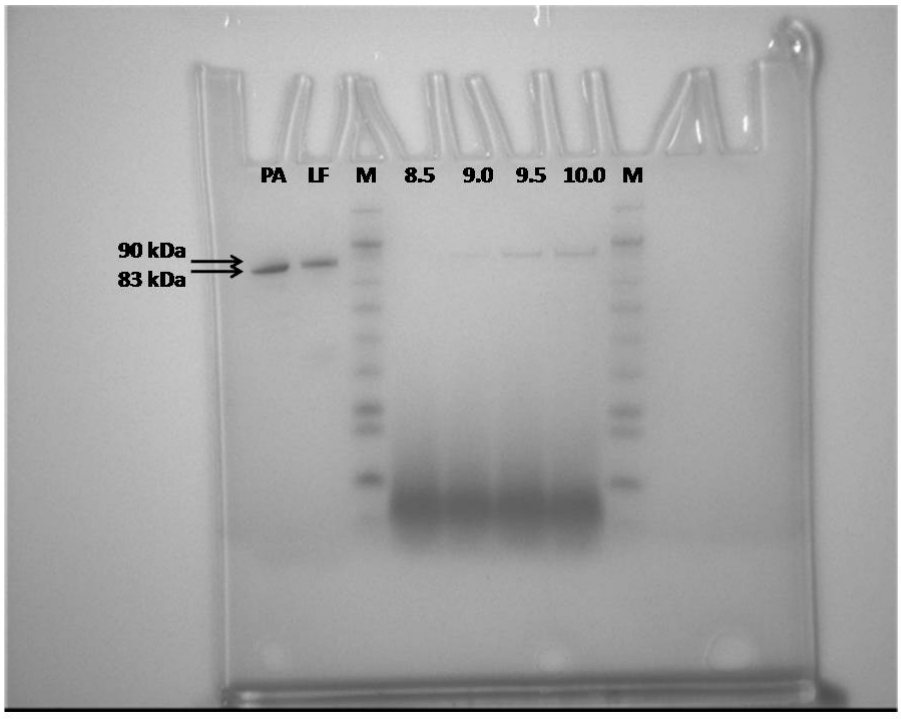

Figure 4.3 *B. anthracis* filtered supernatent from growth curve timepoints. Timepoints 8 ½ hours to 10 hours. Lanes 1 and 2 contain positive control Protective Antigen (PA) and Lethal Factor (LF), Lanes 3 and 8 (labelled M) contain the simply blue protein marker.

These data clearly show that toxin protein production becomes detectable at 9.0 hours of growth onwards gradually becoming more distinct. Toxin production begins late in the exponential phase of growth when grown in high nutrient BHI broth.

In order to distinguish between the two toxin proteins a western blot was also performed on the same time point samples. The positive control PA and LF can be seen marked with an arrow and expected size. LF western blot results can be seen in Figure 4.4 and PA western blot results can be seen in Figure 4.5.

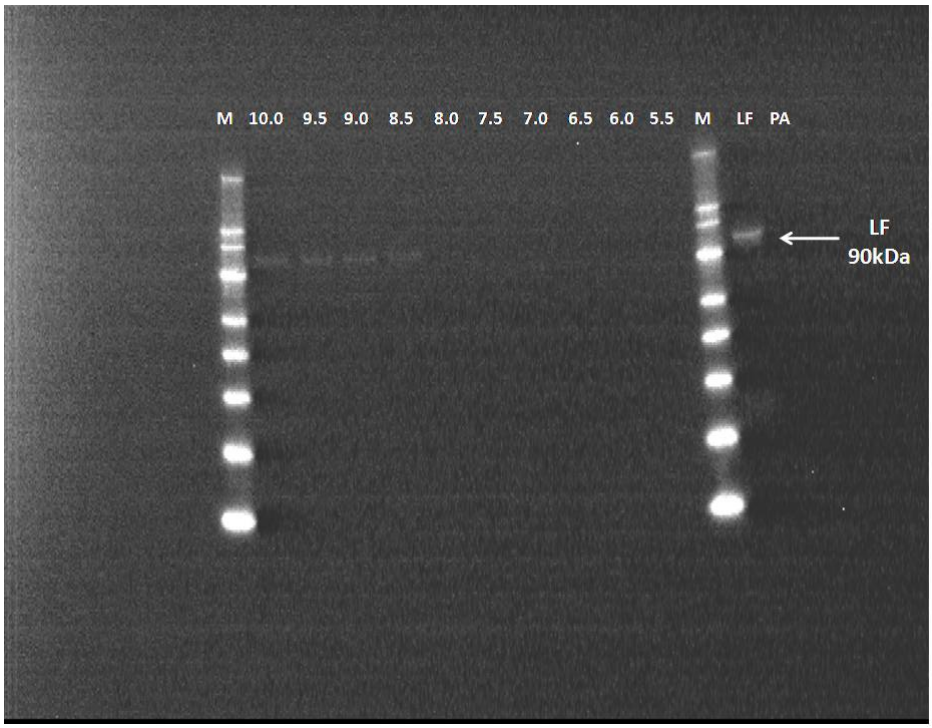

Figure 4.4 Western blot for LF: *B. anthracis* time point samples; 5.5 hours to 10 hours. Western blot was incubated with αLF Rab 727B followed by anti-rabbit horse radish peroxidise conjugate. Lanes 1 and 12 (labelled M) contains the protein marker, lanes 2 – 11 contain the timepoint samples 5.5 to 10.0 hours. Lanes 13 and 14 contain the positive control Lethal Factor (LF) and the negative control Protective Antigen (PA) respectively. LF positive control is marked with an arrow.

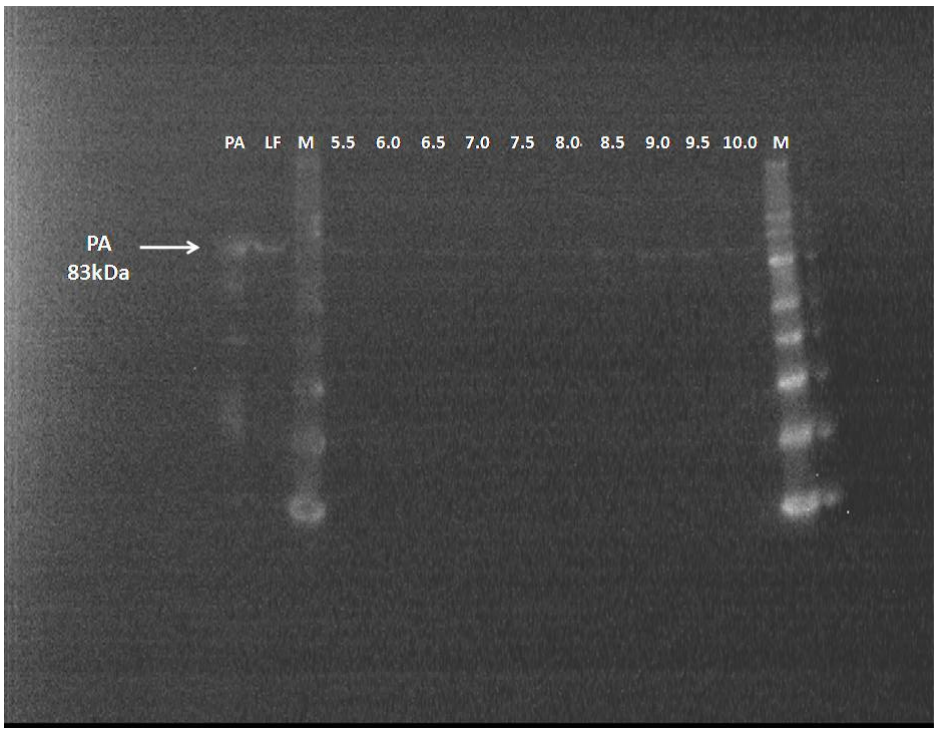

Figure 4.5 Western Blot for PA: *B. anthracis* time point samples; 5.5 hours to 10 hours. Western blot was incubated with αPA Rab 446B followed by anti-rabbit horse radish peroxidise conjugate. Lanes 1 and 2 contain the positive control Protective Antigen (PA) and negative control Lethal Factor (LF) respectively. Lanes 3 and 14 (labelled M) contains the protein marker. Lanes 4 – 13 timepoint samples 5.5 to 10 hours.

From these blot results it is clear that LF toxin levels are detectable from 8.0 hours which shows that the western blot is a more sensitive assay than the protein gel. The PA western blot results also shows that PA is detectable earlier and seems as though there is some amount of PA present from the first time point sample which may have been an ambiguous result which can also be supported by the positive result of the LF negative control on this particular blot.

Both the protein gels and western blot results show that the PA and LF toxins are expressed in the late exponential phase of growth. This is expected as similar results are achieved using the vaccine production media, however, these experiments were performed in a high nutrient media.

4.2 Development and optimisation of the real time RT-PCR assay

There are many aspects to consider when developing a real time PCR protocol for use in gene expression studies. Each step from the initial RNA extraction to the data analysis must be carefully designed and optimised in order to produce the accurate reliable data.

The main steps performed during a real time PCR experiment are highlighted in Figure 4.6.

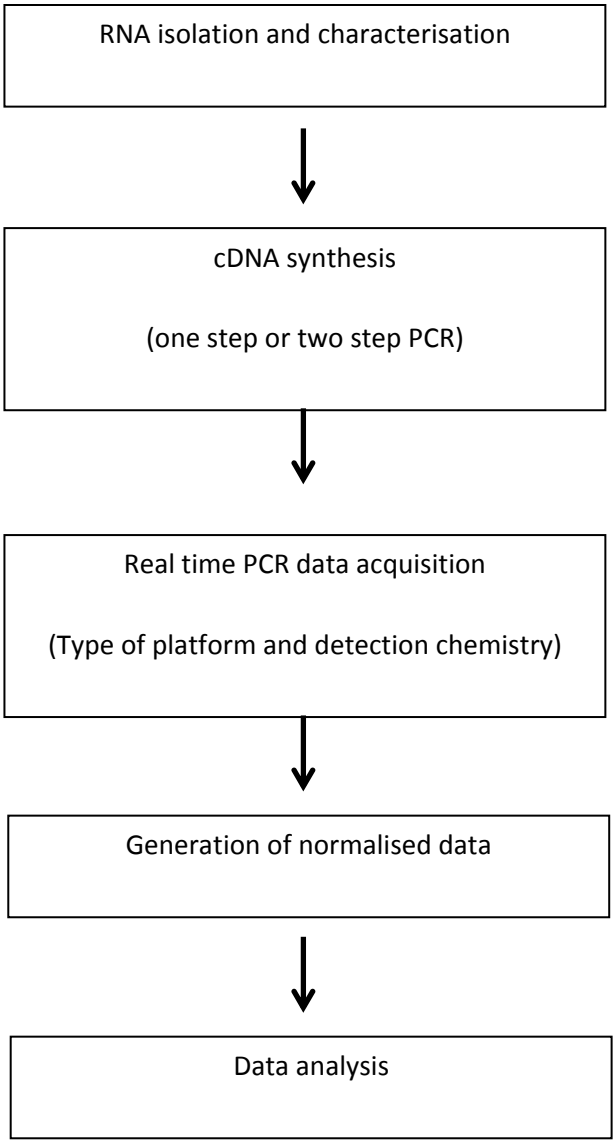

Figure 4.6. Steps performed when measuring gene expression using real time PCR. (Adapted from Wong & Medrano, 2005).

4.2.1 mRNA Isolation and Characterisation.

Isolation and characterisation of mRNA is one of the most important steps in the development of the real time RT-PCR assay. If there is not enough transcript or the quality of the yield is sub-

standard then the data produced will not accurately reflect the true nature of the gene expression levels.

During this study, mRNA extraction methods were optimised from three different kits:

1. RNA Ribopure™ Bacteria, Ambion
2. RNA Protect Bacteria RNeasy Kit, QIAgen
3. Trizol, Invitrogen

One problem occurred when extracting mRNA from the earlier time point samples due to the low levels of biomass. Initial amounts of mRNA were extremely low and after extraction and DNAse digest using the QIAgen spin columns, levels of mRNA were even more reduced. Contaminating DNA also proved to be a problem requiring additional DNA clean up steps which consequently further reduced the final yield of mRNA. In order to extract enough mRNA for the real time PCR assay the method using Trizol was adopted. This method reproduced the highest levels of mRNA and retained a sufficient amount after additional DNA digest steps.

Quality and integrity of the mRNA was measured on a Nanodrop Spectrophotometer. When measuring the absorbance ratios of DNA and RNA the ideal reading should be between 1.8 - 2.0 (Sambrook J. *et al.*, 1989). This is important for both ratios of OD 260/280 and OD 260/230. Results that fall within this range indicate that the DNA/RNA is pure. When comparing measurements from all three extraction methods, the Trizol extraction produced a higher quality yield of mRNA with a higher number of samples falling within this required range.

4.2.2 Optimisation of primers and probes and calculation of primer efficiencies between targets

The real-time PCR assay was designed for the target genes *ppk*, *ppx* and *pap* using TaqMan® chemistries. Two endogenous internal control genes (GyrB and 16srRNA) were used in the optimisation steps in order to assess which one may be more effective in the assay. The primer and probe sequences are shown in materials and methods Table 2.4.

Primers were optimised using *B. anthracis* Sterne genomic DNA in a serial dilution to assess the sensitivity of the assay. The 16srRNA and GyrB targets were optimised for use as an endogenous control and used as a normaliser to study the up/down regulation of gene expression in a variety of chemically defined media. The optimised amplification plots are shown in Figure 4.7. The assays were optimised on the ABI 7900HT platform using the ABI universal master mix.

Figure 4.7 a. Amplification plot for the optimised *ppk* assay. b. Amplification plot for the optimised GyrB assay. c. Amplification plot for the optimised 16srRNA assay. Amplification efficiencies of the PCR primers are an important consideration when performing relative quantitation. When calculating gene expression you could assume that the amplification is ideal and that each amplification of the target gene against the endogenous control is equal to each other, conversely, this is often not the case.

PCR primer efficiencies between the endogenous controls and *ppk* (the target gene) were calculated using the comparative Ct ($2^{-\Delta\Delta Ct}$) method. This compares the Ct values of a serial dilution between the endogenous control and the target gene. See Figure 4.8.

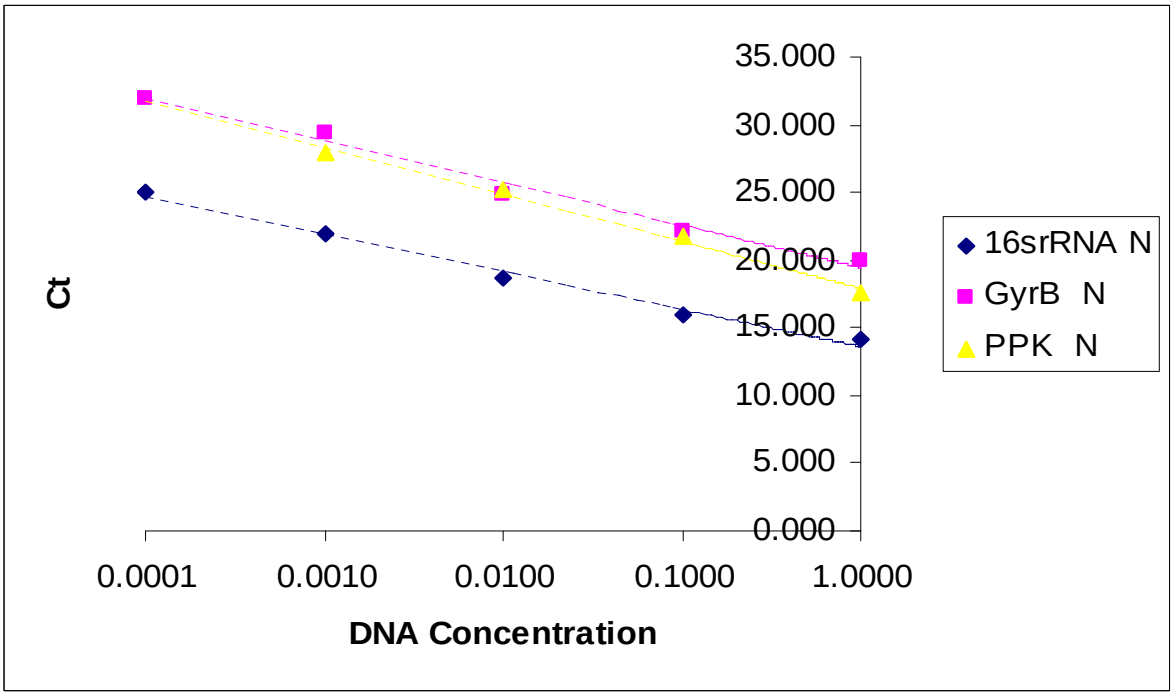

Figure 4.8 Average Ct values of each primer set.

When comparing the average between the sets of primers and probes the plot should be parallel. But as can be seen in Figure 4.9, the plots are not.

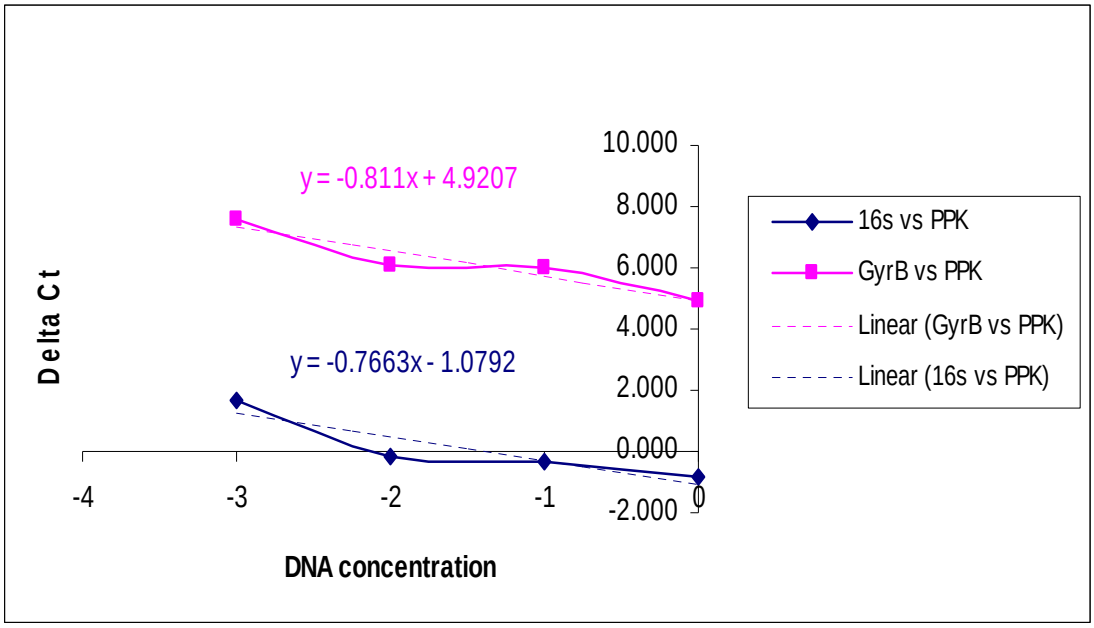

Figure 4.9. Delta Ct values against DNA concentration when comparing the two endogenous controls with the *ppk* target gene.

The primer efficiencies of the endogenous controls and the target genes were not comparable and could not be used in a direct comparison using the comparative Ct ($2^{-\Delta\Delta Ct}$) quantitative method. The standard curve method was then optimised for use in this study.

The standard curve method uses standardised amounts of cDNA to compare the Ct values from the samples. By using the standard curve as a comparison, increased or decreased levels of mRNA expression can be calculated.

4.2.3 Optimisation of assay design

A real time RT-PCR the assay can be done either as a one-step reaction with synthesis of cDNA and PCR amplification performed in a single tube or as a two-step reaction where the cDNA is synthesised in a separate reverse transcription reaction. There are several advantages and disadvantages associated with each method. The one-step method is considered to minimize variation in the assay as both steps are performed in a single tube, but it is likely to be less sensitive than the two-step method. The one-step method uses an RNA starting template each time which can degrade rapidly, therefore, a one-step reaction may not be suitable for samples that are assayed over a period of time in a number of different assays. The two-step method is more sensitive and stable over time but with the extra step there is a risk of introducing DNA contamination into the PCR reaction.

The one-step method was tested in this study but results were not as reliable as the two-step method. It was also decided that due to the amount of samples and the vast amounts of assays to run for each sample it would be more accurate to perform the RT step first and store the cDNA while the assays were being performed. Using the two-step method allowed for optimisation of the RT step with a variety of RT kits that were available. Two kits were tested; QuantiTect Reverse Transcription Kit, QIAgen and High Capacity cDNA Reverse Transcription Kit, Applied Biosystems.

The QuantiTect Reverse Transcription kit included an integrated step for the removal of contaminating genomic DNA which proved to be an important factor. The High Capacity cDNA Reverse Transcription kit did not have this extra step which meant that the RT negative control often came up positive; a sign of genomic DNA contamination. If the High Capacity cDNA Reverse Transcription kit were to be used there would have to be an extra DNA digest step beforehand which increased opportunities for error. The QuantiTect Reverse Transcription kit was chosen for use in the two-step RT-PCR.

There a number of real time PCR master mixes available for use on the ABI 7900HT machine. Two supplied by Applied Biosystems were tested. The TaqMan® Universal PCR Master Mix can be used for basic real time PCR and can also be used for gene expression studies. Applied Biosystems also produce a TaqMan® Gene Expression Master Mix which they claim to be more sensitive for gene expression analysis.

Both of these kits were tested and surprisingly the TaqMan® Universal Master Mix produced higher Ct values and showed a higher sensitivity than the TaqMan® Gene Expression Master Mix. Therefore, the TaqMan® Universal Master Mix was used throughout the study.

4.3 *Bacillus* growth curve studies

B. anthracis and *B. cereus* were used in growth curve studies to analyse the growth characteristics in a variety of nutrient limited media. These growth curves were also used to collect time point samples for analysis using the optimised real time RT-PCR assay for the analysis of *ppk*, *ppx* and *pap* mRNA levels. As mentioned previously, the use of media with varied levels of potassium phosphate represents a phosphate limited environment the result of which would be reflected in the gene expression study.

4.3.1 *B. cereus* growth curve analysis

B. cereus was grown in BHI broth and samples taken at different time points for OD_{600nm} measurement and RNA extraction. The accumulative growth curve results can be seen in Figure 4.10.

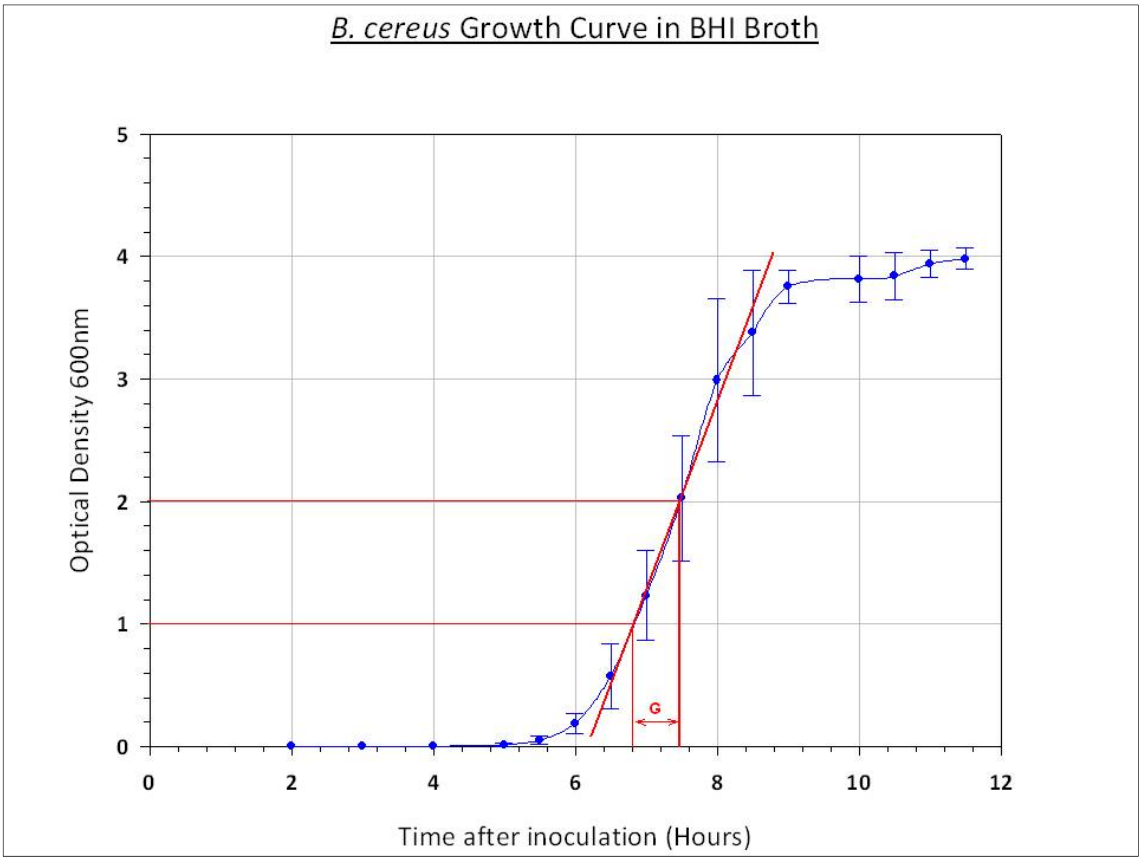

Figure 4.10 *B. cereus* grown in BHI broth. G = Generation Time.

Growth in BHI showed an expected sigmoid growth curve. The lag phase lasted for approximately 5 hours. The exponential phase lasted for approximately 4 hours with a generation time of 42mins which was calculated from the time taken for the OD_{600nm} to double from 1 to 2 during the exponential phase. Stationary phase began between 8 and 9 hours post inoculation.

B. cereus growth in CDM20 (3.2mM potassium phosphate) showed a similar sigmoid growth curve to the one produced by growth in BHI broth. The lag phase lasted for approximately 5 hours. The exponential phase lasted for approximately 7 hours with a generation time of 100 minutes which was calculated from the time taken for the OD_{600nm} to double from 1 to 2 during the exponential phase. The stationary phase began at approximately 12 hours. There were a few unusual OD_{600nm} readings during these experiments and were reproducible in each growth curve. At 8 and 10 hours after inoculation the OD can be seen to spike creating a step like structure to the growth curve. Results can be seen in Figure 4.11.

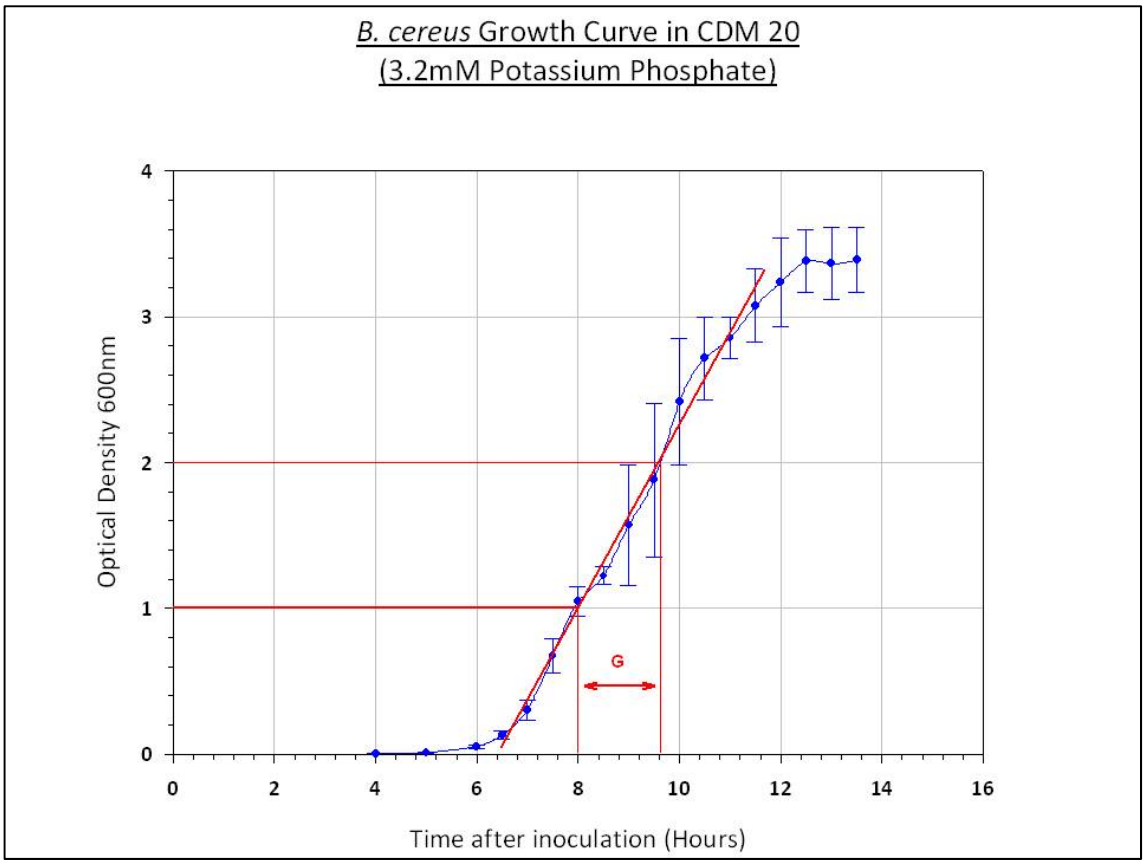

Figure 4.11 *B. cereus* grown in CDM20 (3.2 mM potassium phosphate)

B. cereus growth in CDM20 (0.04 mM potassium phosphate) had a 6 hour lag phase which entered into the exponential phase with a much longer generation time of 100 minutes. This was expected due to the limited nutrient media. The exponential phase lasted for 8 hours but the stationary phase was less defined as growth just seemed to slow very gradually unlike the BHI broth and CDM 20 (3.2 mM potassium phosphate). Results can be seen in Figure 4.12.

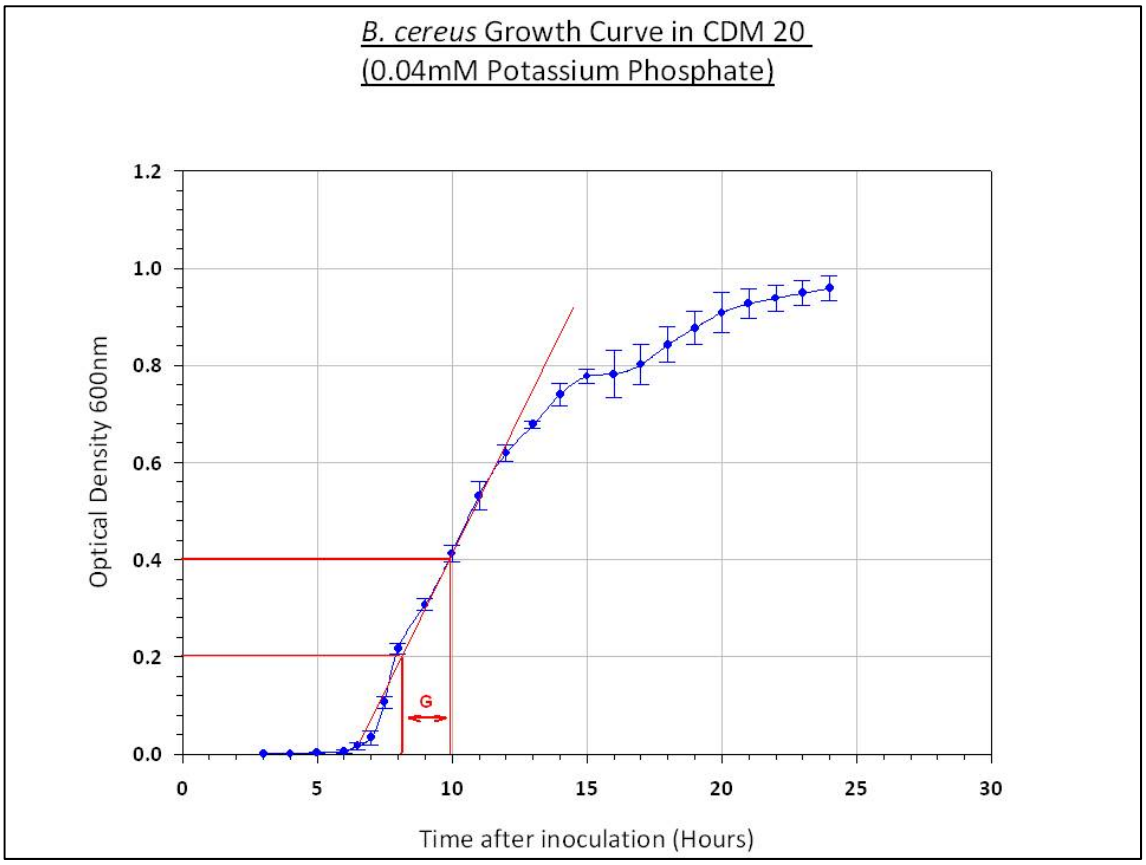

Figure 4.12 *B. cereus* grown in CDM 20 (0.04 mM potassium phosphate)

Growth of *B. cereus* in CDM20 0 mM potassium phosphate showed to be very weak although the lag phase remained at 6 hours which was the same when compared to the higher nutrient media. The exponential phase lasted for around 8 hours, similar to when grown in CDM 20 (0.04 mM potassium phosphate) and generation time was also similar at 100 minutes. The stationary phase started at around 14 hoursbut the OD slowly kept increasing throughout the experiment. Samples were taken for OD measurements up to 36 hours. Results can be seen in Figure 4.13

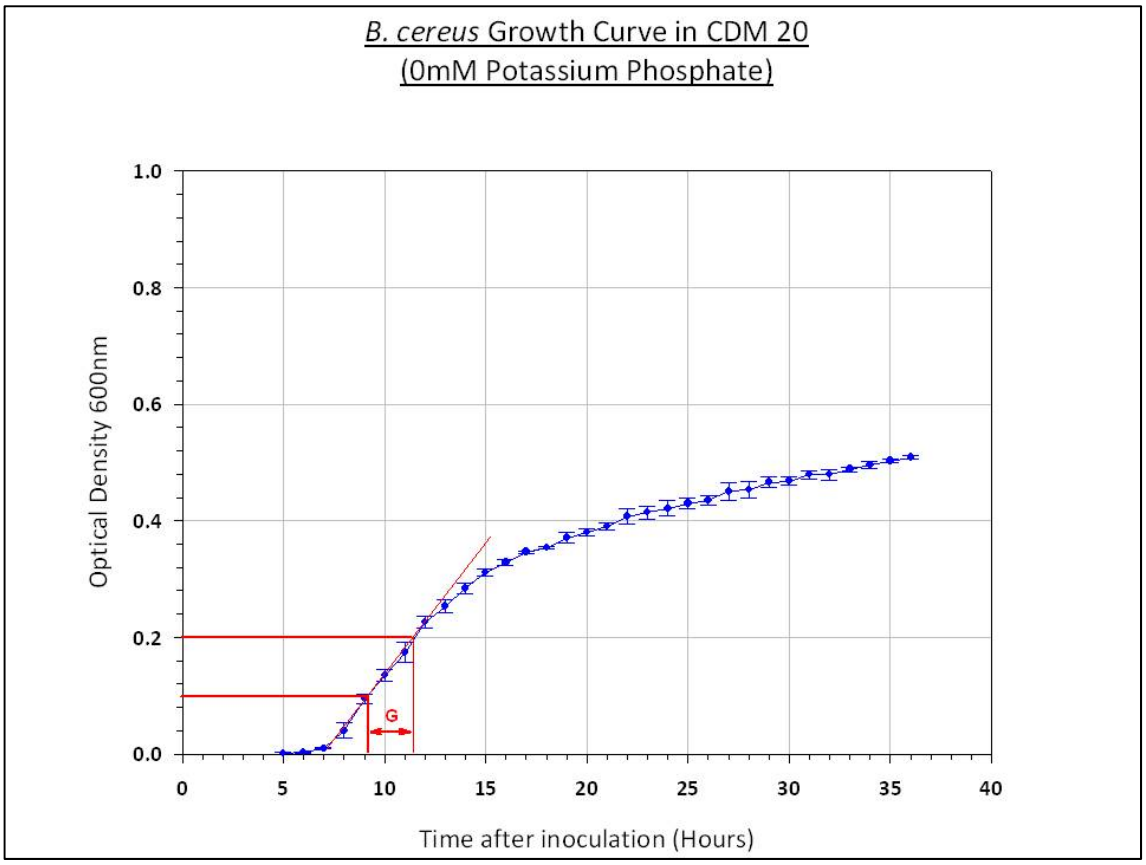

Figure 4.13 *B. cereus* growth in CDM 20 (0 mM potassium phosphate)

B. cereus was also grown in basal medium. Basal medium is the chemically defined medium in which anthrax vaccine is produced. Growth in basal medium produced a similar lag phase at 6 hours followed by a distinct exponential phase that lasted for 7 hours with a generation time of 60 minutes. Stationary phase started at 13 hours after inoculation. The stationary phase in basal medium was very distinct and produced some unexpected OD measurements. The OD_{600nm} spiked at 18 hours from 0.55 to 0.8. This was unusual and a similar effect was not seen in the other media. Results can be seen in Figure 4.14.

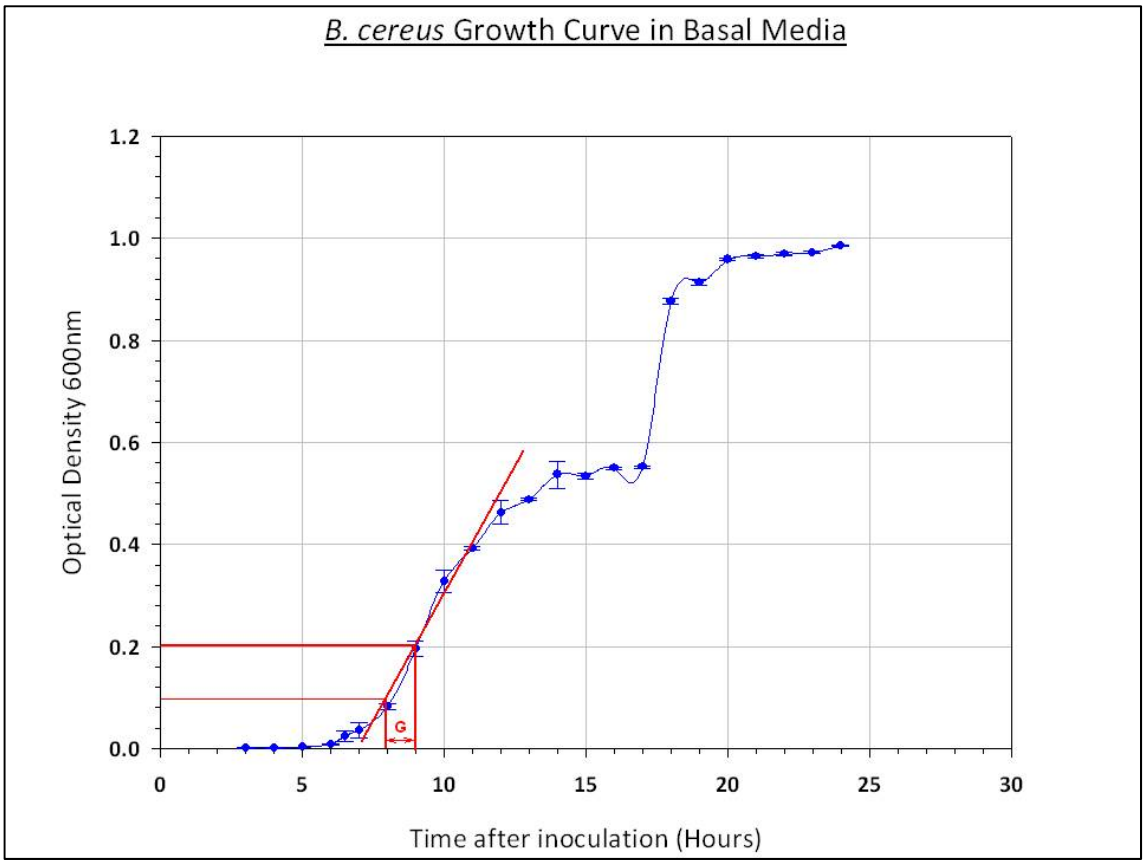

Figure 4.14 *B. cereus* growth in Basal medium

The collective results from the growth curve experiments in Table 4.1 clearly shows that *B. cereus* found the high nutrient conditions of the BHI broth more favourable than the chemically defined medium.

Bacillus strain	**Media**	**Generation Time (Minutes)**
Bacillus anthracis	BHI	42
Bacillus cereus	BHI	42
Bacillus cereus	CDM20 3.2mM Potassium phosphate	100
Bacillus cereus	CDM20 0.04mM Potassium phosphate	100
Bacillus cereus	CDM20 0mM Potassium phosphate	100
Bacillus cereus	Basal Medium	60

Table 4.1 Generation times from growth in all media.

4.3.2 Real time RT-PCR results

The real time RT-PCR was performed on the ABI 7900HT using the optimised assay as discussed previously in section 4.

RNA extracted from various time points was quantified using the NanoDrop. 100ng of RNA was used in each cDNA synthesis reaction. This was then used as a template for the real time PCR comprising of the four targets; *ppk, ppx, pap* and 16srRNA (performed in triplicate). Each single reaction contained 5ng of template. The real time PCR was performed on a 384 well format and incorporated a standard curve on each plate to account for any plate variation. A negative control containing nuclease free water instead of cDNA template was run for each target to control for any DNA/RNA contamination. In addition, a RT negative control was run for each sample to show that there was no residual genomic DNA contamination from the RNA extraction and clean up steps. The baseline threshold for analysis was fixed at 0.2 in order to standardise results from each of the PCR assays.

The raw data consisting of the Ct values from the assays was analysed in the following steps:

1. Average Ct value from triplicate samples
2. All results normalised against the appropriate standard
3. Result normalised against the 16srRNA endogenous control
4. Results compared to the calibrator result (*B. cereus* grown in BHI broth)

The calibrator (*B. cereus* grown in BHI broth) becomes the x1 sample and all other quantities are expressed as an n-fold difference relative to the calibrator. Results can be seen in Figure 4.15.

Figure 4.15 Relative mRNA levels of *B. cereus* in nutrient limited media compared to *B. cereus* in BHI broth

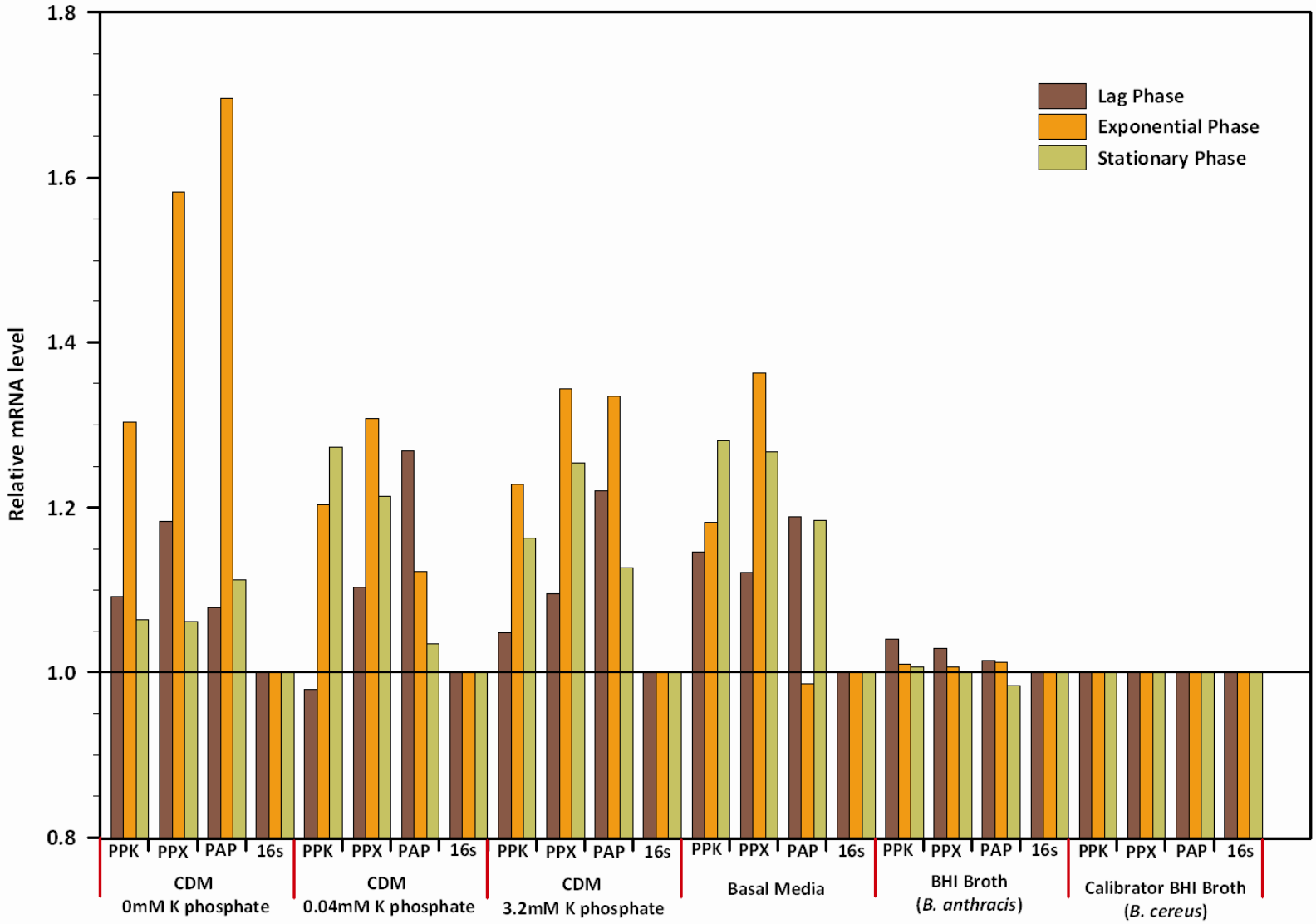

The normalised RT RT-PCR results clearly show differences between levels of mRNA in the high nutrient media when compared to the low nutrient CDM. Elevated levels of *ppk, ppx* and *pap* mRNA can be seen at all phases of growth in CDM 0mM Potassium Phosphate when compared to growth in high nutrient BHI broth. The predominant difference being that of *ppk, ppx* and *pap* during the exponential phase. Levels of *pap* mRNA reach a 0.7 fold increase when compared to *B. cereus* in BHI broth. Levels of *pap* mRNA in CDM 0.04 and 3.2mM potassium phosphate and basal media were lower ranging from a 0 to 0.3 fold increase.

In CDM 0mM potassium phosphate, the most limited nutrient medium; it was interesting to see that the levels of mRNA during the stationary phase did not increase as much as expected. The greatest level of expression during the stationary phase was in fact *pap* mRNA but by a subjectively insignificant 0.05 fold increase.

The mRNA levels expressed in *B. anthracis* when grown in BHI broth were very similar to *B. cereus*. When analysing the target genes there is a slight decrease in mRNA levels through the stages of the growth curve. The lag phase appears to have the highest levels in all three targets which then decrease in steps to exponential phase then stationary phase where the least mRNA is detected.

The most interesting result can be seen in the CDM 0.04mM potassium phosphate when comparing the lag phase and stationary phase. During the lag phase, levels of *ppk* mRNA are far lower than *ppx* and *pap*. When passing through the exponential phase *ppx* mRNA levels become the predominant but this then drops in the stationary phase where *ppk* becomes predominant followed closely by *ppx* and then a lower level of *pap*. This dramatic shift in mRNA level is not reflected quite so obviously in any of the other media, although, a similar pattern can be seen in the lag phase of CDM 3.2mM potassium phosphate and the stationary phase of Basal medium.

4.4 Discussion

Analysing the in vitro growth profiles of *B. cereus* in a variety of nutrient defined media enables a closer examination of the way the bacterium responds to being subjected to a harsh environment. These growth curves provide a foundation with which we can interpret the results of gene expression experiments.

When *B. anthracis* was grown in BHI broth, production levels of PA and LF were comparable to results from previous studies on the vaccine production methods such as Charton *et al*. (Charlton *et al.* 2007). During the vaccine production, toxins were expressed at the end of the exponential phase towards the beginning of the stationary phase (Charlton *et al.*, 2007). In this study, *B. anthracis* was grown in BHI broth to see if the same pattern of toxin expression is reflected in a high nutrient broth when compared to basal media which is used in the vaccine production. Results from the BHI growth curve show that toxin expression can be seen to start at the end of the exponential phase and into the start of the stationary phase (Figure 4.4 and Figure 4.5) which is expected as toxin gene promoter activity and toxin protein yield are highest during these times (Dai & Koehler, 1997).

Growth of *B. cereus* in basal medium was understandably slow with an exponential phase of 7 hours. Nevetheless the OD continued to increase over the whole sampling period (Figure 4.14). The slow growth from the Basal medium growth curve can be explained with reference to the vaccine production experiments (Charlton et al., 2007). When *B. anthracis* is grown in basal medium for vaccine production, the growth is very slow over 32 hours. The growth occurs in stages with a gradual release of nutrients first from the medium then from the degradation of amino acids creating a peak in pH.

In *B. anthracis*, accumulation of (p)ppGpp occurs at the beginning of the stationary phase as nutrient limitation, especially amino acid starvation, becomes apparent. It is the RelA protein that catalases the biosynthesis of the (p)ppGpp effector molecules. The deletion of the *RelA* gene in *B. anthracis* has shown that the accumulation of the effector molecules (p)ppGpp have a crucial role in contributing to sprorulation (van Schaik *et al.*, 2007) and stringent response.

It seems surprising that sporulation conditions are not created during *B. anthracis* vaccine production as nutrient levels are certainly low (Chartlon *et al*. 2007) and the stringent response should be triggered by the degradation of amino acids for a carbon source. Sporulation and maximal production of toxins both occur during entry to the stationary phase. Although mutually exclusive, both seem dependant on a trigger related to nutrient limitation. This intriguing characteristic could be related to the basal media used and it would be interesting to investigate why sporulation seems to be delayed.

Growth in basal medium also showed an unusual OD peak at 17 hours which was reproducible in all of the triplicate curves (Figure 4.14). This peak at 17 hours could be explained by the presence of spores interfering with the OD readings but it is questionable whether this type of interference would be reproducible with very similar OD readings. The vaccine production method has showed that sporulation is delayed and does not occur until much later in the growth curve so this explanation seems unlikely. It could be related to the switch of metabolism in the bacteria to use a new carbon source in the media. Viable cell counts using the plating method could be used to determine if these OD increases reflected actual cell growth some kind of artefact such as extra cellular polysaccharide production. This was an unusual phenomenon which did not occur in any other of the growth curves all of which had been assembled from numerous curves over a long period of time.

The growth curves in these media show a clear difference in the final OD_{600nm} values achieved. As expected there is a clear reduction in final biomass in more nutrient limited medium. Phosphate limitation in the CDM 20 medium also clearly limits final biomass production. For example a decrease from an OD_{600nm} of 3.3 in the 3.2mM potassium phosphate to 1 and then 0.5 in the 0.04mM and 0mM potassium phosphate respectively. Not surprisingly the lower nutrient media have longer generation times of 100 minutes compared to 42 minutes in BHI.

It is interesting to note the similarities between *B. cereus* and *B. anthracis* when grown in BHI broth. It would be expected that they would produce similar growth profiles and they shared a generation time of 42 minutes.

Poly P has been shown to be extremely important in the stringent response of prokaryotes adapting to a harsher environment such as nutrient limitation (Kuroda, 2006). Our RT-PCR analysis revealed the expression levels of the poly P metabolic enzymes of *B. cereus* under nutrient limitation and specifically when the levels of available phosphate are reduced. The RT-PCR analysis was normalised against *B. cereus* grown in BHI broth thus increases or decreases in mRNA levels are in direct comparison to growth in a nutrient rich environment. BHI broth provides the bacteria with no nutrient limitations during lag phase allowing the bacteria to grow exponentially until the nutrients are depleted when the bacteria reach stationary phase.

The mRNA profiles of these three genes in *B. anthracis* and *B. cereus* in BHI broth were very similar (Figure 2.15). One may have expected this to be the case because of the close genetic relationship between these two bacteria. Conversely however gene regulation has been shown to be significantly variable between these bacteria. For example the acquisition of *atxA* and loss of *plcR* in *B. anthracis* has radically altered expression of genes involved in virulence relative to *B. cereus*. These results suggest that the metabolism of poly P is a conserved function in the *B. cereus* group, and part of the bacteria's core-housekeeping activities.

The most notable difference in gene expression was the increase in *ppk, ppx* and *pap* during exponential phase when grown in CDM 20 0mM potassium phosphate (Figure 2.15). During exponential phase, levels of PAP mRNA are higher than *ppx* and *ppk*. This suggests that the phosphate groups from poly P are likely being used to generate ADP from AMP. Levels of *ppx* are higher than *ppk* which also indicates that poly P is being catabolically metabolised, possibly as a source of energy. The functions of *ppx* and *pap* could be are complementary and may work together to release energy which could be used for growth, with excess phosphates released being mopped up by *pap* to generate ADP (which can then be used in ATP production). In addition, ADP can also be used by *ppk* to re-assemble long chain poly P. As discussed in the introduction, it is not clear if poly P has a structural role, catalytic role or indeed as some kind of long term energy store battery.

The mRNA levels of *ppk, ppx* and *pap* genes during lag phase and stationary phase in CDM 20 0mM potassium phosphate are not massively increased and appear to be only slightly higher when compared to a high nutrient environment. This is surprising as poly P is thought to be strongly linked to the stringent response and stressful environments. During stationary phase we would expect to see the activation of the stringent response and production of (p)ppGpp effector molecules which in turn inhibit the activity of *ppx*. This would result in an accumulation of long chain poly P synthesised by the constant levels of the *ppk* enzyme. Results from this study suggest that the expression of all three genes is lowered during stationary phase but that the highest expression levels are from *pap* and not from *ppk*. Interestingly, *ppx* does show the lowest level of mRNA but only slightly less than *ppk*. This combination of expression would result in predominantly an accumulation of ADP instead of long chain poly P. However, *ppk* levels are still higher than *ppx* favouring the assembly and storage of poly P by *ppk* rather than the release of energy from *ppx* activity in the break down down of existing poly P. Overall, this combination of gene expression focuses on the storage of phosphate molecules which would be expected during stationary phase.

During the lag phase, *ppx* shows the highest levels of mRNA suggesting that *ppx* has the highest gene expression. This might be expected during the lag phase in a low nutrient media because *B. cereus* would be struggling to find enough nutrients to grow optimally in exponential phase and releasing stored energy from any poly P would enable the bacteria to grow more efficiently.

In both basal media and in CDM 20 0.04mM potassium phosphate the gene expression profile during stationary phase does reflect that *ppk* levels are at their highest supporting the hypothesis that poly P is accumulated during the stationary phase and during initiation of the stringent response.

Although previous research has shown that the stringent response in *B. anthracis* is not required for virulence (van Schaik et al., 2007) there could still be a relationship between poly P accumulation and the production of the toxins which are produced at the same time during stationary phase. These studies could be continued looking into the mRNA gene expression levels of the toxin genes rather than protein expression to produce more accurate data.

5 *Bacillus* and Amoebae interactions

Bacillus sps. are present naturally in the soil and therefore will regularly come into contact with environmental amoebae such as *A. polyphaga*. Interactions between these species have not been analysed fully.

Previous studies with *B. cereus* vegetative cells have shown that they can be eaten by *A. polyphaga* (de Moraes & Alfieri, 2008). In their natural soil environment however, these *Bacilli* will often likely exist in their spore form which may provide greater resistance to being digested by the phagosomal enzymes. *B. subtilis* has been shown to show resistance to the amoeba *Tetrahymena thermophila* when in its spore form (Klobutcher *et al.*, 2006) so *B. cereus, B. thuringiensis* and *B. anthracis* might be expected to show a similar resistance. In addition, inhaled *B. anthracis*, spores have been shown to germinate only after phagocytosis by lung macrophages. Indeed exposure to superoxide radicals produced in the phagolysosome has been shown to act as a germination signal (Guidi-Rontani *et al.*, 1999). After bacterial phagocytosis amoebae demonstrate an oxidative metabolism which is strikingly similar to the respiratory oxidase burst of neutrophils. This led to the hypothesis that *Bacillus cereus* group spores may also respond in a similar way to phagocytosis by amoebae. In addition, several previous published studies have suggested that a normal ecological niche for *B. cereus* may be to exist as long filaments anchored onto cell surfaces with the lumen of invertebrate (Insect, Woodlouse and Earthworm) guts (Feinberg *et al.*, 1999, Margulis *et al.*, 1998).

Investigations were performed on the interaction of several *B. cereus* group strains with *A. polyphaga* under a range of conditions in an attempt to develop both a model system for the evasion of phagocytic destruction and to understand the impact of environmental interactions between these species.

The specific aims of the experiments presented in this chapter were:

1) To test the effect of temperature on bacteria, amoebae co-culture.

2) Test the effect of bacterial cell number on the outcomes of the interactions.

3) To test the differences of amoebal interactions with bacillus spores and vegetative cells.

4) To test the physiological growth characteristics of the bacillus strains in media alone.

5) To test the physiological growth characteristics of the bacillus strains in spent cell free amoeba supernatants.

6) To test the effects of specific inhibitors of amoeba cellular functions on bacillus uptake by the amoebae.

5.1 Results

5.1.1 The interactions between *B. anthracis, B. cereus* and *B. thuringiensis* vegetative cells with *A. polyphaga* over 24 hours

The strains used in this experiment were *B. anthracis*, *B. cereus* and three different strains of *B. thuringiensis*. *B. anthracis* Sterne ASC 1 is a non-pathogenic strain of *B. anthracis* which is used in the production of the *B. anthracis* vaccine. It is the Sterne strain which is characterised as $pX01^+$ and $pX02^-$, so it is toxigenic but does not produce the immunogenic capsule. *B. cereus* ATCC 14579 is the type strain of *B. cereus* which has a fully sequenced and published genome (Ivanova *et al.*, 2003). *B. thuringiensis* subs. *israelensis* strain 4Q5 has been cured of all plasmids except for the pBtoxis which encodes for all six of the toxins in this isolate (Cry4Aa, Cry4Ba, Cry10Aa, Cry11Aa, Cyt1Aa and Cyt2Ba)(Berry *et al.*, 2002). *B. thuringiensis* subs. *israelensis* strain 4Q7 has been cured of all plasmids. *B. thuringiensis* subs. *israelensis* strain 4Q7gfp is the same 4Q7 strain but labelled with a construct expressing the green fluorescent protein, allowing it to be visualised by fluorescence microscopy.

B. cereus and *B. thuringiensis* Q5, Q7 and Q7gfp were co-cultured for 24 hours with *Acanthamoeba polyphaga* in 100% PYG (amoeba) medium, 10% PYG and PBS. Ratios of vegetative bacterial cells to amoeba cells were 100:1, 10:1, 1:1, 1:10, 1:100 as described in the methods. Incubations were performed at 8°C, 18°C, 25°C and at 37°C. In addition each assay plate was duplicated in order to incubate one in the light and one in the dark to control for any effects of ambient light.

Controls included *Acanthamoeba* in 100% PYG, 10% PYG and PBS, and the bacterial strains in 100% PYG, 10% PYG and PBS and sterile PYG alone.

Real time microscopic analysis of the initial interactions

Within 2-4hours of co-incubation the freshly seeded amoebae had attached to the base of the plate (by 20 minutes) and were activity moving around and beginning to phagocytose the *Bacilli,* which were both on the base of the plate and also swimming in the "water column" of the medium. In 100% and 10% PYG vegetative *B. cereus* and *B. thuringiensis* could be seen to actively swim up to the amoebae and then attach onto their exterior. This was a very dynamic situation and difficult to quantify. However it was clear that in some cases the amoebae would proceed to phagocytose the bacteria, seen by motile *Bacilli* present in vacuoles (See Video 5.1) while in other cases bacteria remained in place and then began increasing in numbers on the surface of the amoebae. Typically clumps of bacteria formed in specific areas of the amoeba surface by the accumulation of attaching bacteria (See Figure 5.1). It was less clear whether the attached bacteria were increasing their numbers by dividing in situ. It appeared that the bacteria were using chemotaxis to seek out the amoebae, as they would often change direction toward the amoebae. Once attached many of the *Bacilli* were seen to elongate, growing larger than the normal vegetative cell length.

Figure 5.1 *B. cereus* and *Acanthamoeba* after 4 hours co-incubation at a ratio of 10:1 respectively. A "microcolony" can be seen on the surface of the amoeba. (Red arrow). ×40 magnification.

Experiments with the non-motile *B. anthracis* showed that during early interactions the amoebae were actively predating the vegetative cells but on occasion, as shown with *B. cereus* and *B. thuringiensis*, the bacteria would seemingly attach and increase their numbers. Given the lack of motility we speculate this was mainly due to bacterial proliferation. The microscope within the CL3 containment facility did not have a camera so we are not able to show a micrograph of this.

It should be noted that the PYG containing media are nutrient rich allowing both bacteria and amoeba to replicate irrespective of any interactions. When comparing the co-cultures at different temperatures during the initial interactions, it was clear to see accelerated growth at 25°C and 37°C which was expected as *Bacilli* have an optimum temperature between 25°C and 37°C. At these temperatures *B. cereus* and *B. thuringiensis* were also more motile. Conversely, at 8°C and 18°C growth was very limited and motility was substantially reduced.

There were a lot less interactions in PBS when compared to PYG media during the first 4 hours. The bacterial cells were significantly less motile which would reflect the lack of amoebae interactions. If the bacterial cells have less energy to move around they would be less likely to be able to swim into the amoebae or chemotact toward them. The amoebae were healthy and could be seen moving across the surface of the micoplate.

Real time microscopic analysis of 24 hour interactions

After 24 hours incubation, the control samples were as expected. *Acanthamoeba* appeared healthy in the 100% PYG, 10% PYG and 1xPBS. As expected there were a greater number of *Acanthamoeba* in the 100% PYG control than in PBS. The *B. cereus* controls showed bacterial overgrowth in 100% and 10% PYG and no growth in the PBS control. Some vegetative bacterial cells were seen to have sprorulated in response to the nutrient limitation of the PBS.

The *Acanthamoeba* appeared healthy and normal at 18°C and 22-25°C temperatures. Conversely at 8°C and 37°C a significant number of the *Acanthamoeba* had formed cysts. This prescribed the limits of temperature for use of the amoeba as a model host.

The results from the 8°C co-incubations showed very little growth of the vegetative bacterial cells of all Bacillus strains, and in addition some of the amoebae had formed cysts. There were very few, if any vegetative bacterial cells (of any strain) able to persist when challenged with amoebae at this temperature. At the lower ratios of 1:1, 1:10 and 1:100 free vegetative cells could not be seen at all suggesting complete predation by the amoebae.

After 24hours incubation, in each of bacteria-amoebae challenge experiments in 100% PYG medium showed overgrowth of the bacteria. Some amoebae had become detached from the surface of the wells indicating either cyst formation or cell death. See Figure 5.2. This reflects the greater replication rate of the bacteria versus the amoeba in nutrient rich media.

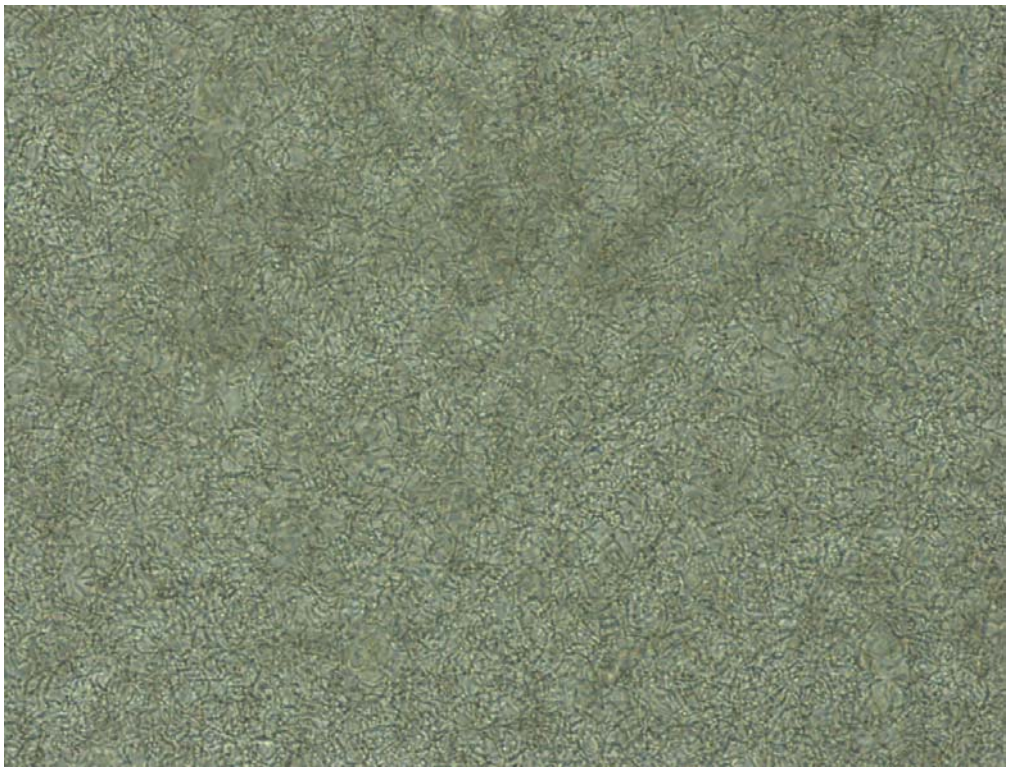

Figure 5.2. Overgrowth of *B. cereus* in a 100:1 bacteria to *A. polyphaga* challenge cultured in 100% PYG.×20 magnification.

Results from co-incubation assays using the more dilute 10% PYG or nutrient free 1xPBS proved to be more revealing regarding our investigations into the interactions between the bacteria and amoebae. In 10% PYG, at the higher ratios of 100:1, and 10:1 bacteria to amoebae, the *Bacillus* again could be seen to outgrow the amoebae and specific interactions could not be visualised. Large clumps of bacterial growth could be seen in areas of the well and often these clumps formed a spiralling growth composed of longer chains of bacillus. This occurred in all strains; *B. anthracis, B. cereus* and all three strains of *B. thuringiensis*. See Figure 5.3.

Figure 5.3. Clumped bacterial growth in a spiralling structure (red arrows).*B. cereus* and *Acanthamoeba polyphaga* at 10:1 bacteria to amoebae in 10% PYG. × 20 magnification.

Importantly, at the lower ratios, 1:1 and 1:10 bacteria to amoebae, cellular interactions could be studied more easily. The *Acanthamoeba* could be seen grazing on the *Bacilli*, engulfing them and holding them within vacuoles, presumably for digestion. However, in many cases the bacteria were seen to attach and form microcolonies on the surface of the amoebae. In many cases the *Bacilli* were seen to form long filaments. See Figure 5.4.

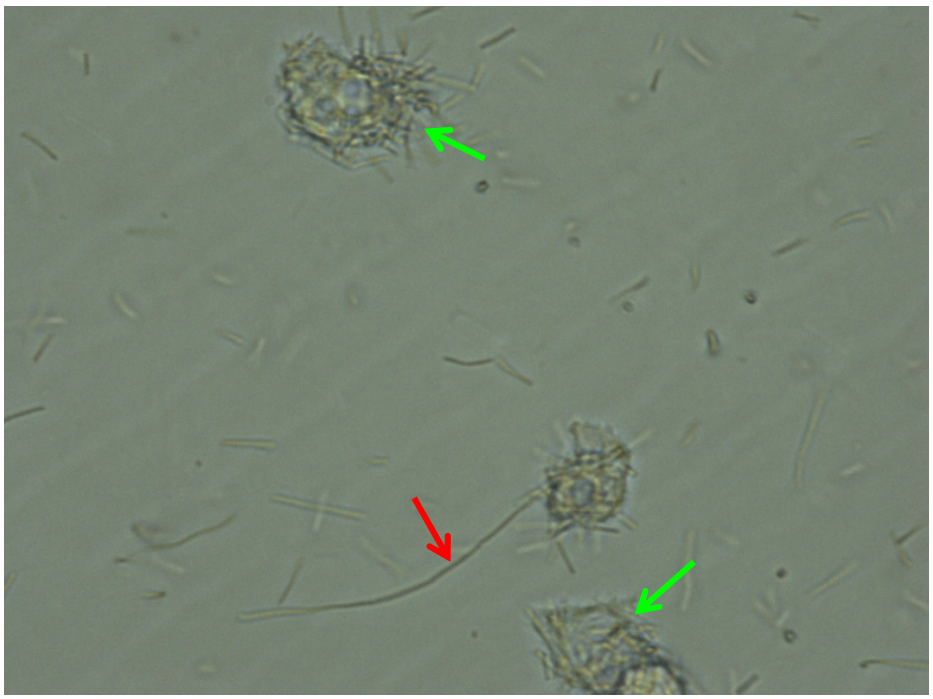

Figure 5.4. *B. cereus* and *Acanthamoeba* at 1:10 ratio in 10% PYG media after 23 hours. Clumped bacterial microcolonies can be seen attached to the amoeba (green arrows) and filamented *B. cereus* (red arrows).× 20 magnification.

Even with the presence of the attached microcolonies the *Acanthamoeba* cells typically remained motile and continued to move around, engulfing single celled *Bacilli* (Video 5.2) Some of the *Bacilli* attached to the surface of the amoebae became filamented, exceeding the normal 2-5µm size of the bacillus rod. It should be noted that motile filamented *Bacilli* could also be seen free in the growth media unattached to amoebae at the lower ratios of 1:10 and 1:1 amoebae to bacteria.

As expected in 100% PBS alone the bacteria could not grow and unsurprisingly most of the vegetative cells were seen to sporulate. Interestingly however we did observe significant bacterial growth when *Acanthamoeba* was also present after overnight incubation. This suggested that the bacteria are able to acquire nutrients from the amoebae cells, either through pathogenic interaction, necromonic scavenging or by a “commensal” utilization of nutrients excreted by the A*canthamoeba* into the PBS medium.

At the lower ratios of *Bacillus* to amoebae (1:10, 1:100) in all strains in both 10% PYG and in PBS we regularly observed the formation of very long filaments. These filaments were often motile and typically entwined together forming rope like structures twisted helically

with a loop at one end where the "rope" had then twisted back on itself producing a complex tertiary structure. See Figure 5.5.

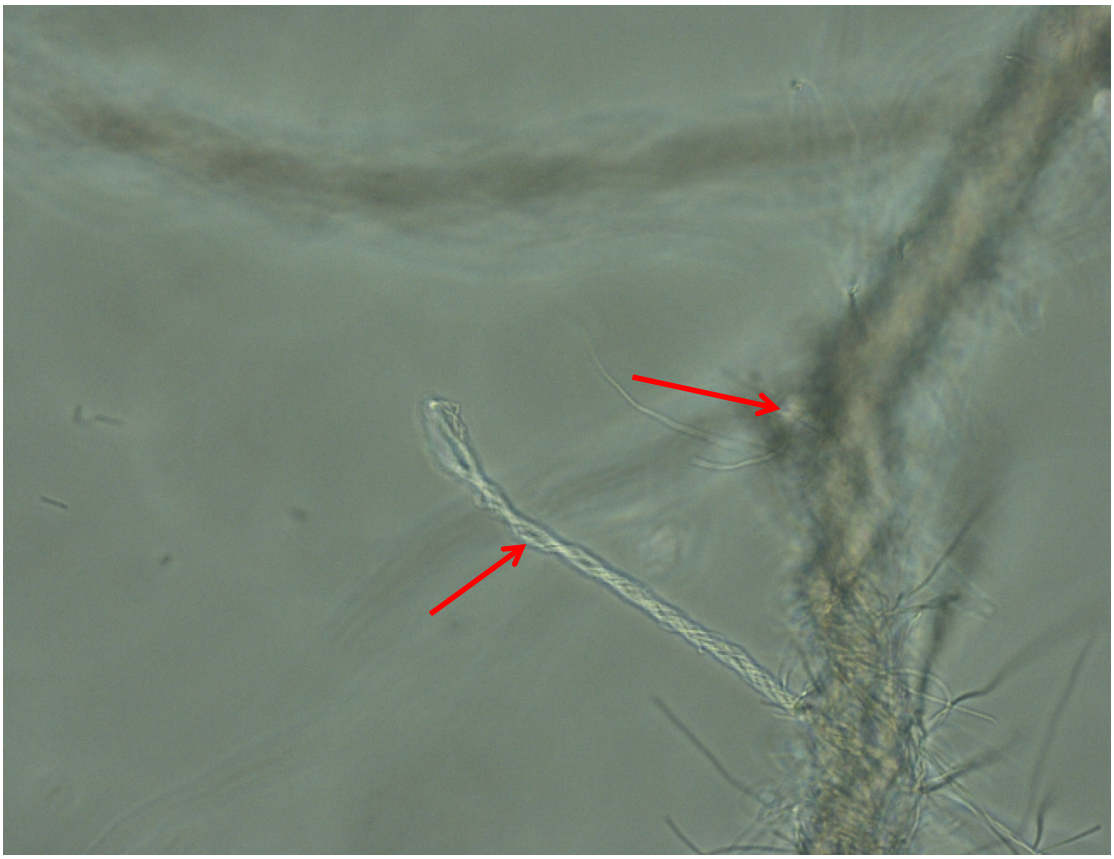

Figure 5.5. Complex rope structure formed by *B. cereus* bacterial growth (red arrow). *B. cereus* at 1:10 bacteria to amoebae after 23 hours in 10% PYG at × 20 magnification.

These rope structures often became very large, some over 1-2 mm long and visible by the naked eye. The *Acanthamoeba* cells did not appear overtly affected by the presence of the ropes, and indeed in many cases the amoebae could be seen moving over the surface of these structures. In any one co-culture not all the *Bacilli* formed ropes, and attached microcolonies in addition to many single motile cells were also still present in these cases. This indicates that these bacteria are capable of complex stociometric developmental switches, with different sub-populations within a clonal culture presuming strikingly different phenotypes. It should be noted that these rope-like structures were formed by all the strains used in these experiments including *B. anthracis*. These data are not shown due to containment limitations of the ACDP III pathogen. It also confirms that this developmental state is a consequence of chromosomal genes shared by all 3 species.

5.1.2 The interactions between *B. anthracis*, *B. cereus* and *B. thuringiensis* spores with *A. polyphaga* over 24 hours

Experiments discussed above in section 5.1.1 were repeated using spores of *B. anthracis*, *B. cereus, B. thuringiensis* Q5, Q7 and Q7gfp instead of vegetative cells. In these experiments the initial interactions for the first 2-4 hours were again examined in addition to the outcomes after 24 h.

Initial interactions

Within 2 hours, spores from all bacillus strains could be seen within the vacuoles of the amoeba at 22-25°C and 37°C See Figure 5.6 and Video 5.3.

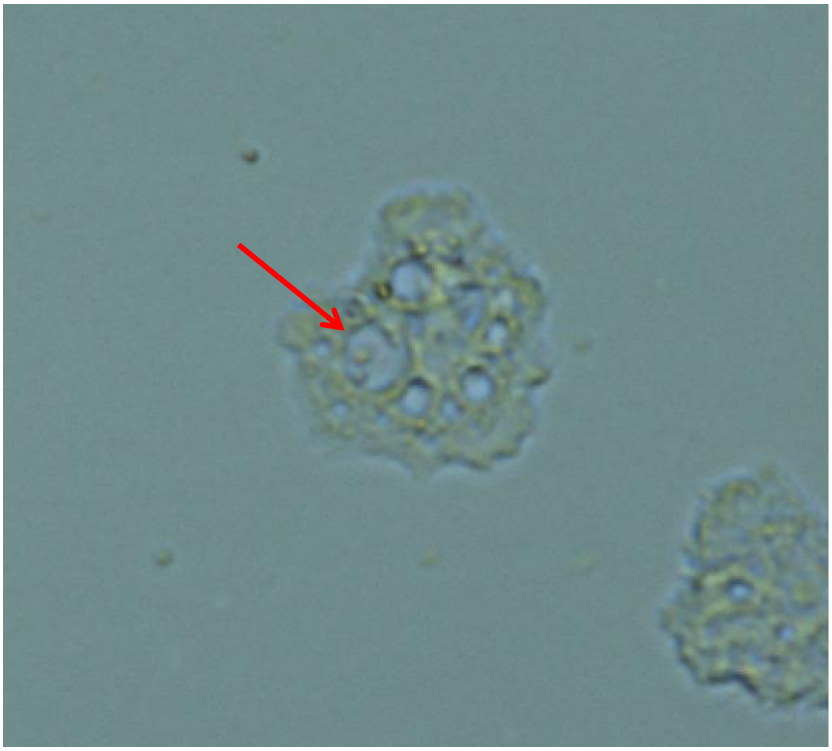

Figure 5.6. *B. cereus* spores contained within amoeba vacuoles (red arrow). *B. cereus* and *Acanthamoeba* at a ratio of 10:1 after 2 hours of co-incubation in 10% PYG at 22-25°C. x 40 magnification.

Both at 8°C and 18°C within the first 4 hours there were no changes from the initial co-inoculation; spores were not seen within vacuoles and spores were not seen to germinate.

After 2-3 hours in 100% PYG and 10% PYG at 37°C, some spores could be seen germinating in the surrounding media and bacterial cells were seen to attach to the external surfaces of the *Acanthamoeba* where they then began to grow as long filaments. Germinated *Bacilli* and spores could also be seen in the vacuoles of the amoebae. It was not clear if these spores had germinated in the surrounding medium before phagocytosis, or if they had germinated within the phagosome. See Figure 5.7 Figure 5.8.

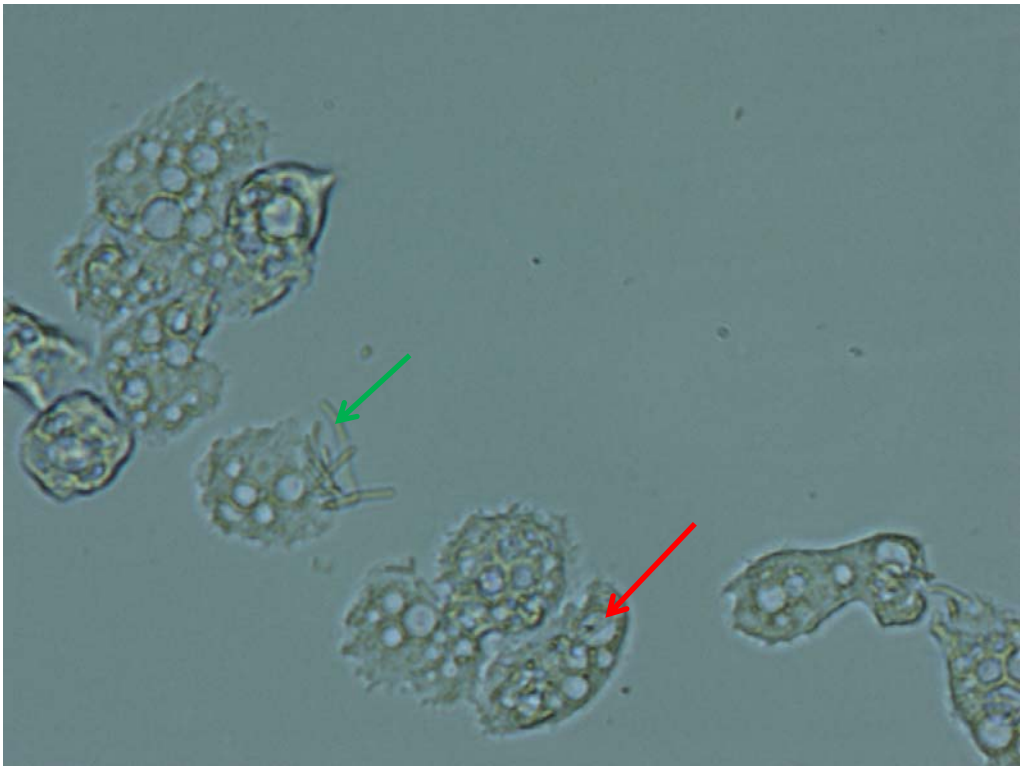

Figure 5.7. *B. thuringiensis* 4Q7 attached to the surface of *Acanthamoeba* and growing in filaments (green arrow). Germinated *Bacilli* are also visible in the vacuoles of the amoebae (red arrow). *B. thuringiensis* and *Acanthamoeba* at ratio 10:1 in 10% PYG at 37°C after 3 hours of co-incubation with *Acanthamoeba*. × 40 magnification.

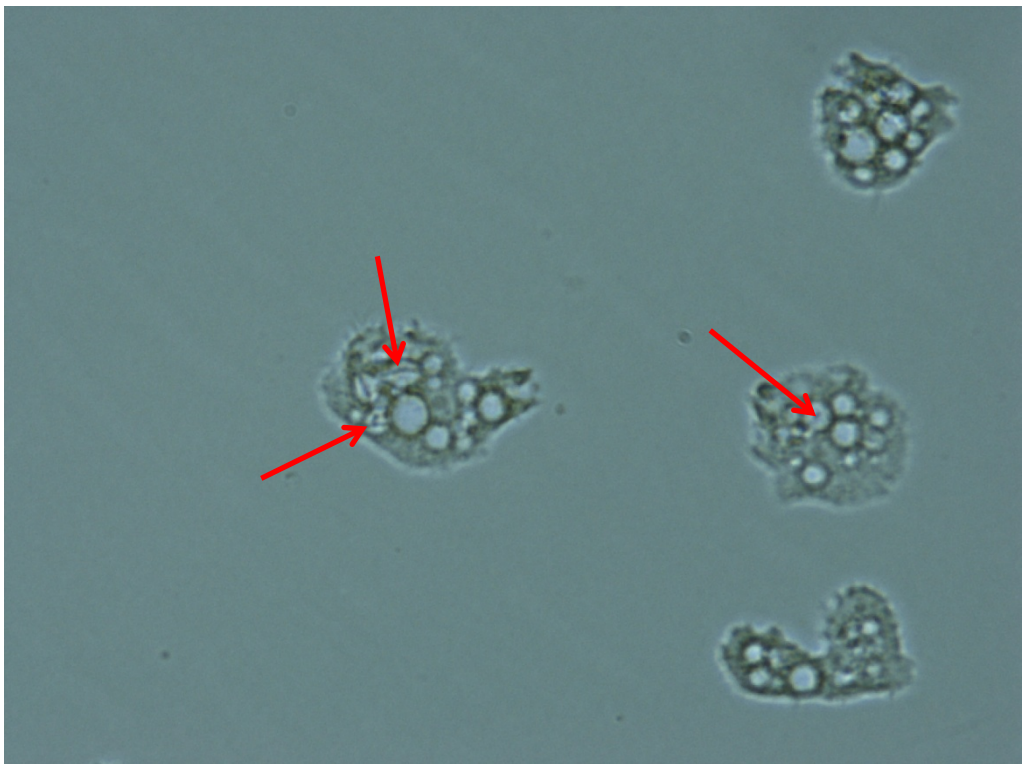

Figure 5.8. Germinated *B. cereus* in vacuoles of amoeba (red arrows). *B. cereus* and *Acanthamoeba* at ratio 10:1 bacteria to amoebae in 10% PYG 37°C after 3 hours of co-incubation. ×40 magnification.

After 5 hours incubation at 37°C some of the *Bacillus* filaments became very long. Some were attached to the amoebae while others remained free in the media. See Figure 5.9. In many cases it was possible to see *Acanthamoeba* cells presumably attempting to graze on these filamented *Bacillus* cells. In the cases of the shorter filaments (cell lengths of less than approximately 5µm), the amoebae were successful at phagocytosis and digestion. However with longer filaments this became impossible for them.

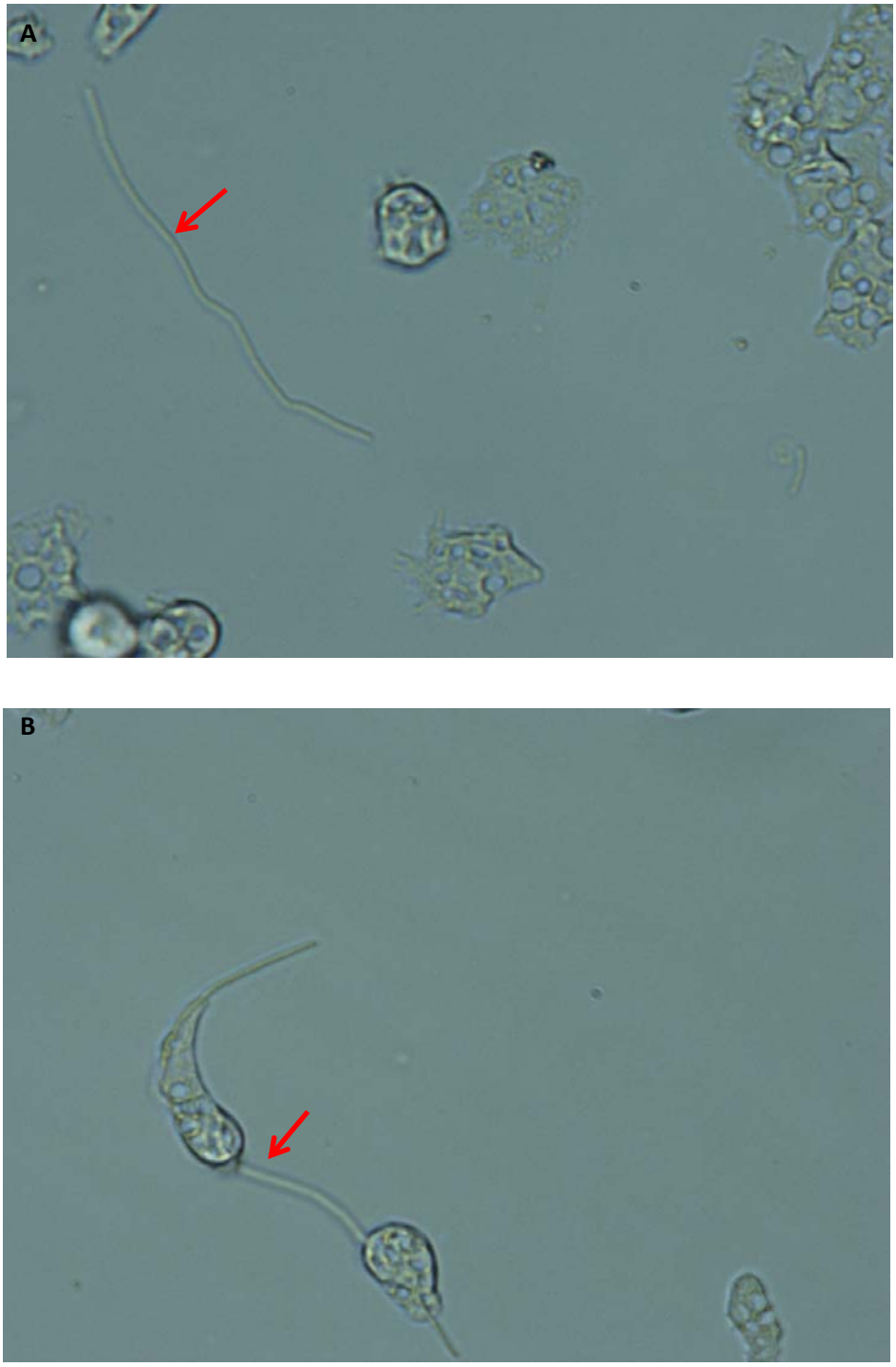

Figure 5.9. A. an unattached, *B. thuringiensis* Q5 filament free in the media (red arrow).**B.** *B. thuringiensis* Q5 filament with attached amoeba. *B. thuringiensis* Q5 and *Acanthamoeba* at a ratio of 10:1 bacteria to amoebae after 5 hours at 37°C. Both pictures were taken from the same experimental plate well at × 40 magnification.

24h interactions

As expected we saw no germination of spores of any of the strains incubated in 1xPBS alone. Conversely, when co-incubated with *Acanthamoeba* in 1x PBS, germination was seen to occur for all strains and again significant filamentation/elongation of the cells. See Figure 5.10.

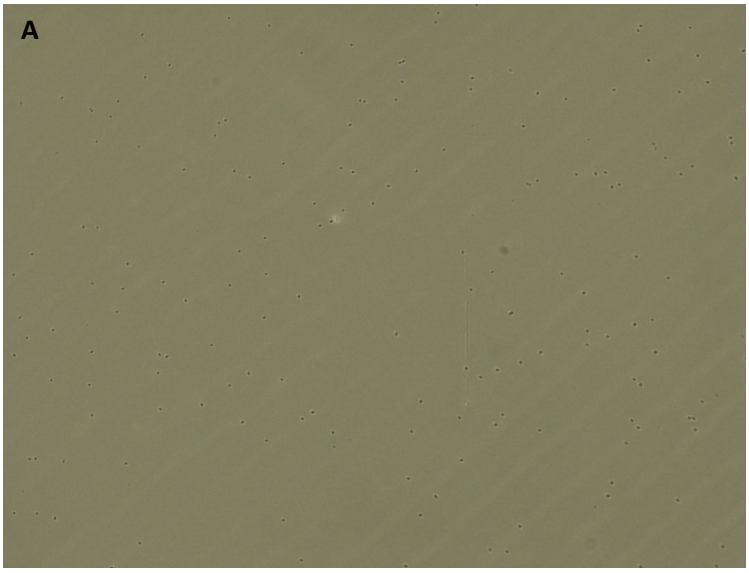

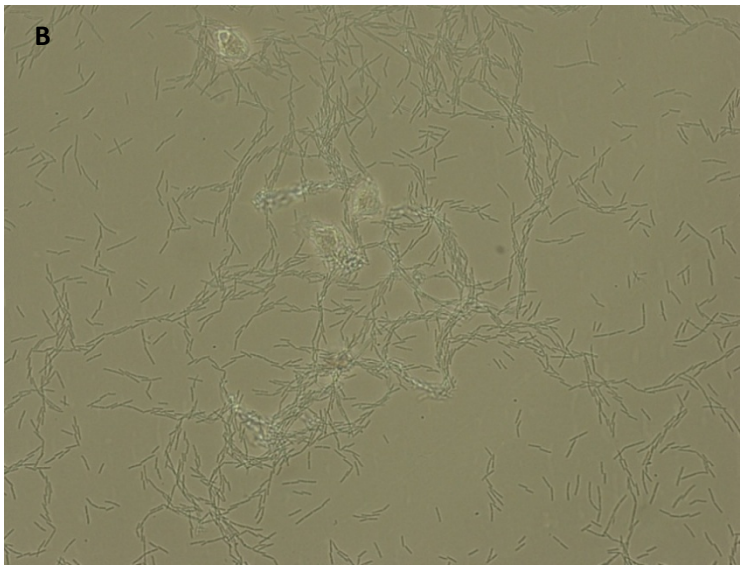

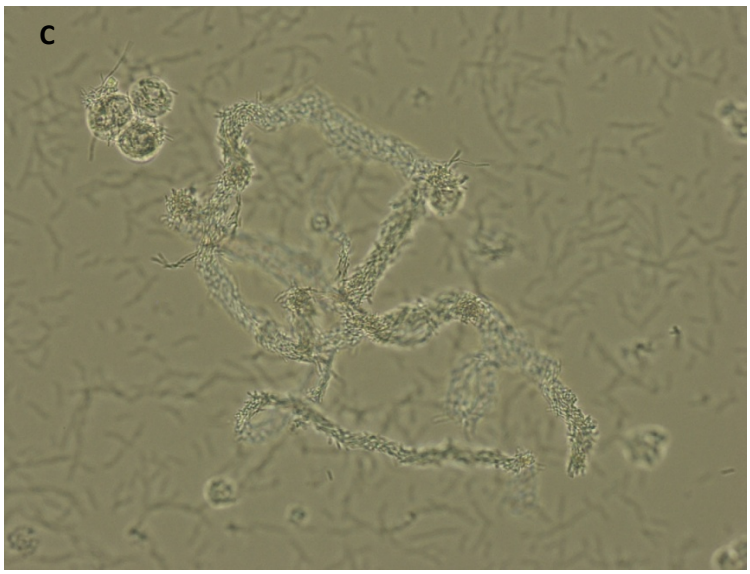

Figure 5.10. A, *B. thuringiensis* Q5 spores alone in 1xPBS after 24 hours at 25°C. **B** and **C** *B. thuringiensis* Q5 spores and *Acanthamoeba* in 1xPBS after 24 hours at 25°C. ×20 magnification.

We saw very little spore germination after 24 hours in co-incubation assays performed at 8°C and 18°C. At both temperatures spores were present in vacuoles and also remained present in the surrounding media. We notice that at 8°C, some of the amoebae had formed cysts, and it is interesting to speculate if any bacterial spores were included in these cysts, which would have provided a very resistant structure if the spores could survive amoeba germination.

There was an increased incidence of filamentation and rope formation or germinated spores at the lower ratios of bacteria to amoebae; specifically 1:10 and 1:100. These filaments were present predominantly at 25°C and 37°C and in all media.

While it was possible to watch the formation of ropes from filamenting vegetative cells using time lapse microsocopy, we nevertheless used fluorescent microscopy of *B. thuringiensis* Q7gfp to demonstrate that the rope-like formations were indeed bacillus. See Figure 5.11. The ropes formed in Figure 5.11 were the result of an overnight co-incubation with spores and amoebae after 24 hours in 10% PYG. These results further demonstrate the extent of rope formation after spore germination when in the presence of amoebae.

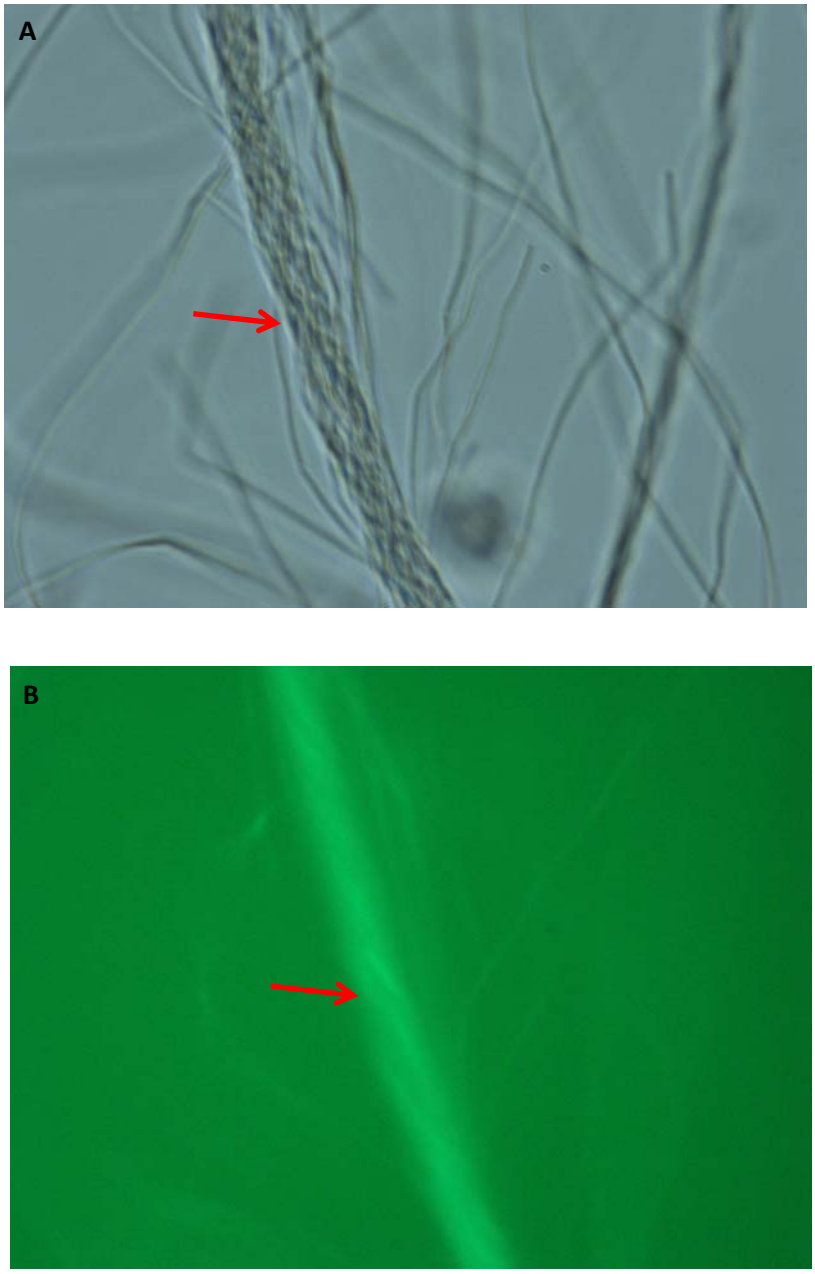

Figure 5.11. *B. thuringiensis* Q7gfp forming rope-like structures (red arrows) after 24 hours incubation at 22-25°C in 10% PYG at a ratio of 1:10 bacteria to amoebae. **A**, *B. thuringiensis* Q7gfp under light microscope, × 40 magnification. **B**, *B. thuringiensis* Q7gfp under fluorescence illumination, × 40 magnification.

In an attempt to visualise in greater detail the cellular interactions between amoebae and germinating bacteria we used Scanning Electron Microscopy (SEM). We used samples of *Acanthamoeba* co-incubated with *B. cereus* for 24 hours at 25°C in 1x PBS. It should be noted that under these conditions there had been some germination of the spores

overnight. We were not able to say if the germination occurred inside the amoebae or outside. Repeated time lapse microscopic analysis did not allow us to determine this. We hoped the SEM may provide clues to answer this question. Neverthelss these conditions were selected as they gave a diversity of bacterial phenotypes overnight and apparently healthy amoebae. The SEM images showed *Acanthamoeba* with clumped bacterial growth on the surface as expected. Interestingly there was no indication of any excess extracellular matrix suggesting the bacteria were simply attached rather than in the process of forming a classical biofilm. Some of the amoebae could be seen to be producing what looks like a phagocytic cup in attempts to engulf the vegetative cells via phagocytosis (see Figure 5.14). Filamented *B. cereus* could also be seen in association with the *Acanthamoeba* often at 5 x their normal length. These are the initial stages of much larger filamentation seen in the light microscopy. See Figure 5.12, 5.13, 5.14 and 5.15.

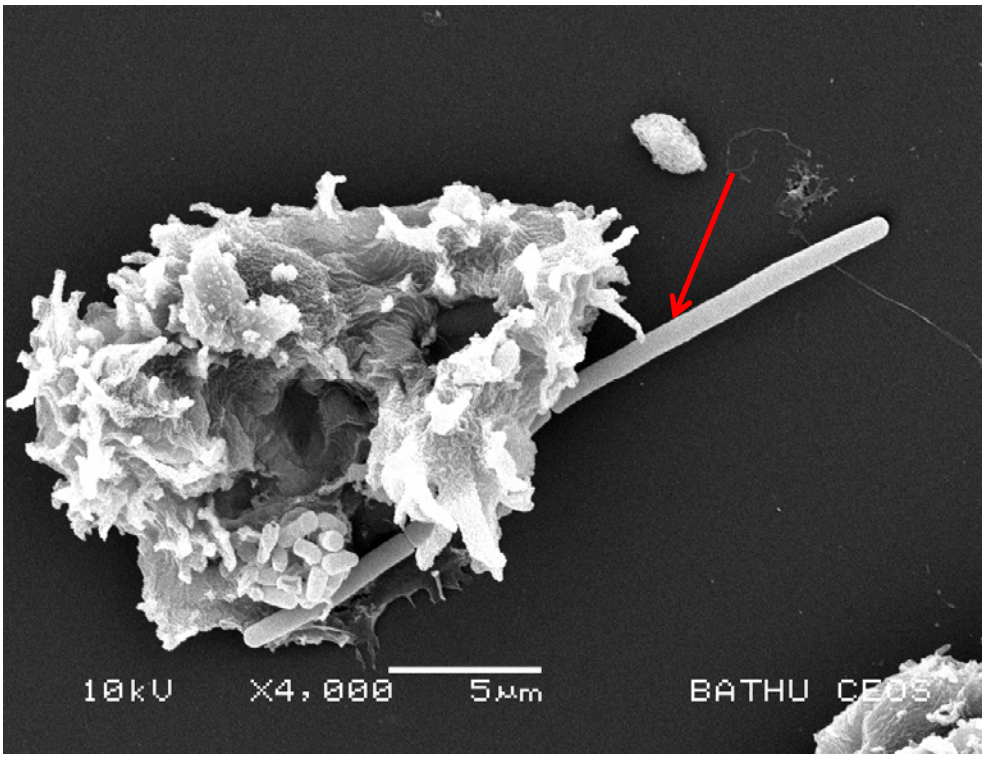

Figure 5.12. Filamented *B. cereus* in close association to *Acanthamoeba*. *B. cereus* is almost 15µm long (red arrow). × 4,000 magnification.

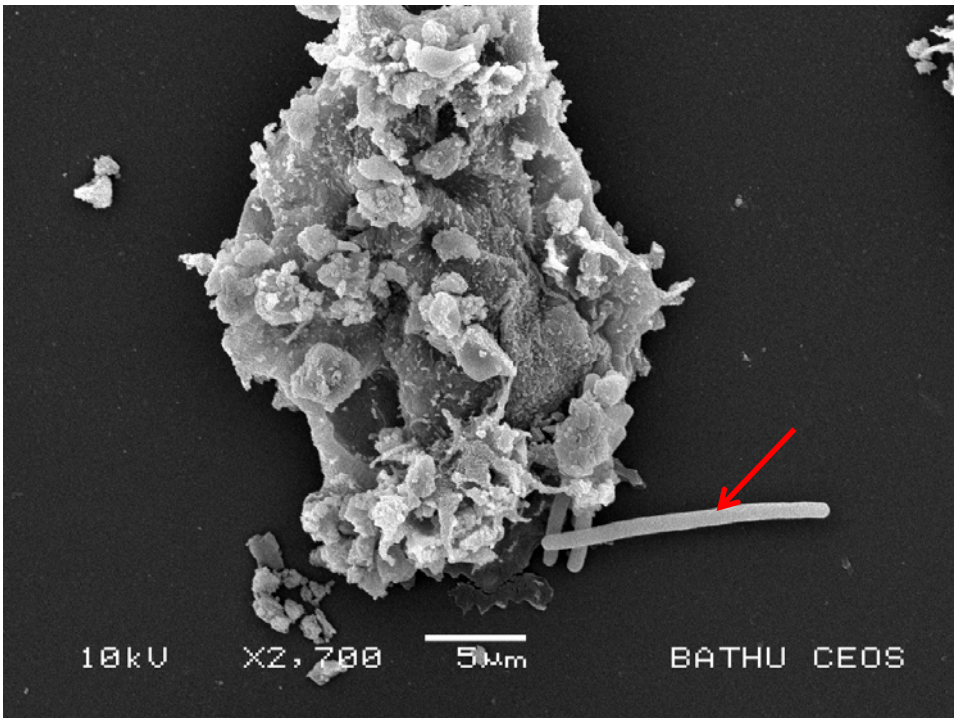

Figure5.13. Filamented *B. cereus* in close association to *Acanthamoeba* (red arrow). × 2,700 magnification.

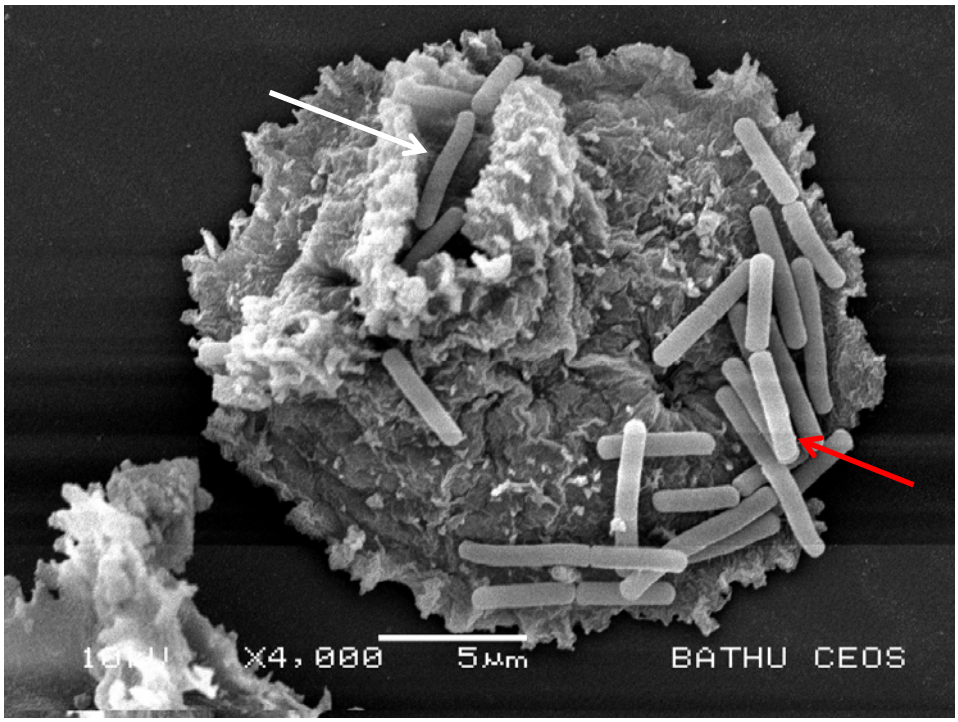

Figure 5.14. Microcolony of *B. cereus* on the surface of the *Acanthamoeba* (red arrow) and phagocytosis of *B. cereus* (white arrow). × 4,000 magnification.

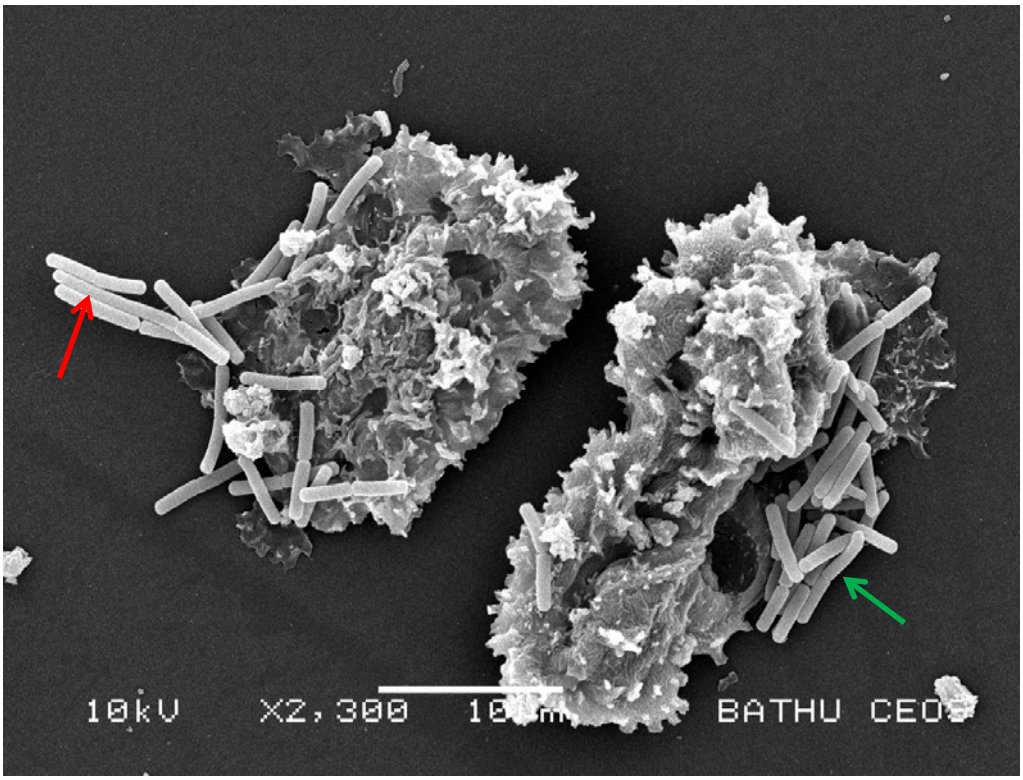

Figure 5.15. Microcolony of *Bacillus cereus* on the surface of *Acanthamoeba* (green arrow) and start of filamented growth (red arrow). × 2,300 magnification.

These SEM images show good examples of the clumped bacterial growth that settles on the surface of the *Acanthamoeba* to form microcolonies. It should be noted that the methods used to acquire these samples for SEM takes only cells attached to the base of the culture plate and would have eliminated any amoebae or bacterial vegetative cells free in the media. As a result any of the longer unattached rope-like structures were not visualised by SEM in these experiements.

Overnight co-culture assays performed with spores (of all strains) in 10% or 100% PYG could not be analysed due to germination and overgrowth by the bacteria, obscurring close observations. In attempt to reduce this overgrowth we supplimemted the medium of *B. cereus* and *B. thuringiensis* spore co-incubations with the antibiotic gentamycin, which should inhibit all germinating extracellular bacteria. This significantly reduced the numbers of unattached bacteria and after 3 washes in 1xPBS the healthy amoebae with attached bacteria could be observed more clearly. Analysis of these results clearly showed that

numerous amoebae contained a large number of *Bacillus* vegetative cells within them, and yet appeared healthy and remained highly motile (See Video 5.4). When analysing the *Acanthamoeba* at × 40 with a light microscope it was impossible to differentiate whether the bacteria were free in the cytoplasm or contained within the membrane bound vesicles. It should be noted that these *B. cereus* and *B. thuringiensis* cells were highly motile within the amoebae cytoplasm and several occasions vegetative cells were seen exiting the amoebae and swimming away. Real time microscopic analysis suggested that some bacteria could end up in what appeared to be large clear food vacuoles while others in either much smaller vesicles (which could not be seen) or free in the cytoplasm. *B. anthracis* was seen both within apparent food vacuoles and on the surface of the amoebae but other cytoplasmic invasion was hard to visualise due to their non-motile nature (data not shown).

Transmission Electron Microscopy (TEM) was utilised for a detailed analysis of the exact location of the bacteria within the amoebae. Samples were prepared from an overnight co-incubation with *B. cereus* spores and *Acanthamoeba* at a ratio of 1 bacterium to 10 amoebae in 10% PYG at 25°C. In order to remove some of the unassociated single bacterial cells from the overnight incubation, the amoeba were subjected to 3 gentamycin treatments in the micoplate well before proceeding to fix for TEM preparation. These data from the TEM preparations suggested that the majority of *Bacillus* were contained within small “tight fitting” vesicles. Some of the larger vacuoles contained numbers of up to 10 *Bacilli* which corroborates the video footage of *Acanthamoeba* containing large numbers of *B. cereus*. See Figure 5.16 and 5.17.

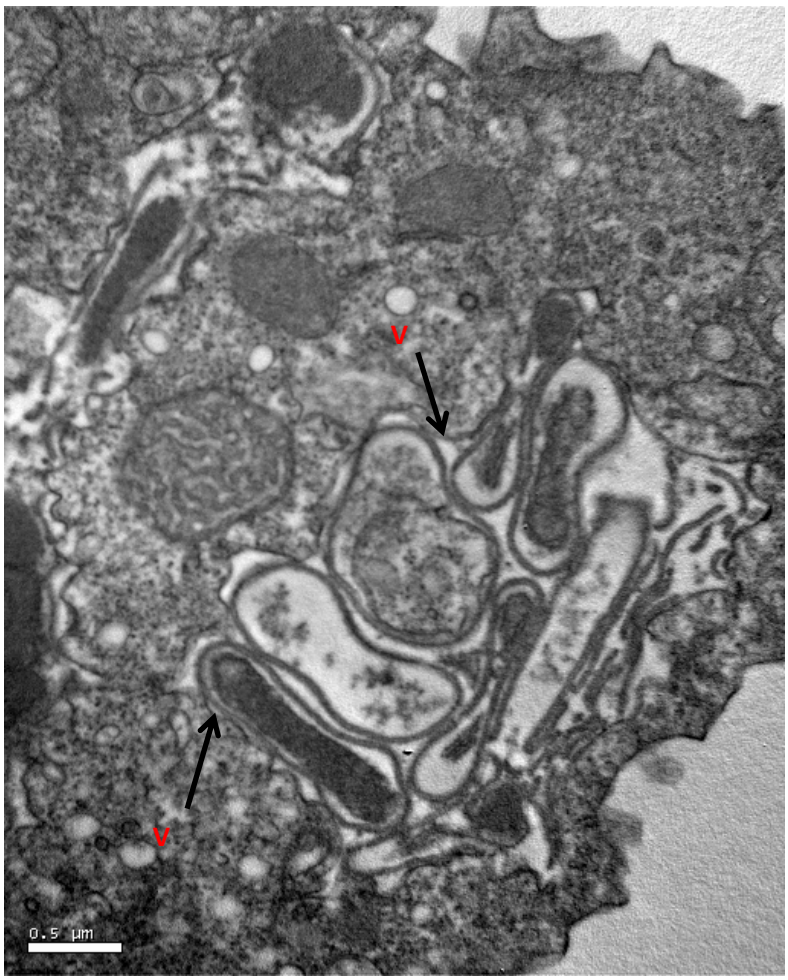

Figure 5.16. *Acanthamoeba* full of *B. cereus* after an overnight co-incubation with *B. cereus* spores. *B. cereus* can be seen contained tightly within a vacuole labelled V.

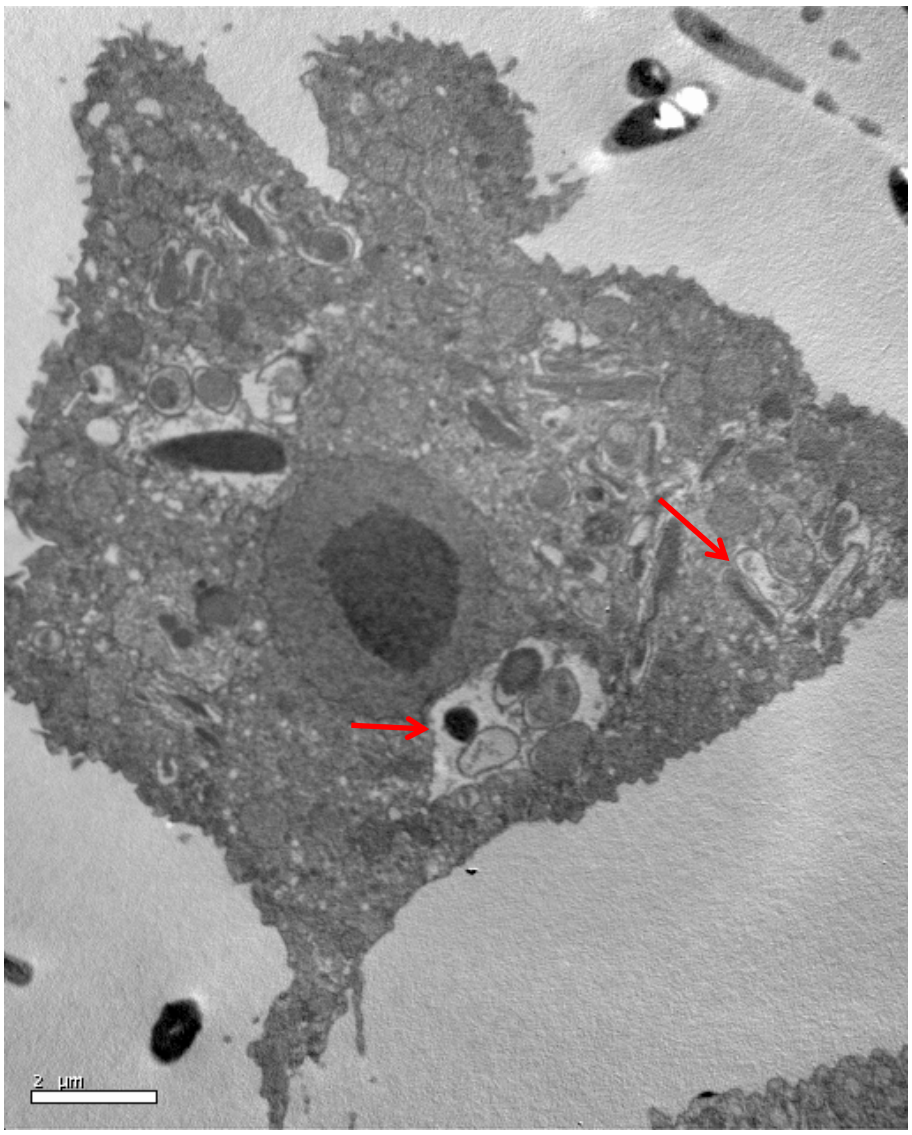

Figure 5.17. TEM of *Acanthamoeba* full of *B. cereus* after an overnight co-incubation. *B. cereus* can be seen contained within vacuoles/vesicles (red arrows).

We also prepared some TEM samples from *B. cereus* spore and *Acanthamoeba* co-incubations for analysis after 4 hours in PBS. Co-incubations were set up with a ratio of 10 bacteria to 1 amoeba in order to increase the likelihood of interactions for analysis. These samples did not need the gentamycin wash as there was very limited bacterial growth present. These data presented some interesting results for analysis. In some TEMs we could see the external attachment of bacterial spores on the surface of amoebae and also the possible germination of a bacterial spore inside a vacuole (See Figure 5.18). Also in one particular TEM (Figure 5.19) the vesicle is different and is much tighter around the bacteria than the spores in other parts of the amoeba.

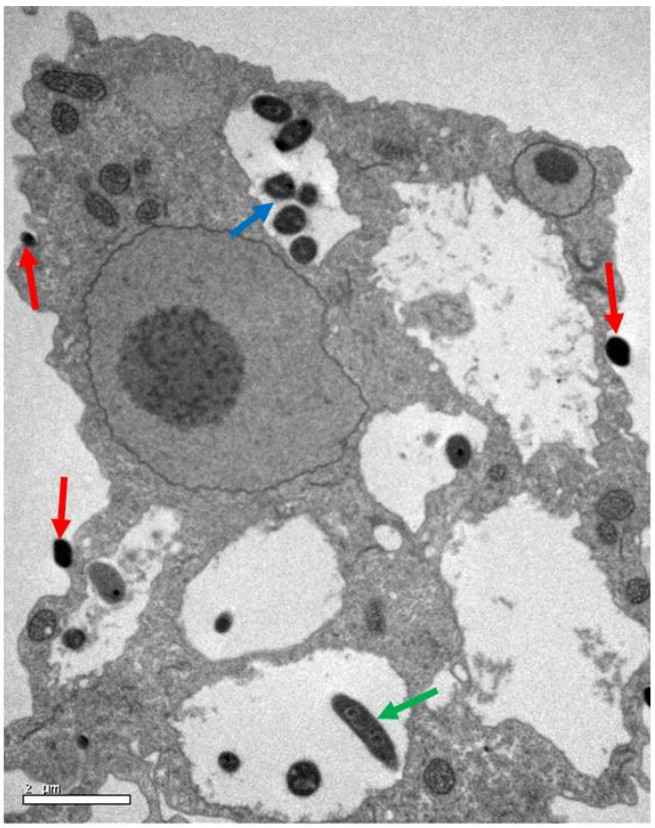

Figure 5.18 TEM of *Acanthamoeba* and *B. cereus* after a 4 hour co-incubation in PBS. *B. cereus* spores can be seen contained within a vacuole/vesicle (blue arrow). *B. cereus* spores can be seen attached to the external surface of the *Acanthamoeba* (red arrows). A germinated *B. cereus* can be seen in a vacuole/vesicle (green arrow).

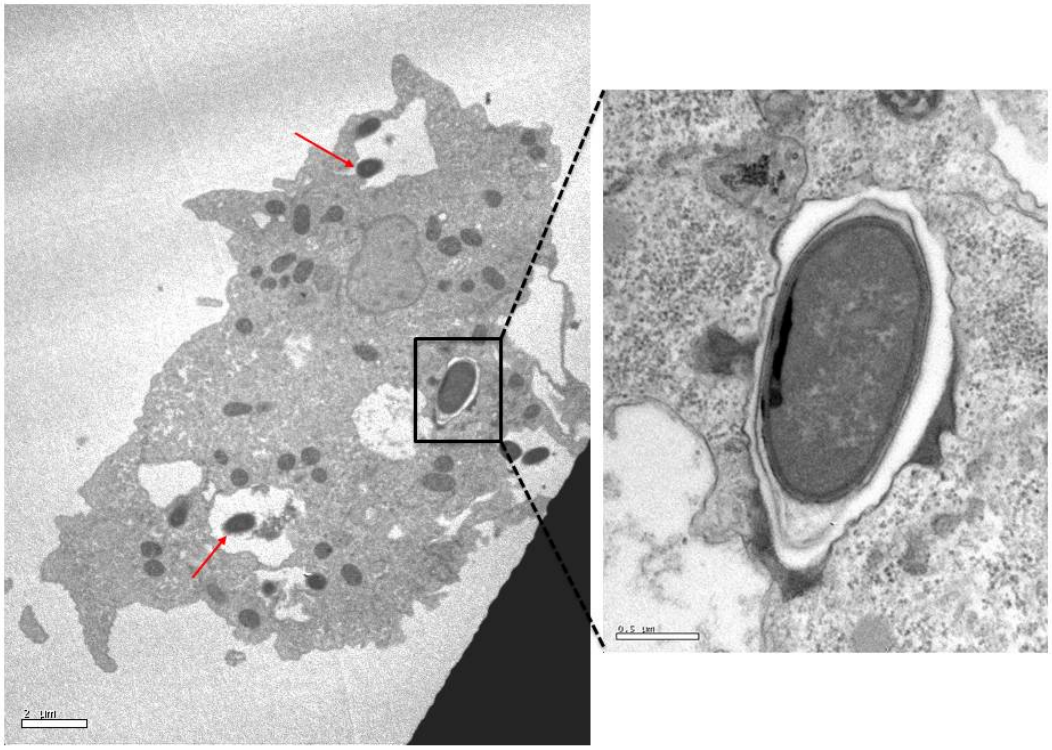

Figure 5.19 TEM of *Acanthamoeba* and *B. cereus* after a 4 hour co-incubation in PBS. *B. cereus* spores can be seen contained within vacuoles/vesicles (red arrows). Enlarged image shows a germinating *B. cereus* spore with a tighter vacuole/vesicle.

Previous images show germinated *B. cereus* cells (Figure 5.18 and 5.19), however, this germination is only from a snapshot in time and there is no conclusive evidence to support germination within the vacuole as the *Bacillus* could have been phagocytosed after germination was initiated. Conversely, some images suggest that the spore could well be preparing to germinate by shedding it's outer spore coat. Figures 5.20 and 5.21 show an unknown residue surrounding the spore which may well represent this stage of germination; conversely it is also a possibility that this could be the first stages of digestion. It is unclear as to what the image portrays, however, it is known that the amoebae struggle to digest the spores as seen in the video footage of spores being expelled by amoeba after what seems to be an unsuccessful digestion (See Video 5.5). Therefore, the evidence suggests the possibility of germination within the amoeba but further work would certainly be needed to confirm this theory.

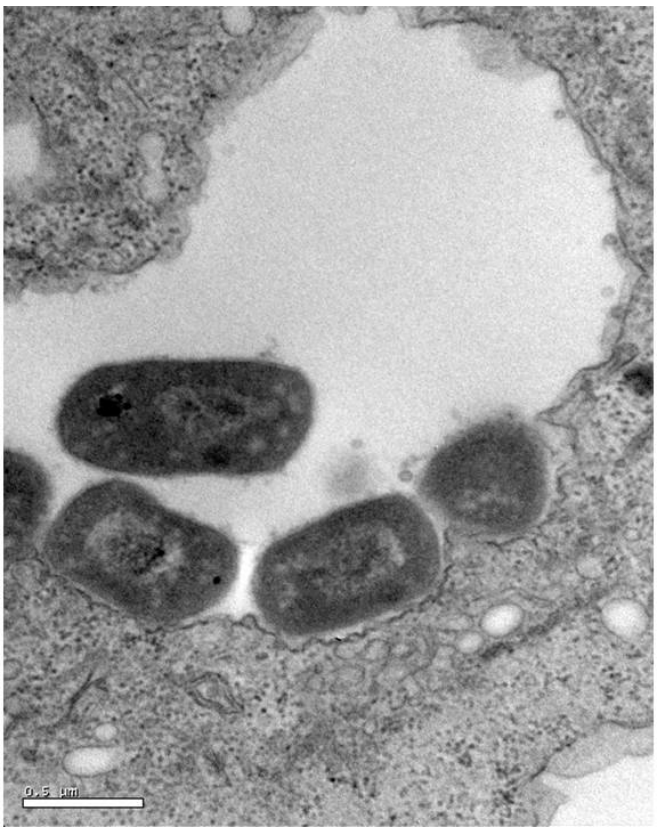

Figure 5.20 TEM showing intimate association of *B. cereus* spores and *Acanthamoeba* within vacuoles after a 4 hour co-incubation in PBS.

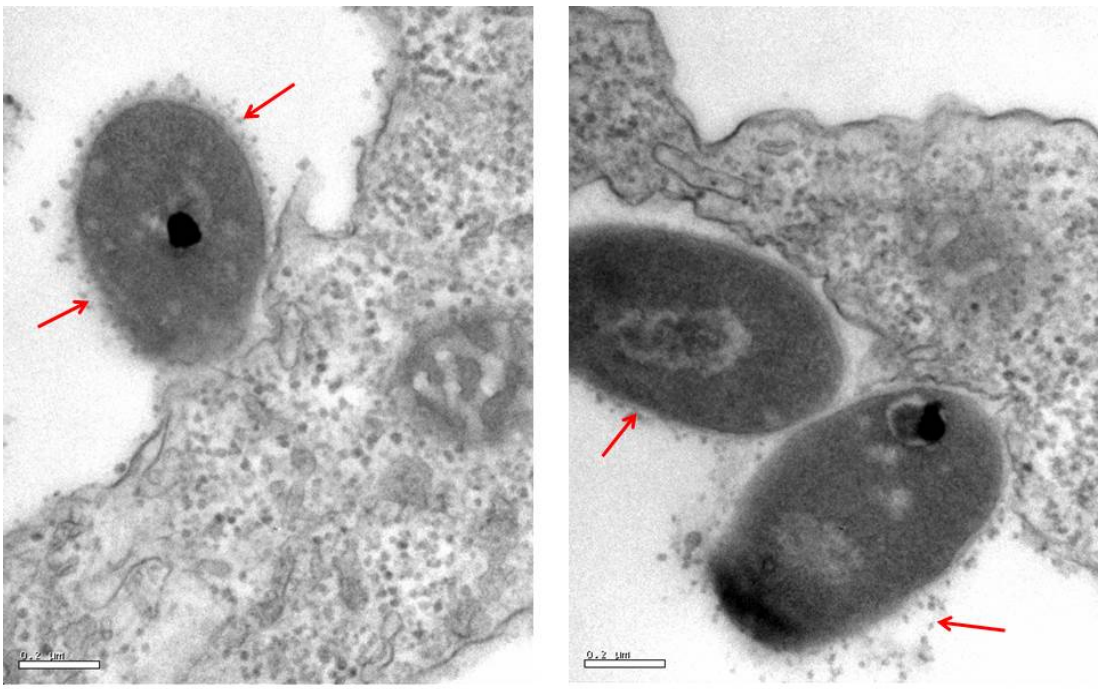

Figure 5.21 TEM showing close association of *B. cereus* spores and *Acanthamoeba* within vacuoles after a 4 hour co-incubation in PBS. Red arrows point to an unknown residue surrounding the spore which could be shedding of the spore coat prior to germination.

5.1.3 Development of *B. cereus* in these conditions in the absence of amoebae.

As a companion control study to the amoebae co-incubation work *B. cereus* was subjected to growth in a variety of media concentrations, diluted with PBS and examined microscopically. Cultures were grown using the same static 25 well experiment plate conditions. In most previous published experiments *Bacillus sp*. are typically grown in shaking cultures to optimise distribution and aeration however, in these experiments cultures were grown statically (in Thompson bottles), which is more similar to the conditions used in *B. anthracis* vaccine production procedure.

The media used in this comparison consisted of L broth, PYG, and Basal media. Basal media is the media used in vaccine production and was included to observe how growth occurs during vaccine production. To examine if nutrient availability has an effect on the physical

growth of *B. cereus*, the media used was diluted with PBS. Media was used at 100%, 50%, 25%, 10% and 1% (v/v). Both spores and vegetative cells were added at 2 x 10^5 spores/cells per well and incubated at 25°C overnight for 24 hours.

24 Hour incubation studies

L broth assays confirmed that *B. cereus* vegetative cells could form rope like structures in all media used at different concentrations. Some level of filamentous growth could be observed in all wells with all the media, however, the longer filaments seemed to be more prevalent at the lower concentrations. See Figure 5.22.

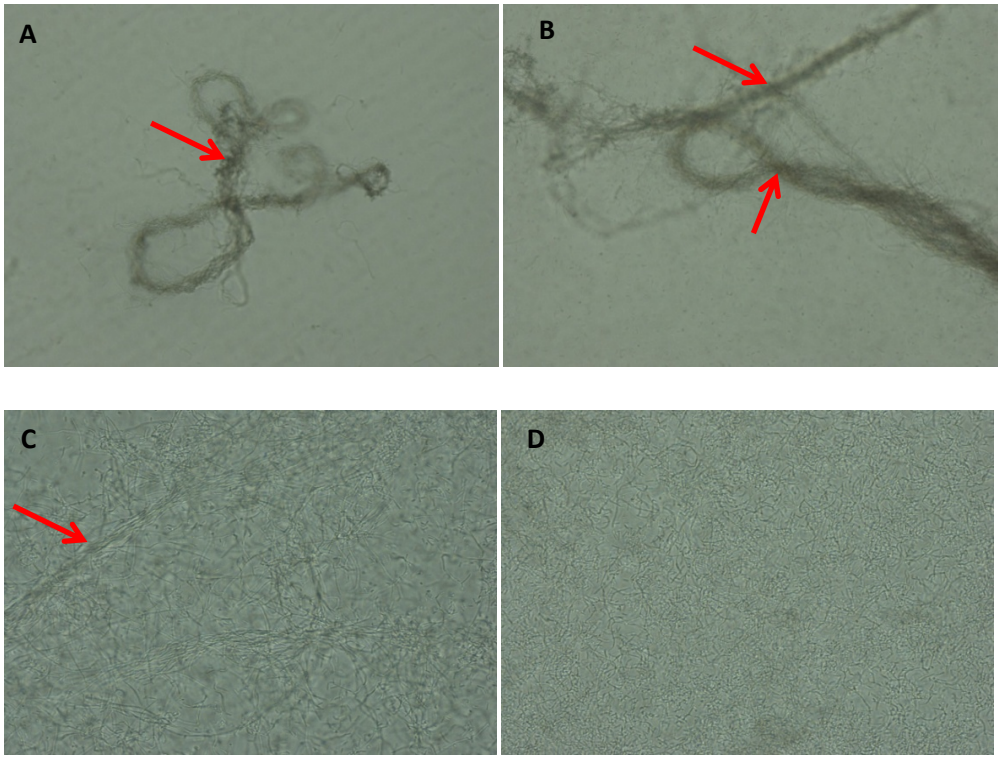

Figure 5.22. Filamentation of *B. cereus* in L broth (red arrows). Inoculated with spores and statically incubated at 25°C for 24 hours. **A**, 1% L broth, **B**, 10% L broth, **C**, 25% L broth, **D**, 50 % L broth. x 20 magnification.

Experiments in L broth show rope formation and filamentation of bacterial cells at 1% and 10% L broth concentrations. At 25% L broth filamentation occured but growth lacked the rope-like formation seen in the lower media concentrations. At 50% and 100% (data not shown) the majority of cells existed as single cells with only limited filamentation and no rope like growth present. These observations suggest that the limitation of nutrients during growth may lead to increased cell elongation. As expected, overall bacterial growth increased in density comparatively with the increased percentage of L broth in the media.

Experiments with vegetative cells gave slightly different results even though both spores and vegetative cells were added at the same densities in each experiment.

Results from the vegetative cell incubations showed that every dilution of L broth could produce filamentous cells coupled with rope-like formations. The structure of the rope-like formations were tightly twisted. In all cases, normal sized *B. cereus* rods were also present. As expected, overall bacterial growth increased in density comparatively with the increased percentage of L broth in the media. See Figure 5.23.

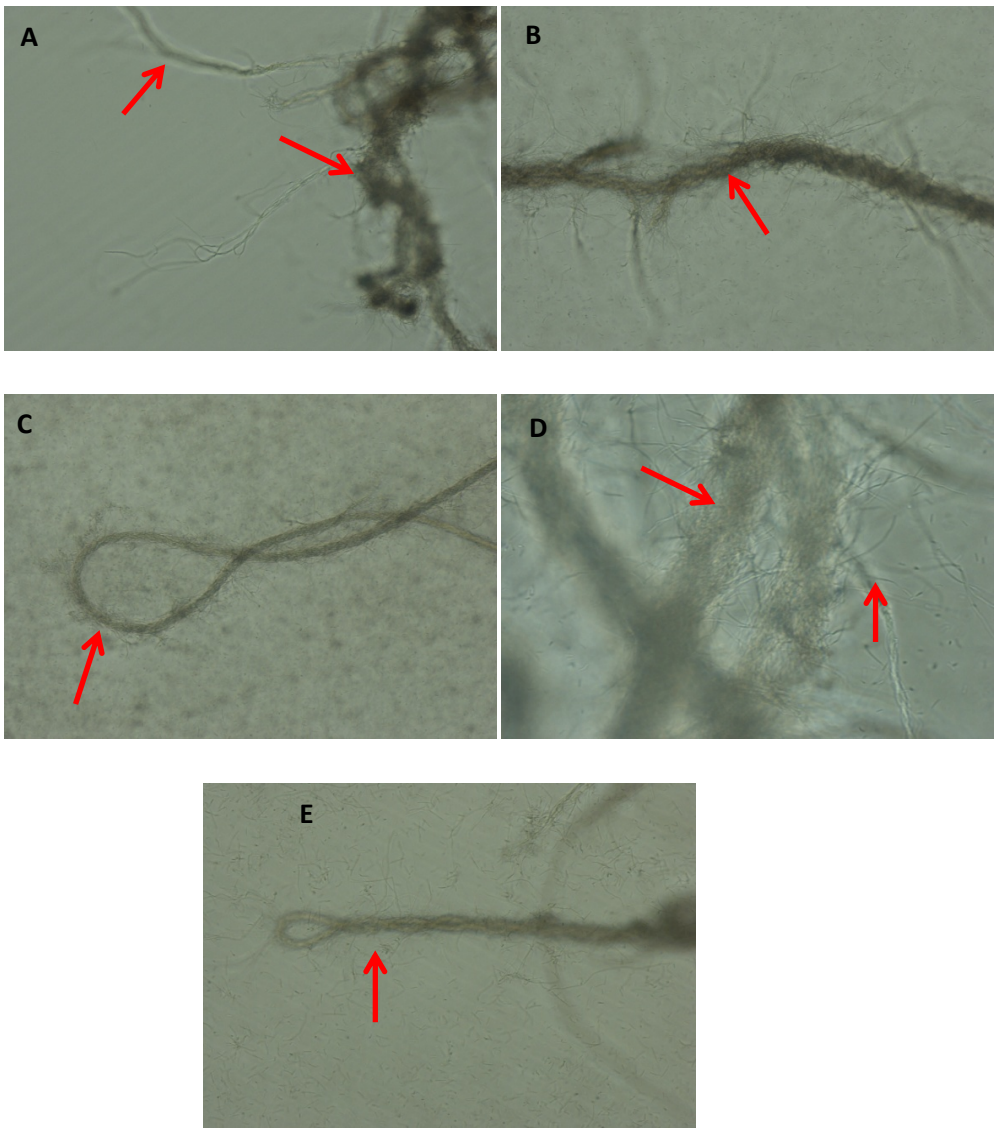

Figure 5.23. Rope-like *B. cereus* formations in L broth (red arrows). Inoculated with vegetative cells and statically incubated at 25°C for 24 hours. A, 1% L broth, B,10% L broth, C, 25% L broth, D, 50 % L broth, E, 100% L broth. 20 x magnification.

Results from using dilutions of PYG showed similar results to the L broth. Rope like growth was present in all dilutions of PYG when using vegetative cells. See Figure 5.24.

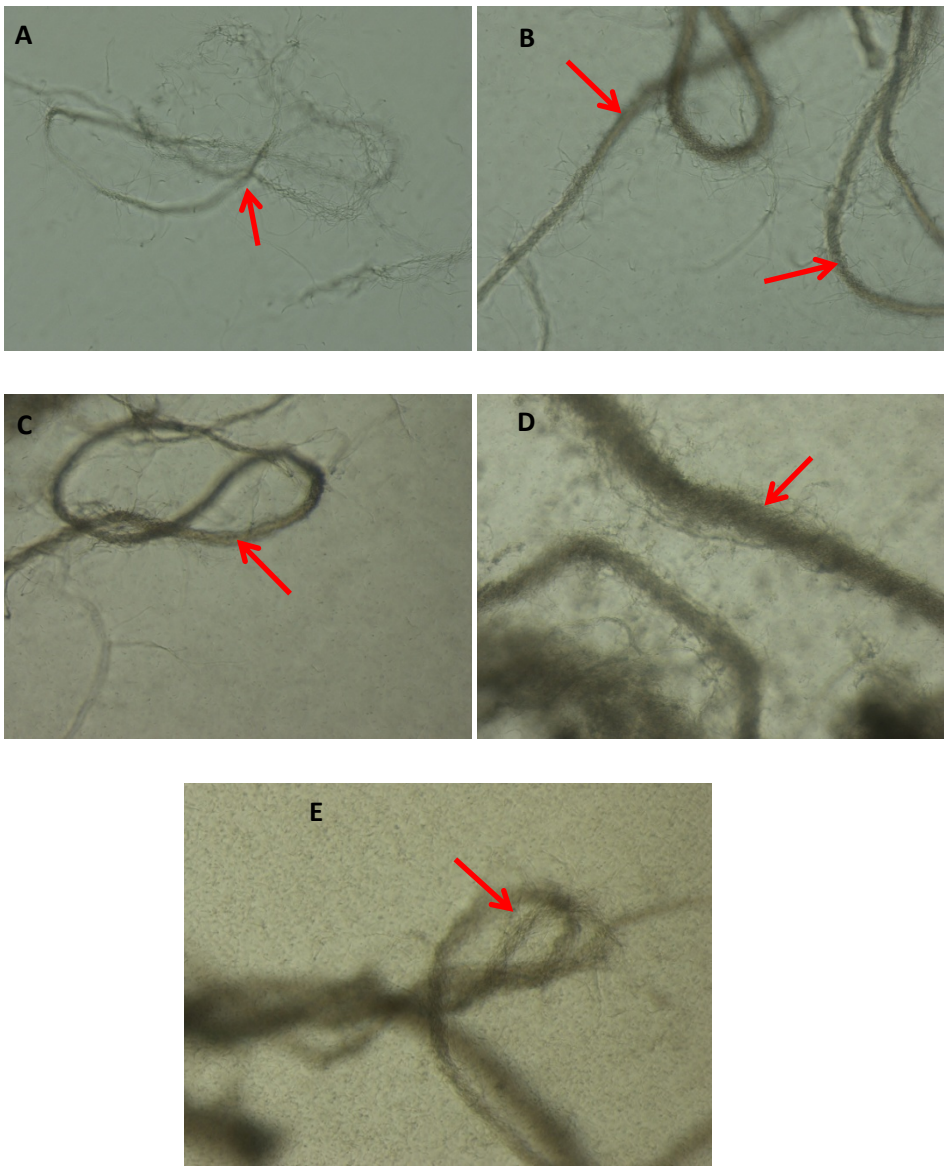

Figure 5.24. Rope-like *B. cereus* growth in PYG media (red arrows). Inoculated with vegetative cells and statically incubated at 25°C for 24 hours. A, 1% PYG, B,10% PYG, C, 25% PYG, D, 50 % PYG, E, 100% PYG. x 20 magnification.

These experiments also revealed the presence of rope-like structures forming as the PYG concentration was increased. Normal length vegetative cells could be seen in all PYG dilutions tested in addition to the long filaments. This suggests that the two morphologies represent two developmentally distinct phenotypes. As expected bacterial growth density increased with increasing percentage of PYG media.

When comparing the growth of spores in the PYG dilutions, we observed that increasing the PYG in the media gave rise to clumped growth. Filamented growth was also present but with less rope-like structures. As expected, bacterial growth increased in density comparatively with the increased percentage of PYG media. See Figure 5.25.

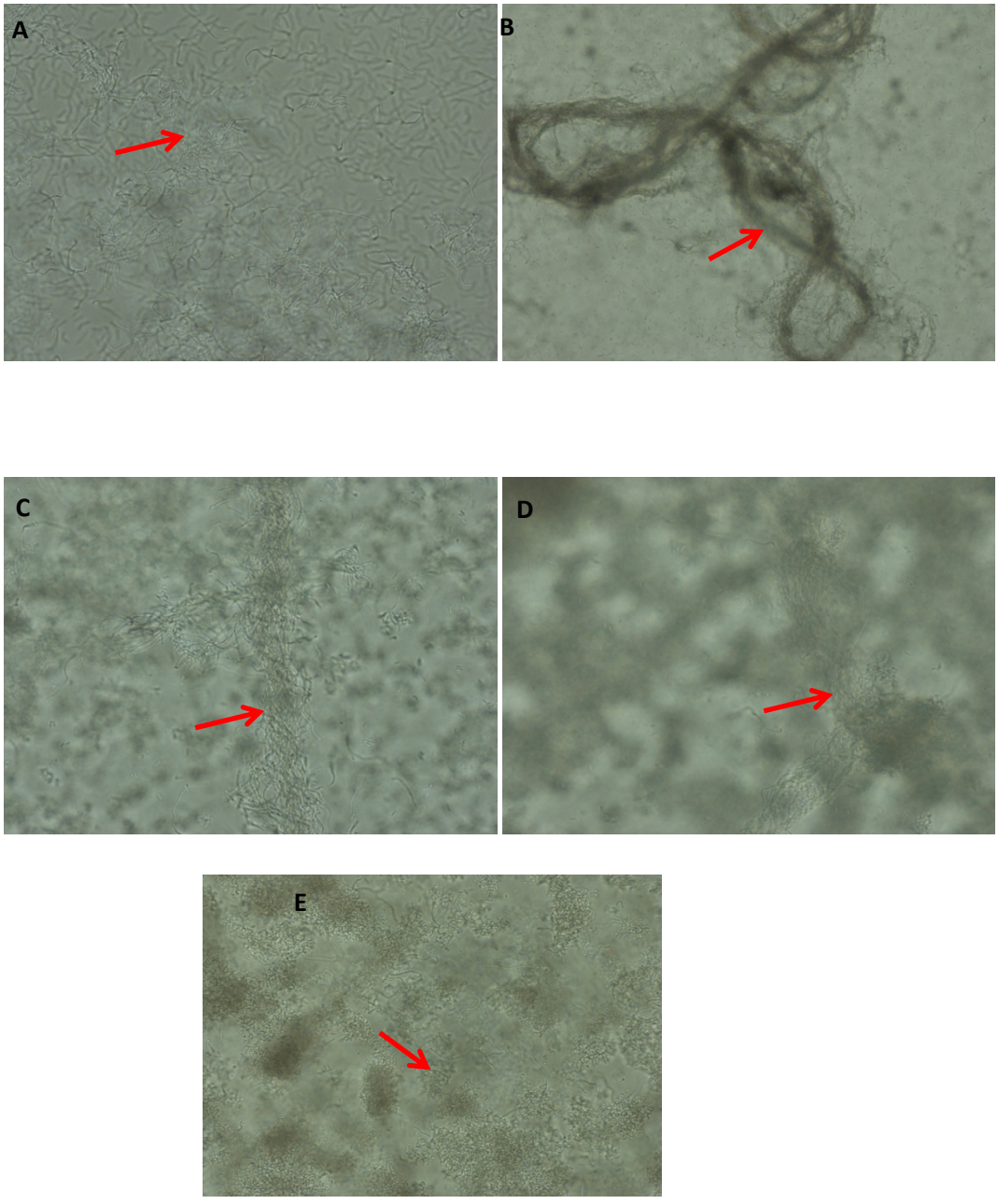

Figure 5.25. Filamented (B) and clumpy (E) *B. cereus* growth in PYG media (red arrows). Inoculated with spores and statically incubated at 25°C for 24 hours. A, 1% PYG, B,10% PYG, C, 25% PYG, D, 50 % PYG, E, 100% PYG. 20 x magnification.

When inoculated with spores we saw filamentous growth throughout the range of PYG concentrations. Rope-like structures could be more clearly defined in the lower percentages of PYG up to 1-25% after which the bacterial growth could still seen to be filamented but often in dense clumps.

B. cereus growth in basal media gave interesting results. There was no *B. cereus* growth visible in 1% Basal medium inoculated with spores or vegetative cells compared to the L broth, and PYG in which there was at least limited growth. None of the spores had germinated or outgrown in the 1% media suggesting there is not enough nutrients present at this dilution of Basal medium. There was very poor growth in the 10% Basal medium, growth that was present occurred as long filaments and virtually no "normal" length rods. Filamented growth and rope like formation were seen in 25%, 50% and 100% Basal medium but all results showed very poor growth throughout. See Figure 5.26.

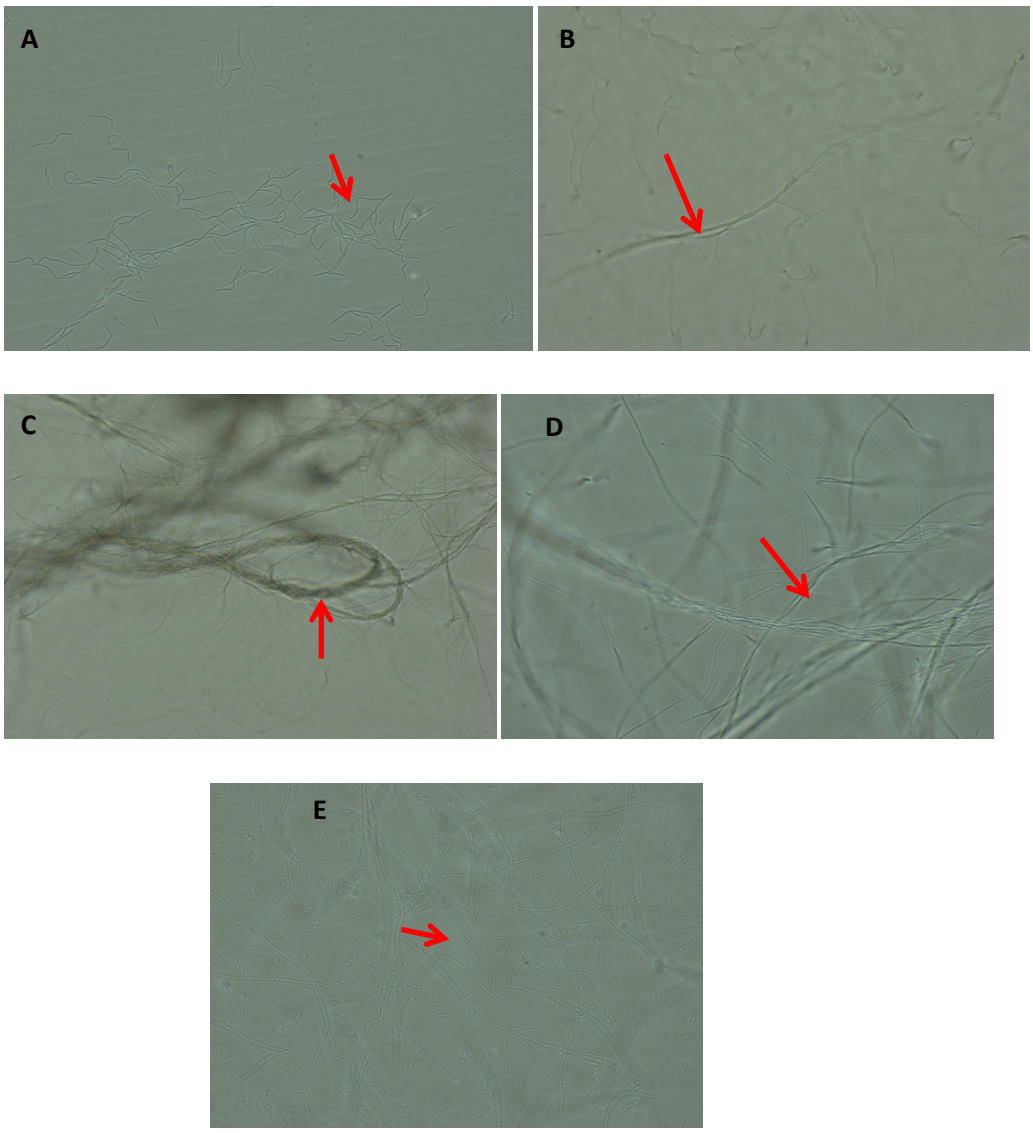

Figure 5.26. Filamented *B. cereus* growth in basal media (red arrows).Inoculated with spores and statically incubated at 25°C for 24 hours. A, 10% Basal, B,25% Basal, C, 50% Basal, D, 100 % Basal, E, 100% Basal. 20 x magnification.

The *B. cereus* vegetative cells also produced very low levels of growth in basal medium. Results showed less dense growth than when spores were used to innoculate the basal medium. See Figure 5.27.

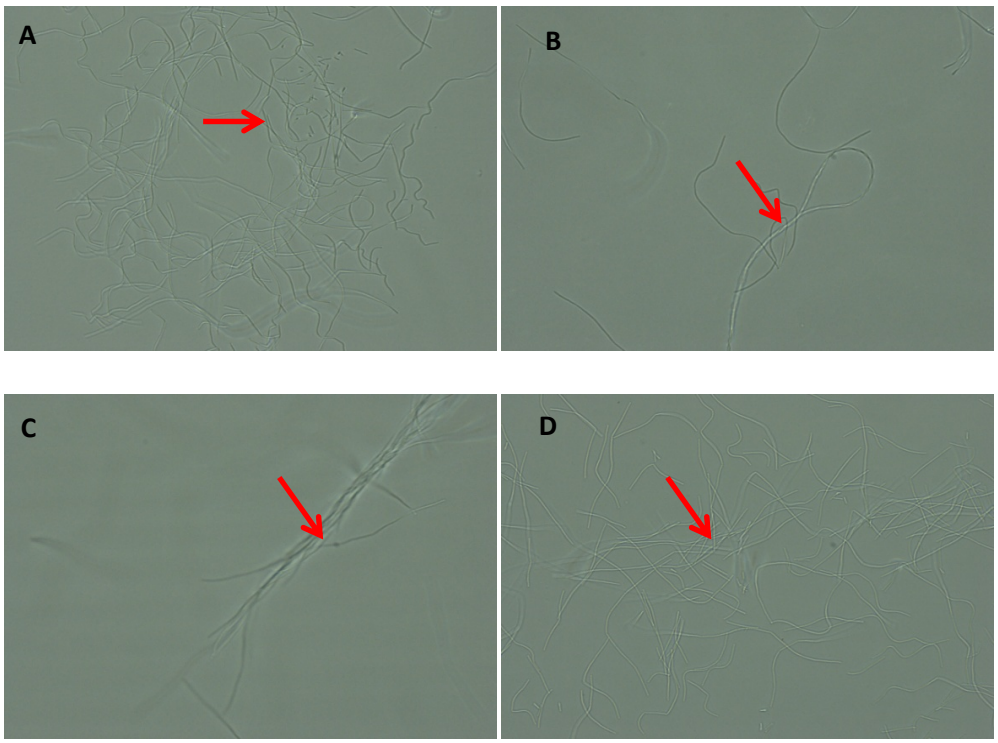

Figure 5.27. Filamented *B. cereus* growth in basal media (red arrows). Inoculated with vegetative cells and statically incubated at 25°C for 24 hours. A, 25% Basal, B,50% Basal, C, 100% Basal, D, 100 % Basal.20 x magnification.

There was no bacterial growth visible in either the 1% or 10% basal medium after 24 hours of incubation at 25°C. Very poor growth was seen in 25% and 50% basal medium all of which was filamented with the formation of small rope-like structures. In 100% basal medium, growth was still very poor but slightly denser than 50%.

5.1.4 Effect of *Acanthamoeba* supernatant on the germination of *Bacillus* spores.

Our previous findings confirmed that *Bacillus* spores could germinate in the presence of *Acanthamoeba* even in nutrient free 1xPBS. In addition we saw increases in the numbers of these *Bacillus sp*. vegetative cells when co-incubated with amoeba also in nutrient free 1xPBS. See Figure 5.28.

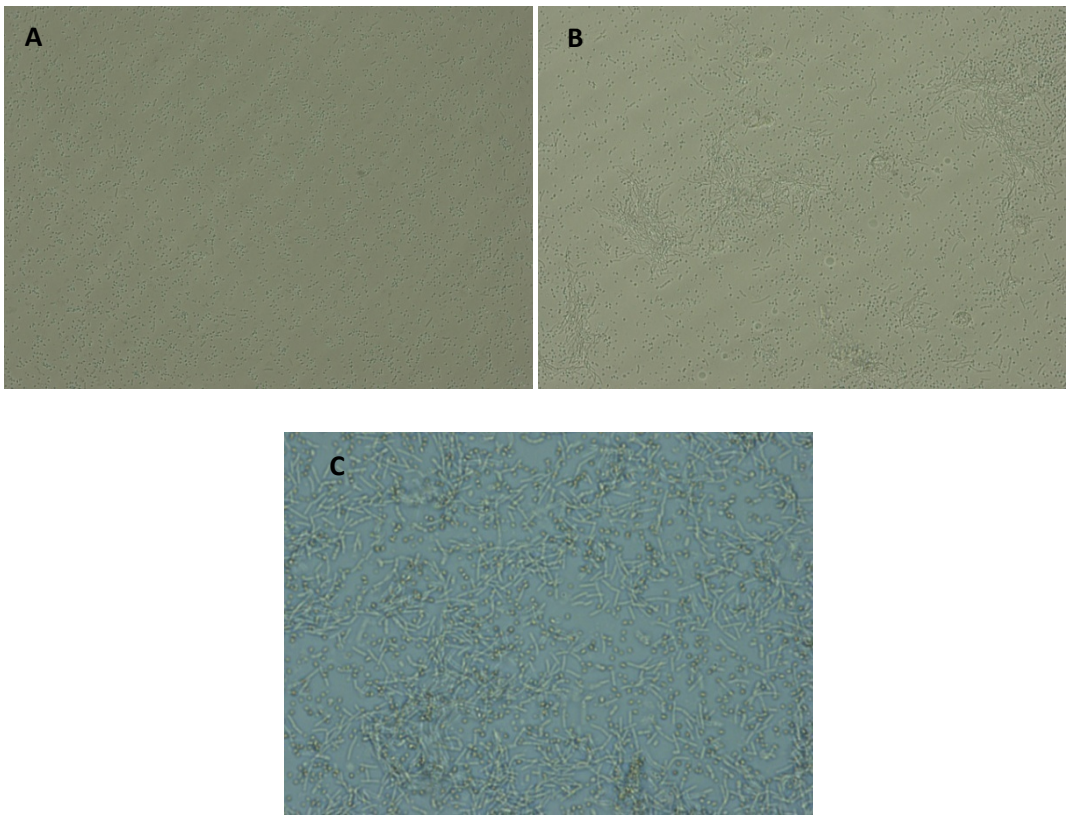

Figure 5.28. Germination of *B. cereus* spores. **A.** *B. cereus* spores in PBS alone. x 20 Magnification **B.** *B. cereus* spores in PBS with *Acanthamoeba*. x 20 Magnification **C.** *B. cereus* spores in PBS with *Acanthamoeba* supernatant. x40 magnification.

In order to test if the presence of live amoebae cells is required for the germination of spores or the maintenance of vegetative cells we incubated amoebae in 1xPBS overnight and then took the supernatant and added 100µl into each well of spores and PBS. The *B. cereus* spores germinated when incubated in the presence of the *Acanthamoeba* supernatant but the level of growth was still very limited. When added to vegetative cells growth did occur but again at a limited level.

These observations confirm that the spores are able to sense and use secreted or excreted molecules produced by the *Acanthamoeba* to support their germination and outgrowth. In order to investigate what these molecules might be the "PBS soak" amoebae supernatants were analysed in several ways. Initially the supernatants were heated to 70°C for 15 minutes, which would denature most protein structures. Nevertheless the spores were still able to germinate and outgrow confirming that the products are not heat-sensitive.

To investigate the size(s) of the important molecules, size fractioning columns were used. Different size fractions of the *Acanthamoeba* supernatant were separated out to use independently to assess the germination of the spores.

Using size cut off columns we were able to prepare fractions as follows; >30kDa, <30kDa, >10kDa, < 10kDa, >5kDa and <5kDa. Using these fractions we were able to show that after 24hours incubation that the *B. cereus* spores only germinated and outgrew in the presence of fractions which contained molecules less than 5kDa. See Figure 5.29.

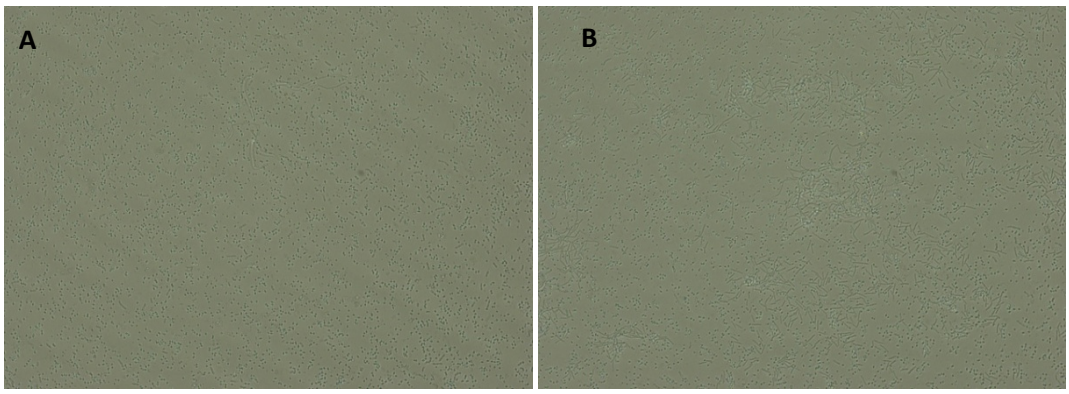

Figure 5.29. Effect of size fractionated *Acanthamoeba* supernatant.**A.** *B. cereus* spores in PBS with *Acanthamoeba* supernatant fraction of > 5kDa molecules. **B.** *B. cereus* spores in PBS with *Acanthamoeba* supernatant fraction of < 5kDa molecules. x 40 magnification.

These results suggest that the product that the spores are utilising consists of small molecules and not large complex proteins. Mass spectrum analysis of molecules present in PBS supernatants from overnight *Acanthamoeba* incubations show a range of molecules sizes (data not show). The nature of these molecules remains obscure. It should be noted that *B. cereus* appeared to grow to a higher cell number when co-incubated with the amoebae rather than the supernatant (data not shown). This is presumably because by adding the supernatant to the wells, a limited pool of nutrients is created and is used up with the absence of amoebae cells available to keep replenishing the supply.

5.1.5 Studies with *Acanthamoeba* after treatment with phagocytosis inhibitors

Phagocytosis inhibitors have been used previously to study the uptake mechanisms involved in the life cycle of *Legionella* and *A. castellanii* (Declerck *et al.*, 2007). By inhibiting different modes of phagocytosis the mechanism of uptake for *B. cereus* spores and vegetative cells can be explored. In some cases pathogens are able to invade a cells cytoplasm using mechanisms independent of normal phagocytic processes.

Uptake inhibitors were selected based on a variety of studies which looked at the modes of phagocytosis of different protozoa. Cycloheximide inhibits eukaryotic protein synthesis (Declerck et al., 2007) by interfering with the translocation step in protein synthesis. It is commonly used in *in vitro* studies as it is highly effective and its effect can be reversed by removing it from the culture medium. Cyctochalasin D inhibits actin polymerisation. It disrupts actin microfilaments and activates the p53-dependent pathways causing arrest of the cell cycle at the G1-S transition which would inhibit any microfilament dependant phagocytosis in amoebae (King *et al.*, 1991). Methylamine is an inhibitor of transglutaminase a plasma membrane enzyme involved in the aggregation of ligand-receptor complexes and is required for receptor-mediated pinocytosis in fibroblasts and macrophages (Teshigawara *et al.*, 1985). Bafilomycin A1 is a specific inhibitor of vacuolar type H^+ATPasewhich can also be used to look at the effect of acidification on the vacuole by halting the acidification of the phagosomal vacuole (Lamothe *et al.*, 2004). If the vacuoles have a less acidic pH bacterial cells may survive for longer and be more prevalent in the bafilomycin treated amoebae, thus evaluating the effect of the natural uptake and survival with regards to the vacuole acidity.

Co-culture assays with *Acanthamoeba* and *B. cereus* were repeated with the addition of a 2 hour treatment with 3 different uptake inhibitors. By treating the *Acanthamoeba* with uptake inhibitors which effect different aspects of the phagocytic process the actual mechanisms involved can be studied in more detail. Amoebae were exposed to the inhibitor treatment for 2 hours before the addition of spores or vegetative cells (the inhibitors were maintained in the medium to ensure continued exposure). After a further 2 hour incubation to allow for any phagocytosis of spores or cells, 20 amoebae per well were examined microscopically (in triplicate biological replicate wells) giving total test number of

60 amoebae per assay. This was repeated 3 times and data was collated and analysed. Spores and vegetative cells were counted inside the amoebae vacuoles from these randomly selected amoeba cells. It should be noted that unfortunately the vegetative cells were often difficult to count due to rapid movement inside the amoeba. We suggest that the large number of cells counted per treatment (n = 180 per treatment) may go someway to offset any errors arising from this. Nevertheless the data should be interpreted with this caveat. We decided to use microscopic counting to assess amoebae uptake of cells rather than the more typical gentamycin intracellular protection assays because of problems associated with spores. Essentially the spores are very sticky and will adhere to the plastic surface of the assay culture plates and also are inherently resistant to gentamycin. This makes the gentamycin assay impossible.

Both the Anderson-Darling and Kolmogorov-Smirnov normality tests were performed on all the data sets generated to establish the data distribution type. Results indicated that the data from these assays were not normally distribution. The non-parametric Mann-Whitney statistical test was therefore employed to compare the treated and untreated amoebae uptake counts.

Results show that the untreated amoebae had phagocytosed more bacterial spores than the amoebae treated with cycloheximide (median of 3 spores and median of 1 spore per amoeba respectively; p value of < 0.001).

Interestingly, the amoebae treated with bafilomycin appeared to contain more spores than the untreated amoebae (median of 4 spores and median of 3 spores per amoeba respectively; p value of <0.001).

Comparison of the untreated amoebae and cytochalasin D and methylamine showed no significant difference. See Figure 5.30 for results.

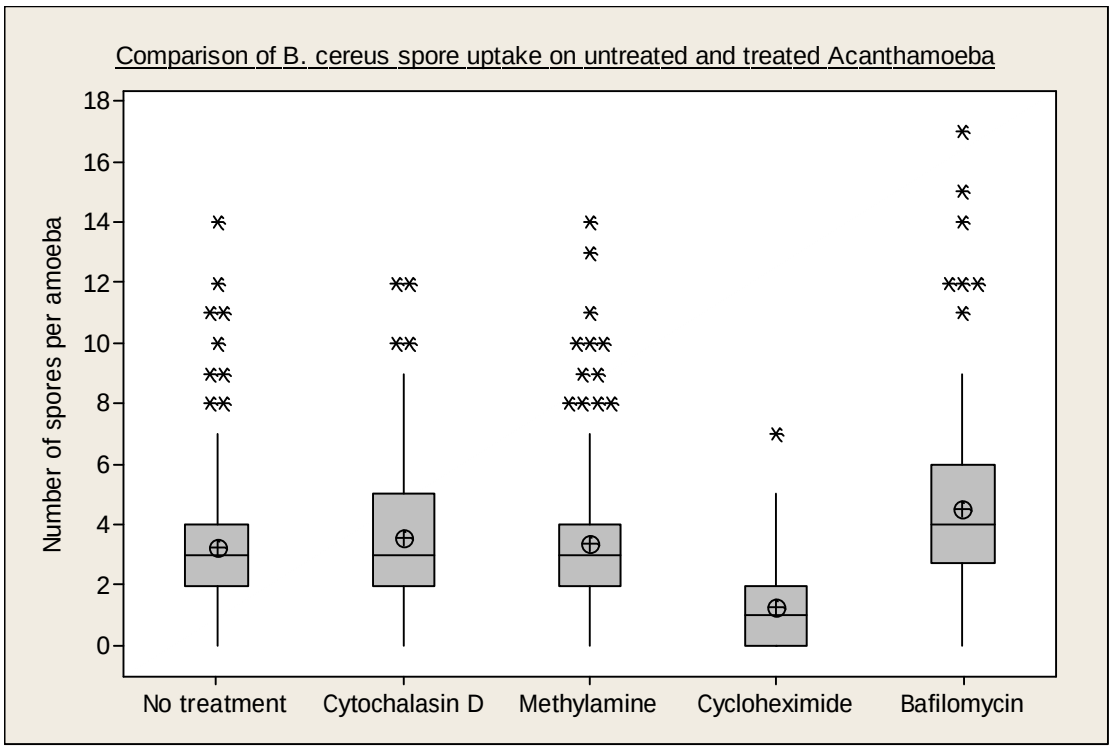

Figure 5.30. *B. cereus* spore uptake of the untreated amoebae compared to treatment with uptake inhibitors Cytovhalsin D, Methylamine and Cycloheximide. Bafilomycin is also shown to show the effect of reduced acidification of the amoebal vacuoles. Cross hatch shows the mean of each set of data.

Table showing levels of significance for untreated amoebae compared to the different amoeba treatments for spore uptake:

Cytochalasin	Methylamine	Cycloheximide	Bafilomycin
p = <1.0 (Not Significant)	p = <1.0 (Not Significant)	p = < 0.001	p = < 0.05

Results from the vegetative cell counts show that the untreated amoebae (median of 1 cell per amoeba) contained more vegetative cells than the cytochalasin D and cyclohexamide treated amoebae (both with a median of 0 and p value of < 0.001).

Bafilomycin treated amoebae contained more vegetative cells than untreated amoebae (both with a median of 1; p value of <0.05)

Comparisons between untreated amoebae and methylamine treated amoebae showed no significant difference. See Figure 5.31 for results.

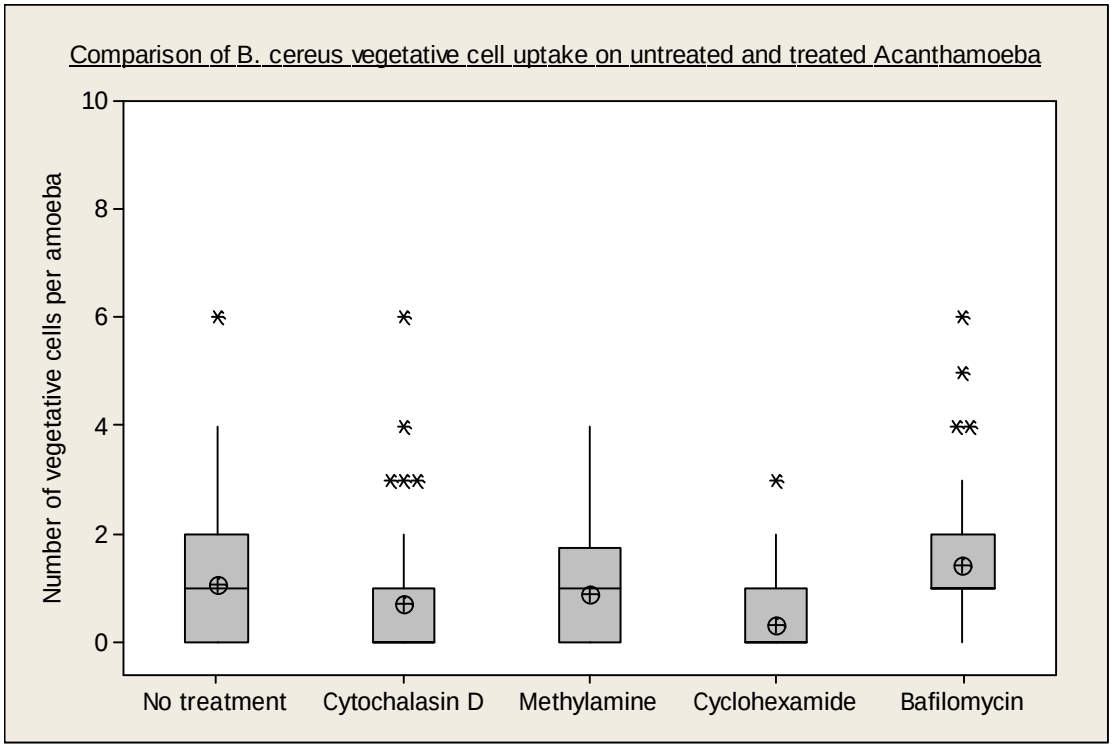

Figure 5.31. *B. cereus* vegetative cell uptake of the untreated amoebae compared to treatment with uptake inhibitors Cytovhalsin D, Methylamine and Cycloheximide. Bafilomycin is also shown to show the effect of reduced acidification of the amoebal vacuoles. Cross hatch shows the mean of each set of data.

Table showing levels of significance for untreated amoebae compared to the different amoeba treatments for vegetative cell uptake:

Cytochalasin D	Methylamine	Cycloheximide	Bafilomycin
P = <0.001	P = <0.1 (Not Significant)	P = < 0.001	P = < 0.05

When comparing the levels of internalised bacteria between the *B. cereus* spores and vegetative cells it is clear that more spores were phagocytosed than vegetative cells. When comparing the spore and vegetative cell counts with each treatment every test gave a significant difference with p values of <0.001. See Figure 5.32 for results.

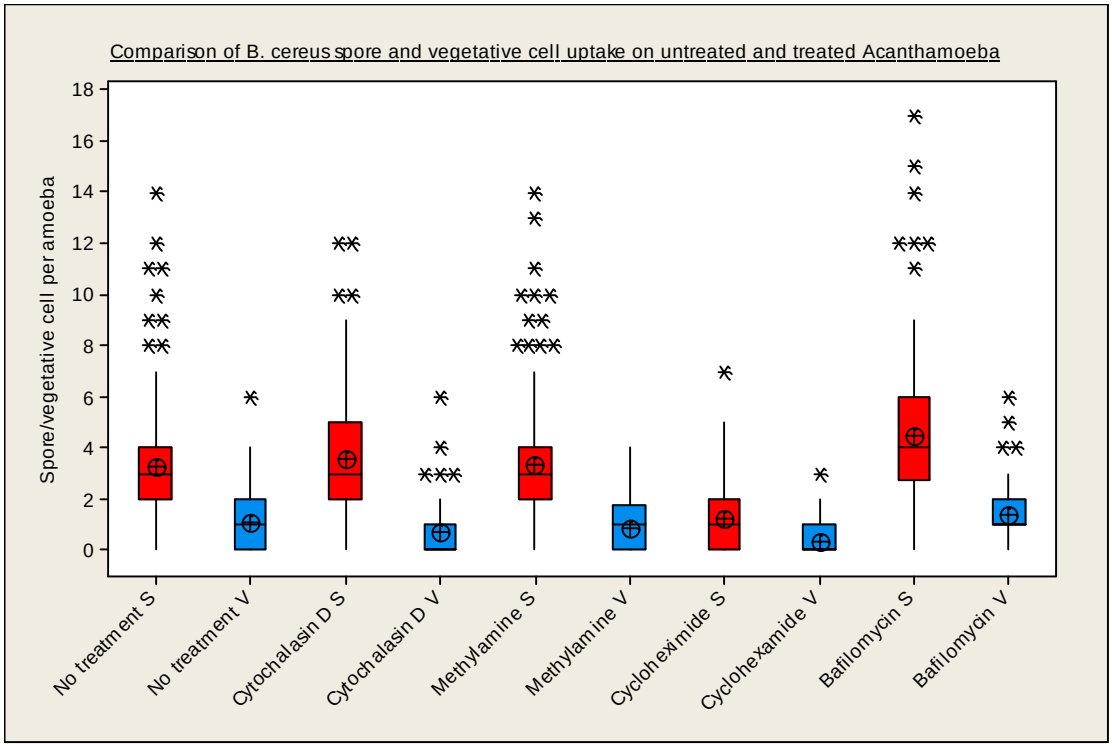

Figure 5.32. Comparison of uptake rates of *B. cereus* vegetative cells and spores of the untreated amoebae compared to treated amoebae with uptake inhibitors Cytovhalsin D, Methylamine and Cycloheximide. Bafilomycin is also shown to show the effect of reduced acidification of the amoebal vacuoles. Cross hatch shows the mean of each set of data. Spore uptake is represented by red boxes, vegetative cell uptake is represented with blue boxes.

Table showing levels of significance for phagocytosis of vegetative cells compared to spores with the different amoeba treatments:

No treatment	Cytochalasin D	Methylamine	Cycloheximide	Bafilomycin
p = <0.001	p = <0.001	p = <0.001	p = <0.001	p = <0.001

Results show that the cyclohexamide treatment of amoebae significantly reduced levels of phagocytosis of *B. cereus* spores when compared to untreated amoebae. Conversely, the Bafilomycin treatment of amoebae either significantly increased the uptake of *B. cereus* spores or increased the survival within the vacuoles when compared to the untreated amoebae.

The levels of vegetative cell uptake were significantly less than the uptake rates of the spores. This suggests that the vegetative cells actively resist phagocytic uptake relative to the spores. This correlates with the microscopic observations of stable colonisation of the bacteria on the amoebae surface. Treatments with Cytochalsin D and Cycloheximide both showed a significantly reduced rate of phagocytosis when compare to the untreated amoebae. Numbers of *B. cereus* vegetative cells were significantly increased after the treatment of Bafilomycin which we suggest indicates a better survival rate in the amoebae vacuoles due to the lower levels of acidification.

5.2 Discussion

Protozoa have been established as an environmental host for numerous bacterial pathogens (Jeong *et al.*, 2007, Huws *et al.*, 2006, Brown *et al.*, 2002, Barker *et al.*, 1992, Abd *et al.*, 2003). Most of these bacteria are human pathogens and amoebae have been suggested to represent a potential environmental reservoir (Barker & Brown, 1994). These adaptations to the intracellular environment have led to the suggestion that bacteria may have used protozoa as an evolutionary "training ground" to develop virulence in mammalian cells such as macrophages (Molmeret *et al.*, 2005, Barker & Brown, 1994).

These important connections between mammalian cell survival and survival from amoebal predation led to our investigation of amoebal interactions with *B. cereus*, *B. thuringiensis* and *B. anthracis*. *B. anthracis* can clearly survive phagocytosis by macrophages during the anthrax infection process. It has been shown to survive intracellularly, germinate and

escape from the macrophage for further dissemination around the host (Guidi-Rontani, 2002, Dixon *et al.*, 2000).

A limited investigation on *B. cereus* and *Acanthamoeba polyphaga* has recently been published (Huws *et al.*, 2008). In these studies it was found that *B. cereus* vegetative cells were not able to survive and replicate within *Acanthamoeba polyphaga*. Bacterial cell numbers decreased significantly over a period of 72 hours in the presence of the amoebae when compared to cell counts from controls in the absence of amoebae. The *Acanthamoeba polyphaga* showed to increase in numbers when co-incubated with *B. cereus*. These data indicate predation of the bacterial cells by the amoebae. Results present in this project, do show that *Acanthamoeba* can graze on the vegetative forms of *B. cereus*. Video footage has shown the *Bacilli* being engulfed and then digested within food vacuoles of the *Acanthamoeba* (See Video 5.1). As seen by the TEM images, tens of cells can be present in one vacuole. Nevertheless we have also seen *B. cereus* vegetative cells persisting inside amoebae for long periods, apparently not in the large clear food vacuoles and showing very high motility within the cell. TEM analysis suggest these may also be within vesicles although this is not clear and requires greater study. We have also seen vegetative cells emerge from amoebae and swim away.

At higher concentrations of bacteria, the vegetative *Bacilli* can be seen to chemotact toward the amoebae, attach onto the surface and then grow in micro-colony like clumps, much like that seen by *B. anthracis* when grown with macrophages (Dixon et al., 2000). These observations were not discussed by Huws *et al.* along with the unusual growth of *B. anthracis*, *B. cereus* and *B. thuringiensis* in very large filamented forms when in the presence of the amoebae.

It is known that *Bacilli* can grow in chains (Turnbull, 2002b), however, at x 40 magnification and SEM these very long filamented *Bacilli* certainly did not show any suggestion of septation, that is separate cells attached as chains, neither do they show signs of cell division occurring. The images present a smooth continuous filament with no regular light or surface distortion. Furthermore, real time microscopic analysis played back at higher speeds shows a smooth elongation of the filaments, essentially similar to fungal hyphal growth. This raises the intriguing possibility that these bacterial filaments contain multiple chromosomes in a continuous cytoplasm, again much like fungi. It has been observed that

B. anthracis grows in a filamentous manner in the rhizosphere of grass plants, but again however, their descriptions indicate that the *Bacilli* grew in chains of single cells not one elongated cell without any signs of cell division (Saile & Koehler, 2006). We did attempt to use TEM analysis to determine if these large filaments contained internal septae however due to the probability of finding a longitudinal section of a filament at such a scale we were unsuccessful and could only see oblique cross-sections of cells.

We noticed that the filamented forms of these *Bacilli* were far less likely to be engulfed by amoebae simply due to their cell length. Other bacteria have previously been seen to grow in length, as "filaments", when in the presence of amoebae and this phenotypic growth has been suggested as a defence mechanism to avoid predation from protozoa (Matz & Kjelleberg, 2005). This primitive yet effective defence mechanism might explain the differences between the uptake of spores and vegetative cells in the phagocytosis inhibitor studies. Spores were phagocytosed significantly more when compared to vegetative cells. The vegetative cells would be more difficult to phagocytose if they grow in length but also their motility would enable them to escape the advances of an amoeba whereas a spore is more likely to adhere to a solid surface where it can be grazed upon with ease by the predatory amoeba. However in addition to these effects we also see stable surface attachment of single cells suggesting they are able to prevent phagocytosis by other means.

A facultative filamentous bacterium; *Flectobacillus sp*. was isolated from lake water (Hahn *et al.*, 1999). It was found to grow in a filamentous form independently from stressful conditions when under predation from *Ochromonas sp*. However, the grazing of the flagellate *Ochromonas* positively influenced the growth of the filamentous phenotype by increasing growth rates and indirectly stimulating filamentation (Hahn et al., 1999). These observations could be applied to the results from this study as the filamentous forms of *Bacilli* were often found in association with the *Acanthamoeba*.

In this project we also showed that while they may make it more likely, that amoebae do not need to be present for filamentous growth and the formation of the complex rope-like structures. The comparison of natural growth of spores and vegetative cells in the variety of media has shown that filamentous growth is frequently observed in a range of environments at both high and low nutrient levels. The filamentous growth also occurred

at different temperatures. Due to the close relationships between *B. anthracis*, *B. cereus* and *B. thuringiensis* it is not surprising that all three strains have shown this growth characteristic. It is possible that the filamentation phenotype might be triggered by several possible environmental cues. One common factor in all our assays was the growth of bacteria in static conditions. We suggest that these conditions would lead to micro-aerophillic environment, especially when the free oxygen is being used by both bacteria and amoebae.

A close bacterial relative that has been studied in detail exhibiting the unusual rope-like growth characteristics is *B. subtilis*. Filamentous growth by *B. subtilis* has been studied closely by Mendelsons group at the University of Arizona. They have shown that a bacterial filament is the precursor for the production of a microfiber (Mendelson, 1976), analogous to the "ropes" described in this thesis. Filamented growth is produced from the outcome of the suppression of the autolytic enzyme required for cell division (Mendelson, 1990). The complex structure of the macrofiber is a result of the compensatory distortion of the cells as they are unable to rotate during growth (Mendelson, 1982). This causes a simple cylinder shaped cell to grow into a helix and further develop into an even more complex microfiber or "rope".

As seen in this study, macrofibers are formed by *B. thuringiensis*, *B. cereus* and *B. anthracis*. It would be reasonable to assume that motility may have some effect on the formation of the complex structures however, *B. anthracis* is characteristically non-motile. Motility is not required for the formation of macrofibers, as the suppression of cell division blocks the assembly of flagella rendering the bacteria non-motile (Fein & Rogers, 1976) which helps support the findings of macrofiber production from all strains used within this project.

The study of macrofibers has shown that they start from a single filament, gradually forming a helical thread and developing into a more complex macrofiber. It has been shown that regardless of the growth conditions straight cells are always produced as well as the elongated helical cells (Mendelson, 1976). Mendelson (1990) states that intercellular adhesions and cell/environment interactions play a significant role in the formation of a macrofiber. When existing in a macrofiber complex, cell to cell communication would be more efficient than quorum sensing.

Bacillus cereus has been connected to some unusual filamentous growth within the intestines of invertebrates (Margulis *et al*., 1998). These findings have been suggested to be a distinct stage of the *B. cereus* life cycle which reflects a different phenotype of growth termed "Arthromitus" (Margulis *et al.*, 1990). This filamentous growth was first described as "delicate filamentous plants" (Leidy, 1881). Since then, the term Arthromitus has been used to describe these segmented filamentous bacteria and DNA analysis has shown that they are closely related to group 1 *Bacilli*. This filamentous growth by *B. cereus* occurs in the intestines of animals and insects where the endospore forms attachment fibres and latches on to the epithelium, to protists, trichomycete fungi or to other intestinal substrata that prevent defecation by peristalsis (Margulis et al., 1998). The attachment to protists is an interesting finding as in these experiments the *B. cereus* cells were often found in association and attached the to surface of the amoeba. We suggest that our assays are mimicking the natural microaerophillic conditions inside invertebrate guts and the amoebae are presenting a substitute for the epithelial cells or other protist residents of the gut.

This Arthomitus stage of growth may be a common way of how this group of bacteria normally survive in the intestine of the host (Margulis et al., 1998), maybe even passing unrecognised as their true known selves as bacteriologists normally concentrate on growth characteristics in culture rather than *in vivo* (Margulis et al., 1990). The genome of the *B. cereus* group bacteria indicate that they are evolved to survive through the degradation of animal tissues rather than the plant derived complex carbohydrates typical of the *B. subtilis* species. If the *B. cereus* group can form a stable association within invertebrate guts as Arthromitus, they can pass spores out from their distal ends while the insect is alive and there is flow through the gut, and remain associated with the animal until it dies, whereupon it will have a large ready source of animal tissue for digestion.

During the production of the UK Anthrax Vaccine, small white filaments have been noted in the medium (personal communication). These small white filaments are very likely to be the production of these macrofibres as seen by *B. cereus* in natural culture in Basal medium. This type of growth has never been investigated so the effect of this type of growth on the production of the vaccine is unknown, although the method has not changed since it was first licensed in the 1950's, therefore this type of growth is likely to have been produced without any knowledge over the past 60 years.

In the natural environment in the soil *B. cereus* and *B. anthracis* are much more likely to be in their spore form due to the constant exposure to adverse environmental conditions. Therefore it seems logical to assess the interactions between amoebae and *B. cereus* spores at lower temperatures reflecting that of a more common environment. When spores of *B. cereus* were engulfed by *A. polyphaga,* digestion in the food vacuoles was not apparent and on occasion the spores were even seen being expelled from the amoebae vacuoles back into the surrounding media. In these cases it was not known if the spores remained viable however. The bacterial spore coat is extremely well built for the protection of the bacteria from adverse environmental conditions. It is possible therefore that the spore coat can also protect the bacteria from the amoebal digestion system. A similar finding has recently shown that the *B. subtilis* spore coat is resistant to the lysosomal enzymes when ingested by the protozoa *Tetrahymena thermophila* (Klobutcher et al., 2006). Survival of *B. subtilis* spores in co-culture with *Tetrahymena thermophila* were compared using strains of wild type *B. subtilis* and *B. subtilis* mutants containing spore coat defects. The *B. subtilis* wild type showed to be phagocytosed but were not digested or killed. The spore coat mutants were phagocytosed, digested and killed leaving the outer "rind" of the spore thus supporting the growth of the *Tetrahymena*.

We were not able to directly prove and image germination inside the amoebae in this study. Although certain TEM images and overnight incubations of co-cultured amoebae and spores with gentamycin did suggest this was occurring. The environment of the amoeba phogosome is likely to be similar to that of the alveolar macrophage, in which *B. anthracis* spores germinate. Germination continued to occur in the surrounding media even in very low nutrient conditions. Results showed that the *Bacillus* spores do not germinate in PBS over night but they germinate and outgrow in PBS when co-cultured in the presence of the *Acanthamoeba*. Results also showed that limited germination and outgrowth occurred when spores were incubated in PBS in the presence of the supernatant from an *Acanthamoeba* culture. Growth was more substantial when cultured in the presence of the amoebae as the amoebae secreted/excreted product(s) utilised by the *Bacillus* were presumably being continually replenished whereas a specific amount of supernatant added to the culture would be limited and therefore used up quickly by the germinating *Bacilli*. The stable attachment of the *B. cereus* onto the surface of the amoebae and the ability to grow using material released by the amoebae raises an intriguing possibility for symbiosis.

We did note that on occasion an amoeba would phagocytose individual bacterial cells from the clumps resident on their surface. We suggest the amoeba may "attract" bacteria and allow them to colonise an area of the cell surface. The bacteria are able to feed off material released by the amoeba and in return are occasionally consumed by the amoeba. This "cellular farming" may be an example of a precursor of more tightly evolved complex symbiotic associations between bacteria and eukaryotes. Conversely depending on the prevailing conditions the bacteria seem able to evade phagocytic destruction by invading the cytoplasm of the bacteria. Under other conditions the amoebae seem to be able to wipe out the bacteria by over grazing. A complex situation of factors such as nutrient availability and relative cell numbers seems to govern the outcome of the interactions and while this is clearly an excellent model system will require significant further work to unravel.

Germination of a *Bacillus* spore requires the combination of monovalent cations and nutrient germinants (Foerster & Foster, 1966). It has been shown that the size of the molecules involved in the germination of the *Bacillus* spores are <5kDa which would suggest that small molecules/ions such as monovalent cations are causing the spores to germinate. These are likely to have been secreted/excreted by the amoebae into the surrounding media. The germination of a *Bacillus* spore starts from the rehydration of the inner membrane which resumes the permeability and ion fluxes and restarts the movement of cations across the spore membrane. Then follows the degradation of the peptidoglycan of the spore cortex and coat layers. After ATP synthesis and oxidative metabolism have begun the DNA complexing small acid-soluble proteins are degraded which are used as a source of amino acids for continuing the spore outgrowth (Moir *et al.*, 2002). Once this process has been initiated the cascade is likely to complete through to the outgrowth into the vegetative cell. The supernatant of the *Acanthamoeba* obviously contains enough nutrient germinants and monovalent cations in order to initiate the start of the germination cascade.

The studies involving the treatment of *Acanthamoeba* with phagocytosis inhibitors showed some interesting results. When looking at the uptake of *B. cereus* spores, the treatment with cycloheximide showed a significant decrease in phagocytosis levels. Cycloheximide inhibits eukaryotic protein synthesis (Declerck et al., 2007) by interfering with the

translocation step in protein synthesis. By blocking this in *Acanthamoeba*, endocytosis is stopped and therefore uptake of cells by endocytosis would not be able to continue. It is interesting however that some bacteria are still found within the vacuoles even with this treatment suggesting that the amoebae are not totally sensitive to this drug. Treatments with Cytochalasin D and Methylamine show no significant reduction in uptake of *B. cereus* spores. This suggests that the spores are not phagocytosed by microfilament-dependant phagocytosis or receptor mediated endocytosis. Alternatively the *Acanthamoeba* pathways may be diverged sufficiently for these drugs not to function. *B. anthracis* spores are phagocytosed by macrophages in the presence of PA antibodies. *B. anthracis* spores have been found to use receptor based phagocytosis to enable entry into professional phagocytes. The integrin Mac-1 is essential for the recognition of the *B. anthracis* exosporium protein BclA for phagocytosis into the macrophage (Oliva *et al.*, 2008). These experiments should be performed with *B. anthracis* spores to see if the cytochalasin D and methylamine treatments affect the uptake into amoebae reflecting a receptor-mediated phagocytosis as in macrophages.

The vegetative cells were phagocytosed at extremely reduced rates when compared to the levels of the spore ingestions. These reduced levels might be due to a number of factors; the motility of the vegetatvive cells enabling them to avoid phagocytosis; filamented growth to become too large to ingest and also an active mechanism coupled to surface colonisation . Interestingly, in the case of the vegetative cells, treatments with cytochalsin D and cycloheximide both showed significantly reduced uptake of cells when compared to the untreated amoebae. These results suggest that microfilament dependant phagocytosis may be part of the uptake of *B. cereus* vegetative cells as well as the expected lack of phagocytosis from stopped protein synthesis caused by the cycloheximide treatment.

Bafilomycin treatment of the amoebae would stop the acidification of the amoebal vacuole and hamper digestion of internalised bacteria. Results from uptake of both spores and vegetative cells showed a significantly more bacteria in bafilomycin treated amoebae which would suggest that both spores and vegetative cells are less likely to survive or stay within the vacuoles if fully acidified.

6 Conclusion and Future areas of work

There are still some significant areas of work that need to be investigated surrounding the importance of inorganic polyp and its relationship with *B. anthracis*.

If inhibition or genetic ablation of the enzymes Ppk, Ppx and Pap has the same detrimental effects as it does in *B. cereus* (Shi et al., 2004) then this would represent an ideal target for a focus of new therapies and prophylactics against anthrax. The current UK Anthrax vaccine is a crude and simple procedure that hasn't changed in many years. Side effects of the current vaccine can be substantial sometimes resulting in illness leading to days off work. With new information and new vaccine targets becoming available, improvement of this vaccine is of great importance. If making the knockout mutants continued to prove difficult an alternative approach would be to use overexpression of *ppx.* This leads to depletion of cellular poly P, resulting in the same cellular effects that would result knocking out the *ppk* gene and these particular studies could be completed.

The current vaccine procedure uses basal medium as a method of growing *B. anthracis*. These studies have shown that *B. anthracis* and *B. cereus* behave and grow in an unusual form when grown statically in low nutrient media like the basal medium. The macrofibres seem to be produced in varying levels of nutrient availability ranging from a 1% L broth in PBS to a limited macrofibre production at 100% L broth, but interestingly the basal media growth was very slow and limited. It should be noted that following a culture growth with optical density is not useful if the bacterial biomass production switches to the fungal hyphal like forms represented by the Macrofibres. This growth dominated over the "normal" short distinct rod shaped bacteria when grown in basal medium which would surely have an important role in the types of protein expressed in this environment. It has been noted that *B. anthracis* does form small "spindles" of growth which are visible to the naked eye (similar to macrofibre experiments during this study) during the incubation in the Thompson bottles for vaccine production (personal communication). This correlates with the results found in this study.

The studies on *ppk*, *ppx* and *pap* gene expression have shown some interesting results but these studies could be expanded to look into the specific gene expression of the toxins which could include PA, LF and EF rather than looking at PA and LF alone. The use of a real

time RT-PCR assay is useful for looking at specific gene expression but looking at the growth of *B. anthracis* in production for the vaccine, it would be far more revealing to use a *Bacillus* microarray to examine the wider aspects of the different genes expressed. This would be especially fascinating when focusing on macrofibre growth as well as interactions with amoebae.

A microarray could focus in on the genes required for macrofibre growth and distinguish any similarities between this form of growth and the production of biofilm within the vaccine production method. If specific genes were to be identified these could then be targeting for further investigations such as knockout mutants and look into whether these specific genes are essential for macrofibre growth and whether their expression is vital in the current vaccine procedure.

Macrofibre growth does not appear to be limited to a specific *Bacillus* strain (demonstrated in *B. anthracis*, *B. cereus* and *B. thuringiensis* and previously published work on *B. subtilis*) and it may be interesting to examine more Bacillus strains and then further these studies to other similar bacteria such as *Clostridium difficle* which shares a number of physiological similarities with *B. anthracis* (i.e. Rod shaped, gram positive, spore former).

Maybe this strange form of fibrous growth is common in the bacterial world but with the focus of scientific research on molecular and downstream applications are we missing the basics of physiology under the microscope? Our real time microscopic studies of the interactions of these bacteria with one amoeba species has made it clear that they can form several unique developmental morphologies or stages. These include (i) single motile rods; (ii) cell-attached single rods; (iii) intracellular single rods, (iv) large attached or motile filaments; (v) large multi-filamented macrofibres and (vi) spores. The biotic and abiotic factors and the genes responsible that trigger the transitions between these stages in most cases require elucidation. The ecological implications of this diverse behaviour is also important when considering monitoring the impacts of spraying large quantities of *B. thuringiensis* as pest control agent and also in the management of anthrax infected soil sites.

Recent work on macrofibres was published on *B. subtilis* (Mendelson *et al.*, 2001) but this research has now turned to focus on the actual motions of the macrofibres and how they

are formed. The reasons as to why they form and the environmental factors that initiate the stimulation of the elongation of the cells is an area of research that could certainly be exploited in future endeavours.

The amoebae interactions performed in this study used only one strain of amoeba and it would be beneficial to investigate this further by looking at interactions with different species of protozoa. *B. subtilis* and *B. thuringiensis* have shown interact with *Tetrahymena* so this would be the next logical step. In other endosymbiotic relationships there is typically a particular protozoa that the bacteria can invade, or in the case of *L. pneumophila* there are 13 strains, so this should be considered when further investigating growth and replication in amoebae for *Bacillus sps*. and especially *B. anthracis* which shares so many intracellular growth characteristics with other bacterial endosymbionts.

There is clearly a great deal of diverse selection pressures exerted upon soil bacteria and the studies presented here indicate that the *B. cereus* group have evolved a number of behaviours and metabolic regulatory mechanisms to respond to these changing biotic and abiotic environmental stresses.

7 References

Abd, H., T. Johansson, I. Golovliov, G. Sandstrom & M. Forsman, (2003) Survival and growth of *Francisella tularensis* in *Acanthamoeba castellanii*. *Applied and environmental microbiology* **69**: 600-606.

Abd, H., A. Saeed, A. Weintraub, G. B. Nair & G. Sandstrom, (2007) *Vibrio cholerae* O1 strains are facultative intracellular bacteria, able to survive and multiply symbiotically inside the aquatic free-living amoeba *Acanthamoeba castellanii*. *FEMS microbiology ecology* **60**: 33-39.

Abrami, L., N. Reig & F. G. van der Goot, (2005) Anthrax toxin: the long and winding road that leads to the kill. *Trends Microbiol* **13**: 72-78.

Ahn, K. & A. Kornberg, (1990) Polyphosphate kinase from *Escherichia coli*. Purification and demonstration of a phosphoenzyme intermediate. *J Biol Chem* **265**: 11734-11739.

Arnaud, M., A. Chastanet & M. Debarbouille, (2004) New vector for efficient allelic replacement in naturally nontransformable, low-GC-content, gram-positive bacteria. *Applied and environmental microbiology* **70**: 6887-6891.

Ayraud, S., B. Janvier, A. Labigne, C. Ecobichon, C. Burucoa & J. L. Fauchere, (2005) Polyphosphate kinase: a new colonization factor of *Helicobacter pylori*. *FEMS Microbiol Lett* **243**: 45-50.

Bach, H., D. Errampalli, K. T. Leung, H. Lee, A. Hartmann, J. T. Trevors & J. C. Munch, (1999) Specific detection of the gene for the extracellular neutral protease of *Bacillus cereus* by PCR and blot hybridization. *Appl Environ Microbiol* **65**: 3226-3228.

Baillie, L., R. Hebdon, H. Flick-Smith & D. Williamson, (2003) Characterisation of the immune response to the UK human anthrax vaccine. *FEMS immunology and medical microbiology* **36**: 83-86.

Barker, J. & M. R. Brown, (1994) Trojan horses of the microbial world: protozoa and the survival of bacterial pathogens in the environment. *Microbiology* **140**: 1253-1259.

Barker, J., M. R. Brown, P. J. Collier, I. Farrell & P. Gilbert, (1992) Relationship between *Legionella pneumophila* and *Acanthamoeba polyphaga*: physiological status and susceptibility to chemical inactivation. *Applied and environmental microbiology* **58**: 2420-2425.

Barker, J., T. J. Humphrey & M. W. Brown, (1999) Survival of *Escherichia coli* O157 in a soil protozoan: implications for disease. *FEMS microbiology letters* **173**: 291-295.

Berry, C., S. O'Neil, E. Ben-Dov, A. F. Jones, L. Murphy, M. A. Quail, M. T. Holden, D. Harris, A. Zaritsky & J. Parkhill, (2002) Complete sequence and organization of pBtoxis, the toxin-coding plasmid of *Bacillus thuringiensis* subsp. *israelensis*. *Applied and environmental microbiology* **68**: 5082-5095.

Brown, E. R. & W. B. Cherry, (1955) Specific identification of *Bacillus anthracis* by means of a variant bacteriophage. *J Infect Dis* **96**: 34-39.

Brown, M. R. & A. Kornberg, (2004) Inorganic polyphosphate in the origin and survival of species. *Proc Natl Acad Sci U S A* **101**: 16085-16087.

Brown, M. R. & A. Kornberg, (2008) The long and short of it - polyphosphate, PPK and bacterial survival. *Trends in biochemical sciences*.

Brown, M. R., A. W. Smith, J. Barker, T. J. Humphrey & B. Dixon, (2002) *E. coli* O157 persistence in the environment. *Microbiology* **148**: 1-2.

Carlson, C. R., D. A. Caugant & A. B. Kolsto, (1994) Genotypic Diversity among *Bacillus cereus* and *Bacillus thuringiensis* Strains. *Applied and environmental microbiology* **60**: 1719-1725.

Charity, J. C., L. T. Blalock, M. M. Costante-Hamm, D. L. Kasper & S. L. Dove, (2009) Small molecule control of virulence gene expression in *Francisella tularensis*. *PLoS pathogens* **5**: e1000641.

Charlton, S., M. Herbert, J. McGlashan, A. King, P. Jones, K. West, A. Roberts, N. Silman, T. Marks, M. Hudson & B. Hallis, (2007) A study of the physiology of *Bacillus anthracis* Sterne during manufacture of the UK acellular anthrax vaccine. *J Appl Microbiol* **103**: 1453-1460.

Chawla, A., S. Midha & R. Bhatnagar, (2009) Efficacy of recombinant anthrax vaccine against *Bacillus anthracis* aerosol spore challenge: preclinical evaluation in rabbits and Rhesus monkeys. *Biotechnology journal* **4**: 391-399.

Choma, C. & P. E. Granum, (2002) The enterotoxin T (BcET) from *Bacillus cereus* can probably not contribute to food poisoning. *FEMS microbiology letters* **217**: 115-119.

Chopra, A. P., S. A. Boone, X. Liang & N. S. Duesbery, (2003) Anthrax lethal factor proteolysis and inactivation of MAPK kinase. *The Journal of biological chemistry* **278**: 9402-9406.

Cirillo, J. D., S. Falkow, L. S. Tompkins & L. E. Bermudez, (1997) Interaction of *Mycobacterium avium* with environmental amoebae enhances virulence. *Infection and immunity* **65**: 3759-3767.

Dahl, J. L., C. N. Kraus, H. I. Boshoff, B. Doan, K. Foley, D. Avarbock, G. Kaplan, V. Mizrahi, H. Rubin & C. E. Barry, 3rd, (2003) The role of RelMtb-mediated adaptation to stationary phase in long-term persistence of *Mycobacterium tuberculosis* in mice. *Proc Natl Acad Sci U S A* **100**: 10026-10031.

Dai, Z. & T. M. Koehler, (1997) Regulation of anthrax toxin activator gene (atxA) expression in *Bacillus anthracis*: temperature, not CO2/bicarbonate, affects AtxA synthesis. *Infection and immunity* **65**: 2576-2582.

Dalebroux, Z. D., S. L. Svensson, E. C. Gaynor & M. S. Swanson, (2010) ppGpp conjures bacterial virulence. *Microbiol Mol Biol Rev* **74**: 171-199.

Datsenko, K. A. & B. L. Wanner, (2000) One-step inactivation of chromosomal genes in *Escherichia coli* K-12 using PCR products. *Proc Natl Acad Sci U S A* **97**: 6640-6645.

de Maagd, R. A., A. Bravo, C. Berry, N. Crickmore & H. E. Schnepf, (2003) Structure, diversity, and evolution of protein toxins from spore-forming entomopathogenic bacteria. *Annual review of genetics* **37**: 409-433.

de Moraes, J. & S. C. Alfieri, (2008) Growth, encystment and survival of *Acanthamoeba castellanii* grazing on different bacteria. *FEMS microbiology ecology* **66**: 221-229.

Declerck, P., J. Behets, B. De Keersmaecker & F. Ollevier, (2007) Receptor-mediated uptake of *Legionella pneumophila* by *Acanthamoeba castellanii* and *Naegleria lovaniensis*. *Journal of applied microbiology* **103**: 2697-2703.

Dempsey, L. A. & Dubnau, D. A. (1989) Localization of the replication origin of plasmid pE194. **171** (5): 2866-2869.

Dixon, T. C., A. A. Fadl, T. M. Koehler, J. A. Swanson & P. C. Hanna, (2000) Early *Bacillus anthracis*-macrophage interactions: intracellular survival survival and escape. *Cell Microbiol* **2**: 453-463.

Donovan, W. P., Y. Tan & A. C. Slaney, (1997) Cloning of the nprA gene for neutral protease A of *Bacillus thuringiensis* and effect of in vivo deletion of nprA on insecticidal crystal protein. *Appl Environ Microbiol* **63**: 2311-2317.

Drobniewski, F. A., (1993) *Bacillus cereus* and related species. *Clin Microbiol Rev* **6**: 324-338.

Drysdale, M., A. Bourgogne, S. G. Hilsenbeck & T. M. Koehler, (2004) atxA controls *Bacillus anthracis* capsule synthesis via acpA and a newly discovered regulator, acpB. *Journal of bacteriology* **186**: 307-315.

Etienne-Toumelin, I., J. C. Sirard, E. Duflot, M. Mock & A. Fouet, (1995) Characterization of the *Bacillus anthracis* S-layer: cloning and sequencing of the structural gene. *J Bacteriol* **177**: 614-620.

Ezzell, J. W. & S. L. Welkos, (1999) The capsule of *Bacillus anthracis*, a review. *J Appl Microbiol* **87**: 250.

Fein, J. E. & H. J. Rogers, (1976) Autolytic enzyme-deficient mutants of *Bacillus subtilis* 168. *Journal of bacteriology* **127**: 1427-1442.

Feinberg, L., J. Jorgensen, A. Haselton, A. Pitt, R. Rudner & L. Margulis, (1999) Arthromitus (*Bacillus cereus*) symbionts in the cockroach Blaberus giganteus: dietary influences on bacterial development and population density. *Symbiosis* **27**: 109-123.

Fenner, L., H. Richet, D. Raoult, L. Papazian, C. Martin & B. La Scola, (2006) Are clinical isolates of *Pseudomonas aeruginosa* more virulent than hospital environmental isolates in amebal co-culture test? *Critical care medicine* **34**: 823-828.

Ferrari, M. E., G. Hermanson & A. Rolland, (2004) Development of anthrax DNA vaccines. *Curr Opin Mol Ther* **6**: 506-512.

Fields, B. S., (1996) The molecular ecology of *legionellae*. *Trends in microbiology* **4**: 286-290.

Firth, J. D., E. E. Putnins, H. Larjava & V. J. Uitto, (1997) Bacterial phospholipase C upregulates matrix metalloproteinase expression by cultured epithelial cells. *Infection and immunity* **65**: 4931-4936.

Fitzpatrick, D. J., P. C. Turnbull, C. T. Keane & L. F. English, (1979) Two gas-gangrene-like infections due to *Bacillus cereus*. *The British journal of surgery* **66**: 577-579.

Flores, I., A. C. Martinez, Y. A. Hannun & I. Merida, (1998) Dual role of ceramide in the control of apoptosis following IL-2 withdrawal. *J Immunol* **160**: 3528-3533.

Foerster, H. F. & J. W. Foster, (1966) Response of *Bacillus* spores to combinations of germinative compounds. *J Bacteriol* **91**: 1168-1177.

Fortier, A. H., S. J. Green, T. Polsinelli, T. R. Jones, R. M. Crawford, D. A. Leiby, K. L. Elkins, M. S. Meltzer & C. A. Nacy, (1994) Life and death of an intracellular pathogen: *Francisella tularensis* and the macrophage. *Immunol Ser* **60**: 349-361.

Friedlander, A. M., S. L. Welkos, M. L. Pitt, J. W. Ezzell, P. L. Worsham, K. J. Rose, B. E. Ivins, J. R. Lowe, G. B. Howe, P. Mikesell & et al., (1993) Postexposure prophylaxis against experimental inhalation anthrax. *J Infect Dis* **167**: 1239-1243.

Fukao, T., (2004) Immune system paralysis by anthrax lethal toxin: the roles of innate and adaptive immunity. *Lancet Infect Dis* **4**: 166-170.

Galloway, D. R. & L. Baillie, (2004) DNA vaccines against anthrax. *Expert Opin Biol Ther* **4**: 1661-1667.

Gao, L. Y., O. S. Harb & Y. Abu Kwaik, (1997) Utilization of similar mechanisms by *Legionella pneumophila* to parasitize two evolutionarily distant host cells, mammalian macrophages and protozoa. *Infection and immunity* **65**: 4738-4746.

Gaze, W. H., N. Burroughs, M. P. Gallagher & E. M. Wellington, (2003) Interactions between *Salmonella typhimurium* and *Acanthamoeba polyphaga*, and observation of a new mode of intracellular growth within contractile vacuoles. *Microbial ecology* **46**: 358-369.

Gonzalez, J. M., Jr. & B. C. Carlton, (1980) Patterns of plasmid DNA in crystalliferous and acrystalliferous strains of *Bacillus thuringiensis*. *Plasmid* **3**: 92-98.

Granum, P. E., (1994) *Bacillus cereus* and its toxins. *Soc Appl Bacteriol Symp Ser* **23**: 61S-66S.

Granum, P. E. & T. Lund, (1997) *Bacillus cereus* and its food poisoning toxins. *FEMS microbiology letters* **157**: 223-228.

Guidi-Rontani, C., (2002) The alveolar macrophage: the Trojan horse of *Bacillus anthracis*. *Trends Microbiol* **10**: 405-409.

Guidi-Rontani, C., M. Weber-Levy, E. Labruyere & M. Mock, (1999) Germination of *Bacillus anthracis* spores within alveolar macrophages. *Mol Microbiol* **31**: 9-17.

Hahn, M. W., E. R. Moore & M. G. Hofle, (1999) Bacterial filament formation, a defense mechanism against flagellate grazing, is growth rate controlled in bacteria of different phyla. *Applied and environmental microbiology* **65**: 25-35.

Harb, O. S., C. Venkataraman, B. J. Haack, L. Y. Gao & Y. A. Kwaik, (1998) Heterogeneity in the attachment and uptake mechanisms of the Legionnaires' disease bacterium,

Legionella pneumophila, by protozoan hosts. *Applied and environmental microbiology* **64**: 126-132.

Heid, C. A., J. Stevens, K. J. Livak & P. M. Williams, (1996) Real time quantitative PCR. *Genome research* **6**: 986-994.

Heinz, E., I. Kolarov, C. Kastner, E. R. Toenshoff, M. Wagner & M. Horn, (2007) An *Acanthamoeba* sp. containing two phylogenetically different bacterial endosymbionts. *Environmental microbiology* **9**: 1604-1609.

Helgason, E., O. A. Okstad, D. A. Caugant, H. A. Johansen, A. Fouet, M. Mock, I. Hegna & A. B. Kolsto, (2000) *Bacillus anthracis, Bacillus cereus*, and *Bacillus thuringiensis*--one species on the basis of genetic evidence. *Appl Environ Microbiol* **66**: 2627-2630.

Hernandez-Ruiz, L., I. Gonzalez-Garcia, C. Castro, J. A. Brieva & F. A. Ruiz, (2006) Inorganic polyphosphate and specific induction of apoptosis in human plasma cells. *Haematologica* **91**: 1180-1186.

Higuchi, R., C. Fockler, G. Dollinger & R. Watson, (1993) Kinetic PCR analysis: real-time monitoring of DNA amplification reactions. *Bio/technology (Nature Publishing Company)* **11**: 1026-1030.

Hoffmaster, A. R., K. K. Hill, J. E. Gee, C. K. Marston, B. K. De, T. Popovic, D. Sue, P. P. Wilkins, S. B. Avashia, R. Drumgoole, C. H. Helma, L. O. Ticknor, R. T. Okinaka & P. J. Jackson, (2006) Characterization of *Bacillus cereus* isolates associated with fatal pneumonias: strains are closely related to *Bacillus anthracis* and harbor *B. anthracis* virulence genes. *J Clin Microbiol* **44**: 3352-3360.

Hoffmaster, A. R., J. Ravel, D. A. Rasko, G. D. Chapman, M. D. Chute, C. K. Marston, B. K. De, C. T. Sacchi, C. Fitzgerald, L. W. Mayer, M. C. Maiden, F. G. Priest, M. Barker, L. Jiang, R. Z. Cer, J. Rilstone, S. N. Peterson, R. S. Weyant, D. R. Galloway, T. D. Read, T. Popovic & C. M. Fraser, (2004) Identification of anthrax toxin genes in a *Bacillus cereus* associated with an illness resembling inhalation anthrax. *Proc Natl Acad Sci U S A* **101**: 8449-8454.

Hofte, H. & H. R. Whiteley, (1989) Insecticidal crystal proteins of *Bacillus thuringiensis*. *Microbiological reviews* **53**: 242-255.

Horn, M., M. D. Harzenetter, T. Linner, E. N. Schmid, K. D. Muller, R. Michel & M. Wagner, (2001) Members of the Cytophaga-Flavobacterium-Bacteroides phylum as intracellular bacteria of *acanthamoebae*: proposal of 'Candidatus Amoebophilus asiaticus'. *Environmental microbiology* **3**: 440-449.

Horn, M. & M. Wagner, (2004) Bacterial endosymbionts of free-living amoebae. *The Journal of eukaryotic microbiology* **51**: 509-514.

Horwitz, M. A. & S. C. Silverstein, (1980) Legionnaires' disease bacterium (*Legionella pneumophila*) multiples intracellularly in human monocytes. *J Clin Invest* **66**: 441-450.

Howard, K. & T. J. Inglis, (2003) The effect of free chlorine on *Burkholderia pseudomallei* in potable water. *Water Res* **37**: 4425-4432.

Howard, K. & T. J. Inglis, (2005) Disinfection of *Burkholderia pseudomallei* in potable water. *Water Res* **39**: 1085-1092.

Huws, S. A., R. J. Morley, M. V. Jones, M. R. Brown & A. W. Smith, (2008) Interactions of some common pathogenic bacteria with *Acanthamoeba polyphaga*. *FEMS Microbiol Lett* **282**: 258-265.

Huws, S. A., A. W. Smith, M. C. Enright, P. J. Wood & M. R. Brown, (2006) Amoebae promote persistence of epidemic strains of MRSA. *Environmental microbiology* **8**: 1130-1133.

Inglesby, T. V., D. A. Henderson, J. G. Bartlett, M. S. Ascher, E. Eitzen, A. M. Friedlander, J. Hauer, J. McDade, M. T. Osterholm, T. O'Toole, G. Parker, T. M. Perl, P. K. Russell & K. Tonat, (1999) Anthrax as a biological weapon: medical and public health management. Working Group on Civilian Biodefense. *Jama* **281**: 1735-1745.

Ishige, K., H. Zhang & A. Kornberg, (2002) Polyphosphate kinase (PPK2), a potent, polyphosphate-driven generator of GTP. *Proc Natl Acad Sci U S A* **99**: 16684-16688.

Ivanova, N., A. Sorokin, I. Anderson, N. Galleron, B. Candelon, V. Kapatral, A. Bhattacharyya, G. Reznik, N. Mikhailova, A. Lapidus, L. Chu, M. Mazur, E. Goltsman, N. Larsen, M. D'Souza, T. Walunas, Y. Grechkin, G. Pusch, R. Haselkorn, M. Fonstein, S. D. Ehrlich, R. Overbeek & N. Kyrpides, (2003) Genome sequence of *Bacillus cereus* and comparative analysis with *Bacillus anthracis*. *Nature* **423**: 87-91.

Jeong, H. J., E. S. Jang, B. I. Han, K. H. Lee, M. S. Ock, H. H. Kong, D. I. Chung, S. Y. Seol, D. T. Cho & H. S. Yu, (2007) *Acanthamoeba*: could it be an environmental host of Shigella? *Experimental parasitology* **115**: 181-186.

Josenhans, C. & S. Suerbaum, (2002) The role of motility as a virulence factor in bacteria. *Int J Med Microbiol* **291**: 605-614.

Keim, P., J. M. Gruendike, A. M. Klevytska, J. M. Schupp, J. Challacombe & R. Okinaka, (2009) The genome and variation of *Bacillus anthracis*. *Molecular aspects of medicine* **30**: 397-405.

Keim, P., L. B. Price, A. M. Klevytska, K. L. Smith, J. M. Schupp, R. Okinaka, P. J. Jackson & M. E. Hugh-Jones, (2000) Multiple-locus variable-number tandem repeat analysis reveals genetic relationships within Bacillus anthracis. *J Bacteriol* **182**: 2928-2936.

Khan, N. A., (2006) *Acanthamoeba*: biology and increasing importance in human health. *FEMS microbiology reviews* **30**: 564-595.

Kilvington, S. & J. Price, (1990) Survival of *Legionella pneumophila* within cysts of *Acanthamoeba polyphaga* following chlorine exposure. *J Appl Bacteriol* **68**: 519-525.

Kim, K. S., N. N. Rao, C. D. Fraley & A. Kornberg, (2002) Inorganic polyphosphate is essential for long-term survival and virulence factors in *Shigella* and *Salmonella* spp. *Proc Natl Acad Sci U S A* **99**: 7675-7680.

King, C. H., B. S. Fields, E. B. Shotts, Jr. & E. H. White, (1991) Effects of cytochalasin D and methylamine on intracellular growth of *Legionella pneumophila* in amoebae and human monocyte-like cells. *Infection and immunity* **59**: 758-763.

Kintzer, A. F., K. L. Thoren, H. J. Sterling, K. C. Dong, G. K. Feld, Tang, II, T. T. Zhang, E. R. Williams, J. M. Berger & B. A. Krantz, (2009) The protective antigen component of anthrax toxin forms functional octameric complexes. *Journal of molecular biology* **392**: 614-629.

Kirby, J. E., (2004) Anthrax lethal toxin induces human endothelial cell apoptosis. *Infect Immun* **72**: 430-439.

Klee, S. R., M. Ozel, B. Appel, C. Boesch, H. Ellerbrok, D. Jacob, G. Holland, F. H. Leendertz, G. Pauli, R. Grunow & H. Nattermann, (2006) Characterization of *Bacillus anthracis*-like bacteria isolated from wild great apes from Cote d'Ivoire and Cameroon. *J Bacteriol* **188**: 5333-5344.

Klobutcher, L. A., K. Ragkousi & P. Setlow, (2006) The *Bacillus subtilis* spore coat provides "eat resistance" during phagocytic predation by the protozoan *Tetrahymena thermophila*. *Proc Natl Acad Sci U S A* **103**: 165-170.

Koehler, T. M., (2009) *Bacillus anthracis* physiology and genetics. *Mol Aspects Med* **30**: 386-396.

Koehler, T.M., (2002) *Bacillus anthracis* Genetics and Virulence Gene Regulation. In Anthrax, T. M. Koehler ed. (Springer) pp. 143-164.

Kolsto, A. B., N. J. Tourasse & O. A. Okstad, (2009) What sets *Bacillus anthracis* apart from other *Bacillus* species? *Annu Rev Microbiol* **63**: 451-476.

Kornberg, A., (1995) Inorganic polyphosphate: toward making a forgotten polymer unforgettable. *J Bacteriol* **177**: 491-496.

Kornberg, A., N. N. Rao & D. Ault-Riche, (1999) Inorganic polyphosphate: a molecule of many functions. *Annu Rev Biochem* **68**: 89-125.

Kotiranta, A., K. Lounatmaa & M. Haapasalo, (2000) Epidemiology and pathogenesis of *Bacillus cereus* infections. *Microbes Infect* **2**: 189-198.

Kumble, K. D. & A. Kornberg, (1995) Inorganic polyphosphate in mammalian cells and tissues. *J Biol Chem* **270**: 5818-5822.

Kumble, K. D. & A. Kornberg, (1996) Endopolyphosphatases for long chain inorganic polyphosphate in yeast and mammals. *J Biol Chem* **271**: 27146-27151.

Kuroda, A., (2006) A polyphosphate-lon protease complex in the adaptation of *Escherichia coli* to amino acid starvation. *Biosci Biotechnol Biochem* **70**: 325-331.

Kuroda, A., H. Murphy, M. Cashel & A. Kornberg, (1997) Guanosine tetra- and pentaphosphate promote accumulation of inorganic polyphosphate in *Escherichia coli. J Biol Chem* **272**: 21240-21243.

Lamothe, J., S. Thyssen & M. A. Valvano, (2004) *Burkholderia cepacia* complex isolates survive intracellularly without replication within acidic vacuoles of *Acanthamoeba polyphaga*. *Cellular microbiology* **6**: 1127-1138.

Leidy, J., (1881) The parasites of termites. *Journal of the Academy of Natural Sciences of Philadelphia* **8**: 425-447.

Leppla, S. H., (1982) Anthrax toxin edema factor: a bacterial adenylate cyclase that increases cyclic AMP concentrations of eukaryotic cells. *Proc Natl Acad Sci U S A* **79**: 3162-3166.

Li, L., N. N. Rao & A. Kornberg, (2007) Inorganic polyphosphate essential for lytic growth of phages P1 and fd. *Proc Natl Acad Sci U S A* **104**: 1794-1799.

Lorence, A., A. Darszon, C. Diaz, A. Lievano, R. Quintero & A. Bravo, (1995) Delta-endotoxins induce cation channels in *Spodoptera frugiperda* brush border membranes in suspension and in planar lipid bilayers. *FEBS letters* **360**: 217-222.

Lorenz, B., J. Munkner, M. P. Oliveira, A. Kuusksalu, J. M. Leitao, W. E. Muller & H. C. Schroder, (1997) Changes in metabolism of inorganic polyphosphate in rat tissues and human cells during development and apoptosis. *Biochim Biophys Acta* **1335**: 51-60.

Lund, T., M. L. De Buyser & P. E. Granum, (2000) A new cytotoxin from *Bacillus cereus* that may cause necrotic enteritis. *Mol Microbiol* **38**: 254-261.

Lund, T. & P. E. Granum, (1997) Comparison of biological effect of the two different enterotoxin complexes isolated from three different strains of *Bacillus cereus*. *Microbiology* **143:** 3329-3336.

Luxananil, P., S. Tanapongpipat, B. Promdonkoy, H. Atomi, T. Imanaka & S. Panyim, (2003) Expression of binary toxin genes in the mosquito-colonizable bacteria, *Bacillus cereus*, leads to high toxicity against *Culex quinquefasciatus* larvae. *Current microbiology* **47**: 372-375.

M'Fadyean, J., (1903) A peculiar staining reaction of the blood of animals dead of anthrax. *Journal of Comparative Pathology.* **16**: 35-41.

Makino, S., I. Uchida, N. Terakado, C. Sasakawa & M. Yoshikawa, (1989) Molecular characterization and protein analysis of the cap region, which is essential for encapsulation in *Bacillus anthracis*. *J Bacteriol* **171**: 722-730.

Manasherob, R., E. Ben-Dov, A. Zaritsky & Z. Barak, (1998) Germination, growth, and sporulation of *Bacillus thuringiensis* subsp. *israelensis* in excreted food vacuoles of the protozoan *Tetrahymena pyriformis*. *Applied and environmental microbiology* **64**: 1750-1758.

Margulis, L., J. Z. Jorgensen, S. Dolan, R. Kolchinsky, F. A. Rainey & S. C. Lo, (1998) The Arthromitus stage of *Bacillus cereus*: intestinal symbionts of animals. *Proc Natl Acad Sci U S A* **95**: 1236-1241.

Margulis, L., L. Olendzenski & B. A. Afzelius, (1990) Endospore-forming filamentous bacteria symbiotic in termites: ultrastructure and growth in culture of Arthromitus. *Symbiosis* **8**: 95-116.

Matz, C. & S. Kjelleberg, (2005) Off the hook--how bacteria survive protozoan grazing. *Trends in microbiology* **13**: 302-307.

Mendelson, N. H., (1976) Helical growth of *Bacillus subtilis*: a new model of cell growth. *Proc Natl Acad Sci U S A* **73**: 1740-1744.

Mendelson, N. H., (1982) Bacterial growth and division: genes, structures, forces, and clocks. *Microbiological reviews* **46**: 341-375.

Mendelson, N. H., (1990) Bacterial macrofibres: the morphogenesis of complex multicellular bacterial forms. *Science progress* **74**: 425-441.

Mendelson, N. H., J. E. Sarlls & J. J. Thwaites, (2001) Motions caused by the growth of *Bacillus subtilis* macrofibres in fluid medium result in new forms of movement of the multicellular structures over solid surfaces. *Microbiology* **147**: 929-937.

Meselson, M., J. Guillemin, M. Hugh-Jones, A. Langmuir, I. Popova, A. Shelokov & O. Yampolskaya, (1994) The Sverdlovsk anthrax outbreak of 1979. *Science (New York, N.Y* **266**: 1202-1208.

Mesnage, S., E. Tosi-Couture, M. Mock, P. Gounon & A. Fouet, (1997) Molecular characterization of the *Bacillus anthracis* main S-layer component: evidence that it is the major cell-associated antigen. *Mol Microbiol* **23**: 1147-1155.

Mignot, T., S. Mesnage, E. Couture-Tosi, M. Mock & A. Fouet, (2002) Developmental switch of S-layer protein synthesis in *Bacillus anthracis*. *Mol Microbiol* **43**: 1615-1627.

Mock, M. & A. Fouet, (2001) Anthrax. *Annu Rev Microbiol* **55**: 647-671.

Moir, A., B. M. Corfe & J. Behravan, (2002) Spore germination. *Cell Mol Life Sci* **59**: 403-409.

Molmeret, M., M. Horn, M. Wagner, M. Santic & Y. Abu Kwaik, (2005) Amoebae as training grounds for intracellular bacterial pathogens. *Applied and environmental microbiology* **71**: 20-28.

Mourez, M., D. B. Lacy, K. Cunningham, R. Legmann, B. R. Sellman, J. Mogridge & R. J. Collier, (2002) 2001: a year of major advances in anthrax toxin research. *Trends Microbiol* **10**: 287-293.

Okinaka, R., T. Pearson & P. Keim, (2006) Anthrax, but not *Bacillus anthracis*? *PLoS pathogens* **2**: e122.

Okinaka, R., Cloud, K., Hampton, O., Hoffmaster, A., Hill, K., Keim, P., Koehler, T. M., Lamke, G., Kumano, S.,Mahillon,J .,Manter, D., Martinez, Y., Ricke, D., Svensson, R., & Jackson, P. J. (1999) Sequence and Organisation of pX01, the large *Bacillus anthracis* plasmid harbouring the anthrax toxin genes. *J Bacteriol.* **181**: 6509-6515.

Oliva, C. R., M. K. Swiecki, C. E. Griguer, M. W. Lisanby, D. C. Bullard, C. L. Turnbough, Jr. & J. F. Kearney, (2008) The integrin Mac-1 (CR3) mediates internalization and directs *Bacillus anthracis* spores into professional phagocytes. *Proc Natl Acad Sci U S A* **105**: 1261-1266.

Oyston, P. C., (2008) *Francisella tularensis*: unravelling the secrets of an intracellular pathogen. *J Med Microbiol* **57**: 921-930.

Page, F. C., (1988) *A New Key to Freshwater and Soil Gymnamoebae with Instructions for Culture*. Freshwater Biological Association, Ambleside.

Pellizzari, R., C. Guidi-Rontani, G. Vitale, M. Mock & C. Montecucco, (1999) Anthrax lethal factor cleaves MKK3 in macrophages and inhibits the LPS/IFNgamma-induced release of NO and TNFalpha. *FEBS Lett* **462**: 199-204.

Priest, F. G., M. Barker, L. W. Baillie, E. C. Holmes & M. C. Maiden, (2004) Population structure and evolution of the *Bacillus cereus* group. *J Bacteriol* **186**: 7959-7970.

ProMed, (2006) Anthrax, Human, Fatal - UK (Scotland).

ProMed, (2008) Anthrax, Human - UK (04) : Death.

ProMed, (2010) Anthrax, Human - United Kingdom (Scotland).Archive number: 20100602.1833.

Ramsay, C. N., A. Stirling, J. Smith, G. Hawkins, T. Brooks, J. Hood, G. Penrice, L. M. Browning & S. Ahmed, (2010) An outbreak of infection with *Bacillus anthracis* in injecting drug users in Scotland. *Euro Surveill* **15**.

Rashid, M. H. & A. Kornberg, (2000) Inorganic polyphosphate is needed for swimming, swarming, and twitching motilities of *Pseudomonas aeruginosa*. *Proc Natl Acad Sci U S A* **97**: 4885-4890.

Rashid, M. H., N. N. Rao & A. Kornberg, (2000) Inorganic polyphosphate is required for motility of bacterial pathogens. *J Bacteriol* **182**: 225-227.

Rasko, D. A., M. R. Altherr, C. S. Han & J. Ravel, (2005) Genomics of the *Bacillus cereus* group of organisms. *FEMS Microbiol Rev* **29**: 303-329.

Rodgers, F. G. & F. C. Gibson, 3rd, (1993) Opsonin-independent adherence and intracellular development of *Legionella pneumophila* within U-937 cells. *Canadian journal of microbiology* **39**: 718-722.

Roh, J. Y., J. Y. Choi, M. S. Li, B. R. Jin & Y. H. Je, (2007) *Bacillus thuringiensis* as a specific, safe, and effective tool for insect pest control. *Journal of microbiology and biotechnology* **17**: 547-559.

Rowbotham, T. J., (1980) Preliminary report on the pathogenicity of *Legionella pneumophila* for freshwater and soil amoebae. *J Clin Pathol* **33**: 1179-1183.

Saile, E. & T. M. Koehler, (2006) *Bacillus anthracis* Multiplication, Persistence, and Genetic Exchange in the Rhizosphere of Grass Plants. *Appl Environ Microbiol* **72**: 3168-3174.

Sambrook J., Fritsch E.F. & Maniatis T., (1989) *Molecular Cloning: A Laboratory Manual, 2nd edition*. Cold Spring Harbor Laboratory Press.

Schneerson, R., J. Kubler-Kielb, T. Y. Liu, Z. D. Dai, S. H. Leppla, A. Yergey, P. Backlund, J. Shiloach, F. Majadly & J. B. Robbins, (2003) Poly(gamma-D-glutamic acid) protein conjugates induce IgG antibodies in mice to the capsule of *Bacillus anthracis*: a potential addition to the anthrax vaccine. *Proc Natl Acad Sci U S A* **100**: 8945-8950.

Scorpio, A., T. E. Blank, W. A. Day & D. J. Chabot, (2006) Anthrax vaccines: Pasteur to the present. *Cell Mol Life Sci* **63**: 2237-2248.

Segal, G. & H. A. Shuman, (1999) *Legionella pneumophila* utilizes the same genes to multiply within *Acanthamoeba castellanii* and human macrophages. *Infection and immunity* **67**: 2117-2124.

Shi, X., N. N. Rao & A. Kornberg, (2004) Inorganic polyphosphate in *Bacillus cereus*: motility, biofilm formation, and sporulation. *Proc Natl Acad Sci U S A* **101**: 17061-17065.

Shiba, T., H. Itoh, A. Kameda, K. Kobayashi, Y. Kawazoe & T. Noguchi, (2005) Polyphosphate:AMP phosphotransferase as a polyphosphate-dependent nucleoside monophosphate kinase in *Acinetobacter johnsonii* 210A. *J Bacteriol* **187**: 1859-1865.

Sierecka, J. K., (1998) Purification and partial characterization of a neutral protease from a virulent strain of *Bacillus cereus*. *The international journal of biochemistry & cell biology* **30**: 579-595.

Sinclair, R., S. A. Boone, D. Greenberg, P. Keim & C. P. Gerba, (2008) Persistence of category A select agents in the environment. *Applied and environmental microbiology* **74**: 555-563.

Smith, S. A., N. J. Mutch, D. Baskar, P. Rohloff, R. Docampo & J. H. Morrissey, (2006) Polyphosphate modulates blood coagulation and fibrinolysis. *Proc Natl Acad Sci U S A* **103**: 903-908.

Solomon, J. M., A. Rupper, J. A. Cardelli & R. R. Isberg, (2000) Intracellular growth of *Legionella pneumophila* in *Dictyostelium discoideum*, a system for genetic analysis of host-pathogen interactions. *Infection and immunity* **68**: 2939-2947.

Spencer, R. C., (2003) *Bacillus anthracis*. *J Clin Pathol* **56**: 182-187.

Steinmetz, M. & R. Richter, (1994) Plasmids designed to alter the antibiotic resistance expressed by insertion mutations in *Bacillus subtilis*, through in vivo recombination. *Gene* **142**: 79-83.

Sterne, M., (1939) The use of anthrax vaccines prepared from avirulent (uncapsulated) varients of Bacillus anthracis. *Onderstepoort Journal of Vetinary Science and Animal Industry* **13**: 307-312.

Stewart, G. S., K. Johnstone, E. Hagelberg & D. J. Ellar, (1981) Commitment of bacterial spores to germinate. A measure of the trigger reaction. *Biochem J* **198**: 101-106.

Taylor, C. M., M. Beresford, H. A. Epton, D. C. Sigee, G. Shama, P. W. Andrew & I. S. Roberts, (2002) *Listeria monocytogenes* relA and hpt mutants are impaired in surface-attached growth and virulence. *J Bacteriol* **184**: 621-628.

Teshigawara, K., R. Kannagi, N. Noro & T. Masuda, (1985) Possible involvement of transglutaminase in endocytosis and antigen presentation. *Microbiology and immunology* **29**: 737-750.

Titball, R. W., A. Johansson & M. Forsman, (2003) Will the enigma of *Francisella tularensis* virulence soon be solved? *Trends in microbiology* **11**: 118-123.

Trieu-Cuot, P., C. Carlier, C. Poyart-Salmeron & P. Courvalin, (1991) An integrative vector exploiting the transposition properties of Tn1545 for insertional mutagenesis and cloning of genes from gram-positive bacteria. *Gene* **106**: 21-27.

Turnbull, P. C., (1991) Anthrax vaccines: past, present and future. *Vaccine* **9**: 533-539.

Turnbull, P. C., (2000) Current status of immunization against anthrax: old vaccines may be here to stay for a while. *Curr Opin Infect Dis* **13**: 113-120.

Turnbull, P. C., (2002a) Introduction: anthrax history, disease and ecology. *Curr Top Microbiol Immunol* **271**: 1-19.

Turnbull, P. C., (2002b) Introduction: Anthrax history, disease and Ecology. In: Anthrax. T. M. Koehler (ed). Springer, pp. 1-20.

Turnbull, P. C., K. Jorgensen, J. M. Kramer, R. J. Gilbert & J. M. Parry, (1979) Severe clinical conditions associated with *Bacillus cereus* and the apparent involvement of exotoxins. *J Clin Pathol* **32**: 289-293.

Turnbull, P. C., N. M. Sirianni, C. I. LeBron, M. N. Samaan, F. N. Sutton, A. E. Reyes & L. F. Peruski, Jr., (2004) MICs of selected antibiotics for *Bacillus anthracis*, *Bacillus cereus, Bacillus thuringiensis*, and *Bacillus mycoides* from a range of clinical and environmental sources as determined by the Etest. *J Clin Microbiol* **42**: 3626-3634.

Tzeng, C. M. & A. Kornberg, (1998) Polyphosphate kinase is highly conserved in many bacterial pathogens. *Mol Microbiol* **29**: 381-382.

Van Delden, C. & B. H. Iglewski, (1998) Cell-to-cell signaling and *Pseudomonas aeruginosa* infections. *Emerg Infect Dis* **4**: 551-560.

Van Ert, M. N., W. R. Easterday, L. Y. Huynh, R. T. Okinaka, M. E. Hugh-Jones, J. Ravel, S. R. Zanecki, T. Pearson, T. S. Simonson, J. M. U'Ren, S. M. Kachur, R. R. Leadem-Dougherty, S. D. Rhoton, G. Zinser, J. Farlow, P. R. Coker, K. L. Smith, B. Wang, L. J. Kenefic, C. M. Fraser-Liggett, D. M. Wagner & P. Keim, (2007) Global genetic population structure of *Bacillus anthracis*. *PloS one* **2**: e461.

van Schaik, W., J. Prigent & A. Fouet, (2007) The stringent response of *Bacillus anthracis* contributes to sporulation but not to virulence. *Microbiology* **153**: 4234-4239.

Wang, L., C. D. Fraley, J. Faridi, A. Kornberg & R. A. Roth, (2003) Inorganic polyphosphate stimulates mammalian TOR, a kinase involved in the proliferation of mammary cancer cells. *Proc Natl Acad Sci U S A* **100**: 11249-11254.

Widmann, C., S. Gibson, M. B. Jarpe & G. L. Johnson, (1999) Mitogen-activated protein kinase: conservation of a three-kinase module from yeast to human. *Physiological reviews* **79**: 143-180.

Williamson, E. D., I. Hodgson, N. J. Walker, A. W. Topping, M. G. Duchars, J. M. Mott, J. Estep, C. Lebutt, H. C. Flick-Smith, H. E. Jones, H. Li & C. P. Quinn, (2005) Immunogenicity of recombinant protective antigen and efficacy against aerosol challenge with anthrax. *Infection and immunity* **73**: 5978-5987.

Winiecka-Krusnell, J., K. Wreiber, A. von Euler, L. Engstrand & E. Linder, (2002) Free-living amoebae promote growth and survival of *Helicobacter pylori*. *Scandinavian journal of infectious diseases* **34**: 253-256.

Wong, M. L. & J. F. Medrano, (2005) Real-time PCR for mRNA quantitation. *BioTechniques* **39**: 75-85.

Young, J. A. & R. J. Collier, (2007) Anthrax toxin: receptor binding, internalization, pore formation, and translocation. *Annu Rev Biochem* **76**: 243-265.

Zhang, H., M. R. Gomez-Garcia, M. R. Brown & A. Kornberg, (2005a) Inorganic polyphosphate in *Dictyostelium discoideum*: influence on development, sporulation, and predation. *Proc Natl Acad Sci U S A* **102**: 2731-2735.

Zhang, H., K. Ishige & A. Kornberg, (2002) A polyphosphate kinase (PPK2) widely conserved in bacteria. *Proc Natl Acad Sci U S A* **99**: 16678-16683.

Zhang, H., N. N. Rao, T. Shiba & A. Kornberg, (2005b) Inorganic polyphosphate in the social life of *Myxococcus xanthus*: motility, development, and predation. *Proc Natl Acad Sci U S A* **102**: 13416-13420.

8 Appendix

Figure 8.1 Poster presented at the Bacillus ACT 2007 conference.

Development of a Relative Real-Time Gene Expression Assay for Polyphosphate kinase in *Bacillus anthracis*

Deborah J. Nash[1,2], S. Charlton[2], N. Waterfield[1], N. J. Silman[2], M. J. Hudson[2], M. R. W. Brown[3]

[1] Department of Biology and Biochemistry, University of Bath, Claverton Down, Bath, UK, BA2 7AY
[2] Health Protection Agency, Centre for Emergency Preparedness and Response, Porton Down, Salisbury, UK, SP4 0JG.
[3] School of Applied Sciences, University of Wolverhampton, Wulfruna Street, Wolverhampton, UK, WV1 1SB

Introduction

Inorganic polyphosphate (Poly P) is a polymer made from tens to hundreds of phosphate residues linked by high energy bonds. It has generally been regarded as a molecular fossil but its importance in all living cells is beginning to unfold.

Four enzymes of PolyP metabolism have been identified in a variety of microrganisms:

- PPK 1 – Polyphosphate Kinase
- PPX – Exopolyphosphatase
- PAP – PolyP/AMP Phosphotransferase
- PPN – Endopolyphosphatase

PPK is key to the assembly of PolyP and is therefore the target in this study.

Kornberg *et al.* have shown that PPK, PPX and PAP knockouts of *B. cereus* are impaired in sporulation, motility, swimming and swarming, biofilm formation and have increased sensitivity to antibiotics.

B. anthracis homlogs of PPK, PPX and PAP show ~90% identity to *B. cereus* which suggests that PolyP may be of similar metabolic importance in *B. anthracis*. We are interested to investigate this with respect to toxin expression in *B. anthracis* Sterne, particularly in the context of acellular anthrax vaccine manufacture.

Correlations between the expression of PPK and production of anthrax toxin components are being studied during the various phases of growth, such that RNA extractions from various time points should show a "snap shot" of the expression at that particular stage of growth. Using a relative real-time gene expression assay these samples will be analysed and compared to an endogenous control which can be used to normalise the level of gene expression.

Method and Results

A real-time PCR assay was designed for the PPK target gene using TaqMan® chemistries. Two endogenous control genes (GyrB and 16srRNA) were used in the optimization steps in order to assess which one may be more effective in the assay. The primer and probe sequences are shown in Table 1.

Primers were optimised using *B. anthracis* Sterne genomic DNA in a serial dilution to assess the sensitivity of the assay. The 16srRNA and GyrB targets were optimised for use as an endogenous control and used as a normaliser to study the up/down regulation of gene expression. The optimised amplification plots are shown in See Figure 1. The assays were optimised on the ABI 7900 platform using the ABI universal master mix.

Table 1. Real-time Primer and Probe sequences.

Gene Target	Sequence 5' – 3'
16s rRNA fwd	FAM – TTCGGGAGCAGAGTG– BHQ1
16s rRNA rvs	FAM – AACATCTCACGACACGAG– BHQ1
16s rRNA Probe	FAM – CAGGTGGTGCATGGTTGTC– BHQ1
GyrB fwd	FAM – ACTTGAAGGACTAGAAGCAG – BHQ1
GyrB rvs	FAM – TCCTTTTCCACTTGTAGATC – BHQ1
GyrB Probe	FAM – CGAAAACGCCCTGGTATGTATA – BHQ1
PPK fwd	FAM – CCCAACAACACTAACTACCCGAAT– BHQ1
PPK Rvs	FAM – AACTCATCGTTCGAGGAACATGT– BHQ1
PPK Probe	FAM – TTTTCACTTACATTTGGAATACCAGGTCGTAGGC– BHQ1

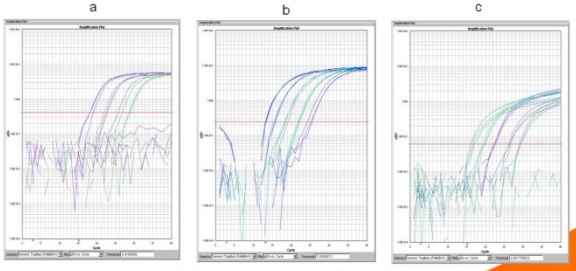

Figure 1. a. Amplification plot for the optimised PPK assay. b. Amplification plot for the optimised GyrB assay. c. Amplification plot for the optimised 16srRNA assay.

The PCR efficiencies of the endogenous control and target gene have been established in order to maximise the reliability of the gene expression assay. This was done by assaying a dilution series of DNA and comparing the difference in Ct between control and target genes. The plot of average Ct values should look parallel between the target gene and the endogenous control, but close inspection showed some slight deviation (Figure 2). Plotting the ΔCt against DNA concentration should produce a straight line with a gradient of 0 ± 0.1(Figure 3) whereas analysis shows this not to be the case.

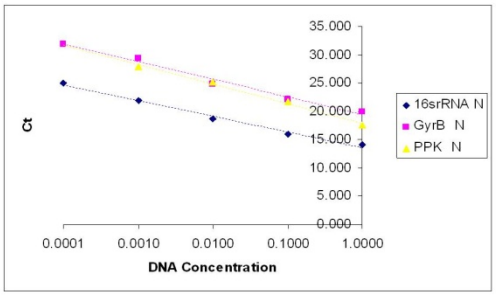

Figure 2. A graph showing the average Ct values of each of the three sets of primers and probes.

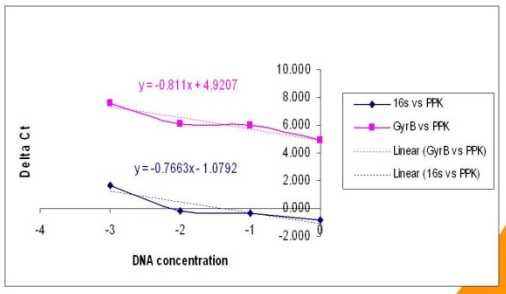

Figure 3. A graph showing the ΔCt values against the DNA concentration when comparing the two endogenous controls with the PPK target gene.

Conclusion

After analysing the two endogenous controls it became clear that the 16srRNA target produced the best results throughout, as the sensitivity of the 16srRNA target was substantially better than the GyrB target.

When comparing the 16srRNA and the PPK target gene it was clear that the PCR efficiencies are not close enough to be able to compare gene expression values accurately. In these preliminary studies, the GyrB gradient was -0.8 and the 16srRNA was -0.7, whereas the optimal value should be 0 ± 0.1.

The PPK target primers and probes were less sensitive than the 16srRNA, but we do not anticipate this being a major problem to our studies as extracted mRNA will be added at the same concentration to each reaction.

Further optimisation of this assay is ongoing prior to analysing samples, together with assay development of comparable assays for the other polyphosphate gene targets (PPX, PAP, PPN).

Acknowledgments

I would like to thank the Society of General Microbiology and the University of Bath for the funding to attend this conference.

References:
Shi, X. Rao. N., and Kornberg, A. (2004) Inorganic polyphosphate in *Bacillus cereus*: Motility, biofilm formation and sporulation. PNAS. **101:** (49) 17061-17065.